ZooKeys 1084: 1–26 (2022)
doi: 10.3897/zookeys.1084.71576
https://zookeys.pensoft.net

RESEARCH ARTICLE

A peer-reviewed open-access journal
ZooKeys
Launched to accelerate biodiversity research

# Complete mitogenomes of four *Trichiurus* species: A taxonomic review of the *T. lepturus* species complex

Mu-Rong Yi[1,2*], Kui-Ching Hsu[1*], Sui Gu[1], Xiong-Bo He[1], Zhi-Sen Luo[1], Hung-Du Lin[3*], Yun-Rong Yan[1,2,4*]

**1** *College of Fisheries, Guangdong Ocean University, Zhanjiang 524088, China* **2** *Marine Resources Big Data Center of South China Sea, Southern Marine Science and Engineering Guangdong Laboratory, Zhanjiang 524088, China* **3** *The Affiliated School of National Tainan First Senior High School, Tainan 701, Taiwan* **4** *Guangdong Provincial Engineering and Technology Research Center of Far Sea Fisheries Management and Fishing of South China Sea, Guangdong Ocean University, Zhanjiang 524088, China*

Corresponding authors: Hung-Du Lin (varicorhinus@hotmail.com), Yun-Rong Yan (tuna_ps@126.com)

Academic editor: Yahui Zhao | Received 14 July 2021 | Accepted 31 December 2021 | Published 26 January 2022

*http://zoobank.org/86853D87-0004-417C-9A34-E0A24DF63CC8*

Citation: Yi M-R, Hsu K-C, Gu S, He X-B, Luo Z-S, Lin H-D, Yan Y-R (2022) Complete mitogenomes of four *Trichiurus* species: A taxonomic review of the *T. lepturus* species complexe. ZooKeys 1084: 1–26. https://doi.org/10.3897/zookeys.1084.71576

## Abstract

Four *Trichiurus* species, *T. japonicus*, *T. lepturus*, *T. nanhaiensis*, and *T. brevis*, from the coasts of the China Seas, have been identified and their entire mitochondrial genomes (mitogenomes) have been sequenced by next-generation sequencing technology. A comparative analysis of five mitogenomes was conducted, including the mitogenome of *T. gangeticus*. The mitogenomes contained 16.568–16.840 bp and encoded 36 typical mitochondrial genes (13 protein-coding, 2 ribosomal RNA-coding, and 21 transfer RNA-coding genes) and two typical noncoding control regions. Although $tRNA^{Pro}$ is absent from *Trichiurus* mitogenomes, when compared with the 22 tRNAs reported in other vertebrates, the gene arrangements in the mitogenomes of the studied species are consistent with those in most teleost mitogenomes. The full-length sequences and protein-coding genes (PCGs) in the mitogenomes of the five species had obvious AT biases and negative GC skew values. Our study indicate that the specimens in the Indian Ocean are neither *T. lepturus* nor *T. nanhaiensis* but they are *T. gangeticus*; the *Trichiurus* species composition in the Indian Ocean is totally different from that in Pacific and Atlantic oceans; there are at least two *Trichiurus* species in Indian Ocean; and the worldwide systematics and diversity of the genus *Trichiurus* need to be reviewed.

* These authors have contributed equally to this work

**Keywords**
Characterization, mitogenome, molecular tool, phylogeny, taxonomy, *Trichiurus*

## Introduction

The cutlassfishes include ten genera and 47 species in Eschmeyer's Catalog of Fishes (ECoF, Fricke et al. 2021). These species are predatory fishes in the family Trichiuridae (Scombriformes) and found in seas throughout the world (Nelson et al. 2016). Among the ten genera, members of the genus *Trichiurus* Linnaeus, 1758 are the most common and most well studied. *Trichiurus* species are important commercial marine fishes (FAO 2004); however, their systematics remain unresolved because of the high degree of similarity among species in the genus in terms of bodily appearance and silvery coloration. As many as 31 nominal species of the genus *Trichiurus* have been described to date, but only nine are valid species (FishBase, Froese and Pauly 2021). However, according to ECof, *Trichiurus* has 31 nominal names and eleven valid species. The difference between the two databases is due to *T. japonicus* Temminck & Schlegel, 1844 and *T. nitens* Garman, 1899. FishBase considers these two species to be synonymous with *T. lepturus*, based on Nakamura and Parin (1993). However, Chakraborty et al. (2006a) established that *T. japonicus* is a valid species based on the differences in mitochondrial 16S rRNA. Moreover, Burhanuddin and Parin (2008) proved the validity of *T. nitens* based on the morphometric parameters.

According to ECoF, these eleven valid species are divided between two species complexes, the *T. lepturus* complex and the *T. russelli* complex. The *T. lepturus* complex is referred to as the large-headed or long-tailed species complex. This species complex, which has the anal opening positioned vertically at the 38$^{th}$–41$^{st}$ dorsal fin rays, includes seven species: *T. lepturus* Linnaeus, 1758, *T. japonicus*, *T. auriga* Klunzinger, 1884, *T. nitens*, *T. gangeticus* Gupta, 1966, *T. margarites* Li, 1992 and *T. nanhaiensis* Wang & Xu, 1992. The *T. russelli* complex is referred to as the short-tailed species complex, and the anal opening is positioned vertically at the 34$^{th}$ and 35$^{th}$ dorsal fin rays (Burhanuddin et al. 2002). The short-tailed species complex includes four species: *T. australis* Chakraborty, Burhanuddin & Iwatsuki, 2005, *T. brevis* Wang & You, 1992, *T. nickolensis* Burhanuddin & Iwatsuki, 2003 and *T. russelli* Dutt & Thankam, 1967. Although there were many studies about the systematics of the genus *Trichiurus* (e.g., Lee et al. 1977; Nakabo 2000; Chakraborty et al. 2006b; Tzeng et al. 2007; Hsu et al. 2009), the taxonomic identification within the *T. lepturus* complex has long been confusing.

Many studies have suggested that *Clupea haumela* Fabricius, 1775 is a synonym of *T. lepturus* (Nakamura and Parin 1993, 2021; Fricke 2008; Golani and Fricke 2018); however, a recently published study (Zheng et al. 2019) mentioned this species as a valid *Trichiurus* species without taxonomic evidence and presented its complete mitochondrial genome. In addition, many studies (Tucker 1956; Nakamura and Parin 1993; Nelson 1994) suggested that *T. japonicus* Temminck & Schlegel, 1844 is synonymous

with *T. lepturus*, but other studies (Lee et al. 1977; Nakabo 2000; Chakraborty et al. 2006a, b; Tzeng et al. 2007; Hsu et al. 2009; He et al. 2014; Fricke et al. 2021) suggested that *T. japonicus* is a valid species. *Trichiurus lepturus* is known to be found in tropical and temperate waters throughout the world (Froese and Pauly 2021). Chakraborty et al. (2006a) sampled specimens of *T. lepturus* in the Indian Ocean, but Hsu et al. (2009) re-examined the taxonomic status of *Trichiurus* species and suggested that these specimens from the Indian Ocean might not be *T. lepturus*. There are thus several outstanding questions regarding the systematics and distributional patterns of *Trichiurus* species.

The accurate identification of species is important both for scientists and the broader community. However, correctly identifying species remains a major challenge for the general public. Hebert et al. (2003) proposed that the DNA barcoding can be used to facilitate species identification. For animals, the universal barcoding region is the cytochrome c oxidase subunit 1 (COI) in mitochondrial DNA. COI has become a valuable molecular tool for studies characterizing interspecific and intraspecific diversity and evolutionary relationships (e.g., Conway et al. 2015; Ahti et al. 2016; Salcioglu et al. 2020). However, Mirande (2018) proposed that incomplete mitochondrial gene sequences have a limited ability to facilitate the identification of complex evolutionary relationships in many fishes. The use of mitogenomes would be expected to provide more information for species identification, phylogenetics and population genetics (Liu et al. 2020; Phillips and Zakaria 2021; Wang et al. 2021). To address these problems about the taxonomy of the genus *Trichiurus*, the COI, mitogenome, and morphology were used.

In this study, we completed four tasks. First, COI sequences were used to identify *Trichiurus* species to determine the number of species found along the coast of China. Second, the complete mitogenomes of four *Trichiurus* species in the China Seas were sequenced using next-generation sequencing. Third, we obtained the mitogenome sequences of the family Trichiuridae from the NCBI database (https://www.ncbi.nlm.nih.gov) to clarify the systematics of the genus *Trichiurus* and to facilitate comparison of the molecular evolutionary characteristics between *Trichiurus* species and other cutlassfishes. Finally, traditional caliper measurements were performed, which identified 14 landmarks that were used to evaluate morphological differences among *Trichiurus* species. These results provide further insight into the systematics and diversity of the genus *Trichiurus*.

## Materials and methods

### Sampling and species identification

Our teams sampled *Trichiurus* specimens from the China Seas, including the Yellow Sea, East China Sea, and South China Sea in October 2017 and August 2019 by longline, gill net, and trawl net with fishermen (Fig. 1A, Suppl. material 1: Table S1). In total, 1.311 specimens were collected. Traditional caliper measurements were performed, which identified 14 landmarks (a–n, Fig. 2).

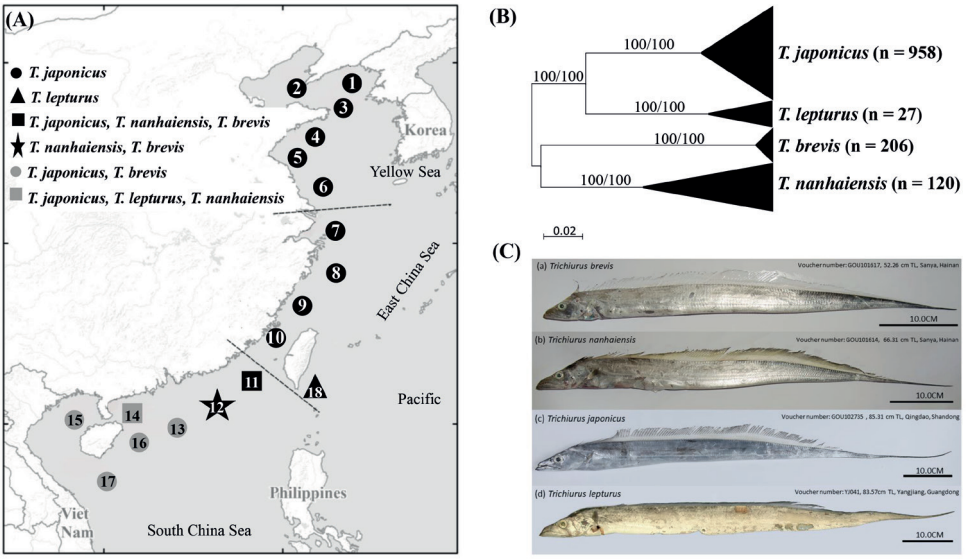


**Figure 1. A** Eighteen sampling localities of the genus the *Trichiurus* along the Chinese coast and the species composition after our surveys. Refer to Suppl. material 1: Table S1 for the abbreviations of localities. **B** The maximum-likelihood (ML) tree of these four *Trichiurus* species along the coast based on the COI gene. The numbers at the nodes are bootstrap values of the ML and NJ (neighbor-joining) analyses. The sampling size (n) indicated in parentheses **C** The photographs of four Trichiurus species used in the mitogenomes analyses.

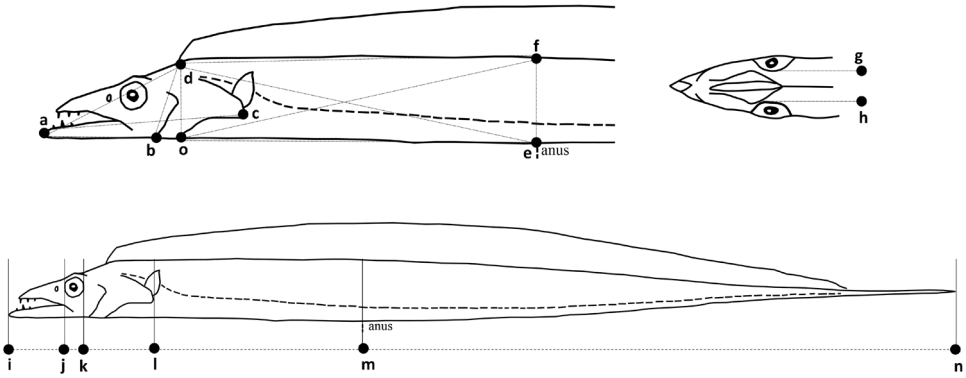


**Figure 2.** Positions of 14 (a–n) landmarks used to contrast the morphological differences between *Trichiurus* species.

A portion of the muscle tissues from 1.311 specimens was stored in 100% ethanol. Total genomic DNA was extracted from muscle tissue using a Genomic DNA Purification Kit (Gentra Systems, Valencia, CA). The COI gene was amplified by polymerase chain reaction (PCR) using the primers Fish-F2 (5′-ACCTCTGTGTGTGGGGCTAC-3′) and Fish-R2 (5′-GTGATGCATTGGCTTGAAA-3′) (Gu et al. 2021). Each

50-μl PCR mixture contained 5 ng of template DNA, 5 μl of 10× reaction buffer, 4 μl of dNTP mix (10 mM), 5 pmol of each primer and 2 U of Taq polymerase (TaKaRa, Taq polymerase). PCR was conducted on an MJ Thermal Cycler using the following cycling parameters: one cycle of denaturation at 94 °C for 3 min, 40 cycles of denaturation at 94 °C for 30 s, annealing at 55 °C for 30 s and extension at 72 °C for 1 min and 30 s, followed by a 72 °C extension for 10 min and storage at 4 °C. The purified PCR products were sequenced using an ABI 377 automated sequencer (Applied Biosystems, Foster City, CA, U.S.A.). The resulting chromatograms were assessed using CHROMAS software (Technelysium), and the sequences were manually edited using BIOEDIT 6.0.7 (Hall 1999). In totally, 1.311 sequences were obtained, and the haplotypes were deposited in GenBank under accessions MZ959870 - MZ959999, MZ960057-MZ960127, OK053821 - OK054341 and OL539388-OL539398. The nucleotide sequences were aligned in Clustal X 1.81 (Thompson et al. 1997). Selection of the best-fit nucleotide substitution models was performed using the Bayesian information criterion (BIC) in jModelTest 2.0 (Darriba et al. 2012). The most appropriate nucleotide substitution model was GTR+I+G for COI. Maximum likelihood (ML) and neighbor-joining (NJ) phylogenetic analysis were performed with MEGA-X (Kumar et al. 2018). Bootstrapping was implemented with 1000 replications. In addition, Shen et al. (2016) proposed that the use of the K2P (Kimura's two-parameter) distance in barcode analyses has been challenged and the p-distance has been proposed to be a better model. Thus, the p-distances between *Trichiurus* species were estimated in MEGA-X.

## Sequence assembly, annotation, and analysis

Next-generation sequencing (NGS) was performed to obtain complete mitogenome sequences. Complete mitogenomes were obtained from high-throughput sequencing with a HiSeqX Ten platform (Illumina, San Diego, CA) with a paired-end, 150-bp approach. All the reads were mapped to the full mitogenome reference sequences of other *Trichiurus* species (Table 1) using SOAPdenovo v.2.04 (https://github.com/aquaskline/SOAPdenovo2). The remaining high-quality reads were assembled using SPAdes v3.10 (https://github.com/ablab/spades). Compared with the corresponding complete mitogenome sequences of the genus *Trichiurus* (Liu and Cui 2009; Liu et al. 2013; Xu et al. 2019; Zheng et al. 2019; Mukundan et al. 2020; Table 1), protein-coding genes (PCGs), tRNA-coding genes and ribosome-coding genes were identified by BLAST. Codon usage, nucleotide substitution and base composition were determined using MEGA-X and DnaSP version 5.10 (Librado and Rozas 2009), and the rules for the vertebrate mitochondrial genetic code was used. AT skewing and GC skewing of the nucleotide composition were measured according to the following formulae: AT skew = (A – T)/(A + T) and GC skew = (G – C)/(G + C) (Perna and Kocher 1995).

The relative synonymous codon usage (RSCU), nonsynonymous codon usage (Ka) and synonymous codon usage (Ks) of all PCGs were analyzed using DnaSP. Comparison of the rates of Ka/Ks provides insight into changes in selective pressure: Ka/Ks values > 1 indicate positive selection; Ka/Ks = 1 indicates neutral selection; and Ka/Ks < 1 indicates negative or purifying selection. Some mitogenomes of the family Trichiuridae

**Table 1.** Information on the mitogenomes used in this study.

| Species | Accession no. | Genome size | References |
|---|---|---|---|
| *Trichiurus japonicus* | EU339148 | 16.796 bp | Liu and Cui (2009) |
| | MK292708 | 16.798 bp | Xu et al. (2019) |
| | MW719077 | 16.685 bp | This study |
| *T. haumela* | MH846121 | 16.855 bp | Zheng et al. (2019) |
| *T. lepturus* | MK333401 | 16.840 bp | Mukundan et al. (2020) |
| *T. nanhaiensis* | MW719078 | 16.568 bp | This study |
| | JX477078 | 17.060 bp | Liu et al. (2013) |
| | MW719076 | 16.801 bp | This study |
| *T. brevis* | MW694877 | 16.733 bp | This study |
| *Benthodesmus tenuis* | AP012522 | 16.864 bp | Miya et al. (2013) |
| *Aphanopus carbo* | AP012944 | 16.406 bp | Miya et al. (2013) |
| *Evoxymetopon poeyi* | AP012509 | 16.475 bp | Miya et al. (2013) |
| *Assurger anzac* | AP012508 | 16.510 bp | Miya et al. (2013) |

were downloaded from GenBank (NCBI database, Table 1). The most appropriate nucleotide substitution model was GTR+I+G for the mitogenome. The ML and NJ phylogenetic analysis were performed with MEGA-X. Bootstrapping was implemented with 1000 replications. The p-distances between *Trichiurus* species (interspecific) and between genera within Trichiuridae (intergeneric) were estimated in MEGA-X.

### Morphological analyses

Measurements were referred to the truss network (Humphries et al. 1981) and some additional landmarks, forming 19 distances from 14 landmarks (Fig. 2). The morphometric characteristics were measured to nearest 0.1 and 0.01 cm using traditional calipers. In total, 225 specimens from South China Sea were measured. Values of the distances between landmarks were measured, and their means and standard deviations (S.D.) were calculated.

## Results

### Species identification

A total of 1.311 specimens were collected. Species were first identified by morphology. Two species groups were recognized, the *T. lepturus* complex, which has the anal opening positioned vertically at the 38$^{th}$–41$^{st}$ dorsal fin rays, and the *T. russelli* complex, which has the anal opening positioned vertically at the 34$^{th}$ and 35$^{th}$ dorsal fin rays (Burhanuddin et al. 2002). Within the *T. lepturus* complex, *T. japonicus* has a longer tail, and *T. lepturus* has a whitish dorsal fin when fresh; by contrast, *T. nanhaiensis* has a yellowish green dorsal fin (Hsu et al. 2009). Besides, our study found that from the front view of the heads preserved specimens, the frontal bone of *T. nanhaiensis* is very smooth (Suppl. material 1: Fig. S1A), the frontal bone of *T. japonicus* is slightly inverted (Suppl. material 1: Fig. S1B), and the frontal bone of *T. lepturus* is obviously

inverted and bulges in the upper part of the orbit and is accompanied by an indentation (Suppl. material 1: Fig. S1C). Four species belonging to the two species complexes were collected. We used COI sequences to identify species (Hebert et al. 2003). Our study sequenced complete COI gene (1551 bp) in all specimens. The phylogenetic trees reconstructed within ML and NJ were identical. In the ML tree (Fig. 1B), all specimens were grouped into four lineages with strong bootstrap support. After BLAST, we ensured these four lineages corresponded to four *Trichiurus* species: *T. japonicus* (*n* = 958), *T. lepturus* (*n* = 27), *T. nanhaiensis* (*n* = 120) and *T. brevis* (*n* = 206).

*Trichiurus japonicas* is distributed in the China Sea; *T. lepturus*, *T. nanhaiensis*, and *T. brevis* are distributed in the South China Sea. The results from the morphological and molecular data were the same. However, our study revealed that *T. lepturus* is very rare in the South China Sea (Fig. 1, Suppl. material 1: Table S1). Additionally, the results showed that *T. lepturus* complex was not a monophyletic group because *T. brevis*, belonging to *T. russelli* complex, was nested with *T. nanhaiensis*. Our study considers that this is because information is lacking.

After identifying species by morphology and DNA barcoding, the complete mitochondrial genomes of four *Trichiurus* species were sequenced (Fig. 1C). These four specimens were fixed in 10% formalin, transferred to 70% ethanol, and deposited in the Guangdong Ocean University, Zhanjiang, China as voucher specimens (GOU101614, GOU101617, GOU102735, and TLYJ041). The lengths of the complete mitogenomes of *T. japonicus* (MW719077), *T. lepturus* (MW719078), *T. nanhaiensis* (MW719076), and *T. brevis* (MW694877) were 16.685 bp, 16.568 bp, 16.801 bp, and 16.733 bp, respectively. To confirm the taxonomy of *Trichiurus* species, the phylogeny of Trichiuridae was analyzed using mitogenome sequences (Fig. 3, Table 1). The phylogenetic trees reconstructed within ML and NJ were identical. In ML tree (Fig. 3), the sequences of the genus *Trichiurus* were grouped into five lineages (I–V). *Trichiurus haumela* (MH846121 in Zheng et al. 2019) was included within *T. japonicus* (lineage I), and *T. lepturus* (MW719078) in our study and "*T. lepturus*" (MK333401 in Mukundan et al. 2020) were not considered monophyletic (lineages II and III). Thus, our study used COI sequences to examine the taxonomic status of *Trichiurus* species. All COI sequences of *Trichiurus* species in GenBank (NCBI database) were downloaded. After alignment, 477 bp were analyzed. The phylogenetic trees reconstructed within ML and NJ were identical, with only small differences in bootstrap values. In the COI phylogenetic analyses (ML tree, Fig. 4), all sequences were grouped into six lineages (A–F). Lineage F included *T. brevis* within the *T. russelli* complex. *Trichiurus haumela* (MH846121 in Zheng et al. 2019) was also included within *T. japonicus* in lineage A. The specimen from the Indian Ocean (MK333401 in Mukundan et al. 2020) might be not *T. lepturus*, as it was grouped with other specimens of *T. gangeticus* in lineage E. The genetic distance within the six lineages ranged from 0.0013 (lineage F, *T. brevis*) to 0.0333 (lineage C, *T. lepturus*), and the genetic distance between lineages ranged from 0.0435 (between *T. japonicus* and *T. auriga*) to 0.1600 (between *T. japonicus* and *T. brevis*) (Table 2). Based on the mitogenomes, the genetic distances between these five species ranged from 0.0507 (*T. nanhaiensis* and *T. gangeticus*) to 0.1331 (*T. gangeticus* and *T. brevis*), including the d-loop region, and from 0.0476 (*T. nanhaiensis* and *T.*

*gangeticus*) to 0.1288 (*T. lepturus* and *T. brevis*), excluding the d-loop region (Table 2). Moreover, the mitogenome p-distances between *T. japonicus* and *T. haumela*, including and excluding the d-loop region, were 0.0067 and 0.0047, respectively.

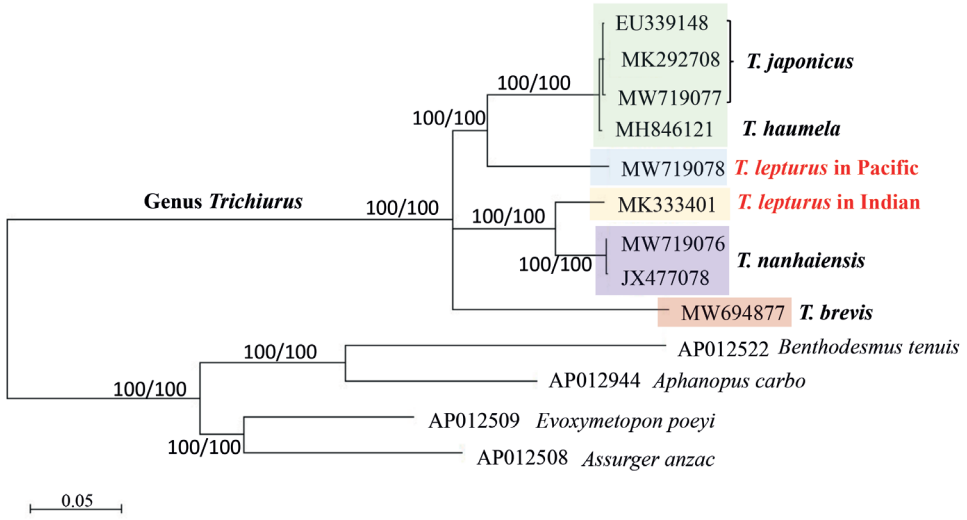


**Figure 3.** The maximum-likelihood (ML) tree of the Trichiuridae based on the sequences of mitogenome (excluding d-loop). The numbers at the nodes are bootstrap values of the ML and NJ (neighbor-joining) analyses.

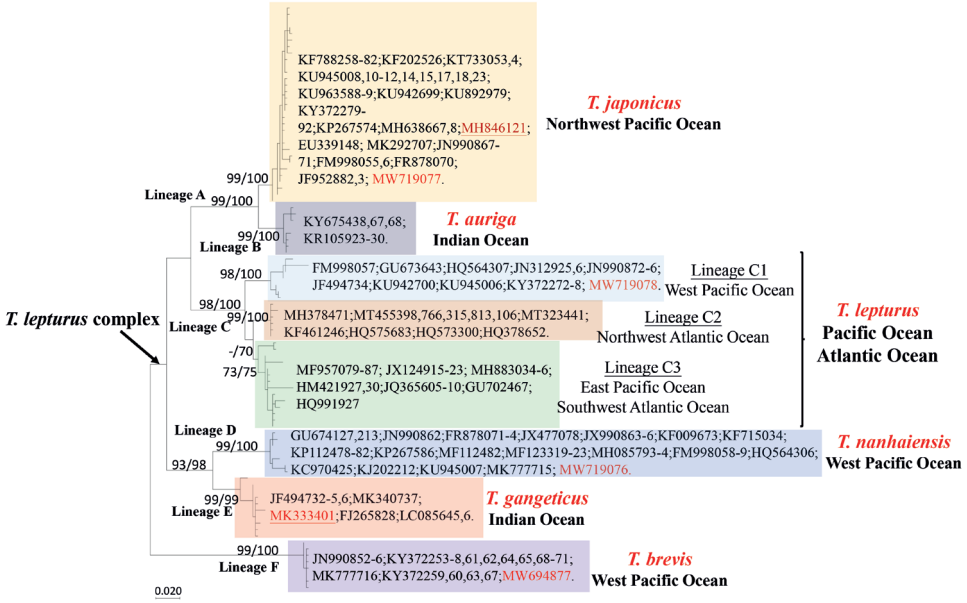


**Figure 4.** The maximum-likelihood (ML) tree of six *Trichiurus* species in the world based on the COI gene. The numbers at the nodes are bootstrap values of the ML and NJ (neighbor-joining) analyses.

**Table 2.** The p-distance based on sequences of partial COI (below) and mitogenome (above, excluding d-loop in brackets). Bold indicates the mean COI divergence within groups.

| | *T. japonicus* | *T. auriga* | *T. lepturus* | *T. nanhaiensis* | *T. gangeticus* | *T. brevis* |
|---|---|---|---|---|---|---|
| *T. japonicus* | **0.0054** | – | 0.0984 (0.0965) | 0.1160 (0.1127) | 0.1140 (0.1114) | 0.1306 (0.1280) |
| *T. auriga* | 0.0435 | **0.0069** | – | – | – | - |
| *T. lepturus* | 0.1078 | 0.1149 | **0.0333** | 0.1127 (0.1118) | 0.1119 (0.1107) | 0.1310 (0.1288) |
| *T. nanhaiensis* | 0.1277 | 0.1171 | 0.1255 | **0.0037** | 0.0507 (0.0476) | 0.1308 (0.1244) |
| *T. gangeticus* | 0.1251 | 0.1156 | 0.1093 | 0.0750 | **0.0090** | 0.1331 (0.1279) |
| *T. brevis* | 0.1600 | 0.1505 | 0.1475 | 0.1282 | 0.1357 | **0.0013** |

## Morphological analyses

After identifying species by morphological characters and phylogenetic analysis, traditional caliper measurements were performed, which produced 14 landmark sites (a–n, Fig. 2). *Trichiurus brevis* could not be identified by these standard morphological characteristics (Table 3), but it is easy to distinguish from *T. lepturus* complex in the anal opening positioned vertically at the 34$^{th}$ and 35$^{th}$ dorsal fin rays. Thus, our morphological comparison is mainly concentrated in the *T. lepturus* complex (Table 3, Fig. 5). Our study compared many numerical values based on the external morphology of various body ratios (more than 20 counts, Suppl. material 1: Fig. S2). Our study found

**Table 3.** Summary statistics of body measurements for four *Trichiurus* species.

| | Mean ± S.D. | | | |
|---|---|---|---|---|
| **Measurement (cm)** | ***T. japonicus*** | ***T. lepturus*** | ***T. nanhaiensis*** | ***T. brevis*** |
| Total length [D(i,n)*] | 74.7 ± 12.8 | 79.8 ± 6.2 | 55.6 ± 9.2 | 50.6 ± 7.3 |
| D(i,m) | 23.7 ± 0.6 | 30.5 ± 0.2 | 20.5 ± 0.2 | 28.0 ± 0.3 |
| D(i,l) | 8.7 ± 2.6 | 11.4 ± 1.0 | 7.8 ± 0.8 | 6.4 ± 1.2 |
| D(m,n) | 50.8 ± 10.5 | 49.7 ± 5.0 | 35.5 ± 5.2 | 32.8 ± 4.6 |
| D(i,j) | 3.0 ± 1.1 | 3.8 ± 0.5 | 2.6 ± 0.3 | 2.2 ± 0.4 |
| D(j,k) | 1.3 ± 0.4 | 1.9 ± 0.1 | 1.1 ± 0.2 | 1.0 ± 0.1 |
| D(k,l) | 4.4 ± 1.0 | 5.7 ± 0.5 | 4.1 ± 0.4 | 3.3 ± 0.6 |
| D(a,b) | 5.2 ± 1.6 | 5.6 ± 0.7 | 5.3 ± 0.5 | 3.9 ± 1.0 |
| D(a,c) | 8.3 ± 1.8 | 11.0 ± 1.0 | 7.4 ± 0.9 | 6.1 ± 1.0 |
| D(a,d) | 6.0 ± 2.0 | 8.1 ± 0.7 | 5.9 ± 0.7 | 4.4 ± 0.7 |
| D(b,c) | 3.9 ± 1.5 | 5.8 ± 0.6 | 2.8 ± 0.4 | 2.5 ± 0.7 |
| D(b,d) | 3.9 ± 1.2 | 5.1 ± 0.5 | 4.0 ± 0.3 | 3.3 ± 0.5 |
| D(b,e) | 28.6 ± 4.8 | 24.5 ± 2.2 | 17.4 ± 1.1 | 13.8 ± 2.8 |
| D(b,f) | 19.2 ± 5.0 | 25.1 ± 1.7 | 18.2 ± 1.3 | 14.4 ± 3.0 |
| D(c,d) | 3.9 ± 0.8 | 4.6 ± 0.5 | 3.4 ± 0.5 | 3.1 ± 0.5 |
| D(d,e) | 18.2 ± 4.6 | 23.1 ± 1.9 | 17.5 ± 1.3 | 14.2 ± 2.6 |
| D(d,f) | 17.9 ± 5.8 | 22.7 ± 1.8 | 17.0 ± 1.4 | 13.9 ± 2.6 |
| D(d,o) | 3.8 ± 0.3 | 4.1 ± 0.2 | 4.1 ± 0.2 | 3.3 ± 0.3 |
| D(e,f) | 4.2 ± 0.1 | 4.8 ± 0.5 | 4.7 ± 0.4 | 3.6 ± 0.6 |
| D(g,h) | 1.3 ± 0.4 | 1.7 ± 0.3 | 1.0 ± 0.2 | 0.9 ± 0.1 |
| D(i,n)/D(i,m) | 3.08 ± 0.32 | 2.61 ± 0.09 | 2.74 ± 0.18 | 2.86 ± 0.11 |
| D(m,n)/D(i,m) | 2.08 ± 0.32 | 1.62 ± 0.09 | 1.74 ± 0.18 | 1.86 ± 0.11 |
| D(i,m)/D(e,f) | 5.59 ± 0.57 | 6.29 ± 0.45 | 4.47 ± 0.79 | 4.91 ± 0.43 |
| D(m,n)/D(e,f) | 11.60 ± 1.79 | 10.29 ± 0.87 | 7.77 ± 1.38 | 9.13 ± 0.69 |
| D(i,l)/D(d,o) | 2.22 ± 0.14 | 2.73 ± 0.13 | 1.92 ± 0.18 | 2.55 ± 0.13 |
| D(d,o)/D(g,h) | 3.10 ± 0.42 | 2.42 ± 0.36 | 3.88 ± 0.67 | 3.57 ± 0.56 |
| D(d,o)/D(j,k) | 3.00 ± 0.42 | 2.20 ± 0.32 | 3.57 ± 0.44 | 3.31 ± 0.41 |
| Sample size | 75 | 27 | 27 | 96 |

* D(i,n), distance between landmarks i and n in Fig. 2.

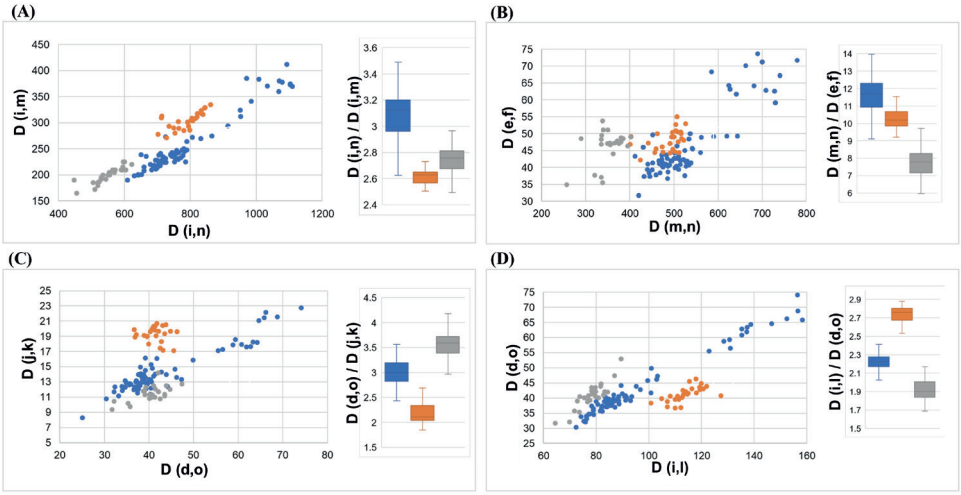


**Figure 5.** The simple regression and the boxplot analysis in *T. japonicus* (blue), *T. lepturus* (orange) and *T. nanhaiensis* (grey) **A** Total length [D(i,n)] and Preanal length [D(i,m)] **B** Caudal length [D(m,n)] and Body depth at anus [D(e,f)] **C** Head depth [D(d,o)] and Orbital length [D(j,k)] and **D** Head length [D(i,l)] and Head depth [D(d,o)]. The landmarks are illustrated in Fig. 2.

that the caudal length is longer in *T. japonicus* [D(i,n/i,m) = 3.08 ± 0.32, 2.61 ± 0.09 and 2.74 ± 0.18 in *T. japonicus*, *T. lepturus*, and *T. nanhaiensis*; Table3, Fig. 5A]; the body depth at the anus is wider in *T. nanhaiensis* [D(m,n/e,f) = 11.60 ± 1.79, 10.29 ± 0.87 and 7.77 ± 1.38 in *T. japonicus*, *T. lepturus*, and *T. nanhaiensis*; Table 3, Fig. 5B]; the orbital length is larger in *T. lepturus* [D(d,o/j,k) = 3.00 ± 0.42, 2.20 ± 0.32 and 3.57 ± 0.44 in *T. japonicus*, *T. lepturus*, and *T. nanhaiensis*; Table 3, Fig. 5C]; and the head is slenderer in *T. lepturus* [D(i,l/d,o) = 2.22 ± 0.14, 2.73 ± 0.13 and 1.92 ± 0.18 in *T. japonicus*, *T. lepturus* and *T. nanhaiensis*; Table 3, Fig. 5D].

## Genome organization, base composition and rates

The mitogenomes of all four *Trichiurus* species contain 36 mitochondrial genes (13 PCGs, 21 tRNA-coding genes and 2 rRNA-coding genes) and two noncoding regions (OL and d-loop, control region) (Table 4). One of the 13 PCGs (ND6), seven tRNA-coding genes (Gln, Ala, Asn, Cys, Tyr, Ser, Glu), and one noncoding region (OL) are encoded on the L-strand, and the other 28 genes (12 PCGs, 14 tRNA-coding genes, and 2 rRNA-coding genes) and d-loop are encoded on the H-strand. The composition and arrangement of the mitochondrial genes in these four species were the same as those in *T. gangeticus* in the Indian Ocean (MK333401 in Mukundan et al. 2020). To characterize variation among the *Trichiurus* mitogenomes, we analyzed the base composition of *T. gangeticus* in the Indian Ocean (Mukundan et al. 2020). We found the mean AT nucleotide content of the five complete mitogenomes to be similar (55.0% in *T. japonicus*, 55.1% in *T. lepturus*, 54.4% in *T. nanhaiensis*, 54.3% in *T. gangeticus* and

**Table 4.** Characteristics of the four newly determined *Trichiurus* mitogenomes.

| Gene | Position | | Codons | | | | Intergenic nucleotides |
|---|---|---|---|---|---|---|---|
| | From | To | Start | Stop | anticodon | Strand | |
| $tRNA^{Phe}$ | 1/1/1/1 | 69/69/69/70 | | | GAA | H | 0/0/0/-1 |
| 12S rRNA | 70/70/70/70 | 1027/1027/1026/1028 | | | | H | 0/0/0/0 |
| $tRNA^{Val}$ | 1028/1028/1027/1029 | 1098/1098/1097/1099 | | | TAC | H | 0/0/0/0 |
| 16S rRNA | 1099/1099/1098/1100 | 2836/2840/2824/2830 | | | | H | 0/0/0/0 |
| $tRNA^{Leu}$ | 2837/2841/2825/2831 | 2910/2914/2898/2904 | | | TAA | H | 0/0/0/0 |
| ND1 | 2921/2923/2910/2916 | 3899/3894/3884/3890 | TTA | TAA | | H | 10/9/11/11 |
| $tRNA^{Ile}$ | 3900/3900/3890/3895 | 3969/3969/3959/3965 | | | GAT | H | 0/5/5/5 |
| $tRNA^{Gln}$ | 3968/3969/3959/3965 | 4038/4039/4029/4035 | | | TTG | L | -2/-1/-1/-1 |
| $tRNA^{Met}$ | 4038/4039/4029/4035 | 4108/4109/4099/4105 | | | CAT | H | -1/-1/-1/-1 |
| ND2 | 4110/4111/4101/4107 | 5156/5157/5147/5153 | ATG | TAA | | H | 1/1/1/1 |
| $tRNA^{Trp}$ | 5156/5157/5147/5153 | 5228/5229/5220/5226 | | | TCA | H | -1/-1/-1/-1 |
| $tRNA^{Ala}$ | 5229/5231/5222/5229 | 5297/5299/5290/5297 | | | TGC | L | 0/1/1/2 |
| $tRNA^{Asn}$ | 5299/5301/5292/5299 | 5371/5373/5364/5371 | | | GTT | L | 1/1/1/1 |
| $O_L$ | 5374/5376/5367/5374 | 5403/5405/5396/5403 | | | | L | 2/2/2/2 |
| $tRNA^{Cys}$ | 5403/5405/5396/5403 | 5468/5470/5461/5468 | | | GCA | L | -1/-1/-1/-1 |
| $tRNA^{Tyr}$ | 5469/5471/5462/5469 | 5535/5537/5528/5535 | | | GTA | L | 0/0/0/0 |
| COI | 5537/5539/5530/5537 | 7087/7089/7080/7087 | GTG | TAA | | H | 1/1/1/1 |
| $tRNA^{Ser}$ | 7088/7090/7081/7088 | 7158/7160/7151/7158 | | | TGA | L | 0/0/0/0 |
| $tRNA^{Asp}$ | 7162/7164/7154/7162 | 7234/7236/7226/7230 | | | GTC | H | 3/3/2/3 |
| COII | 7236/7240/7229/7235 | 7926/7930/7919/7925 | ATG | TAA | | H | 1/3/2/4 |
| $tRNA^{Lys}$ | 7927/7931/7920/7926 | 7998/8003/7992/7998 | | | TTT | H | 0/0/0/0 |
| ATP8 | 7999/8005/7995/8000 | 8166/8172/8162/8167 | ATG | TAA | | H | 0/1/2/1 |
| ATP6 | 8157/8163/8153/8158 | 8840/8846/8836/8841 | ATG | TAA | | H | -10/-10/-10/-10 |
| COIII | 8840/8846/8836/8841 | 9625/9631/9621/9626 | ATG | TAA | | H | -1/-1/-1/-1 |
| $tRNA^{Gly}$ | 9625/9631/9621/9626 | 9693/9699/9689/9694 | | | TCC | H | -1/-1/-1/-1 |
| ND3 | 9694/9700/9690/9695 | 10044/10050/10040/10045 | ATT | TAA | | H | 0/0/0/0 |
| $tRNA^{Arg}$ | 10043/10049/10039/10044 | 10111/10117/10107/10112 | | | TCG | H | -2/-2/-2/-2 |
| ND4L | 10112/10118/10108/10113 | 10408/10414/10404/10409 | ATG | TAA | | H | 0/0/0/0 |
| ND4 | 10402/10408/10398/10403 | 11772/11778/11768/11773 | ATG | AGA | | H | -7/-7/-7/-7 |
| $tRNA^{His}$ | 11781/11787/11776/11781 | 11849/11856/11844/11849 | | | GTG | H | 8/8/7/8 |
| $tRNA^{Ser}$ | 11850/11857/11845/11850 | 11920/11927/11915/11920 | | | GCT | H | 0/0/0/0 |
| $tRNA^{Leu}$ | 11923/11930/11918/11923 | 11994/12001/11989/11994 | | | TAG | H | 2/2/2/2 |
| ND5 | 11997/12004/11992/11997 | 13877/13884/13872/13877 | ATG | TAA | | H | 2/2/2/2 |
| ND6 | 13874/13881/13869/13874 | 14395/14402/14390/14395 | ATG | TAG | | L | -4/-4/-4/-4 |
| $tRNA^{Glu}$ | 14396/14403/14391/14396 | 14464/14471/14459/14464 | | | TTC | L | 0/0/0/0 |
| Cyt b | 14469/14476/14464/14469 | 15609/15616/15604/15609 | ATG | TAA | | H | 4/4/4/4 |
| $tRNA^{Thr}$ | 15610/15617/15605/15610 | 15683/15692/15678/15683 | | | TGT | H | 0/0/0/0 |
| d-loop | 15684/15693/15679/15684 | 16685/16568/16801/16733 | | | | H | |

54.6% in *T. brevis*; Table 5). All mitogenomes had high A + T content: 54.3%–55.1% (53.3%–54.1% for PCGs, 54.5%–56.9% for light tRNA genes, 53.4%–54.5% for heavy tRNA genes, 52.3%–52.6% for rRNA genes, and 63.5%–67.1% for d-loop). The overall AT skews in the five entire mitogenomes were 0.06006, 0.04465, 0.05775, 0.04891 and 0.06789, and the overall GC skews were -0.17695, -0.17258, -0.18480, -0.18396 and -0.19633 (Table 5).

The total lengths of PCGs in the five *Trichiurus* species ranged from 11.530 to 11538 bp, accounting for 68.47%–69.59% of the entire mitogenome. The mitogenomes could be translated into 3.809–3.810 amino acid-coding codons, excluding

stop codons. ND5 and ATP8 were the largest and smallest genes, respectively. The majority of PCGs start with an NTN (ATG/GTG/ATT) start codon and are terminated with the stop codons TAA, TAG, and AGA (Table 4). Most of the AT skew and GC skew values of the PCGs in the five species were negative, indicating that the bases T and C were more plentiful than A and G (Table 5). Moreover, the A + T content and AT skew differed among PCGs (Suppl. material 1: Table S2, Fig. 6). The AT skew values of five genes (ND2, COII, ATP8, ND4 and ND5) were positive, and those of other genes were negative. The GC skew value was positive only for ND6.

To better understand the role of selection in the evolution of the PCGs, the Ka/Ks value of each PCG was calculated (Fig. 7A). All the PCGs, excluding ND6, showed signatures of purifying selection (Ka/Ks < 1). The ND6 and ATP8 genes had the highest Ka/Ks values (1.18 and 0.13), and the COI and cyt b genes had the lowest Ka/Ks values (0.04). A lower Ka/Ks value indicates less variation in amino acids. For the ND6 gene, the highest Ka/Ks value was observed between *T. nanhaiensis* and *T. gangeticus* (Fig. 7B). For the ATP8 gene, the highest Ka/Ks value was observed between *T. brevis* and other *Trichiurus* species (Fig. 7C). Summaries of the relative synonymous codon usage and number of amino acids in the annotated PCGs are presented in Figs 8, 9 and Suppl. material 1: Table S3. Overall codon usage among the sequenced *Trichiurus* mitogenomes was similar; Leu, Ala, Thr, Ile, and Ser were the five most common amino acids.

The lengths of 16S rRNA genes ranged from 1.725 (*T. gangeticus*) to 1.742 (*T. lepturus*), whereas those of 12S rRNAs ranged from 957 (*T. gangeticus* and *T. nanhaiensis*) to 959 (*T. brevius*). These rRNA genes are located between $tRNA^{Phe}$ and $tRNA^{Leu}$ and are separated by $tRNA^{Val}$. The AT content of the rRNA genes ranged from 52.3% to 52.6% (Table 5). The total lengths of the 21 tRNA genes ranged from 1.483 (*T.*

**Table 5.** Nucleotide compositions of *T. japonicus*, *T. lepturus*, *T. nanhaiensis*, *T. brevis*, and *T. gangeticus*.

| | | Whole genome | Protein-coding genes | Light tRNAs[1] | Heavy tRNAs[2] | 2 rRNA | d-loop |
|---|---|---|---|---|---|---|---|
| AT% | *T. japonicus* | 55.0 | 53.4 | 56.9 | 53.4 | 52.4 | 66.3 |
| | *T. lepturus* | 55.1 | 54.0 | 56.4 | 54.1 | 52.3 | 64.4 |
| | *T. nanhaiensis* | 54.4 | 53.3 | 55.0 | 54.1 | 52.5 | 66.7 |
| | *T. gangeticus*[3] | 54.3 | 53.5 | 54.5 | 54.5 | 52.3 | 67.1 |
| | *T. brevis* | 54.6 | 54.1 | 55.3 | 53.5 | 52.6 | 63.5 |
| AT-skew | *T. japonicus* | 0.06006 | -0.05230 | 0.11991 | 0.11993 | 0.20156 | 0.04072 |
| | *T. lepturus* | 0.04465 | -0.06827 | 0.09293 | 0.11745 | 0.21332 | 0.00621 |
| | *T. nanhaiensis* | 0.05775 | -0.05444 | 0.11080 | 0.11620 | 0.21268 | -0.01349 |
| | *T. gangeticus*[3] | 0.04891 | -0.05679 | 0.10329 | 0.10850 | 0.21337 | -0.03428 |
| | *T. brevis* | 0.06789 | -0.04365 | 0.11892 | 0.13515 | 0.23956 | 0.02992 |
| GC-skew | *T. japonicus* | -0.17695 | -0.29641 | -0.05917 | -0.20854 | -0.16176 | -0.11573 |
| | *T. lepturus* | -0.17258 | -0.29303 | -0.03277 | -0.23999 | -0.15737 | -0.15169 |
| | *T. nanhaiensis* | -0.18480 | -0.30426 | -0.04978 | -0.25498 | -0.17127 | -0.09910 |
| | *T. gangeticus*[3] | -0.18396 | -0.30589 | -0.05000 | -0.23819 | -0.16780 | -0.11246 |
| | *T. brevis* | -0.19633 | -0.30975 | -0.07410 | -0.24391 | -0.19198 | -0.16164 |

AT% = [A+T]/[A+T+G+C], AT-skew = [A-T]/[A+T], GC-skew = [G-C]/[G+C].

[1] Light tRNAs are those transcribed from the heavy strand mitochondrial DNA, including Phe, Val, Leu, Ile, Met, Trp, Asp, Lys, Gly, Arg, His, Leu, Thr.

[2] Heavy tRNAs are those transcribed from the light strand, including Gln, Ala, Asn, Cys, Tyr, Ser, Glu.

[3] MK333401 in Mukundan et al. 2020.

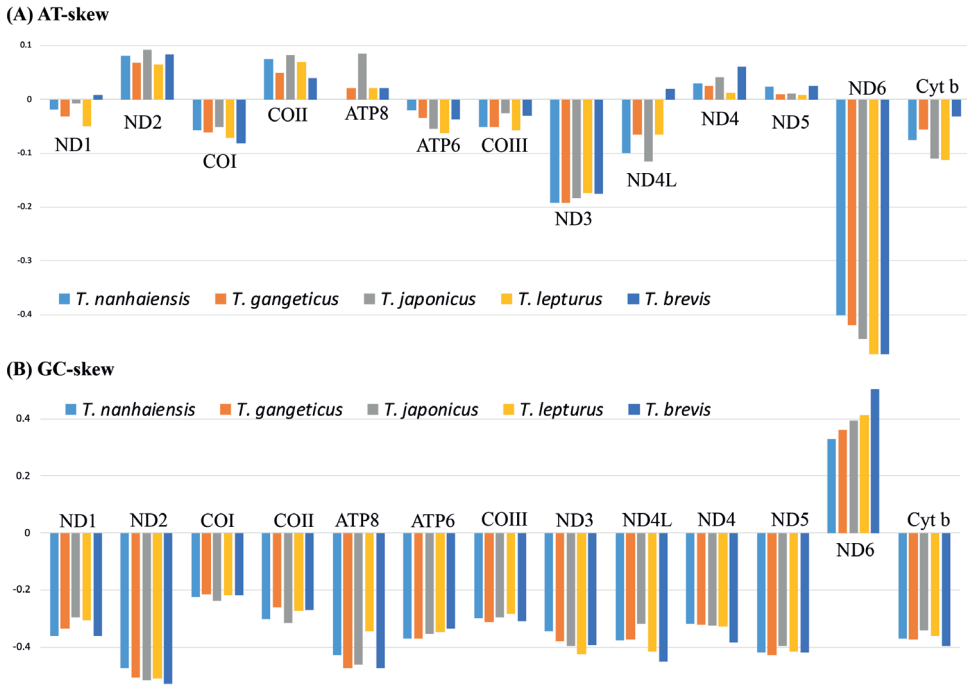


**Figure 6. A** AT-skew in 13genes. **B** GC-skew in in 13 genes.

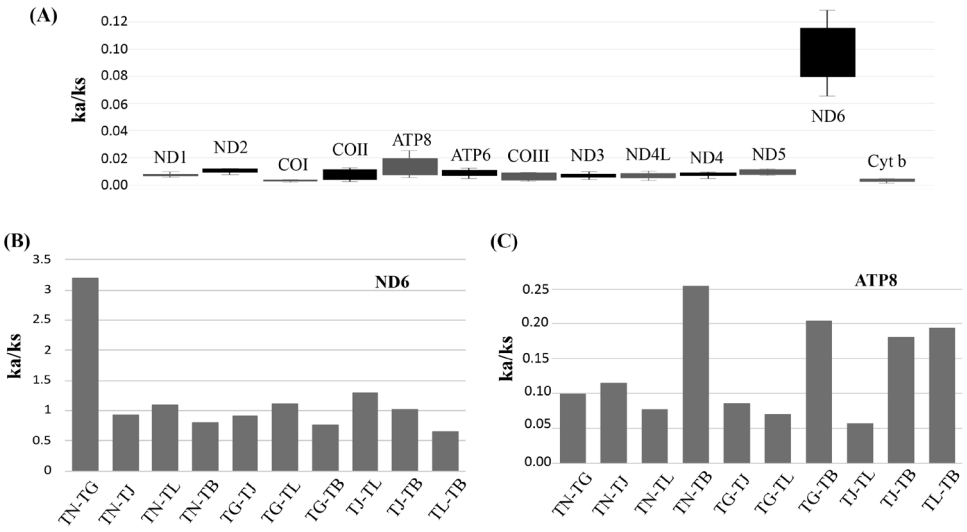


**Figure 7. A** Mean evolutionary rates for each protein coding gene in mitogenomes of five *Trichiurus* species **B** Evolutionary rates of ND6 gene of five *Trichiurus* species. **C** Evolutionary rates of Ka/Ks in ATP8 gene of five *Trichiurus* species. Indicated the rates of non-synonymous substitutions to the rate of synonymous substitutions (ka/ks). *T. japonicus* (TJ), *T. lepturus* (TL), *T. nanhaiensis* (TN), *T. gangeticus* (TG) and *T. brevis* (TB).

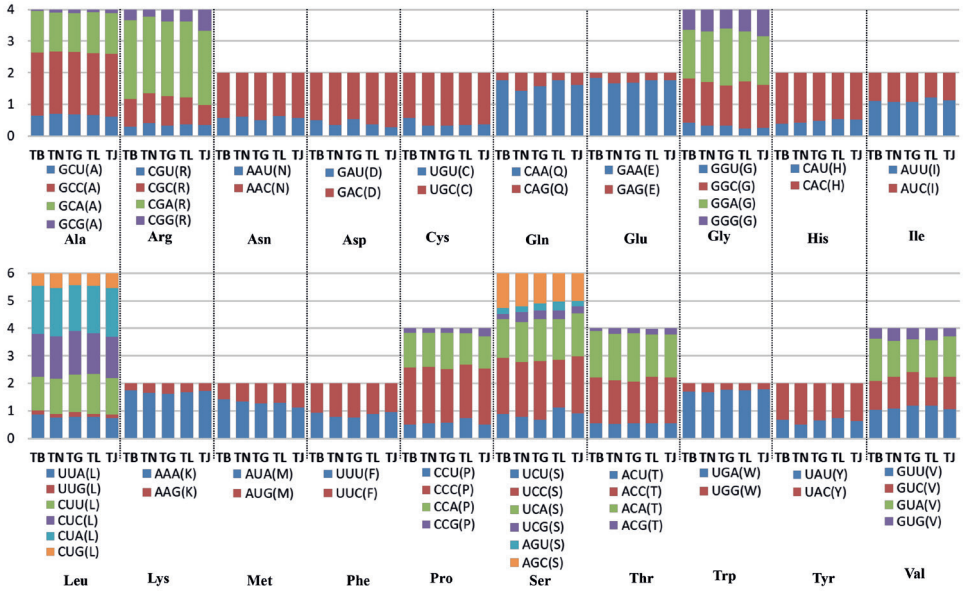


**Figure 8.** Relative synonymous codon usage (RSCU) of the mitogenomes of the five *Trichiurus* species; the stop codon is not included. *T. japonicus* (TJ), *T. lepturus* (TL), *T. nanhaiensis* (TN), *T. gangeticus* (TG) and *T. brevis* (TB).

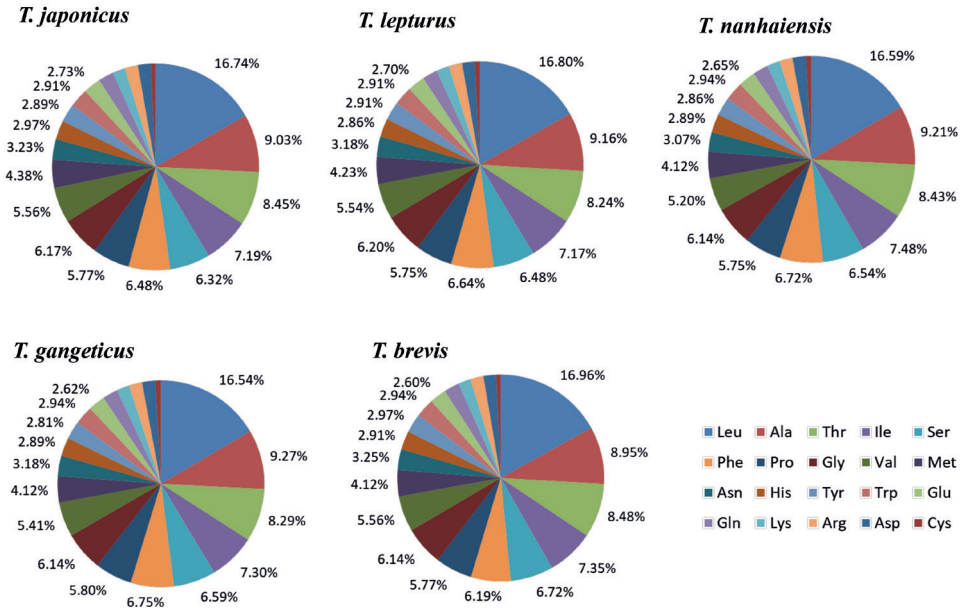


**Figure 9.** Frequencies of different amino acids in the mitogenomes of the five *Trichiurus* species; the stop codon is not included.

*japonicus* and *T. brevis*) to 1.487 bp (*T. lepturus*), and individual tRNA genes typically ranged in size from 66 to 76 bp. No sequence similarity to the $tRNA^{Pro}$ gene was observed elsewhere in the mitogenome. The d-loop in *Trichiurus* mitogenomes is located between $tRNA^{Phe}$ and $tRNA^{Thr}$. The A + T content (63.5%–67.1%) of the d-loop was higher than that of the whole genome (54.3%–55.1%), rRNA-coding genes (52.3%–52.6%), and tRNA-coding genes (54.4%–55.2%) (Table 5). Furthermore, compositional analysis revealed that the mitogenome of *T. nanhaiensis* and *T. gangeticus* had a negative AT skew (-0.01349 and -0.03428) in the d-loop.

## Molecular tool

To determine molecular markers that could be used to examine the phylogeny and identify species, the overall interspecific and intergeneric p-distance was used to describe the evolutionary rate of two rRNA-coding genes, 13 PCGs and the mitogenome, excluding the d-loop region (Fig. 10, Table 6, Suppl. material 1: Table S4). The maximum interspecific p-distance (mean = 0.189, range = 0.073-0.241) was observed for the ND6 gene, and the maximum intergeneric p-distance (mean = 0.369, range = 0.257-0.470) was observed for the ATP8 gene. Among these 16 markers, 9 markers (e.g., 12S rRNA, ATP6 and ND1 genes) displayed overlapping interspecific and intergeneric p-distances (Fig. 10). Among the four genes in the oxidase family, only COII showed overlap between interspecific and intergeneric p-distances. Furthermore, the range of pairwise interspecific p-distances among five *Trichiurus* species based on the 16S rRNA and cyt b genes ranged from 0.015 (between *T. gangeticus* and *T. nanhaiensis*) to 0.077 (between *T. lepturus* and *T. brevis*) and from 0.072 (between *T. gangeticus* and *T. nanhaiensis*) to 0.143 (between *T. nanhaiensis* and *T. brevis*) (Table 6). In addition, our study found that the 16S rRNA genetic distances between *T. brevis* (short-tailed species complex) and other *Trichiurus* species (*T. lepturus* complex or large-head species complex) were not higher than those within the *T. lepturus* complex (Table 6). The results based on cyt b and 16S rRNA differed.

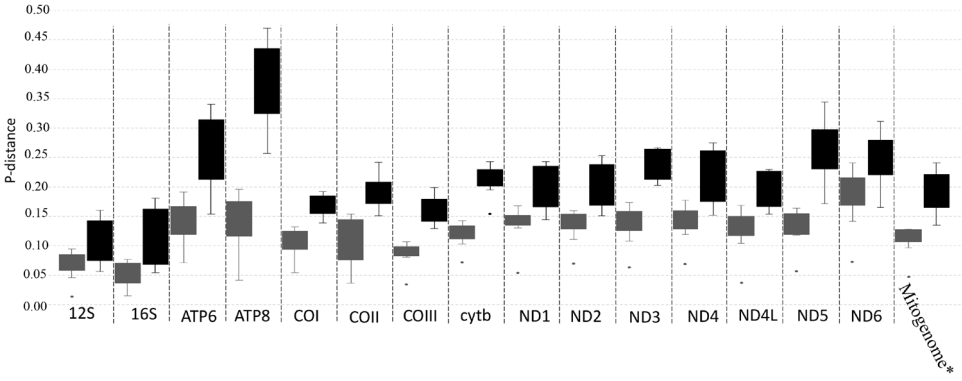


**Figure 10.** The mean partwise interspecific (gray) and intergeneric (black) p-distance in each gene.

**Table 6.** The p-distance ($*10^{-2}$) between *Trichiurus* species (interspecific) and between genera within Trichiuridae (intergeneric) in each gene and mitogenome (excluding d-loop). *T. japonicus* (TJ), *Trichiurus lepturus* (TL), *Trichiurus nanhaiensis* (TN), *T. gangeticus* (TG), *Trichiurus brevis* (TB), *Trichiurus* (T), *Benthodesmus* (B), *Aphanopus* (C), *Evoxymetopon* (E), and *Assurger* (A).

| | 12S | 16S | atp6 | atp8 | COI | COII | COIII | cytb | ND1 | ND2 | ND3 | ND4 | ND4L | ND5 | ND6 | genome |
|---|---|---|---|---|---|---|---|---|---|---|---|---|---|---|---|---|
| TG/TB | 9.4 | 3.9 | 17.0 | 17.3 | 12.4 | 14.6 | 8.3 | 14.1 | 13.6 | 15.0 | 15.5 | 17.7 | 13.8 | 16.4 | 23.0 | 12.8 |
| TG/TJ | 6.2 | 6.2 | 12.4 | 11.9 | 10.5 | 8.8 | 8.0 | 11.4 | 14.3 | 14.5 | 13.2 | 14.6 | 12.8 | 13.0 | 20.3 | 11.1 |
| TG/TL | 6.5 | 6.6 | 14.5 | 13.1 | 9.4 | 7.7 | 8.4 | 12.6 | 14.9 | 14.8 | 14.6 | 14.0 | 12.1 | 11.8 | 20.7 | 11.1 |
| TG/TN | 1.4 | 1.5 | 7.2 | 4.2 | 5.4 | 3.6 | 3.4 | 7.2 | 5.4 | 7.0 | 6.3 | 6.9 | 3.7 | 5.7 | 7.3 | 4.8 |
| TB/TJ | 7.6 | 7.4 | 14.8 | 15.5 | 13.2 | 13.9 | 10.3 | 13.2 | 16.8 | 14.9 | 16.5 | 15.7 | 16.8 | 15.3 | 17.8 | 12.8 |
| TB/TL | 8.3 | 7.7 | 19.2 | 19.6 | 12.8 | 15.3 | 10.7 | 13.2 | 15.7 | 15.6 | 15.1 | 15.2 | 14.8 | 14.1 | 19.7 | 12.9 |
| TB/TN | 9.4 | 2.8 | 16.7 | 18.5 | 11.5 | 14.3 | 9.5 | 14.3 | 13.0 | 13.5 | 17.4 | 16.8 | 15.5 | 16.1 | 24.1 | 12.4 |
| TJ/TL | 4.6 | 4.9 | 12.1 | 10.7 | 9.4 | 9.0 | 9.7 | 10.3 | 15.1 | 11.1 | 10.8 | 12.0 | 10.4 | 12.2 | 14.2 | 9.7 |
| TJ/TN | 6.4 | 6.4 | 11.1 | 13.1 | 9.7 | 8.3 | 8.9 | 11.9 | 14.3 | 16.0 | 14.5 | 13.9 | 14.8 | 13.7 | 21.1 | 11.3 |
| TL/TN | 6.5 | 6.9 | 14.5 | 15.5 | 9.6 | 7.5 | 9.4 | 12.5 | 14.7 | 15.3 | 15.7 | 13.1 | 13.5 | 11.9 | 20.9 | 11.2 |
| T/B | 16.0 | 18.1 | 34.0 | 47.0 | 19. | 24.2 | 19.9 | 22.6 | 23.3 | 25.3 | 26.6 | 26.6 | 22.6 | 34.4 | 31.1 | 24.1 |
| T/C | 15.2 | 17.0 | 31.4 | 43.3 | 18.9 | 22.1 | 18.9 | 24.3 | 23.5 | 23.6 | 26.5 | 25.3 | 23.0 | 31.7 | 30.0 | 22.9 |
| T/E | 14.0 | 15.4 | 30.7 | 40.6 | 17.5 | 20.4 | 16.3 | 20.4 | 24.3 | 23.8 | 25.2 | 26.0 | 23.0 | 28.8 | 27.3 | 21.5 |
| T/A | 14.0 | 16.0 | 31.5 | 44.3 | 18.3 | 20.4 | 17.6 | 21.2 | 23.5 | 24.0 | 23.1 | 27.5 | 22.3 | 29.1 | 26.9 | 21.9 |
| B/C | 7.6 | 7.0 | 21.6 | 26.3 | 13.9 | 17.1 | 12.9 | 19.5 | 14.4 | 15.2 | 21.5 | 15.2 | 15.4 | 28.7 | 19.3 | 16.1 |
| B/E | 9.7 | 9.1 | 25.1 | 35.7 | 17.0 | 19.9 | 16.8 | 20.9 | 16.9 | 19.6 | 22.6 | 17.7 | 17.1 | 26.4 | 24.3 | 18.2 |
| B/A | 11.6 | 10.1 | 24.9 | 37.4 | 16.4 | 20.3 | 15.9 | 20.7 | 17.5 | 18.5 | 26.4 | 20.2 | 19.1 | 27.9 | 25.5 | 18.9 |
| C/E | 7.2 | 6.5 | 20.2 | 34.5 | 16.4 | 18.2 | 14.4 | 22.2 | 16.7 | 17.7 | 21.8 | 17.0 | 18.1 | 22.4 | 23.0 | 16.7 |
| C/A | 7.7 | 7.3 | 21.8 | 34.5 | 15.9 | 17.2 | 15.3 | 24.2 | 17.5 | 17.4 | 20.6 | 19.5 | 18.8 | 23.3 | 23.4 | 17.0 |
| E/A | 5.6 | 5.4 | 15.4 | 25.7 | 14.2 | 15.1 | 13.5 | 15.4 | 16.2 | 15.1 | 20.3 | 17.9 | 15.4 | 17.2 | 16.5 | 13.5 |

## Discussion

### Mitogenomic features of *Trichiurus* species

The mitogenomes of *Trichiurus* species encode 36 typical mitochondrial genes (13 protein-coding, 2 ribosomal RNA-coding genes, and 21 transfer RNA-coding genes) and two typical noncoding control regions, the d-loop and origin of the light strand (OL) (Table 4). Overall, the mitogenomes of four *Trichiurus* species in the present study have a gene order and composition similar to other *Trichiurus* mitogenomes in previous studies (e.g., Liu and Cui 2009; Liu et al. 2013; Zheng et al. 2019; Mukundan et al. 2020). The gene order of the mitogenomes in Trichiuridae was similar to that in most teleosts, although different types of gene rearrangements were observed within Pleuronectiformes (Gong et al. 2015) and Stomiiformes (Arrondo et al. 2020).

In addition, our study found that the $tRNA^{Pro}$ gene was absent in the *Trichiurus* mitogenomes. Previous studies of the complete mitogenomes of *Trichiurus* species have also obtained similar findings (e.g., Liu and Cui 2009; Liu et al. 2013; Zheng et al. 2019; Mukundan et al. 2020). Our data indicate that this event only occurred in the genus *Trichiurus* and not in other teleosts. Adams and Palmer (2003) proposed that the mitochondrial gene content is highly variable across eukaryotes. However, most previous studies have been conducted on plants (Adams et al. 2001; Adams and Palmer 2003). In addition, the loss of genes in vertebrate mitogenomes is rare. In teleosts, loss of the ND6 gene was observed only in Antarctic fish mitogenomes (Papetti et al. 2007), and no cases of tRNA gene loss were observed.

## Molecular tool assessment

Because the systematics of many species remain unresolved, many studies have employed molecular, phylogenetics and DNA barcoding approaches (e.g., Hebert et al. 2003; Hsu et al. 2009; Han et al. 2019). Among all molecular markers, the mtDNA COI and cyt b genes have been the most frequently used (Yang et al. 2016; Han et al. 2019; Hsu et al. 2020; Ju et al. 2021). In addition, some studies have used mtDNA rRNA (12S and 16S) sequences to resolve phylogenetic relationships and taxonomy (Byrne et al. 2010; Herler et al. 2013; Zheng et al. 2016). However, the results of pairwise p-distances based on 16S rRNA and cyt b genes differed in this study (Table 6). These results, coupled with the results of the Ka/Ks analyses (Fig. 7), suggested that the evolutionary rates of these genes differed. Our study indicated that overlap between the interspecific and intergeneric distances might affect phylogenetic reconstruction and molecular species identification. For example, the intergeneric 12S rRNA p-distance between *Evoxymetopon* and *Assurger* was 0.056, which is smaller than the interspecific 12S rRNA p-distance of *Trichiurus* (Table 6, Fig. 10). Thus, some genes that were used to resolve the phylogeny and identify species should be evaluated. Actually, this question has been intensively discussed, and has been applied to mitochondrial genes (i.e., Zardoya and Meyer 1996; Miya and Nishida 2000). However, some studies ignored this question (our observations).

Moreover, variation in the Ka/Ks values was greater for ATP8 than for other genes (Fig. 7), and the length of ATP8 (approximately 168 bp) was shorter. Thus, our study suggested that only COI, COIII, cyt b, ND5 and mitogenome (excluding d-loop) sequences could be used to identify *Trichiurus* species and examine the phylogeny of Trichiuridae. However, these genes may also display a limited ability to identify complex evolutionary relationships in many fishes (Mirande 2018). For example, the Ka/Ks values of the COI and cyt b genes were the lowest (0.04). Lower Ka/Ks values indicate less variation in amino acids (Brookfiel 2000; Li et al. 2020; Sun et al. 2021). Therefore, an increasing number of studies have used complete mitogenome data to resolve animal phylogenies and identify species because they provide more information (Ajene et al. 2020; González-Castellano et al. 2020; Irisarri et al. 2020); the results of our study support this hypothesis.

## Systematics of *Trichiurus*

The taxonomy of the genus *Trichiurus* remains unresolved because of the high degree of morphological similarity within the genus in terms of bodily appearance and silvery coloration. Our study also showed that identifying *Trichiurus* species by morphological characters is very difficult (Fig. 5, Table 3). Phylogenetic analyses based on the complete mitogenome (Fig. 3) and COI gene (Fig. 4) showed that *T. haumela* was clustered with *T. japonicus*. Moreover, *T. japonicus* is synonymous with *T. lepturus* in FishBase (Froese and Pauly 2021), but the present results (Figs 3, 4; Table 2) indicated that *T. haumela* is synonymous with *T. japonicus* and that *T. japonicus* is a valid species (Hsu et al. 2009; Fricke et al. 2021). Moreover, the systematic position of *T. brevis* is still

not resolved in this study because we did not analyze other species of *Trichiurus russelli* complex, and did not provide enough information.

In addition, the results suggested that specimens in the Indian Ocean (MK333401 in Mukundan et al. 2020) are not "*T. lepturus*" (Figs 3, 4; Table 2). In the phylogenetic tree based on COI (Fig. 4), MK333401 was grouped with other specimens in the Indian Ocean as lineage E. Within lineage E, most specimens were identified as "*T. lepturus*", and only MK340737 in Bangladesh was identified as *T. gangeticus*. According to these results, members of lineage E could not be identified as *T. lepturus*; our data suggest that they should be recognized as *T. gangeticus*. Similarly, within lineage B, some specimens were identified as *Trichiurus* sp. (Isari et al. 2017), and some specimens were identified as *T. auriga*. We thus recognized lineage B as *T. auriga* (Fig. 4). Accordingly, our study suggests that the *Trichiurus* specimens in the Indian Ocean are not *T. lepturus* calls into question many previous studies (e.g., Chakraborty et al. 2006a; Jahromi et al. 2016; Mukundan et al. 2020).

Chakraborty et al. (2006a) and Chakraborty and Iwatsuki (2006) found that *T. lepturus* in Indo-Pacific differed from that in Atlantic using 16S rRNA sequences. However, Hsu et al. (2009) identified the specimens of *T. lepturus* in the Indo-Pacific in Chakraborty et al. (2006a) and Chakraborty and Iwatsuki (2006) as "*Trichiurus* sp. 2" (synonym of *T. nanhaiensis*). Jahromi et al. (2016) examined the phylogenetic relationship of *T. lepturus* from the Persian Gulf using 16S rRNA sequences, and suggested homogeneity between Persian Gulf and the other Indo-Pacific individuals. However, Lin et al. (2021) found that the specimens in Jahromi et al. (2016) were identified as *T. japonicus*, *T. lepturus*, and *T. nanhaiensis* and the specimens in the Persian Gulf was nested with *T. nanhaiensis* using 16S rRNA sequences. Besides, Lin et al. (2021) found *T. nanhaiensis* could be divide as two groups, Indo-Pacific and West Indian. The results of our study indicate that *T. gangeticus* was more similar to *T. nanhaiensis* (Fig. 4, Table 2). Thus, our study considers these two groups might be *T. nanhaiensis* and *T. gangeticus*, although we did not collect the COI data of *T. nanhaiensis* in the east Indian Ocean. In addition, our study found some specimens from the Gulf of Oman referred to in Lin et al. (2021) were in fact *T. lepturus*. However, *T. lepturus* had the highest intraspecific diversity (Table 2). Thus, our study suggests that systematics of *T. lepturus* species complex and *T. lepturus* both need to be reviewed.

Bingpeng et al. (2018) used the COI gene to identify fish at the species level in the Taiwan Strait and proposed that the average p-distances within species, genera, families, orders, and classes were 0.0021, 0.0650, 0.2370, and 0.2560, respectively. Our study revealed that the range of COI interspecific distances in *Trichiurus* ranged from 0.0435 to 0.1600, and the intraspecific distance within lineage C (*T. lepturus*) was 0.0333 (Table 2, Fig. 4). These results suggest that there were cryptic species within lineage C. Lineage C could be divided into three sublineages C1–C3 (Fig. 4). Lineage C1 was distributed in the West Pacific Ocean; lineage C2 was distributed in the Northwest Atlantic Ocean; and lineage C3 was distributed in the East Pacific and Southwest Atlantic oceans. The range of the pairwise genetic distances ranged from 0.0308 to 0.0529. Thus, these three sublineages should be recognized as three different species. Within lineage C3, most specimens were identified as *T. lepturus*, but some

specimens (MF957079-MF957087) were identified as *T. nitens*. *Trichiurus nitens* was described in 1899, and it is distributed in the eastern Pacific, from California south to Peru. Nakamura and Parin (1993) considered it synonymous with *T. lepturus*, but some researchers have suggested that it is the real *T. nitens* (Eschmeyer and Herald 1983; Burhanuddin and Parin 2008; Robertson et al. 2017). In addition, *T. margarites* is considered a valid species in FishBase (Froese and Pauly 2021) and ECoF (Fricke et al. 2021). *Trichiurus margarites* is distributed in the South China Sea (Li 1992; Fricke et al. 2021), but this species has not yet been detected along Chinese coastal waters. However, it is possible that the lineage C1 is *T. margarites* (Fig. 4). Thus, our study suggested that the systematics within lineage C require careful evaluation. In future studies, a careful morphological comparative work within lineage C is needed.

### Morphological analyses

Tzeng et al. (2007) analyzed the morphometry from *T. japonicus* and *T. lepturus*, and found that it exhibited high intraspecific variations. Our study also found the same (Fig. 5, Table 3). However, although Tzeng et al. (2007) found a decisive specific gap of non-overlapping scattering using discriminant function analysis, they did not provide a reference key to identify the *Trichiurus* species because it is very difficult. Lee et al. (1977) proposed that *T. japonicus* and *T. lepturus* can been distinguished based on the external morphology of various body ratios. Thus, our study calculated some body ratios (Table 3, Fig. 5) and only found that the ratio between length and depth of head can been used to distinguish *T. lepturus* and other species (Fig. 5D). In *T. lepturus*, the ratio between distance of head length [D(i,l)] and distance of head depth [D(d,o)] was larger than 2.5. Our study also did not find a reference key to distinguish these three species within *T. lepturus* complex; we used the complex indexes to distinguish them. *Trichiurus japonicus* has a longer body and tail (Fig. 5A, B); *T. lepturus* has a shorter tail, longer head, and bigger eye (Fig. 5A, C, D); and *T. nanhaiensis* has a wider tail, smaller eye, and shorter head (Fig. 5B, C, D).

## Conclusions

Accurate species identification is important for fishery purposes. The current study represents the first comparative mitogenomic and phylogenetic analysis within *Trichiurus* and provides new insight into the mitogenomic features and evolution of fishes. Our study suggested that (1) it is difficult to identify species of *T. lepturus* complex by morphology; (2) *T. japonicus* is a valid species; and (3) the specimens in Indian Ocean are neither *T. lepturus* nor *T. nanhaiensis*. Furthermore, Shih et al. (2011) proposed that the von Bertalanffy growth model of three *Trichiurus* species in Taiwanese waters differed. Thus, accurate species identification of *Trichiurus* species for resource management is very important. Our study identified four *Trichiurus* species along the China Sea coasts. The historical records of their distribution were *T. japonicus* in the Northwestern Pacific, China, and Taiwan to Japan, *T. lepturus* in tropical and warm temperate seas, (including Gulf of Mexico, Caribbean Sea, Mediterranean Sea, Sea of

Marmara, Red Sea, Persian Gulf), *T. nanhaiensis* in the West Pacific, and *T. brevis* in the South China Sea (Fricke et al. 2021). Thus, our team wants to sample more specimens in other regions. We hope that our current results can provide more information on the systematics and diversity of *Trichiurus*. Future studies should collect more specimens in the Indian Ocean to re-examine the systematics of *Trichiurus* by mitogenomic, nuclear gene, and morphological data. The results of this study also have implications for the resource management of *Trichiurus* species.

## Acknowledgments

This work was supported by the grants from National Key R&D Program of China (Grant Number: 2018YFD0900905), Southern Marine Science and Engineering Guangdong Laboratory (Zhanjiang), (Grant Number: ZJW-2019-08), Science and Technology Plan Projects of Guangdong Province, China (Grant Number: 2018B030320006), Guangdong Basic and Applied Basic Research Foundation (Grant Number: 2019B1515120064) and Marine Economy Development Special Foundation of Department of Natural Resources of Guangdong Province (Grant Number: GDNRC [2020]052). We are grateful to the anonymous referees for their constructive comments.

## References

Adams KL, Rosenblueth M, Qiu YL, Palmer JD (2001) Multiple losses and transfers to the nucleus of two mitochondrial succinate dehydrogenase genes during angiosperm evolution. Genetics 158: 1289–1300. https://doi.org/10.1093/genetics/158.3.1289

Adams KL, Palmer JD (2003) Evolution of mitochondrial gene content: gene loss and transfer to the nucleus. Molecular Phylogenetics and Evolution 29: 380–395. https://doi.org/10.1016/S1055-7903(03)00194-5

Ahti PA, Coleman RR, DiBattista JD, Berumen ML, Rocha LA, Bowen BW (2016) Phylogeography of Indo-Pacific reef fishes: sister wrasses *Coris gaimard* and *C. cuvieri* in the Red Sea, Indian Ocean and Pacific Ocean. Journal of Biogeography 43: 1103–1115. https://doi.org/10.1111/jbi.12712

Ajene I, Khamis FM, Pietersen G, van Asch B (2020) Mitochondrial genetic variation reveals phylogeographic structure and cryptic diversity in *Trioza erytreae*. Science Reports 10: e8893. https://doi.org/10.1038/s41598-020-65880-7

Arrondo NV, Gomes-dos-Santos A, Marcote ER, Perez M, Froufe E, Castro LFC, (2020) A new gene order in the mitochondrial genome of the deep-sea diaphanous hatchet fish *Sternoptyx diaphana* Hermann, 1781 (Stomiiformes: Sternoptychidae). Mitochondrial DNA B Resource 5: 2859–2861. https://doi.org/10.1080/23802359.2020.1790325

Bingpeng X, Heshan L, Zhilan Z, Chunguang W, Yanguo W, Jianjun W (2018) DNA barcoding for identification of fish species in the Taiwan Strait. PLoS ONE 13: e0198109. https://doi.org/10.1371/journal.pone.0198109

Brookfiel JFY (2000) Evolutionary: what determines the rate of sequence evolution? Current Biology 10: 410–411. https://doi.org/10.1016/S0960-9822(00)00506-6

Burhanuddin AI, Iwatsuki Y, Yoshino T, Kimura S (2002) Small and valid species of *Trichiurus brevis* Wang & You, 1992 and *T. russelli* Dutt & Thankam, 1966, defined as the "*T. russelli* complex" (Perciformes: Trichiuridae). Ichthyological Research 49: 211–223. https://doi.org/10.1007/s102280200030

Burhanuddin AI, Parin NV (2008) Redescription of the trichiurid fish, *Trichiurus nitens* Garman, 1899, being a valid of species distinct from *T. lepturus* Linnaeus, 1758 (Perciformes: Trichiuridae). Journal of Ichthyology 48: 825–830. https://doi.org/10.1134/S0032945208100019

Byrne M, Rowe F, Uthicke S (2010) Molecular taxonomy, phylogeny and evolution in the family Stichopodidae (Aspidochirotida: Holothuroidea) based on COI and 16S mitochondrial DNA. Molecular Phylogenetics and Evolution 56: 1068–1081. https://doi.org/10.1016/j.ympev.2010.04.013

Chakraborty A, Aranishi F, Iwatsuki Y (2006a) Genetic differences of *Trichiurus japonicus* and *T. lepturus* (Perciformes: Trichiuridae) based on mitochondrial DNA analyses. Zoological Studies 45: 419–427. https://doi.org/10.1007/s10228-005-0313-3

Chakraborty A, Aranishi F, Iwatsuki Y (2006b) Genetic differences among three species of the genus *Trichiurus* (Perciformes: Trichiuridae) based on mitochondrial DNA analysis. Ichthyological Research 53: 93–96. https://doi.org/10.1007/s10228-005-0313-3

Chakraborty A, Iwatsuki Y (2006). Genetic variation at the mitochondrial 16S rRNA gene among *Trichiurus lepturus* (Teleostei: Trichiuridae) from various localities: preliminary evidence of a new species from west coast of Africa. Hydrobiologia 563:501–513. https://doi.org/10.1007/s10750-006-0105-4

Conway KW, Ralf B, Jiwan S, Manimekalan A, Rüber L (2015) Molecular systematics of the Asian torrent minnows (Ostariophysi: Psilorhynchidae) inferred from nuclear and mitochondrial DNA sequence data. Journal of Zoological Systematics and Evolutionary Research 53: 33–44. https://doi.org/10.1111/jzs.12090

Darriba D, Taboada GL, Doallo R, Posada D (2012) jModelTest 2: more models, new heuristics and parallel computing. Nature Methods 9: 772–772. https://doi.org/10.1038/nmeth.2109

Eschmeyer WN, Herald ES (1983) A field guide to Pacific Coast fishes of North America from the Gulf of Alaska to Baja California. Peterson Field Guide Series. No. 28. Houghton-Mifflin Co., Boston, 336 pp, pls 1–48.

FAO Fishery Information, Data and Statistics Unit (2004) Capture production 2002, FAO yearbook. Fishery statistics, 94/1. Rome: Food and Agricultural Organisation (FAO).

Froese R, Pauly D (2021) FishBase. World Wide Web electronic publication. www.fishbase.org, version (02/2021).

Fricke, 2008. Authorship, availability and validity of fish names described by Peter (Pehr) Simon Forsskål and Johann Christian Fabricius in the 'Descriptiones animalium' by Carsten Niebuhr in 1775 (Pisces). Stuttgarter Beiträge zur Naturkunde A, Neue Serie 1: 1–76.

Fricke R, Eschmeyer WN, Van der Laan R (2021) Eschmeyer's Catalog of Fishes: genera, species, references. http://researcharchive.calacademy.org/research/ichthyology/catalog/fishcatmain.asp

Golani D, Fricke R (2018) Checklist of the Red Sea fishes with delineation of the Gulf of Suez, Gulf of Aqaba, endemism and Lessepsian migrants. Zootaxa 4509: 1–215. https://doi.org/10.11646/zootaxa.4509.1.1

Gong L, Shi W, Si LZ, Wang ZM, Kong XY (2015) The complete mitochondrial genome of peacock sole *Pardachirus pavoninus* (Pleuronectiformes: Soleidae) and comparative analysis of the control region among 13 soles. Molecular Biology 49: 408–417. https://doi.org/10.1134/S0026893315030061

González-Castellano I, Pons J, González-Ortegón E, Martínez-Lage A (2020) Mitogenome phylogenetics in the genus *Palaemon* (Crustacea: Decapoda) sheds light on species cryptic-ism in the rockpool shrimp *P. elegans*. PLoS One 15: e0237037. https://doi.org/10.1371/journal.pone.0237037

Gu S, Yi MR, He XB, Lin PS, Liu WH, Luo ZS, Lin HD, Yan YR (2021) Genetic diversity and population structure of cutlassfish (*Lepturacanthus savala*) along the coast of mainland China, as inferred by mitochondrial and microsatellite DNA markers. Regional Studies in Marine Science 43: e101702. https://doi.org/10.1016/j.rsma.2021.101702

Hall TA (1999) BioEdit: a user-friendly biological sequence alignment editor and analysis program for Windows 95/98/NT. Nucleic Acids Symposium Series 41: 95–98.

Han CC, Hsu KC, Fang LS, Cheng IM, Lin HD (2019) Geographical and temporal origins of *Neocaridina* species (Decapoda: Caridea: Atyidae) in Taiwan. BMC Genetics 20: e86. https://doi.org/10.1186/s12863-019-0788-y

He L, Zhang A, Weese D, Li S, Li J, Zhang J (2014) Demographic response of cutlassfish (*Trichiurus japonicus* and *T. nanhaiensis*) to fluctuating palaeo-climate and regional oceanographic conditions in the China seas. Science Reports 4: e6380. https://doi.org/10.1038/srep06380

Hebert PDN, Cywinska A, Ball SL, deWarrd JR (2003) Biological identifications through DNA barcodes. Proceedings: Biology Science 270: 313–321. https://doi.org/10.1098/rspb.2002.2218

Hebert PDN, Stoeckle MY, Zemlak TS, Francis CM (2004) Identification of birds through DNA barcodes. PLoS Biology 2: e312. https://doi.org/10.1371/journal.pbio.0020312

Herler J, Bogorodsky SV, Suzuki T (2013) Four new species of coral gobies (Teleostei: Gobiidae: Gobiodon), with comments on their relationships within the genus. Zootaxa 3709: 301–329. https://doi.org/10.11646/zootaxa.3709.4.1

Hsu KC, Shih NT, Ni IH, Shao KT (2009) Speciation and population structure of three *Trichiurus* species based on mitochondrial DNA. Zoology Studies 48: 835–849.

Hsu KC, Wu HJ, Kuo PH, Chiu YW (2020) Genetic diversity of *Cyclina sinensis* (Veneridae): Resource management in Taiwan. Taiwania 66: 165–173.

Humphries JM, Bookstein FL, Chenoff B, Smith DR, Elder RL, Poss SG (1981) Multivaritiate discrimination by shape in relation to size. Systemic Zoology 30: 291–308. https://doi.org/10.2307/2413251

Irisarri I, Uribe JE, Eernisse DJ, Zardoya R (2020) A mitogenomic phylogeny of chitons (Mollusca: Polyplacophora). BMC Evolutionary Biology 20: e22. https://doi.org/10.1186/s12862-019-1573-2

Isari S, Pearman JK, Casas L, Michell CT, Curdia J, Berumen ML, Irigoien X (2017) Exploring the larval fish community of the central Red Sea integrated morphological and molecular approach. PLoS ONE 12: e0182503. https://doi.org/10.1371/journal.pone.0182503

Jahromi ST, Noor SAM, Pirian K, Dehghani R, Nazemi M, Khazaali A (2016) Mitochondrial DNA sequence-based phylogenetic relationship of *Trichiurus lepturus* (Perciformes: Trichiuridae) from the Persian Gulf. Iranian Journal of Veterinary Research Summer 17(3): 194–199.

Ju YM, Wu JH, Hsu KC, Chiu YW, Wang WK, Chen CW, Lin HD (2021) Genetic diversity of *Rhinogobius delicatus* (Perciformes: Gobiidae): origins of the freshwater fish in East Taiwan. Mitochondrial DNA Part A 32: 12–19. https://doi.org/10.1080/24701394.2020.1844678

Kumar S, Steecher G, Li M, Knyaz C, Tamura K (2018) MEGA X: Molecular evolutionary genetics analysis across computing platforms. Molecular Biology and Evolution 35: 1547–1549. https://doi.org/10.1093/molbev/msy096

Lee SC, Chang KH, Wu WL, Yang HC (1977) Formosan ribbonfishes (Perciformes, Trichiuridae). Bulletin of the Institute of Zoology, Academia Sinica 16: 77–84.

Li CS (1992) Hairtail fishes from Chinese coastal waters (Trichiuridae). Marine Science, Academia Sinica 26: 212–219. (in Chinese with English abstract)

Li Z, Li M, Xu S, Liu L, Chen Z, Zhou K (2020) Complete mitogenomes of three Carangidae (Perciformes) fishes: genome description and phylogenetic considerations. International Journal of Molecular Sciences 21: e4685. https://doi.org/10.3390/ijms21134685

Librado P, Rozas J (2009) DnaSP v5: a software for comprehensive analysis of DNA polymorphism data. Bioinformatics 25: 1451–1452. https://doi.org/10.1093/bioinformatics/btp187

Lin HC, Tsai CJ, Wang HY (2021) Variation in global distribution, population structures, and demographic history for four *Trichiurus* cutlassfishes. PeerJ 9: e12639. https://doi.org/10.7717/peerj.12639

Liu Y, Cui Z (2009) The complete mitochondrial genome sequence of the cutlassfish *Trichiurus japonicus* (Perciformes: Trichiuridae): genome characterization and phylogenetic considerations. Marine Genomics 2: 133–142. https://doi.org/10.1016/j.margen.2009.07.003

Liu X, Guo Y, Wang Z, Liu C (2013) The complete mitochondrial genome sequence of *Trichiurus nanhaiensis* (Perciformes: Trichiuridae). Mitochondrial DNA 24: 516–517. https://doi.org/10.3109/19401736.2013.772151

Liu H, Sun C, Zhu Y, Li Y, Wei Y, Ruan H (2020) Mitochondrial genomes of four American characins and phylogenetic relationships within the family Characidae (Teleostei: Characiformes). Gene 762: e145041. https://doi.org/10.1016/j.gene.2020.145041

Mirande JM (2018) Morphology, molecules and the phylogeny of Characidae (Teleostei, Characiformes). Cladistics 35: 282–300. https://doi.org/10.1111/cla.12345

Miya M, Friedman M, Satoh TP, Takeshima H, Sado T, Iwasaki W, Yamanoue Y, Nakatani M, Mabuchi K, Inoue JG, Poulsen JY, Fukunaga T, Sato Y, Nishida M (2013) Evolutionary origin of the Scombridae (tunas and mackerels): members of a paleogene adaptive radiation with 14 other pelagic fish families. PLoS ONE 8: e73535. https://doi.org/10.1371/journal.pone.0073535

Miya M, Nishida M (2000) Use of mitogenomic information in teleostean molecular phylogenetics: a tree-based exploration under the maximum-parsimony optimality criterion. Molecular Phylogenetics and Evolution 17: 437–455. https://doi.org/10.1006/mpev.2000.0839

Mukundan LP, Sukumaran S, Sebastian W, Gopalakrishnan A (2020) Characterization of the whole mitogenome of largehead hairtail *Trichiurus lepturus* (Trichiuridae): insights

into special characteristic. Biochemical Genetics 58: 430–451. https://doi.org/10.1007/s10528-020-09956-z

Nakabo T (2000) Fishes of Japan with Pictorial Keys to the Species, 2nd ed. Tokai University Press, Tokyo, 2428 pp. (in Japanese)

Nakamura I, Parin NV (1993) FAO species catalogue. Snake mackerels and cutlassfishes of the world (families Gempylidae and Trichiuridae). FAO (Food and Agriculture Organization of the United Nations) Fisheries Synopsis 125: 1–136.

Nakamura I, Parin NV (2001) Families Gempylidae, Trichiuridae. In: Carpenter & Niem 2001. Species identification guide for fishery purposes. The living marine resources of the western central Pacific. Bony fishes part 4 (Labridae to Latimeriidae), estuarine crocodiles, sea turtles, sea snakes and marine mammals. FAO, Rome, 6: iii-v.

Nelson JS (1994) Fishes of the World, 3rd ed. J Wiley, New York, 600 pp.

Nelson JS, Grande TC, Wilson MVH (2016) Classification of fishes from Fishes of the World. https://doi.org/10.1002/9781119174844

Papetti C, Lio P, Rüber L, Patarnello T, Zardoya R (2007) Antarctic fish mitochondrial genomes lack ND6 gene. Journal of Molecular Evolution 65: 519–528. https://doi.org/10.1007/s00239-007-9030-z

Perna NT, Kocher TD (1995) Patterns of nucleotide composition at fourfold degenerate sites of animal mitochondrial genomes. Journal of Molecular Evolution 41: 353–35. https://doi.org/10.1007/BF00186547

Phillips MJ, Zakaria SS (2021) Enhancing mitogenomic phylogeny and resolving the relationships of extinct megafaunal placental mammals. Molecular Phylogenetics and Evolution 158: e107082. https://doi.org/10.1016/j.ympev.2021.107082

Robertson DR, Angulo A, Baldwin CC, Pitassy D, Driskell A, Weigt LA, Navarro IJF (2017) Deep-water bony fishes collected by the B/O Miguel Oliver on the shelf edge of Pacific Central America: an annotated, illustrated and DNA-barcoded checklist. Zootaxa 4348: 1–125. https://doi.org/10.11646/zootaxa.4348.1.1

Salcioglu A, Gubili C, Kery G, Sönmez AY, Bilgin R (2020) Phylogeography and population dynamics of the Eastern Mediterranean whiting (*Merlangius merlangus*) from the Black Sea, the Turkish Straits System, and the North Aegean Sea. Fisheries Research 229: e105614. https://doi.org/10.1016/j.fishres.2020.105614

Shen Y, Guan L, Wang D, Gan X (2016) DNA barcoding and evaluation of genetic diversity in Cyprinidae fish in the midstream of the Yangtze River. Ecology and Evolution 6: 2702–2713. https://doi.org/10.1002/ece3.2060

Shih NT, Hsu KC, Ni IH (2011) Age, growth and reproduction of cutlassfishes *Trichiurus* spp. in the southern East China Sea. Journal of Applied Ichthyology 27: 1037–1315. https://doi.org/10.1111/j.1439-0426.2011.01805.x

Sun CH, Liu HY, Xu N, Zhang XL, Zhang Q, Han BP (2021) Mitochondrial genome structures and phylogenetic analyses of two tropical Characidae fishes. Frontiers in Genetics 12: e627402. https://doi.org/10.3389/fgene.2021.627402

Thompson JD, Gibson TJ, Plewniak F, Jeanmougin F, Higgins DG (1997) The CLUSTAL_X windows interface: flexible strategies for multiple sequence alignment aided by quality analysis tools. Nucleic Acids Research 25: 4876–4882. https://doi.org/10.1093/nar/25.24.4876

Tucker DW (1956) Studies on the trichiuroid fishes a preliminary revision of the family Trichiuridae. Bulletin of the Natural History Museum 4: 73–103. https://doi.org/10.5962/p.271719

Tzeng CH, Cheng CS, Chiu TS (2007) Analysis of morphometry and mitochondrial DNA sequences from two *Trichiurus* species in waters of the western North Pacific: taxonomic assessment and population structure. Journal of Fish Biology 70: 1–12. https://doi.org/10.1111/j.1095-8649.2007.01368.x

Wang Q, Huang J, Wu H (2021) Mitogenomes provide insights into phylogeny of mycetophilidae (Diptera: Sciaroidea). Gene 783: e145564. https://doi.org/10.1016/j.gene.2021.145564

Xu L, Wang X, Du F (2019) The complete mitochondrial genome of cutlassfish (*Trichiurus japonicus*) from South China Sea. Mitochondrial DNA B Resource 4: 783–784. https://doi.org/10.1080/23802359.2019.1566791

Yang JQ, Hsu KC, Liu ZZ, Su LW, Kuo PH, Tang WQ, Zhou ZC, Liu D, Bao BL, Lin HD (2016) The population history of *Garra orientalis* (Teleostei: Cyprinidae) using mitochondrial DNA and microsatellite data with approximate Bayesian computation. BMC Evolution Biology 16: e73. https://doi.org/10.1186/s12862-016-0645-9

Zardoya R, Meyer A (1996) Phylogenetic performance of mitochondrial protein-coding genes in resolving relationships among vertebrates. Molecular Biology and Evolution 13: 933–942. https://doi.org/10.1093/oxfordjournals.molbev.a025661

Zheng SY, Liu JH, Jia PF (2019) Complete mitogenome of the cutlassfish *Trichiurus haumela* (Scombriformes: Trichiuridae) from Ningde, Fujian province, Southeast China. Mitochondrial DNA B Resource 4: 87–88. https://doi.org/10.1080/23802359.2018.1536475

Zheng LP, Yang JX, Chen XY (2016) Molecular phylogeny and systematics of the Barbinae (Teleostei: Cyprinidae) in China inferred from mitochondrial DNA sequences. Biochemical Systematics and Ecology 68: 250–259. https://doi.org/10.1016/j.bse.2016.07.012

## Supplementary material 1

**Table S1–S4, Figure S1, S2**

Authors: Mu-Rong Yi, Kui-Ching Hsu, Sui Gu, Xiong-Bo He, Zhi-Sen Luo, Hung-Du Lin, Yun-Rong Yan

Data type: docx file

Explanation note: **Table S1.** Sample sizes of the genus *Trichiurus* in 18 sampling locations in Figure 1A. **Table S2.** Nucleotide compositions of *T. japonicus* (TJ), *T. lepturus* (TL), *T. nanhaiensis* (TN), *T. gangeticus* (TG) and *T. brevis* (TB). **Table S3.** Total number and frequency of the codons in mitogenomes. **Table S4.** The maximum (max.), mean and minimum (min.) p-distances between Trichiurus species (interspecific) and between genera within Trichiuridae (intergeneric) in each gene and mitogenome. **Figure S1.** Frontal view of the heads of preserved specimens of *T. lepturus* species complex. A *T. nanhaiensis*, 83.4 cm TL, ZBL 000440, Zhanjiang; B *T. japonicus*, 85.6 cm TL, ZJ 1902, Zhanjiang; C *T. lepturus*, 76.3 cm TL, ZJ 1906, Zhanjiang. **Figure S2.** The boxplot analyses in *T. japonicus* (blue), *T. lepturus* (orange) and *T. nanhaiensis* (grey). The landmarks are illustrated in Fig. 2.



Link: https://doi.org/10.3897/zookeys.1084.71576.suppl1

ZooKeys 1084: 27–42 (2022)
doi: 10.3897/zookeys.1084.77038
https://zookeys.pensoft.net

RESEARCH ARTICLE

A peer-reviewed open-access journal
ZooKeys
Launched to accelerate biodiversity research

# First records of two genera and thirteen species of Tabanidae (Diptera) from Honduras

Katerin Veroy[1], Jesus Orozco[1], Augusto L. Henriques[2]

**1** *Insect Collection, Agricultural Science and Production Department, Zamorano University (Escuela Agrícola Panamericana), Zamorano, Honduras* **2** *Coordenação de Pesquisas em Biodiversidade, Instituto Nacional de Pesquisas da Amazônia, Manaus, AM, Brazil*

Corresponding author: Jesus Orozco (cucarron1@gmail.com)

Academic editor: T. Dikow | Received 25 October 2021 | Accepted 3 January 2022 | Published 26 January 2022

*http://zoobank.org/3323F2E7-F3A8-49D1-9F46-21DABC882AF2*

**Citation:** Veroy K, Orozco J, Henriques AL (2022) First records of two genera and thirteen species of Tabanidae (Diptera) from Honduras. ZooKeys 1084: 27–42. https://doi.org/10.3897/zookeys.1084.77038

## Abstract

This works presents information on the diversity of the Tabanidae of Honduras as a product of the examination of 386 specimens and a literature review. Thirteen species and two genera (*Bolbodimyia* and *Dasychela*) are recorded from the country for the first time. Eighty-five species distributed in 22 genera, five tribes, and three subfamilies are now known from Honduras. A key to the subfamilies, tribes, and genera of the known Honduran species is also included. All new records are mapped and illustrated to aid in the identification of the species.

## Keywords

Central America, diversity, horse flies, tabanids, taxonomy

## Introduction

Tabanidae is a family of Diptera that includes flies considered of medical and veterinary importance due to the blood sucking habits of the adults. Currently the group contains around 4,400 species worldwide (Pape et al. 2011). The Neotropical region has the highest diversity, with approximately 1,205 species and about 28% of the global fauna (Henriques et al. 2012), but many its areas continue to be unexplored.

The best known tabanid faunas in Central America are those of Costa Rica and Panama thanks in big part to the works of Fairchild (1961), Hogue and Fairchild (1974), Fairchild (1986), and Burger (2002). Currently, 146 species of tabanids are known from Costa Rica (Borkent et al. 2018) and 152 from Panama (Fairchild 1986). For Honduras, few works deal with the diversity of horseflies in the country, i.e., Bequaert (1925), Root (1925), and James (1950). Coscarón and Papavero (2009), in their catalog for the neotropics, listed 70 species of Tabanidae from Honduras. Henriques (2016) added two additional species, *Scione maculipennis* (Schiner) and *Philipotabanus ebrius* (Osten Sacken), for a total of 72 species.

Honduran species diversity is poorly known for many groups. Linares and Orozco (2017) estimated that at least half of the insects in the country are known unknowns, species already described that are not recorded. This poor understanding of the diversity makes conducting ecological and conservation studies very difficult in the country.

This work presents for the first time an overview of the tabanids of Honduras. By nature, this is vastly incomplete as there are many more habitats to sample and collections to revise. In comparison, Costa Rica with less than half the size of Honduras has more than twice the number of known species of tabanids. The aims of this article are: 1) to present the new findings regarding the species diversity in the country, 2) to integrate the records on the tabanid fauna of Honduras scattered in the literature, 3) to provide an updated list of the species, and 4) to create a key for the genera of tabanids known in the country.

## Methods

Material of Tabanidae deposited at the Insect Collection at Zamorano University (EAPZ) (Zamorano, Honduras) was examined. Fieldwork was done using H-traps (Egri et al. 2013), light traps, and an aerial net in several locations in Honduras. Specimens were studied under a Leica EZ4 stereo microscope using the keys provided by Bequaert (1931), Philip (1954), Fairchild and Philip (1960), Fairchild (1976), Wilkerson (1979), Fairchild (1983, 1986), Fairchild and Wilkerson (1986), Coscarón and González (1991), Burger (1996), Henriques (2006), Krolow et al. (2007), Burger (2009), Krolow and Henriques (2010), Turcatel et al. (2010), Carmo and Henriques (2019), and Turcatel (2019).

Distributional records were obtained from label data and from the literature.

A species distribution map was made for the new records using SimpleMappr (https://www.simplemappr.net/) and Microsoft Power Point v. 2112.

Photographs were taken using a Canon 100 mm lens mounted on a Canon Rebel T5i attached to a macro rail. Composite images were obtained using PICOLAY v. 2020–02–06 (http://www.picolay.de). Individual images were organized in plates in GIMP v. 2.10.24 (http://www.gimp.org).

## Results and discussion

Eighteen genera and 47 species were found in the 386 specimens examined. Thirteen species and two genera are recorded for the first time (Fig. 1).

With these new records Honduras has now a diversity of 85 species of horseflies (Table 1). This represents an increase of 15.3% compared to the previously known taxa (72 species) but it's still a low number, and many more species are expected to be discovered in the future. Two additional species, *Tabanus femoralis* Kröber from Escuela Agricola Panamericana Zamorano, Francisco Morazan, and *Stypommisa lerida* (Fairchild) from 15 km west of La Ceiba, Atlántida, are recorded in GBIF (https://www.gbif.org/es/occurrence/3048772282 and https://www.gbif.org/es/occurrence/3385753663). Since this material was not examined, it is not included in the list, but the records are probably valid.

**Table 1.** Species of Tabanidae from Honduras. Distributions according to Coscarón and Papavero (2009), except were indicated.

| Taxon | Distribution |
|---|---|
| **CHRYSOPSINAE** | |
| **CHRYSOPSINI** | |
| *Chrysops soror* Kröber, 1925 | Guatemala, Belize, Honduras, Costa Rica, Panama, Colombia, Venezuela |
| *Chrysops auroguttatus* Kröber, 1930 | Mexico to Colombia |
| *Chrysops latifasciatus* Bellardi, 1859 | Mexico to Nicaragua |
| *Chrysops melaenus* Hine, 1925 | Honduras (new record), Nicaragua, Costa Rica to Venezuela |
| *Chrysops mexicanus* Kröber, 1926 | Mexico to Colombia |
| *Chrysops pachycnemius* Hine, 1905 | Mexico to Honduras |
| *Chrysops scalaratus* Bellardi, 1859 | Mexico to Panama |
| *Chrysops variegatus* (De Geer, 1776) | Mexico to Argentina |
| *Chrysops willistoni* Hine, 1925 | Mexico to Honduras |
| *Silvius melanopterus* (Hine, 1905) | Mexico to Honduras |
| **PANGONIINAE** | |
| **PANGONIINI** | |
| *Esenbeckia illota* (Williston, 1901) | Mexico to Honduras |
| *Esenbeckia mejiai* Fairchild, 1942 | Guatemala to Costa Rica |
| *Esenbeckia prasiniventris* (Kröber, 1929) | Guatemala to Ecuador and Trinidad, Brazil |
| *Esenbeckia translucens* (Macquart, 1846) | Mexico to Peru and Brazil |
| *Esenbeckia wiedemanni* (Bellardi, 1859) | Mexico, Honduras (new record) |
| **SCIONINI** | |
| *Fidena flavipennis* Kröber, 1931 | Mexico to Venezuela |
| *Fidena rhinophora* (Bellardi, 1859) | Mexico to Venezuela and Peru |
| *Scione aurulans* (Wiedemann, 1830) | Mexico to Costa Rica |
| *Scione maculipennis* (Schiner, 1868) | Honduras, Costa Rica to Venezuela, Ecuador* |
| **TABANINAE** | |
| **DIACHLORINI** | |
| *Bolbodimyia atrata* (Hine, 1904) | USA, Mexico, Honduras (new record) |
| *Bolbodimyia erythrocephala* (Bigot, 1892) | Honduras (new record), Costa Rica, Panama, Ecuador |
| *Bolbodimyia galindoi* Fairchild, 1964 | Honduras (new record), Costa Rica to Colombia |
| *Bolbodimyia philipi* Stone, 1954 | Guatemala, El Salvador, Honduras (new record), Costa Rica, Panama, Colombia |
| *Catachlorops baliopterus* Gorayeb, L. Bemúdez, E.M. Bermúdez & Villalba, 1989 | Mexico, Honduras, Costa Rica |

| Taxon | Distribution |
|---|---|
| *Catachlorops fulmineus* (Hine, 1920) | Honduras to Panama, Colombia, Ecuador |
| *Catachlorops scurrus* (Fairchild, 1958) | Mexico to Panama |
| *Chlorotabanus inanis* (Fabricius, 1787) | Mexico to Peru and Brazil |
| *Chlorotabanus mexicanus* (Linnaeus, 1758) | Mexico to Ecuador, Brazil, Trinidad |
| *Dasychela badia* (Kröber, 1931) | Honduras (new record), Costa Rica, Panama |
| *Diachlorus ferrugatus* (Fabricius, 1805) | USA to Costa Rica, Bahamas Islands |
| *Dichelacera costaricana* (Fairchild, 1941) | Honduras, Costa Rica |
| *Dichelacera grandis* Philip, 1943 | Guatemala, Belize, Honduras |
| *Dichelacera marginata* Macquart, 1847 | Honduras (New record), Nicaragua to Brazil and Peru |
| *Dichelacera pulchroides* Fairchild & Philip, 1960 | Mexico, Honduras |
| *Dichelacera regina* Fairchild, 1940 | Honduras to Ecuador |
| *Dichelacera scapularis* Macquart, 1847 | Mexico to Panama |
| *Dichelacera submarginata* Lutz, 1915 | Honduras (new record), Costa Rica to Venezuela, Peru, Bolivia |
| *Lepiselaga crassipes* (Fabricius, 1805) | Mexico to Argentina |
| *Leucotabanus exaestuans* (Linnaeus, 1758) | Mexico to Bolivia, Argentina, and Trinidad |
| *Leucotabanus nigriventris* Kröber, 1931 | Mexico to Panama |
| *Phaeotabanus longiappendiculatus* (Macquart, 1855) | Mexico to Panama |
| *Philipotabanus ebrius* (Osten Sacken, 1886) | Honduras, Costa Rica, Panama* |
| *Philipotabanus elviae* (Fairchild, 1943) | Honduras (new record), Costa Rica, Panama |
| *Philipotabanus kompi* (Fairchild, 1943) | Belize, Honduras |
| *Philipotabanus magnificus* (Kröber, 1934) | Honduras to Venezuela and Ecuador |
| *Philipotabanus nigrinubilus* (Fairchild, 1953) | Honduras, Costa Rica, Panama, Colombia, Ecuador |
| *Philipotabanus plenus* (Hine, 1907) | Guatemala to Colombia |
| *Rhabdotylus venenatum* (Osten Sacken, 1886) | Guatemala to Ecuador |
| *Selasoma tibiale* (Fabricius, 1805) | Mexico to Argentina |
| *Stenotabanus fulvistriatus* (Hine, 1912) | Mexico to Panama |
| *Stenotabanus littoreus* (Hine, 1907) | Mexico to Panama |
| *Stenotabanus maculifrons* (Hine, 1907) | Honduras, Costa Rica, Panama, Trinidad, Venezuela. |
| *Stibasoma chionostigma* (Osten Sacken, 1886) | Mexico to Colombia |
| *Stibasoma flaviventris* (Macquart, 1848) | Mexico to Brazil |
| *Stibasoma panamense* Curran, 1934 | Honduras to Ecuador and Venezuela |
| *Stypommisa captiroptera* (Kröber, 1930) | Mexico to Guyana, Brazil, Paraguay |
| *Stypommisa changena* Fairchild, 1986 | Honduras (new record), Costa Rica, Panama |
| *Stypommisa u-nigrum* Philip, 1977 | Mexico, Guatemala, Honduras |
| **TABANINI** | |
| *Poeciloderas quadripunctatus* (Fabricius, 1805) | Mexico to Argentina |
| *Tabanus abattenuis* Philip, 1969 | Mexico, Guatemala, El Salvador, Honduras, Nicaragua |
| *Tabanus bigoti* Bellardi, 1859 | Mexico to Colombia and Venezuela |
| *Tabanus claripennis* (Bigot, 1892) | Honduras (new record), West Indies, Costa Rica to Paraguay, Brazil, Argentina, and Chile |
| *Tabanus colombensis* Macquart, 1846 | USA to Trinidad, Venezuela, Ecuador, Brazil |
| *Tabanus commixtus* Walker, 1860 | Mexico to Venezuela, Hispaniola, Trinidad, Martinique |
| *Tabanus defilippii* Bellardi, 1859 | Mexico to Panama |
| *Tabanus dorsifer* Walker, 1860 | USA, Mexico, Honduras |
| *Tabanus erebus* Osten Sacken, 1886 | Honduras, Nicaragua, Costa Rica, Panama |
| *Tabanus jilamensis* Hine, 1925 | Honduras |
| *Tabanus morbosus* Stone, 1938 | USA, Mexico to Panama |
| *Tabanus nebulosus* De Geer, 1776 | Belize, Honduras (New record), Costa Rica, Trinidad, Barbados to Brazil and Argentina |
| *Tabanus occidentalis* Linnaeus, 1758 | Mexico to Argentina, Trinidad |
| *Tabanus oculus* Walker, 1848 | Mexico to Panama |
| *Tabanus picturatus* Kröber, 1931 | Mexico, Belize, Honduras |
| *Tabanus polyphemus* Fairchild, 1958 | Mexico to Colombia |
| *Tabanus pruinosus* Bigot, 1892 | USA to Panama |
| *Tabanus pseudoculus* Fairchild, 1942 | Guatemala to Colombia, Venezuela, Ecuador, and Trinidad |

| Taxon | Distribution |
|---|---|
| *Tabanus pungens* Wiedemann, 1828 | USA, Neotropics (except West Indies and Chile), Trinidad |
| *Tabanus quinquepunctatus* Hine, 1925 | Guatemala, Belize, Honduras, Costa Rica, Panama |
| *Tabanus secundus* Walker, 1848 | Guatemala to Peru, Surinam, and Paraguay |
| *Tabanus subruber* Bellardi, 1859 | Mexico, Guatemala, Honduras |
| *Tabanus unipunctatus* (Bigot, 1892) | Mexico to Colombia |
| *Tabanus unistriatus* Hine, 1906 | Guatemala to Ecuador |
| *Tabanus vittiger* ssp. *guatemalanus* Hine, 1906 | USA, Bahamas, West Indies, Mexico to Surinam, French Guiana, and Brazil |
| *Tabanus xenorhynchus* Fairchild, 1947 | Guatemala to Panama |
| *Tabanus yucatanus* Townsend, 1897 | Mexico, Guatemala, El Salvador, Honduras, Nicaragua |

* Distribution according to Henriques (2016).

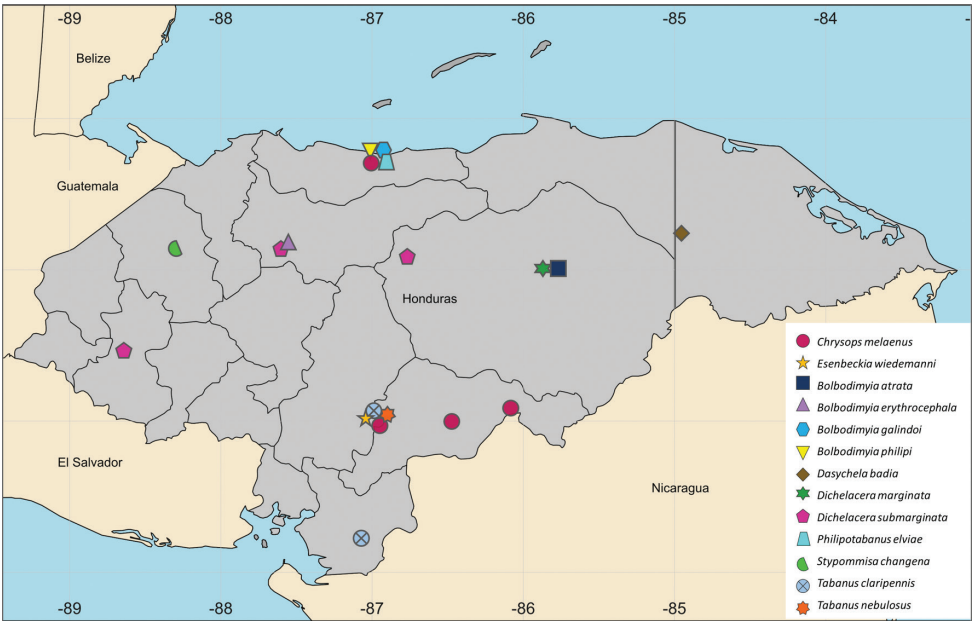


**Figure 1.** Distribution map of new records of Tabanidae from Honduras.

## New Tabanidae from Honduras

### CHRYSOPSINAE
### CHRYSOPSINI

#### *Chrysops melaenus* Hine, 1925
Figure 2A

**Distribution.** Previously known from Nicaragua to Venezuela (Coscarón and Papavero 2009).

**Material examined.** Honduras: 1♂, Atlántida, RVS Cuero y Salado, Salado Barra, 15°46'02"N, 86°59'51"W, 2 m, 25.i.2000, R. Cave, R. Cordero and J. Torres leg.; EAPZ22.445. 1♂, El Paraíso, 5.3 km N Cifuentes, 14°05'48"N, 86°06'57"W, 13.vi.1999, R. Cave and J. Torres leg.; EAPZ69.749. 1♀, El Paraíso, Danlí, Cerro

Apaguiz 14°00'27"N, 86°32'26"W, 20.ii.1988, R. Cordero leg.; EAPZ42.723. 1♀, Francisco Morazán, 32 km Tegucigalpa, El Zamorano, 14°01'N, 87°00'W , J. Cabezas leg.; EAPZ42.698.

**PANGONIINAE**
**PANGONIINI**

***Esenbeckia wiedemanni* (Bellardi, 1859)**
Figure 2B, C

**Distribution.** Previously known exclusively from Mexico (Coscarón and Papavero 2009).

**Material examined.** Honduras: 1♂, 1♀, Francisco Morazán, Masicarán, Uyúca, 14°01'00"N, 87°05'00"W, 10–15.xi.2016, E. van den Berghe leg.; EAPZ42.764.

**TABANINAE**
**DIACHLORINI**

***Bolbodimyia atrata* (Hine, 1904)**
Figure 2D

**Distribution.** Previously known from U.S.A. and Mexico (Coscarón and Papavero 2009).

**Material examined.** Honduras: 2♂♂, Olancho, El Murmullo, Sierra de Agalta, 15°01'00"N, 85°47'00"W, 28.vi.1997, R. Cave leg.; EAPZ69.815.

***Bolbodimyia erythrocephala* (Bigot, 1892)**
Figure 2E

**Distribution.** Previously known from Costa Rica, Panama, Ecuador (Coscarón and Papavero 2009), and Colombia (Wolff and Miranda-Esquivel 2016).

**Material examined.** Honduras: 1♀, Yoro, Par. Nac. Pico Pijol, 15°13'00"N, 87°33'00"W, 22–23.vi.1998, R. Cave leg.; EAPZ42.652.

***Bolbodimyia galindoi* Fairchild, 1964**
Figure 3A, B

**Distribution.** Previously known from Costa Rica to Colombia (Coscarón and Papavero 2009).

**Material examined.** Honduras: 1♂, 1♀, Atlántida, Par. Nac. Pico Bonito, Rio Zacate, 15°41'35"N, 86°55'58"W, 35 m, 5.iii.2000, R. Cave, R. Cordero and J. Torres leg.; EAPZ27.180.

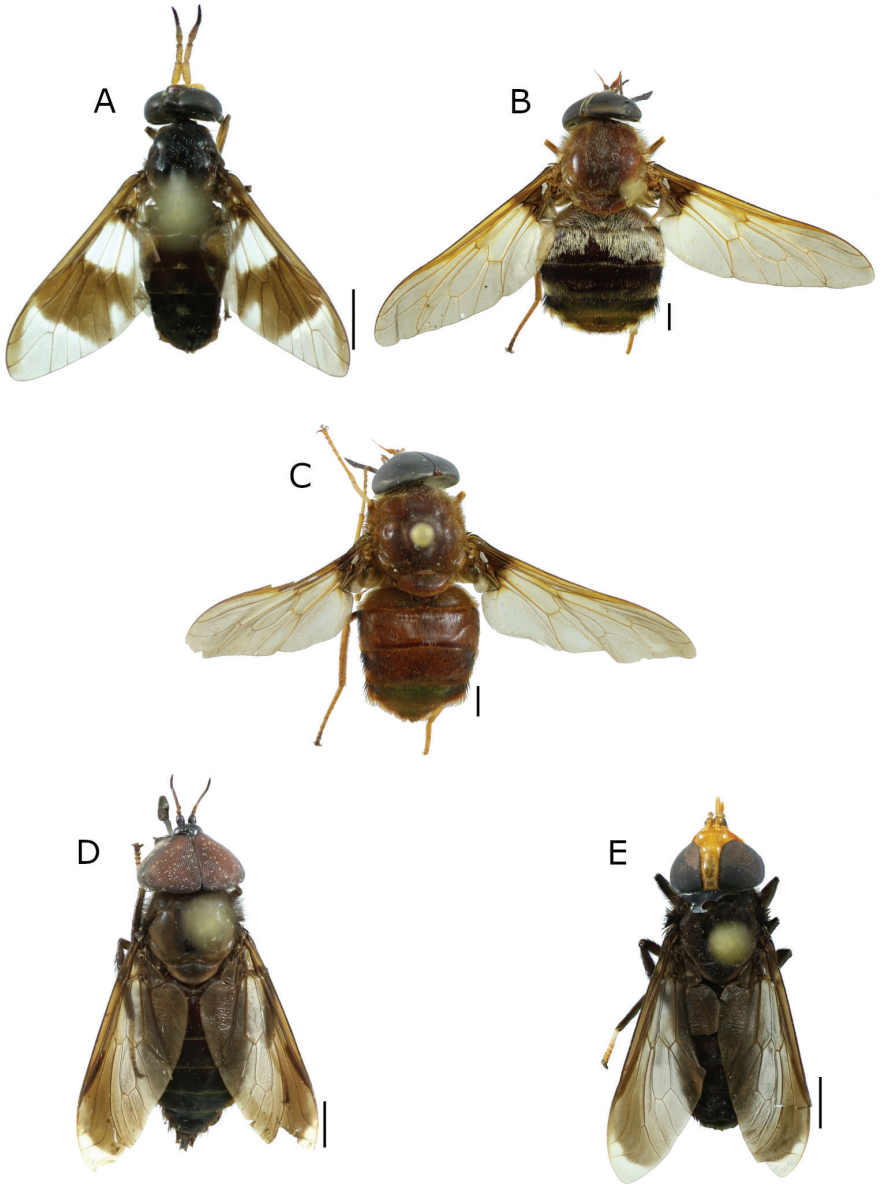


**Figure 2.** New records of Tabanidae from Honduras **A** *Chrysops melaenus* Hine (♀) **B, C** *Esenbeckia wiedemanni* (Bellardi) (♀, ♂) **D** *Bolbodimyia atrata* (Hine) (♂) **E** *B. erythrocephala* (Bigot) (♀). Scale bars: 2 mm.

***Bolbodimyia philipi* Stone, 1954**
Figure 3C

**Distribution.** Previously known from Guatemala, El Salvador, Costa Rica, Panama, and Colombia (Coscarón and Papavero 2009).

**Material examined.** Honduras: 1♂, Atlántida, Cuero y Salado, Salado Barra, 15°46'02"N, 86°59'51"W, 2 m, 25.i.2000, R. Cave, R. Cordero and J. Torres leg.; EAPZ22.452.

***Dasychela badia* (Kröber, 1931)**
Figure 3D

**Distribution.** Previously known from Costa Rica and Panama (Coscarón and Papavero 2009).

**Material examined.** Honduras: 23♀♀, Gracias a Dios, Ciudad Blanca, 15°14'47"N, 84°58'2"W, 250 m, 15–26.ii.2017, E. van den Berghe leg., light trap; EAPZ43.577.

***Dichelacera marginata* Macquart, 1847**
Figure 3E

**Distribution.** Previously known from Nicaragua to Brazil and Peru (Coscarón and Papavero 2009).

**Material examined.** Honduras: 1♀, Olancho, El Murmullo, Sierra de Agalta, 15°01'00"N, 85°47'00"W, 28.vi.1997, R. Cave leg.; EAPZ44.214.

***Dichelacera submarginata* Lutz, 1915**
Figure 4A, B

**Distribution.** Previously known from Costa Rica to Venezuela, Peru, and Bolivia (Coscarón and Papavero 2009).

**Material examined.** Honduras: 1♀, Olancho, La Muralla, 15°04'56"N, 86°45'24"W, 26–30.iii.2013, O. Schlein leg.; EAPZ42.549. 1♂, Lempira, Par. Nac. Celaque, 14°28'46"N, 88°38'35"W, 1400 m, 27.iv.2018, E. van den Berghe leg.; EAPZ69.831. 1♂, Yoro, Par. Nac. Pico Pijol, Linda Vista, 15°10'35"N, 87°35'10"W, 1450 m, 21.iv.1999, R. Cave and J. Torres leg.; EAPZ42.829.

***Philipotabanus elviae* (Fairchild, 1943)**
Figure 4C

**Distribution.** Previously known from Costa Rica and Panama (Coscarón and Papavero 2009).

**Material examined.** Honduras: 12 ♀♀, Atlántida, Par. Nac. Pico Bonito, Rio Zacate, 15°41'35"N, 86°55'58"W, 35 m, 5.v.2000, R. Cave leg.; EAPZ29.665.

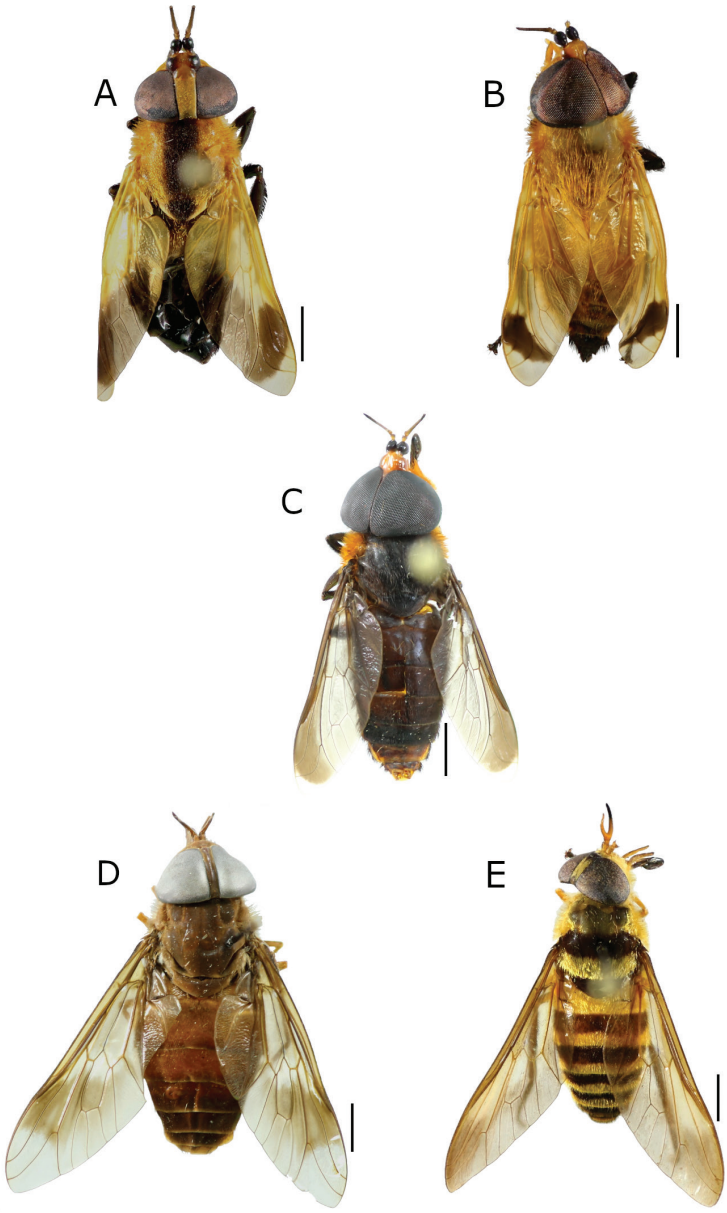


**Figure 3.** New records of Tabanidae from Honduras. **A, B** *Bolbodimyia galindoi* Fairchild (♀, ♂) **C** *B. philipi* Stone (♂) **D** *Dasychela badia* (Kröber) (♀) **E** *Dichelacera marginata* Macquart (♀). Scale bars: 2 mm.

***Stypommisa changena* Fairchild, 1986**
Figure 4D

**Distribution.** Previously known from Costa Rica and Panama (Coscarón and Papavero 2009).

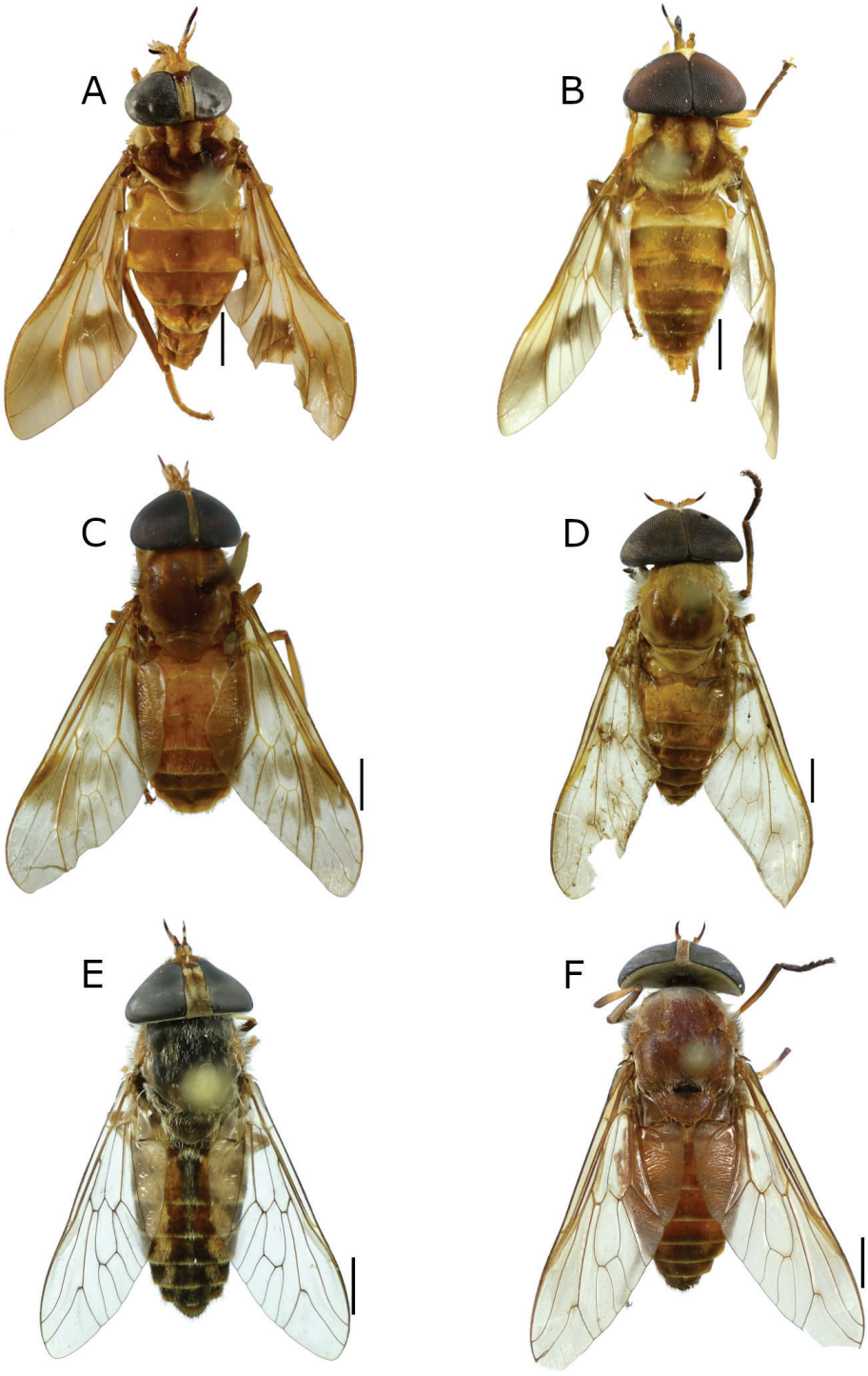


**Figure 4.** New records of Tabanidae from Honduras **A, B** *Dichelacera submarginata* Lutz (♀, ♂) **C** *Philipotabanus elviae* (Fairchild) (♀) **D** *Stypommisa changena* Fairchild (♂) **E** *Tabanus claripennis* (Bigot) (♀) **F** *T. nebulosus* De Geer (♀). Scale bars: 2 mm.

**Material examined.** Honduras: 1 ♂, Santa Bárbara, El Volcán, Trinidad, 15°08'02"N, 88°18'01"W, 1320 m, 26.vi.2000. R. Cordero and J. Torres leg.; EAPZ35.149.

**TABANINI**

***Tabanus claripennis* (Bigot, 1892)**
Figure 4E

**Distribution.** Previously known from the West Indies, Costa Rica to Paraguay, Brazil, Argentina, and Chile (Coscarón and Papavero 2009).

**Material examined.** Honduras: 7 ♀♀, Francisco Morazán, El Zamorano, EAP, 14°01'N, 87°00'W, 5–29.vii.2020, H-trap, R. Argueta leg.; EAPZ43.572. 1♂, Choluteca, 6.7 km SE Santa Ana de Yusguare, 13°15'37"N, 87°04'40"W, 8.ix.1999, R. Cave and J. Torres leg.; EAPZ43.570.

***Tabanus nebulosus* De Geer, 1776**
Figure 4F

**Distribution.** Previously known from Belize (Coscarón and Papavero 2009), Costa Rica (Fairchild 1961), Colombia, Venezuela, Trinidad, Surinam, Brazil, Bolivia, Paraguay, Barbados, and Argentina (Coscarón and Papavero 2009; Henriques 2016).

**Material examined.** Honduras: 2 ♀♀, Francisco Morazán, El Zamorano EAP, 14°01'N, 87°00'W, 850 m, v–vii, Estudiante EAPZ leg.; EAPZ75.022. 1 ♀, Francisco Morazán, El Zamorano EAP, 14°01'N, 87°00'W, 850 m, 31.v.2019, L. Moreno leg.; EAPZ75.023.

## Key to the subfamilies, tribes, and genera of Tabanidae from Honduras

Modified from Fairchild (1969) and Burger (2009).

| | | |
|---|---|---|
| 1 | Hind tibiae without paired terminal spurs or spines; TABANINAE | **6** |
| – | Hind tibiae with paired terminal spurs or spines, spines rarely absent or difficult to see | **2** |
| 2 | Third antennal segment with 7 or 8 distinct flagellomeres; tergite 9 undivided; PANGONIINAE | **3** |
| – | Third antennal segment with no more than 5 distinct flagellomeres; tergite 9 divided; CHRYSOPSINAE | **5** |
| 3 | Eyes bare; frons with ridge-like callus, which may be bare or tomentose; PANGONIINI | ***Esenbeckia* Rondani** |
| – | Eyes pilose; frons flat, without any sort of callus; SCIONINI | **4** |
| 4 | Cell $m_3$ closed at wing margin | ***Scione* Walker** |
| – | Cell $m_3$ open at wing margin | ***Fidena* Walker** |

5 Wings with dark crossband (Fig. 2A), crossband absent at times; eyes in life with pattern of dots and bars ..... ***Chrysops*** **Meigen**

– Wings hyaline or cloudy on cross veins or elsewhere, without distinct crossband; eye pattern in life irregularly speckled..... ***Silvius*** **Meigen**

6 Basicosta without strong setae, if setae present usually less dense than those on adjoining costa; if setae on basicosta as dense as on costa, then vestiges of ocelli present; DIACHLORINI ..... **7**

– Basicosta with numerous strong setae, setae equal in size and density to those on adjoining costa, if setae sparse, then without vestiges of ocelli; TABANINI ..... **22**

7 Third antennal segment with strong dorso-basal tooth or forward-pointing spine that often reaches to or beyond end of first flagellomere..... **8**

– Third antennal segment usually at most with acute dorso-basal angle..... **12**

8 Eyes densely pilose; antennal tooth reaching beyond apex of first flagellomere; proboscis longer than maxillary palpi; maxillary palpi slender, generally exceeding antennae; labella short, membranous; callus club shaped, much narrower than frons; wings with diffuse dark discal marking..... ..... ***Dasychela*** **Enderlein**

– Eyes bare; other characters variable ..... **9**

9 Stout species; body sometimes hairy and beelike; foretibiae usually inflated; long hair fringes on at least hind tibiae; maxillary palpi inflated; antennae short, stout, with dorsal tooth extending beyond apex of first flagellomere; labella shiny and sclerotized ..... **10**

– Slender species; all tibiae slender; rest of characters not as above ..... **11**

10 Abdomen green or greenish, sparsely covered with hairs; hind tibial fringe moderate in length; all tibiae slender; wings hyaline, sometimes yellowish; not resembling bees ..... ***Rhabdotylus*** **Lutz**

– Abdomen not greenish, densely hirsute; hind tibial fringe long; at least foretibia inflated; wings variable, never entirely hyaline or uniformly tinted, generally with black or contrasting pattern; body often resembling bees (see Turcatel et al. 2010)..... ***Stibasoma*** **Schiner**

11 Basal callus thin, ridge-like, narrower than frons; eyes unicolored, bright green in life, rarely bicolored or with faint median line; mesoscutum unicolored or weakly striped, not transversely banded ..... ..... ***Catachlorops*** **Lutz**

– Basal callus as wide as frons; eyes banded or unicolorous blackish in life; mesoscutum often transversely banded ..... ***Dichelacera*** **Macquart**

12 Subcallus, and usually first antennal segment, greatly inflated and shiny; third antennal segment long and slender, with obtuse dorso-basal angle; tibiae slender or slightly incrassate; wings black or partly so, with apex sharply hyaline, apical half of vein $R_4$ bent sharply forward; maxillary palpi moderately slender, tomentose; clypeus tomentose..... ***Bolbodimyia*** **Bigot**

– Without above combination of characters..... **13**

13 Tibiae, especially first two pairs, greatly inflated; subcallus, clypeus, and gena bare; maxillary palpi shiny and flattened; wings black at base, at least to ends of cells br and bm; labella membranous ..... **14**

– Tibiae not or but slightly inflated; without above combination of characters... **15**

14 Large, shiny bluish-black species; wings black from base to middle of cell d.. ..... ***Selasoma*** **Macquart**

– Small species, mesoscutum, and often abdomen, with metallic brassy or greenish scale-like hairs; wings black from base to beyond end of cell d, with hyaline triangle in cells $m_3$ and $cua_1$ ..... ***Lepiselaga*** **Macquart**

15 Mesopleura shiny or pearly tomentose in contrast to rest of pleura; wings usually with dark subapical marking..... ***Diachlorus*** **Osten Sacken**

– Mesopleura not shiny or pearly tomentose, not contrasting with other pleural sclerites; wings without dark subapical marking ..... **16**

16 Basal callus absent..... ***Chlorotabanus*** **Lutz**

– Basal callus present, reduced at times ..... **17**

17 Labella sclerotized; frons narrow, generally over 5 times as long as its basal width; eyes in life unicolored, unbanded; dorsal angle on third antennal segment strong ..... ***Phaeotabanus*** **Lutz**

– Labella membranous; frons generally less than 4 times as long as its basal width; eyes in life usually banded; dorsal angle of third antennal segment variable.... **18**

18 Eyes bare, with at least 2 transverse bands in life; mostly small species with moderately broad frons often with median dark-haired patch; callus rounded or square, generally as wide as frons ..... ***Stenotabanus*** **Lutz**

– Eyes pilose or bare, with at most 1 dark median, generally unicolored, rarely bicolored; rest of characters not as above..... **19**

19 Vertex with well-marked tubercle and/or with clear vestiges of ocelli; eyes bare; frons narrow; basal callus club-shaped or ridge-like ..... **20**

– Vertex without tubercle or clear vestiges of ocelli, slightly raised shiny or discolored tubercle rarely present; if tubercle present, then eyes pilose, or frons broad, or basal callus rounded..... **22**

20 Wings with extensive dark pattern not consisting of spots on cross veins; if wings apparently unmarked, then thorax prominently striped, or frons exceedingly narrow and callus thread-like..... ***Philipotabanus*** **Fairchild**

– Wings hyaline, tinted, or with dark pattern consisting primarily of dark spots around cross veins..... **21**

21 Wings hyaline or evenly tinted, with costal cell often darker, but never with apical clouds or spots on cross veins; frontal callus clavate or ridge-like; abdomen black or brown, nearly always with transverse bands at least on fourth segment, rarely otherwise; appendix on fork of vein $R_4$ absent ..... ***Leucotabanus*** **Lutz**

– Wing with clouds on at least discal cross veins, often with apical infuscation, if entirely hyaline or tinted, then abdomen and thorax not as above; frontal callus variable; wings often with appendix on fork of vein $R_4$ ..... ..... ***Stypommisa*** **Enderlein**

22 Vertex with small, rounded, sometimes indistinct, tubercle; eyes of female usually pilose, densely so on males; wings with all cross veins prominently spotted.....***Poeciloderas* Lutz**

– Vertex rarely with tubercle; without above combination of characters ..... .....***Tabanus* Lutz**

## Acknowledgements

We are grateful to the reviewers, Daniel Carmo and Mauren Turcatel, as well as the editor, Torsten Dikow, for critically reading the manuscript and contributing to improve the quality of this paper. We thank Milena Agila for taking the photographs and arranging the plates for publication. We also thank Ronel Argueta for his help constructing and maintaining the traps at Zamorano.

## References

Bequaert J (1925) Report of an entomological trip to the Truxillo Division, Honduras, to investigate the sand-fly problem. Report of Medical Department of the United Fruit Company 13: 193–206.

Bequaert J (1931) Tabanidae of the peninsula of Yucatan Mexico, with descriptions of new species. Journal of the New York Entomological Society 39(4): 533–553.

Borkent A, Brown BV, Adler PH, Amorim DS, Barber K, Bickel D, Boucher S, Brooks SE, Burger J, Burington ZL, Capellari RS, Costa DNR, Cumming JM, Curler G, Dick CW, Epler JH, Fisher E, Gaimari SD, Gelhaus J, Grimaldi DA, Hash J, Hauser M, Hippa H, Ibáñez-Bernal S, Jaschhof M, Kameneva EP, Kerr PH, Korneyev V, Korytkowski CA, Kung GA, Kvifte GM, Lonsdale O, Marshall SA, Mathis WN, Michelsen V, Naglis S, Norrbom AL, Paiero S, Pape T, Pereira-Colavite A, Pollet M, Rochefort S, Rung A, Runyon JB, Savage J, Silva VC, Sinclair BJ, Skevington JH, Stireman JOI, Swann J, Vilkamaa P, Wheeler T, Whitworth T, Wong M, Wood DM, Woodley N, Yau T, Zavortink TJ, Zumbado MA (2018) Remarkable fly (Diptera) diversity in a patch of Costa Rican cloud forest: why inventory is a vital science. Zootaxa 4402(1): 53–90. https://doi.org/10.11646/zootaxa.4402.1.3

Burger JF (1996) Description of the male and variation in *Bolbodimyia galindoi* Fairchild (Diptera: Tabanidae), and a revised key to species of *Bolbodimyia*. Proceedings of the Entomological Society of Washington 98: 390–395.

Burger JF (2002) Description of five new species of Tabanidae (Diptera) from Costa Rica and revised keys to species for the genera *Fidena* Walker, *Scione* Walker, and *Chrysops* Meigen in Costa Rica. Proceedings of the Entomological Society of Washington 104: 928–940.

Burger JF (2009) Tabanidae (Horseflies, Deer Flies, Tabanos). In: Brown BV, Borkent A, Cumming JM, Wood DM, Woodley NE, Zumbado MA (Eds) Manual of Central American Diptera. First Edition. National Research Council Research Press, Ottawa, 495–504.

Carmo DD, Henriques AL (2019) Taxonomy of *Tabanus trivittatus* species-group (Diptera: Tabanidae), with description of five new species. Zootaxa 4554(1): 63–100. https://doi.org/10.11646/zootaxa.4554.1.2

Coscarón S, González C (1991) Tabanidae from Chile: annotated list of species and key to the genera reported from Chile. Acta Entomológica Chilena 16: 125–150.

Coscarón S, Papavero N (2009) Catalogue of Neotropical Diptera. Tabanidae. Neotropical Diptera 16: 1–199.

Egri Á, Blahó M, Száz D, Barta A, Kriska G, Antoni G, Horváth G (2013) A new tabanid trap applying a modified concept of the old flypaper: Linearly polarising sticky black surfaces as an effective tool to catch polarotactic horseflies. International Journal for Parasitology 43: 555–563. https://doi.org/10.1016/j.ijpara.2013.02.002

Fairchild GB (1961) A preliminary check list of the Tabanidae (Diptera) of Costa Rica. Revista de Biología Tropical 9(1): 23–38. https://doi.org/10.15517/rbt.v9i1.30116

Fairchild GB (1969) Notes on Neotropical Tabanidae XII. Classification and distribution, with keys to genera and subgenera. Arquivos de Zoologia 17(4): 199–255. https://doi.org/10.11606/issn.2176-7793.v17i4p199-255

Fairchild GB (1976) Notes on Neotropical Tabanidae (Dipt.) XVI. The *Tabanus trivittatus* complex. Studia Entomologica 19(1–4): 237–261.

Fairchild GB (1983) Notes on Neotropical Tabanidae (Diptera). XIX. The *Tabanus lineola* complex. Miscellaneous Publications of the Entomological Society of America 57: 1–50.

Fairchild GB (1986) The Tabanidae of Panama. Contributions of the American Entomological Institute 22(3): 1–139.

Fairchild GB, Philip CB (1960) A revision of the Neotropical genus *Dichelacera* subgenus *Dichelacera* Macquart (Diptera, Tabanidae). Studia Entomologica 3(1–4): 1–86.

Fairchild GB, Wilkerson RC (1986) A review of the Neotropical genus *Stypommisa* (Diptera: Tabanidae). Contributions of the American Entomological Institute 22(5): 1–61.

Henriques AL (2006) O gênero *Philipotabanus* Fairchild (Insecta: Diptera: Tabanidae) na Amazônia, com chave para as fêmeas das espécies e descrição de *P. obidensis* sp. nov. Acta Amazonica 36(4): 549–556. https://doi.org/10.1590/s0044-59672006000400017

Henriques AL (2016) Tabanidae (Diptera) of the American Museum of Natural History Collection. Zootaxa 4137(2): 151–186. http://doi.org/10.11646/zootaxa.4137.2.1

Henriques AL, Krolow TK, Rafael JA (2012) Corrections and additions to Catalogue of Neotropical Diptera (Tabanidae) of Coscarón & Papavero (2009). Revista Brasileira de Entomologia 56: 277–280. https://doi.org/10.1590/S0085-56262012005000042

Hogue L, Fairchild G (1974) A revised check list of the Tabanidae (Diptera) of Costa Rica. Revista de Biología Tropical 22(1): 11–27.

James MT (1950) The Diptera collected on the Cockerell and Hubell expeditions to Honduras. Part I: Stratiomyidae, Tabanidae, and Acroceratidae. The Pan-Pacific Entomologist 26(2): 86–90.

Krolow TK, Henriques AL (2010) Taxonomic revision of the New World genus *Chlorotabanus* Lutz, 1913 (Diptera: Tabanidae). Zootaxa 2656(1): 1–40. https://doi.org/10.11646/zootaxa.2656.1.1

Krolow TK, Krüger RF, Ribeiro PB (2007) Chave pictórica para os gêneros de Tabanidae (Insecta: Diptera) do bioma Campos Sulinos, Rio Grande do Sul, Brasil. Biota Neotropica 7(2): 253–264. https://doi.org/10.1590/S1676-06032007000200028

Linares CA, Orozco J (2017) The Coreidae of Honduras (Hemiptera: Coreidae). Biodiversity Data Journal 5: e13067. https://doi.org/10.3897/BDJ.5.e13067

Pape T, Blagoderov V, Mostovski MB (2011) Order Diptera Linnaeus, 1758. In: Zhang Z-Q (Ed.) Animal biodiversity: an outline of higher-level classification and survey of taxonomic richness. Zootaxa 3148(1): 222–229. https://doi.org/10.11646/zootaxa.3148.1.42

Philip CB (1954) New North American Tabanidae. VIII. Notes on and keys to the genera and species of Pagoniinae exclusive of *Chrysops*. Revista Brasileira de Entomologia 2: 13–60.

Root FM (1925) Notes on blood-sucking arthropods collected at Tela, Honduras and Port Limon, Costa Rica, during the summer of 1924. Report of Medical Department of the United Fruit Company 13: 207–209.

Turcatel M (2019) Taxonomic revision of the Neotropical genus *Rhabdotylus* Lutz, 1913 (Diptera: Tabanidae). Biodiversity Data Journal 7: e36277. https://doi.org/10.3897/BDJ.7.e36277

Turcatel M, de Carvalho CJB, Rafael JA (2010) A taxonomic revision of *Stibasoma* Schiner, 1867 (Diptera: Tabanidae). Zootaxa 2368(1): 1–39. https://doi.org/10.11646/zootaxa.2368.1.1

Wilkerson RC (1979) Horse flies (Diptera: Tabanidae) of the Colombian Departments of Choco, Valle, and Cauca. Cespedesia 8(31–32): 99–432. https://doi.org/10.5962/bhl.title.45984

Wolff M, Miranda-Esquivel DR (2016) Family Tabanidae. Zootaxa 4122(1): 249–301. https://doi.org/10.11646/zootaxa.4122.1.23

ZooKeys 1084: 43–64 (2022)
doi: 10.3897/zookeys.1084.69767
https://zookeys.pensoft.net

RESEARCH ARTICLE

A peer-reviewed open-access journal
ZooKeys
Launched to accelerate biodiversity research

# Japanese *Tetramorium* queens: identification key and species diagnoses (Hymenoptera, Formicidae, Myrmicinae)

Seiki Yamane[1], Shingo Hosoishi[2], Fuminori Ito[3]

**1** *Haruyama-chô, Kagoshima-shi 899–2704, Japan* **2** *Institute of Tropical Agriculture, Kyushu University, Motooka 744, Nishi-ku, Fukuoka 819–0395, Japan* **3** *Faculty of Agriculture, Kagawa University, Ikenobe, Miki, Kagawa Pref. 761–0795, Japan*

Corresponding author: Shingo Hosoishi (hosoishi@gmail.com)

Academic editor: Brian Lee Fisher | Received 6 June 2021 | Accepted 7 November 2021 | Published 26 January 2022

*http://zoobank.org/F1B1DAC5-901F-4C42-B694-6A437A1228DE*

**Citation:** Yamane S, Hosoishi S, Ito F (2022) Japanese *Tetramorium* queens: identification key and species diagnoses (Hymenoptera, Formicidae, Myrmicinae). ZooKeys 1084: 43–64. https://doi.org/10.3897/zookeys.1084.69767

## Abstract

In Japan, nine species have been known in the ant genus *Tetramorium*, of which five or more are considered tramps. A key to the queens of nine *Tetramorium* species found in Japan is presented. The tramp species *T. tonganum* Mayr, 1870 is excluded from the key because no queen was available for us, while *T. pacificum* Mayr, 1870 is included because it was once intercepted at a port in Japan and exotic queens were available. Diagnosis of the queen of each species is provided together with differences between the two female castes. *Tetramorium tanakai* Bolton, 1977 is resurrected from synonymy with *T. kraepelini* Forel, 1905 based mainly on the queen characters.

## Keywords

Ant, caste difference, Japan, key to species, queen, species account, stat. rev., *Tetramorium*

## Introduction

*Tetramorium* Mayr, 1855 is a large ant genus containing slightly less than 600 species worldwide, with very few native species in the New World (AntWiki 2021). Most species are found in tropical and subtropical regions of Africa, Madagascar and Asia (e.g. Bolton 1977, 1980; Hita Garcia and Fisher 2012; Agavekar et al. 2017), though one group, the *T. caespitum* (Linnaeus, 1758) complex, has developed into more than ten species in northern Eurasia (e.g. Steiner et al. 2006). Some species are common, encountered during most field surveys on ant species diversity and some others are tramps spreading over non-native areas. In spite of their ubiquity, the nesting biology of *Tetramorium* species has not been studied well and many species are known only from the worker caste. In Japan nine species have been recorded, of which at least five are considered tramps or aliens (Terayama 2020; Yoshimura 2020). Although *Tetramorium tanakai* Bolton, 1977 was synonymized with *T. kraepelini* Forel, 1905 by Japan Ant Database Group (2003), it is highly probable that it is a good species and it is resurrected from synonymy in the present paper. Species accounts for the known *Tetramorium* fauna of Japan are given by Terayama et al. (2014), based on the worker caste, but information about the queen and male is still very poor even for common species. The present paper is the first attempt to provide an identification key and morphological accounts for all the known Japanese species of the genus, except for *T. tonganum* Mayr, 1870. We include *T. pacificum* Mayr, 1870 that was once intercepted at a ferry port in Honshu. This paper is the second part of 'the queens of the Japanese ants' series; the first part dealt with the genus *Pheidole* (Yamane and Hosoishi 2020).

## Materials and methods

We tried to use queen specimens associated with workers, i.e. from colony series, for each species. Although we could examine only one queen for *T.* cf. *kraepelini* Forel, 1905, sampled by general collection, we identified it as *T.* cf. *kraepelini*, based on the key characters of the *T. kraepelini* species-complex, colouration and distribution information in Japan. As no queen of *T. tonganum*, either from Japan or outside Japan, was available, accordingly it has been omitted from the key. In the case of *T. pacificum*, not established yet in Japan, queens collected in Southeast Asia are used for the key and description. Specimens examined are deposited in the Entomological Laboratory, Kyushu University (KUEC: Fukuoka, Japan) and Seiki Yamane Collection (SKYC: Kitakyushu, Japan).

### Measurements

**TBL**: total body length roughly measured from anterior margin of head to tip of gaster; **HL**: maximum head length (in full-face view in a straight line from mid-point of anterior clypeal margin to mid-point of a transverse line spanning apices of projecting posteriormost portions of head); **HW**: maximum head width excluding eyes; **SL**: length of antennal scape; **EL**: maximum eye length (major diameter); **EW**: maxi-

mum eye width (minor diameter); **PtW**: maximum petiolar width; **PptW**: maximum postpetiole width; **CI**: cephalic index (HW divided by HL × 100); **SI**: scape index (SL divided by HW × 100); **ELI**: eye length index (EL divided by head length × 100). All measurements are expressed in mm.

## Identification and species accounts

### List of the Japanese species of *Tetramorium*

*Tetramorium bicarinatum* (Nylander, 1846) [*T. bicarinatum* group; introduced]
*Tetramorium* cf. *kraepelini* Forel, 1905 [*T. scabrosum* group; ?native]
*Tetramorium lanuginosum* Mayr, 1870 [*T. obesa* group; introduced]
*Tetramorium nipponense* Wheeler, 1928 [*T. bicarinatum* group; native]
*Tetramorium simillimum* (F. Smith, 1851) *T. simillimum* group; introduced]
*Tetramorium smithi* Mayr, 1879 [*T. angulinode* group; introduced]
*Tetramorium tanakai* Bolton, 1977, stat. rev. [*T. scabrosum* group; native]
*Tetramorium tonganum* Mayr, 1870 [*T. tonganum* group: introduced]
*Tetramorium tsushimae* Emery, 1925 [*T. caespitum* species group; native]

## Queen characters

The queens of the Japanese *Tetramorium* species, except for *T. tonganum* (queen not available) have the following character conditions in common: i) large eyes, ii) complete set of ocelli present, iii) full wings present (not confirmed in *T*. cf. *kraepelini* but distinct scars are seen at position of wing bases), iv) pronotum demarcated from mesonotum with distinct suture, v) mesonotum divided into mesoscutum and mesoscutellum, vi) notaulix absent, vii) mesopleuron divided into upper and lower portions, viii) distinctly defined metanotum and ix) metapleuron only weakly demarcated from lateral face of propodeum. In all Japanese species, the propodeal spine is moderate to well-developed and often stouter than in the worker. Ogata (1991) also provided a useful diagnosis for the queen caste of the Japanese species, but the species examined was not mentioned.

Amongst the Japanese myrmicine queens, *Tetramorium* queens are easily recognised by the following combination of the conditions: i) antennal club 3-segmented, ii) masticatory margin of mandible generally with seven teeth, iii) lateral portion of clypeus raised into sharp ridge that constitutes part of wall defining antennal insertion and iv) mid- and hind-tibiae each apically with simple spur. Important queen characters for identification of the Japanese *Tetramorium* species are listed below. Character conditions for the *T. tonganum* queen are cited from Bharti and Kumar (2012).

**Head shape.** Much broader than long: *T. tsushimae* Emery, 1925. Longer than broad or rarely almost as long as broad: other species.

**Mandibular sculpture.** Extensively smooth to superficially sculptured, shiny: *T. pacificum*, *T. smithi*. Almost entirely finely and densely striate, mat: other species.

**Antennal segments.** 11: *T. smithi*. 12: other species.

**Sculpture on antennal scrobe.** Of the same type as in surrounding areas: *T. tsushimae*. Simpler and weaker than in surrounding areas: other species.

**Anterior margin of clypeus.** Medially notched or impressed: *T. bicarinatum*, *T. nipponense*, *T. pacificum*. Entire: other species.

**Sculpture on mesonotum.** Principally puncto-reticulate, rugae if any wavy or indistinct: *T. lanuginosum*. Principally longitudinally striate/rugose: other species.

**Lower portion of mesopleuron.** Densely punctate or striate and mat: *T. simillimum* (punctate), *T. tsushimae* (striate). More or less shiny, with weak or superficial sculpture: other species.

**Petiolar length.** Very short; dorsal face seen from above 1/6 to 1/5 as long as broad: *T. tsushimae*. Much longer; dorsal face seen from above much more than 1/5 as long as broad: other species.

**Shape of petiolar node in profile view.** Anterior and dorsal faces confluent with continuous curve (Fig. 1a): *T. pacificum*. Dorsal face curving into posterior face without distinct angle between them (Fig. 1b): *T. lanuginosum*, *T. tonganum*. Anterior and posterior slopes more or less parallel and dorsum of node flat to weakly convex (Fig. 1c, d): other species except for *T. tsushimae* (Fig. 1e) (see above).

**Waist sculpture.** Dorsum of petiole or postpetiole, or both extensively smooth and shiny: *T.* cf. *kraepelini*, *T. smithi*, *T. tanakai*. Dorsum of petiole and postpetiole entirely densely sculptured: other species (in *T. tonganum* postpetiole dorsum almost smooth).

**Basal portion of gastral tergite 1** (abdominal tergite 4). Basal 1/6–1/3 of the tergite longitudinally striate (Fig. 1f): *T. bicarinatum*, *T. nipponense*, *T. pacificum*. Basal 1/3 micropunctate or microsculptured (sculpture can be superficial) and mat or weakly shiny (Fig. 1g): *T. simillimum*. Entire tergite essentially smooth and shiny (Fig. 1h): other species (in *T. tsushimae* this part is sometimes very superficially microsculptured, but this species is easily separable from others in other characters, see above).

**Body pilosity.** Bifid and trifid hairs present on dorsal body: *T. lanuginosum*. All body hairs simple: other species.

**Pilosity on antennal scape and mid- and hindtibiae.** Erect and suberect hairs abundant (in aged foundresses, hairs can be partly missing) (Fig. 1i, l): *T.* cf. *kraepelini*, *T. tanakai*. Principally decumbent or appressed, but variable (hairs on antennal scape can be near suberect, those on tibiae less frequently suberect) (Fig. 1j, m): *T. bicarinatum*, *T. nipponense*, *T. pacificum*, *T. tonganum*. All hairs decumbent or appressed (Fig. 1k, n): *T. lanuginosum*, *T. simillimum*, *T. smithi*, *T. tsushimae*.

For the wing venation in the Japanese species of *Tetramorium*, see Ogata (1991).

## Key to Japanese species (queens) excluding *T. tonganum*

1 Basal 1/6–1/3 of gastral tergite 1 (abdominal tergite 4) with fine longitudinal striae (Fig. 1f) or micropunctures that are sometimes superficial; sculptured area mat or weakly shiny (Fig. 1g) ..... **2**

– Entire gastral tergite 1 (abdominal tergite 4) essentially smooth; punctures very sparse and cuticular surface shiny (microsculpture if any confined to extreme basal area) (Fig. 1h) ..... **5**

2 Gastral tergite 1 basally with micropunctures and mat (sometimes weakly shiny) (Fig. 1g). Erect hairs on dorsum of head and mesosoma not tapering apicad, some with truncate apex. Anterior clypeal margin entire..... ***T. simillum***

– Gastral tergite 1 longitudinally striate at base (Fig. 1f). Erect hairs on dorsum of head and mesosoma tapering apicad, some with pointed apex. Anterior clypeal margin medially with small notch or impression ..... **3**

3 Mandible extensively smooth. Petiolar node longer, with anterior slope gentle, curving into petiolar dorsum (Fig. 1a). Body dark reddish-brown (Fig. 2e). (Japanese specimen not available) ..... ***T. pacificum***

– Mandible entirely striate. Petiolar node shorter, with anterior slope almost vertical (Fig. 1c). Body yellowish-brown to brown often with darker gaster (Fig. 2a).... **4**

4 Petiole in profile with almost flat dorsal outline; its posterior slope generally straight (Fig. 1c). Propodeum with 2–3 strong transverse carinae between propodeal spines. Gaster blackish-brown ..... ***T. bicarinatum***

– Petiole in profile with shallowly convex dorsal outline; its posterior slope often shallowly concave. Transverse propodeal carinae absent or very weak (at most only one distinct carina present). Gaster yellowish-brown to brown .... ..... ***T. nipponense***

5 Larger species with total body length 5.5–6 mm. Entire body dark brown to blackish (Fig. 3c). Petiolar node in profile very short (thin), without distinct dorsal face, with rounded apex (Fig. 1e)..... ***T. tsushimae***

– Smaller species with total body length less than 4 mm. Body yellowish-brown to brown, sometimes with much darker gaster. Petiolar node in profile longer (thicker), generally with more or less distinct dorsal face (in *T. lanuginosum* dorsal face confluent to posterior declivity with smooth curve) (Fig. 1b, d)..... **6**

6 Dorsum of head and mesosoma with many bifid and fewer trifid erect hairs. Petiolar node in profile view longer than high, of peculiar shape, namely dorsum smoothly continuous to posterior declivity. Dorsum of both petiole and postpetiole without smooth area ..... ***T. lanuginosum***

– Dorsum of head and mesosoma without bifid/trifid erect hairs. Petiolar node in profile shallowly convex dorsally or flat, as long as or shorter than high. Dorsum of petiole or postpetiole or both with smooth area ..... **7**

7 Antenna 11-segmented. Antennal scape and mid- and hind-tibiae without erect hairs; hairs appressed, decumbent or at most weakly suberect. Posterior declivity of propodeum without transverse carinae..... ***T. smithi***

– Antenna 12-segmented. Antennal scape and mid- and hind-tibiae with many suberect to erect hairs (Fig. 1i, l). Posterior declivity of propodeum with some transverse carinae ..... **8**

8 Body entirely yellowish-brown (Fig. 2b). Posterior ocelli separated from each other by less than 2.5× ocellar diameter (Fig. 1p). Petiole in profile with anterodorsal corner rather sharply angled..... ***T.* cf. *kraepelini***

– Body entirely dark reddish-brown (Fig. 3b). Posterior ocelli widely separated from each other by 4.5× ocellar diameter (Fig. 1o). Petiole in profile with anterodorsal corner more roundly angled..... ***T. tanakai***

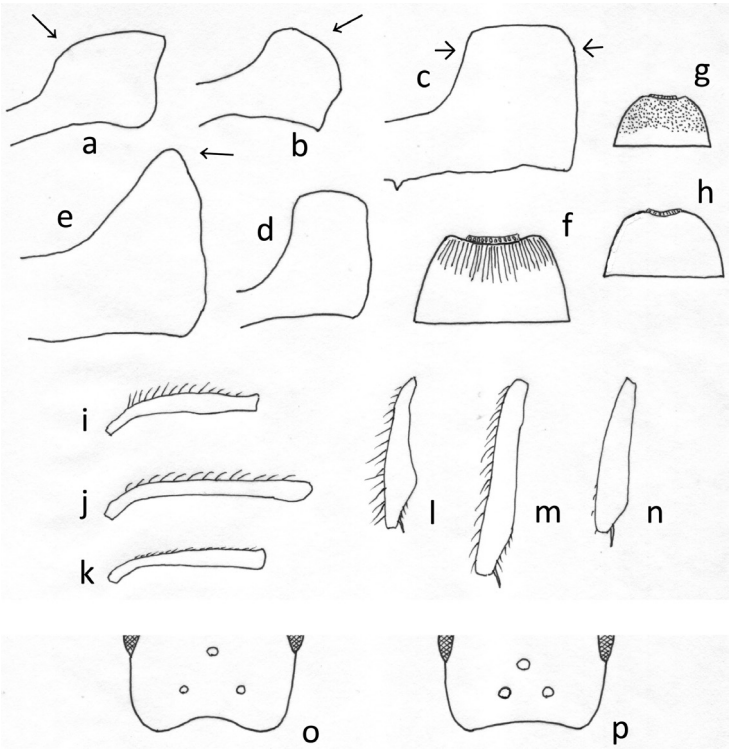


**Figure 1.** Some important characters used in the key to species **a–e** petiole in profile view **a** *T. pacificum* **b** *T. lanuginosum* **c** *T. bicarinatum* **d** *T. smithi* **e** *T. tsushimae* **f–h** anterior half of first gastral tergite **f** *T. bicarinatum* **g** *T. simillimum* **h** *T. lanuginosum* **i–k** antennal scape showing pilosity on its anterior margin **l–n** left hindtibia **i, l** *T.* cf. *kraepelini* **j, m** *T. nipponense* **k, n** *T. simillimum* **o, p** configuration of ocelli **o** *T. tanakai* **p** *T.* cf. *kraepelini*.

## Species accounts

***Tetramorium bicarinatum*** **(Nylander, 1846)**
Figs 1c, 2a, 4a, 5a

**Queen diagnosis.** Measurements (n = 5): TBL 3.9–4.9 (4.4), HL 1.04–1.09 (1.06), HW 0.9–0.95 (0.94), SL 0.64–0.70 (0.68), EL 0.28 (0.28), EW 0.23–0.26 (0.24), PtW 0.39–0.42 (0.41), PptW 0.50–0.52 (0.51), CI 85.7–91.6 (89.0), SI 67.1–75.5 (71.8), ELI 25.7–26.9 (26.5). Head and mesosoma yellowish-brown; gaster blackish-brown. Dorsum of head between frontal carinae with distinct rugae that are weakly waved. Clypeus with three longitudinal carinae; anterior margin with median notch (impression). Vertex, temple, gena, pronotum and nodes of petiole and postpetiole coarsely reticulate. Mandible densely striate. Antennal scape with long decumbent/suberect hairs. Mesonotum covered with rather regular longitudinal rugae. Posterior declivity of propodeum with 2–3 distinct transverse carinae between propodeal spines.

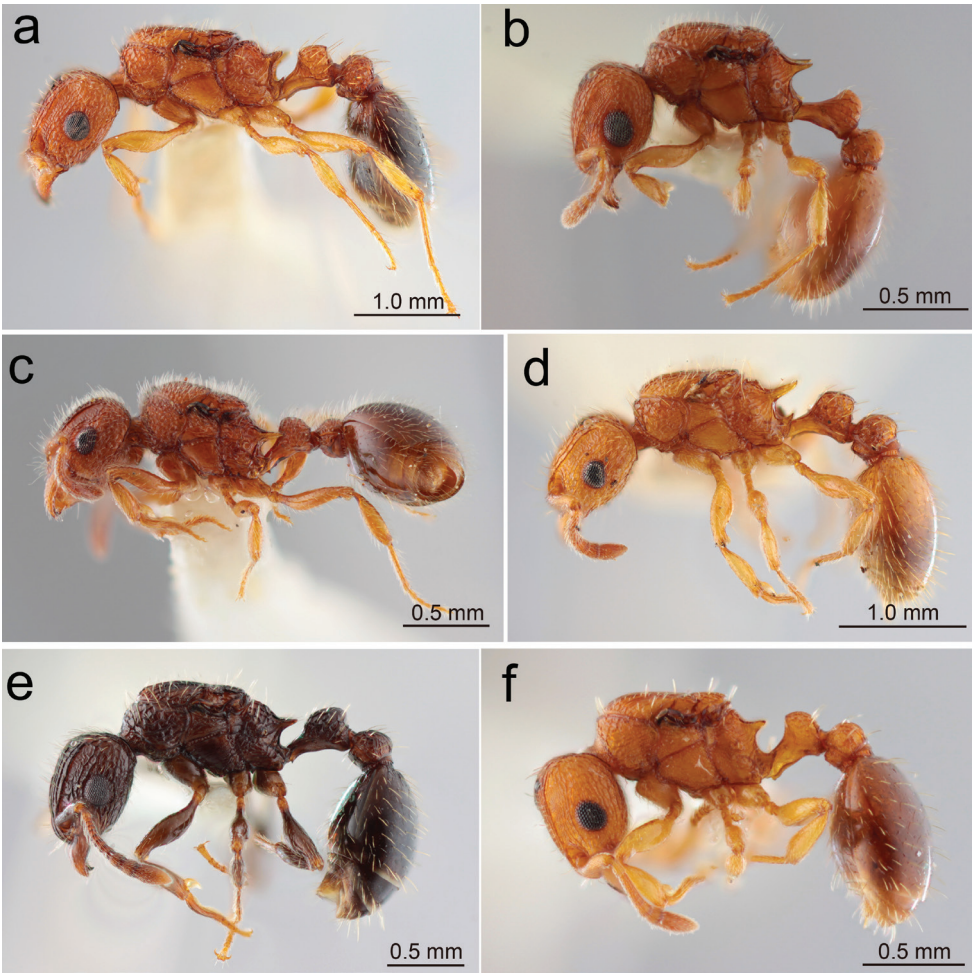


**Figure 2.** Japanese *Tetramorium* queens: habitus in profile view **a** *T. bicarinatum* (Nagashima, Kagoshima-ken, Kyushu) **b** *T.* cf. *kraepelini* (Itoman, Okinawa-jima, Okinawa-ken) **c** *T. lanuginosum* (Komi, Iriomote-jima, Okinawa-ken) **d** *T. nipponense* (Umi-jinja, Shikano-shima, Fukuoka-shi) **e** *T. pacificum* (Upper Thompson Nature Park, Singapore) **f** *T. simillimum* (Yoron-jima, Amami Is., Kagoshima-ken). (Same specimens were used for 'head in full-face view' and 'habitus in dorsal view').

Dorsum of petiole and postpetiole coarsely reticulate. Gastral tergite 1 with fine, dense longitudinal striae at base.

**Caste difference.** Worker measurements (n = 5): TBL 2.5–3.3 (3.0), HL 0.83–0.94 (0.88), HW 0.7–0.8 (0.74), SL 0.56–0.61 (0.58), EL 0.18–0.21 (0.19), EW 0.16–0.18 (0.17), PtW 0.24–0.28 (0.26), PptW 0.31–0.37 (0.34), CI 81.9–85.3 (84.1), SI 76.3–81.4 (79.1), ELI 20.9–22.7 (21.8). Worker much smaller than the queen. Eye smaller; distance between mandibular base and anterior margin of eye longer than major diameter of eye; in the queen, the distance as long as or shorter than major diameter of eye. Mandible more weakly striate and more shiny than in

the queen. Entire dorsum of mesosoma puncto-reticulate; in the queen mesonotum longitudinally rugose. Propodeal spine slender and always up-curved apically; in the queen it tends to be more strongly sclerotised, relatively shorter, with broader base than in the worker and apex not distinctly up-curved. Long hairs on antennal scape and mid- and hind-tibiae frequently near suberect; in the queen, these hairs less frequently near-suberect.

**Specimens examined.** Kyushu mainland: 2q (dealate), Kyushu Univ. Hakozaki Campus, Fukuoka-shi, emerged from colony collected in ix. 2015 by M. Obika and kept in lab; 1q (dealate), Hongôkitakata, Miyazaki-shi, 21.vii.2020, Sk. Yamane & G. Mita; 1q (dealate), Naga-shima, Kagoshima-ken, 31.vii.1979, K. Ogata (Figs 2a, 4a, 5a); 4q (dealate), Kagoshima Univ. Kôrimoto Campus, Kagoshima-shi, 7.vi.2005, rotting log, Sk. Yamane leg. (JP05-SKY-101); 1q (winged), Kamitaniguchi, Kagoshima-shi, 16.ix.2008, attracted to light, Sk. Yamane leg. N. Ryukyus: 1q (dealate), Nakano-shima, Tokara Islands, 31.iii.1991, Y. Yamanouchi leg. C. Ryukyus: 2q (dealate), Takabaru, Yoro-shima, Amami Islands, 2.vii.2015, dead stem on tree, Sk. Yamane leg. (JP15-SKY-34); 1q (dealate), Shuri, Okinawa-jima, 17.vii.2020, in house, Y. Kusui leg.

**Distribution in Japan.** Honshu (Pacific coast), Shikoku, Kyushu, throughout the Nansei Islands, Ogasawara Islands and Iwô Islands (Terayama et al. 2014).

**Remarks.** *Tetramorium bicarinatum* is an alien tramp species found in disturbed areas in warmer regions of the world except in Africa. It belongs to the *T. bicarinatum* species group (Bolton 1977) together with *T. nipponense* in Japan. In the queen this species is most similar to *T. nipponense*, which inhabits forests, preferring wetter conditions. The possession of 2–3 transverse carinae between the propodeal spines is an important characteristic in distinguishing the two species; in *T. nipponense* these carinae are lacking or much weaker (at most one distinct carina present). Furthermore, the propodeal spine is straight throughout its length in *T. bicarinatum*, while it tends to have a slightly up-curved apex in *T. nipponense*. New queens are attracted to light.

### *Tetramorium* cf. *kraepelini* Forel, 1905

Figs 1i, lp, 2b, 4b, 5b

**Queen diagnosis.** Measurements (n = 1): TBL 2.7, HL 0.64, HW 0.58, SL 0.38, EL 0.21, EW 0.16, PtW 0.23, PptW 0.28, CI 90.6, SI 65.5, ELI 32.8. Body yellowish-brown. Frons between frontal carinae with weak longitudinal rugae. Clypeus with some weak longitudinal carinae; anterior margin of clypeus without median notch. Eye large, 2 times as long as distance between anterior margin of eye and mandibular base. Distance between posterior ocelli less than 2.5× ocellar diameter. Vertex, temple including posterolateral corner of head, dorsum of pronotum puncto-reticulate. Entire mesonotum with dense and longitudinal rugae; dorsum of propodeum longitudinally rugose, continuous to anterior margin of posterior declivity that is weakly transversely striate. Lateral face of pronotum and upper portion of mesopleuron distinctly striate; lower portion of mesopleuron only superficially sculptured and shiny. Petiole with

strong carinae on lateral face, superficially sculptured and weakly shiny on dorsum; dorsum of postpetiole smooth and shiny. Gastral tergite 1 basally without carinae, smooth. Antennal scape and mid- and hind-tibiae with erect/suberect hairs.

**Caste difference.** Worker measurements (n = 5): TBL 2.0–2.1 (2.1), HL 0.58–0.61 (0.60), HW 0.53–0.55 (0.54), SL 0.35–0.38 (0.36), EL 0.14–0.16 (0.15), EW 0.09–0.10 (0.10), PtW 0.17–0.18 (0.18), PptW 0.19–0.23 (0.22), CI 88.3–90.2 (90), SI 65.5–69.1 (67.3), ELI 23.7–26.2 (25.1). Worker smaller than the queen. In the worker, head more extensively reticulate, leaving area behind clypeus longitudinally rugose. Eye smaller than in the queen, as long as or only slightly longer than distance between anterior eye margin and mandibular base. Eye strongly converging anteriad; in the queen, eye broadly rounded anteriorly. Mesosomal dorsum entirely densely reticulate; in the queen, mesonotum with dense longitudinal striae. In the worker, both petiole and postpetiole dorsum smooth and shiny.

**Specimens examined.** C. Ryukyus: 1q (dealate), Itoman, Okinawa-jima, 18.viii.1991, Y. Yamanouchi leg. (Figs 2b, 4b, 5b).

**Distribution in Japan.** Kyushu and throughout the Nansei Islands (Terayama et al. 2014).

**Remarks.** *Tetramorium* cf. *kraepelini* belongs to the *T. scabrosum* group (sensu Bolton 1977). The so-called *T. kraepelini* can be a complex of sibling species. As only one queen was available for examination the variation in structure and sculpture is unknown. One queen from a colony collected from Central Thailand and tentatively identified as *T. kraepelini* is very similar to the queen examined above; however, the distance between the posterior ocelli is slightly longer than in the Japanese form.

### *Tetramorium lanuginosum* Mayr, 1870

Figs 1b, h, 2c, 4c, 5c

**Queen diagnosis.** Measurements (n = 5): TBL 2.5–3 (2.7), HL 0.69–0.73 (0.71), HW 0.69–0.73 (0.7), SL 0.45–0.5 (0.46), EL 0.2–0.21 (0.2), EW 0.16–0.18 (0.17), PtW 0.27–0.28 (0.28), PptW 0.29–0.3 (0.29), CI 95.9–101.4 (98.6), SI 61.6–72.5 (65.9), ELI 27.4–30.4 (28.7). Body yellowish-brown, with gaster much darker. Head almost as long as broad. Frons medially with longitudinal rugae; other portions of head puncto-reticulate. Clypeus irregularly and superficially sculptured and shiny, with median carina. Eye large; distance between anterior eye margin and mandibular base much shorter than half eye length. Pronotum, mesonotum, lateral mesosoma, except for lower portion of mesopleuron and petiolar and postpetiole nodes puncto-reticulate except for lower portion of mesopleuron rather shiny (mesoscutum may have rather distinct longitudinal rugae). Peduncle of petiole smooth and shiny; dorsal face of petiole not defined, smoothly continuous to declivity; subpetiolar process almost missing. Gastral tergite 1 without longitudinal carinae at base. Vertex and mesosoma with many bifid and fewer trifid erect hairs; these hairs much fewer on gastral tergites.

**Caste difference.** Worker measurements (n = 5): TBL 2.1–2.6 (2.4), HL 0.64–0.68 (0.65), HW 0.6–0.65 (0.62), SL 0.43 (0.43), EL 0.14–0.15 (0.15), EW 0.09–0.11 (0.1), PtW 0.18–0.23 (0.21), PptW 0.23–0.25 (0.24), CI 93.8–98.4 (95.4), SI 66.2–71.7 (69.2), ELI 22.1–23.4 (22.7). Worker consistently smaller than the queen. Head only slightly longer than broad in the worker. In the worker, dorsum of head rather extensively reticulate, with weak longitudinal rugae, and mesosomal dorsum densely reticulate, completely lacking rugae; in the queen, at least some rugae recognised on mesonotum. Lateral face of mesosoma entirely sculptured; in the queen, lower portion of mesopleuron more or less smooth and shiny. Eye smaller, only slightly longer than distance between anterior eye margin and mandibular base; in the queen, eye distinctly longer than the distance. Bifid hairs denser on gastral tergite 1 than in the queen.

**Specimens examined.** C. Ryukyus: 11q (2 dealated, 9 winged), Takabaru, Yoro-jima, Amami Islands, 2.vii.2015, rotting branch on ground, Sk. Yamane leg. (JP15-SKY-27); 4q (3 winged, 1 dealate), Suehiro Park, Shuri, Okinawa-jima, Okinawa Is., emerged from colony (FI19–25) collected on 11.iii.2019 from soil and reared in lab. S. Ryukyus: 5q (winged), Ishigaki-jima, Yaeyama Is., emerged from colony (FI19–15) collected on 7.ii.2019 from under stone in forest and reared in lab; 1q (dealate), Komi, Iriomote-jima, Yaeyama Is., 16.v.1979, K. Ogata leg. (Figs 2c, 4c, 5c); 7q (4 winged, 3 dealate), Inbi-dake, Yonaguni-jima, Yaeyama Is., emerged from colony (FI15–96) collected on 7.xi.2015 from decayed wood in forest and reared in lab.

**Distribution in Japan.** Nansei Islands. The northern limit lies in Kuchinoerabu-jima and Tanega-shima of the Ôsumi Islands (Yamane and Fukumoto 2017).

**Remarks.** *Tetramorium lanuginosum* belongs to the *T. obesa* species group of the former '*Triglyphothrix* Forel, 1890' (Bolton 1976). This group is characterised by the mixture of simple and bifid hairs on the body, with fewer or no trifid hairs. *Tetramorium lanuginosum* queens have many bifid hairs on the head and mesosoma (very few on gastral tergite 1), but trifid hairs are absent on the gaster and fewer on head and mesosoma. This species is easily distinguished in both the worker and queen by the presence of bifid and trifid hairs on the body, erect hairs on the antennal scape and mid- and hind-tibiae and the petiole without distinction of the dorsum from posterior declivity.

### *Tetramorium nipponense* Wheeler, 1928

Figs 1j, m, 2d, 4d, 5d

**Queen diagnosis.** Measurements (n = 5): TBL 3.5–4 (3.8), HL 0.83–0.86 (0.85), HW 0.69–0.76 (0.72), SL 0.54–0.58 (0.56), EL 0.23–0.25 (0.24), EW 0.18–0.2 (0.19), PtW 0.28–0.33 (0.3), PptW 0.36–0.41 (0.39), CI 82.4–88.4 (85.1), SI 74.7–80 (77.6), ELI 27.1–29.8 (28.1). Body yellowish-brown, with gaster slightly darker; coxae, femora and tibiae of all legs creamy yellow. Head distinctly longer than broad. Head reticulate, except for frons between clypeus and ocellar area with a few longitudinal carinae; clypeus superficially sculptured and shiny, with three longitudinal carinae. Mandible densely striate. Pronotal dorsum coarsely reticulate; mesonotum longitudinally

striate/rugose; propodeum irregularly sculptured and shiny; transverse carinae between propodeal spines absent or weak (at most only one distinct carina present). Lateral face of mesosoma coarsely rugose except for lower portion of mesopleuron weakly sculptured; propodeal spine slender, often weakly up-curved apically. Nodes of petiole and postpetiole entirely puncto-reticulate. Gastral tergite 1 with longitudinal basal striae. Antennal scape and mid- and hind-tibiae with many decumbent to near suberect hairs.

**Caste difference.** Worker measurements (n = 5): TBL 2.8–3.0 (2.9), HL 0.74–0.79 (0.77), HW 0.63–0.7 (0.66), SL 0.49–0.55 (0.53), EL 0.16–0.18 (0.17), EW 0.12–0.14 (0.13), PtW 0.23–0.26 (0.25), PptW 0.28–0.33 (0.30), CI 84.0–88.6 (86.4), SI 75.4–85.7 (80.2), ELI 24.6–27.3 (25.9). Worker very similar to the queen in coloration, structure and sculpture, with the following differences. Body smaller. Eye smaller, distance between anterior margin of eye and mandibular base slightly longer than major diameter of eye; in the queen, the distance slightly shorter than major diameter of eye. Dorsum of mesosoma entirely coarsely reticulate; in the queen, mesonotum with longitudinal rugae/striae that are dense and often irregular. Lower portion of mesopleuron sculptured and slightly mat; in the queen, lower portion with much weaker sculpture and shiny. Propodeal spine up-curved in apical 1/3; in the queen, the spine tending to be straighter throughout. Petiole tends to be longer than in the queen. Long hairs on antennal scape and mid- and hind-tibiae frequently near-suberect; in the queen, these hairs less frequently near suberect.

**Specimens examined.** Kyushu: 1q (dealate), Umi-jinja, Shikano-shima, Fukuoka-shi, 15.ix.1980, K. Ogata leg. (Figs 2d, 4d, 5d); 6q (winged), Yoshino-chô, Kagoshima-shi, 7.ix.2016, attracted to light, T. Tsukada leg.; 3q (dealate), Kenkôno-mori, Inusako-chô, Kagoshima-shi, 20.iv.2019, dry dead twig on ground, Sk. Yamane leg. (JP19-SKY-022); 3q (dealate), near Hetsuka, Minamiôsumi-chô, Kagoshima-ken, 23.vii.2020, nest under moss, Sk. Yamane leg. (JP20-SKY-069). N. Ryukyus: 1q (dealate), Tashiro-Yumugi, Kuchinoerabu-jima, Ôsumi Islands, 26.vii.2016, nest in dead sasa bamboo, Sk. Yamane leg. (JP16-SKY-70); 2q (dealate), Maeda, Kuchinoerabu-jima, in dead twig on ground, Sk. Yamane leg. (JP16-SKY-120). C. Ryukyus: 1q (dealate), Nagakumo, Tatsugô-chô, Amami-ôshima, Amami Islands, 22.xii.2015, in decayed wood, Sk. Yamane leg. (JP15-SKY-72); Takahachi-yama, Amami-ôshima, 5.iii.2017, in decayed wood, Sk. Yamane leg. (JP17-SKY-20); 7q (winged), Chinase, Naze, Amami-ôshima, 28.viii.2019, attracted to light, K. Kanai leg.; 3q (2 winged, 1 dealate), Yonaha, Okinawa-jima, 5.vii–5.viii.2001, Malaise trap, T. Muroi & C. Nakamura.

**Distribution in Japan.** Honshu (southern coast), Shikoku, Kyushu, throughout Nansei Islands, Senkaku Islands.

**Remarks.** *Tetramorium nipponense* belongs to the *T. bicarinatum* species group (Bolton 1977) together with *T. bicarinatum* in Japan. The gaster is generally much paler in colour than in the latter. The shape of the petiole that is frequently used to distinguish between these species in the worker caste is not very useful in the queen, though in *T. nipponense* the petiole tends to be longer and have a weakly convex dorsal face (for further discussion, see *Remarks* under *T. bicarinatum*). Queens of this species are frequently attracted to light and also caught with Malaise traps.

***Tetramorium pacificum* Mayr, 1870**
Figs 1a, 2e, 4e, 5e

**Queen diagnosis.** Measurements (n = 3; material from Southeast Asia): TBL 3.5–3.8 (3.6), HL 0.81–0.86 (0.84), HW 0.70–0.74 (0.73), SL 0.53–0.55 (0.54), EL 0.21–0.23 (0.22), EW 0.16–0.18 (0.17), PtW 0.28–0.30 (0.29), PptW 0.35–0.37 (0.36), CI 86.0–88.1 (86.8), SI 71.6–75.7 (73.9), ELI 24.4–28.4 (26.7). Body brown to dark reddish or blackish-brown. Head in full-face view longer than broad, with almost parallel lateral margins. Frons sparsely longitudinally rugose with interspaces superficially sculptured and often shiny; other portions of head puncto-reticulate; antennal scrobe densely but weakly sculptured and rather shiny. Clypeus with three parallel longitudinal carinae; its anterior margin medially impressed but more weakly than in *T. bicarinatum* and *T. nipponense*. Mandible very superficially sculptured or almost smooth and shiny. Pronotal dorsum puncto-reticulate; mesonotum with parallel longitudinal rugae that are often wavy or irregular; dorsum and lateral face of propodeum puncto-reticulate or irregularly coarsely sculptured; remaining portions of mesosoma mainly striate to rugose but lower portion of mesopleuron generally smoother and shiny. Petiole in profile long; its node longer than high, with anterior slope gentle and not clearly separable from dorsum and steep posterior slope; petiole and postpetiole both dorsally and laterally distinctly sculptured and mat. Basal 1/3 or more of gastral tergite 1 covered with distinct longitudinal striae. Antennal scape and mid- and hind-tibiae without erect hairs.

**Caste difference.** Worker measurements (n = 7; 3 specimens intercepted at Kure Port, Japan and 4 from Southeast Asia): TBL 2.9–3.6 (3.3), HL 0.83–0.95 (0.88), HW 0.70–0.81 (0.75), SL 0.53–0.64 (0.60), EL 0.16–0.20 (0.19), EW 0.13–0.14 (0.13), PtW 0.24–0.29 (0.27), PptW 0.29–0.37 (0.33), CI 83.3–87.9 (85.5), SI 75.7–82.9 (80.0), ELI 19.3–22.7 (21.3). Worker very similar to the queen, but with the following characteristics that are different from those of the latter. Body slightly, but constantly larger than in the queen in terms of HL, HL and SL, but eye size smaller than in the latter with ELI 21.3 (worker) vs. 26.7 (queen). Distance between anterior eye margin and mandibular base distinctly longer than major diameter of eye; in the queen, the distance as long as major diameter of eye. Entire dorsum of mesosoma coarsely puncto-reticulate; in the queen mesonotum longitudinally rugose. Mesopleuron entirely with dense minute punctures; in the queen, lower portion of mesopleuron rather smooth and sculpture in upper portion weak.

**Specimens examined.** No Japanese specimen available. A dealate queen collected in Upper Thompson Nature Park, Singapore on 9.xii.2017 by Sk. Yamane was used for photos (Figs 2e, 4e, 5e).

**Distribution in Japan.** Not established in Japan.

**Remarks.** *Tetramorium pacificum* belongs to the *T. bicarinatum* group, in which the anterior margin of the clypeus is notched or impressed at the middle (Bolton 1977). Amongst the species found in Japan, this species is easily distinguished from the others by having a near-smooth mandible and the anterior and dorsal faces of the petiole confluent with a smooth curve. Workers were found in a container at Kure Port, Hyogo-ken, Honshu, transported by a ferry from Zhongshan, China via Hiroshima Port. Up to now, any established population has not yet been confirmed in Japan.

***Tetramorium simillimum* (F. Smith, 1851)**
Figs 1g, k, n, 2f, 4f, 5f

**Queen diagnosis.** Measurements (n = 4): TBL 2.3–2.6 (2.5), HL 0.60–0.63 (0.62), HW 0.53–0.58 (0.56), SL 0.39–0.43 (0.41), EL 0.17–0.18 (0.18), EW 0.13 (0.13), PtW 0.20–0.23 (0.22), PptW 0.25–0.28 (0.27). Body yellowish-brown, with darker gaster and light brown to yellow legs. Dorsum of head with dense and longitudinal striae that are regular and parallel; interspaces microsculptured and mat. Clypeus with strong median carina; other longitudinal carinae weak, indistinct; anterior margin entire. Distance between anterior eye margin and mandibular base distinctly shorter than major diameter of eye. Dorsum of mesosoma entirely sculptured; pronotum reticulate, with anterolateral corner angulate; entire mesonotum densely with longitudinal striae; in profile lateral face of mesosoma entirely sculptured; upper portion of mesopleuron rugose and lower portion densely punctate (sometimes punctation weak). Propodeum with longitudinally puncto-striate dorsum and transversely puncto-striate declivity, entirely mat, without transverse carinae between propodeal spines; propodeal spine short, apically blunt, only slightly longer than metapleural lobe. Petiolar node anteriorly sharply truncate; petiole and postpetiole entirely sculptured; ventre of petiolar peduncle superficially sculptured and weakly shiny; nodes of both petiole and postpetiole coarsely punctured. Gastral tergite 1 in basal 1/3 densely and minutely punctate or coriaceous, mat or weakly shiny. Antennal scape and mid- and hind-tibiae without erect hairs. Erect body hairs not tapering apicad, apically often truncate or blunt.

**Caste difference.** Worker measurements (n = 5): TBL 1.8–2.1 (1.9), HL 0.53–0.59 (0.56), HW 0.45–0.53 (0.49), SL 0.33–0.39 (0.36), EL 0.11–0.13 (0.12), EW 0.08–0.09 (0.08), PtW 0.16–0.18 (0.17), PptW 0.19–0.23 (0.21), CI 83.3–89.8 (87.4), SI 71.7–77.6 (74.6), ELI 20.0–22.6 (21.1). Worker very similar to the queen, but with the following differences. Body smaller than in the queen. Distance between anterior eye margin and mandibular base as long as or slightly longer than major diameter of eye; in the queen, the distance much shorter than major eye diameter. Mesonotum coarsely rugoso-reticulate, rugae wavy and irregular; in the queen striae fine and regular. Gastral tergite 1 entirely smooth and shiny; in the queen basal area of the tergite micropunctured and mat (sometimes microsculpture very faint and cuticle weakly shiny). Apical truncation of erect hairs on head and mesosoma more distinct; in the queen, erect hairs often not typically truncate.

**Specimens examined.** C. Ryukyus: 1q, (dealate), Nagahama-chô, Naze, Amami-ôshima, 17.vi.2017, in dead twig on ground, F. Ito leg.; 1q (dealate), same loc., date and nesting site, F. Ito (FI17–102); 2q (dealate), Yoron-jima, 28.v–2.vi.1999 (Figs 2f, 4f, 5f).

**Distribution in Japan.** Nansei Islands, Ogasawara Islands, Volcano Island. Northern limit lies in Kodakara-jima of the Tokara Islands (Yamane and Fukumoto 2017).

**Remarks.** *Tetramorium simillimum* belongs to the *T. simillimum* species group (Bolton 1977). In the queen, it is easily distinguished from other Japanese congeners by the following character conditions: i) dorsum of head with regular longitudinal striae, with interspaces densely sculptured and mat; ii) erect body hairs not sharply pointed apically; iii) petiole anteriorly truncate, with dorsal face clearly separated from

anterior slope with sharp angle; iv) basal 1/3 of gastral tergite 1 micropunctate or coriaceous and mat (sometimes weakly shiny). This species is a famous tramp of African origin (Bolton 1977; Yoshimura 2020).

### *Tetramorium smithi* Mayr, 1879

Figs 1d, 3a, 4g, 6a

**Queen diagnosis.** Measurements (n = 2): TBL 3.4/3.1, HL 0.73/0.74, HW 0.70/0.71, SL 0.43/0.43, EL 0.21/0.19, EW 0.17/0.17, PtW o.29/0.27, PpW 0.42/0.38, CI 95.9/95.9, SI 61.4/60.6, ELI 28.8/25.7. Head, mesosoma and waist brown to reddish-brown, with dorsum of head, antenna and legs dark brown; gaster black. Dorsum of head longitudinally rugose; other portions of head puncto-reticulate. Frontal carina strong, defining dorsal margin of antennal scrobe; antennal scrobe superficially sculptured and shiny. Clypeus with three longitudinal carinae, with anterior margin entire. Mandible superficially sculptured and shiny. Antenna with 11 segments. With mesosoma in dorsal view, pronotum sparsely transversely rugose; mesonotum and propodeal dorsum densely with longitudinal parallel rugae; propodeal declivity partly smooth, shiny; transverse carinae absent between propodeal spines; in profile view, pronotum, metapleuron and lateral face of propodeum rugose or irregularly sculptured; mesopleuron, especially on lower portion, with weaker sculpture and somewhat shiny. Petiole and postpetiole with smooth portions on their dorsum; petiolar peduncle and sternite smooth and shiny; lateral face of petiolar node and lateral and ventral faces of postpetiole sculptured; petiole ventrally with sharp longitudinal ridge throughout; postpetiole more than 1.4 times as broad as petiole in dorsal view. Gastral tergite 1 entirely smooth and shiny. Hairs on antennal scape and mid- and hind-tibiae decumbent to appressed; those on tibiae slightly approaching suberect.

**Caste difference.** Worker measurements (n = 5): TBL 2.1–2.3 (2.2), HL 0.64–0.68 (0.65), HW 0.56–0.60 (0.59), SL 0.38–0.41 (0.40), EL 0.15–0.17 (0.16), EW 0.10–0.12 (0.11), PtW 0.19–0.23 (0.21), PptW 0.28–0.30 (0.29), CI 87.5–93.8 (90.5), SI 64.4–69.5 (67.4), ELI 23.4–25.0 (24.0). Worker much smaller than the queen. Eye smaller, distance between anterior eye margin and mandibular base as long as or slightly longer than major diameter of eye; in the queen the distance much shorter than major diameter of eye. Eye anteriorly distinctly tapered; in the queen eye anteriorly broadly rounded. Pronotal dorsum rugose except for small area around anterolateral corner reticulate; in the queen pronotal dorsum coarsely reticulate. Mesonotum longitudinally rugose in both castes. Mesopleuron entirely coarsely sculptured; in the queen, sculpture weaker, especially in lower portion.

**Specimens examined.** S. Ryukyus: 1q (winged), Miyako-jima, 30.x.2019, nest in soil, on forest pass, F. Ito leg. (FI19–209); 1q (winged), Hirarahigashi, Miyako-jima, emerged on 28.vii.2020 in colony (FI19–203) collected on 29.x.2019 and kept in lab., F. Ito leg. (Figs 3a, 4g, 6a)

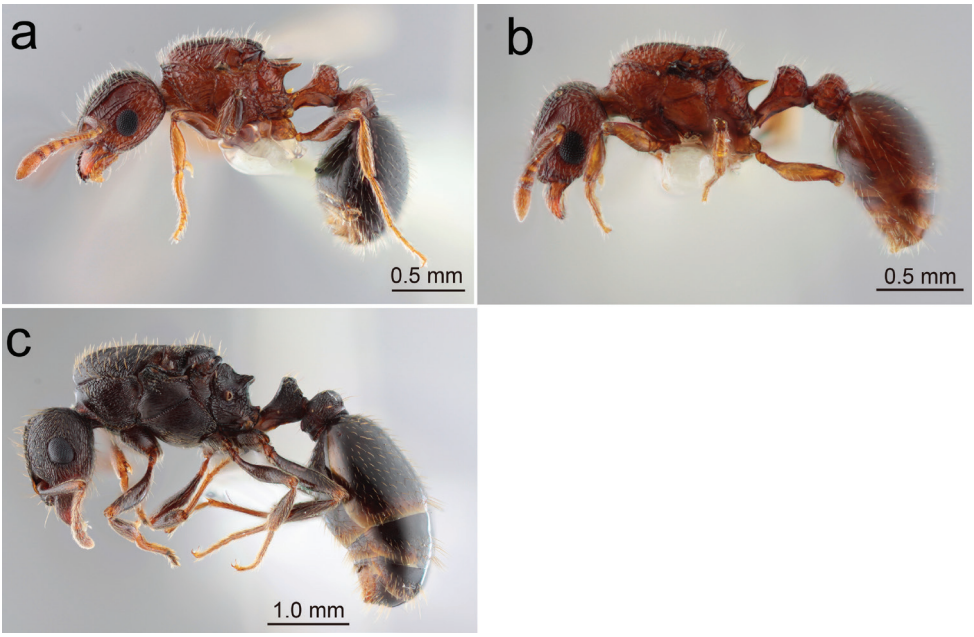


**Figure 3.** Japanese *Tetramorium* queens: habitus in profile **a** *T. smithi* (Hirarahigashi, Miyako-jima, Okinawa-ken) **b** *T. tanakai* (Mandabaru, Yonaguni-jima, Okinawa-ken) **c** *T. tsushimae* (Nokono-shima, Fukuoka-shi). (Same specimens were used for 'head in full-face view' and 'habitus in dorsal view').

**Distribution in Japan.** Nansei Islands. The northern limit lies in Okinawa-jima (Central Ryukyu Islands) (Terayama et al. 2014).

**Remarks.** *Tetramorium smithi* belongs to the *T. angulinode* species group, in which the antenna has only eleven segments in the female castes (Bolton 1977). This species is easily separated from other Japanese congeners by the reduced antennal segments (11), shiny mandible (shared by *T. pacificum*) and black gaster (shared by *T. tsushimae*). This is the only Japanese *Tetramorium* species with the mesonotum entirely regularly rugose in both female castes.

### *Tetramorium tanakai* Bolton, 1977, stat. rev.

Figs 1o, 3b, 4h, 6b

*Tetramorium tanakai* Bolton, 1977: 119–120, Mt. Omoto, Ishigaki I.; Onoyama 1980: 198; Ogata 1991: 102; Bolton 1995: 415.
*Tetramorium kraepelini*: Japanese Ant Database Group 2003: 136; Terayama 2020: 120.

**Queen diagnosis.** Measurements (n = 1): TBL 2.63, HL 0.66, HW 0.61, SL 0.40, EL 0.19, EW 0.16, PtW 0.30, CI 92.4, SI 65.6, ELI 28.8. Body brown to dark reddish-brown, with gaster very dark. Head reticulate, with frons between clypeus and ocellar

region longitudinally rugose. Clypeus with three longitudinal carinae; its anterior margin entire. Posterior ocelli widely separated from each other; distance between them as long as 4.5× ocellar diameter. Dorsum of pronotum and propodeum coarsely reticulate; mesonotum longitudinally rugose (rugae on mesoscutellum irregular); lateral face of pronotum, upper portion of mesopleuron, metapleuron and lateral face of propodeum largely striate/rugose; lower portion and part of upper portion of mesopleuron smooth to very weakly sculptured and shiny; propodeal declivity irregularly sculptured; no transverse carinae between propodeal spines. Petiolar node entirely reticulate; sternite and peduncle microsculptured and mat; postpetiole with smooth area on its dorsum; its lateral face and sternite irregularly sculptured. Gastral tergite entirely smooth and shiny. Antennal scape and mid- and hind-tibiae with many erect hairs.

**Caste difference.** Worker measurements (n = 5): TBL 2.0–2.4 (2.3), HL 0.59–0.63 (0.61), HW 0.53–0.58 (0.56), SL 0.36–0.40 (0.38), EL 0.13–0.16 (0.14), EW 0.08–0.10 (0.09), PtW 0.17–0.23 (0.20), PptW 0.20–0.25 (0.23), CI 86.4–93.2 (91.2), SI 65.5–70.6 (68.6), ELI 22.0–25.4 (23.1). Worker very similar to the queen in structure and sculpture, but differing in the following aspects. Eye smaller, distance between anterior eye margin and mandibular base as long as or slightly longer than major diameter of eye; in the queen the distance much shorter than major diameter of eye. Eye distinctly tapered anteriad; in the queen, eye anteriorly broadly rounded. Mesosomal dorsum entirely coarsely reticulate; mesonotum longitudinally rugose in the queen. Mesopleuron entirely sculptured; sculpture on mesopleuron much weaker especially in lower portion that is extensively smooth and shiny in the queen.

**Specimens examined.** S. Ryukyus: 1q (dealate), Mandabaru, Yonaguni-jima, emerged in v.2020 in colony (FI19–108) collected on 14.iii.2019 by R. Hosokawa and kept in lab (Figs 3b, 4h, 6h). 1q (dealate), Yonaha-dake, Yonaguni-jima, 12.iii.2020, F. Ito (FI20–45).

**Distribution in Japan.** Yaeyama Islands of the Ryukyu Islands (Ishigaki-jima and Yonaguni-jima).

**Remarks.** *Tetramorium tanakai* was originally described based on the worker and queen castes collected on Ishigaki-jima, Yaeyama Islands, Japan (Bolton 1977; no queen description provided). The worker is very similar to the Southeast Asian *T. kraepelini*, but is distinguished from the latter by the bicoloured body (dark brown head and gaster contrasted with lighter mesosoma, waist and legs) and the petiolar dorsum longer than the height of the tergal portion of the petiole (Bolton 1977). The workers sampled from Yonaguni-jima and examined in this study had a nearly entirely dark brown body with yellowish antennae and legs and are clearly different from extensively yellowish-brown workers of *T. kraepelini* and the Japanese *T.* cf. *kraepelini*. The dorsal length of the petiole is variable, generally as long as or slightly longer than the height of the tergal portion. The present study shows that the queen collected from Yonaguni-jima is also similar to that of *T.* cf. *kraepelini* in structure and sculpture, but clearly different from the latter in the widely separated posterior ocelli and coarsely reticulate dorsal propodeum as well as much darker body. We also examined queens and workers from two colonies collected in Shuisheliao, Taiwan. These specimens have a more typical bicolorous body and longer petiolar dorsum as in the original description of *T. tanakai*. The

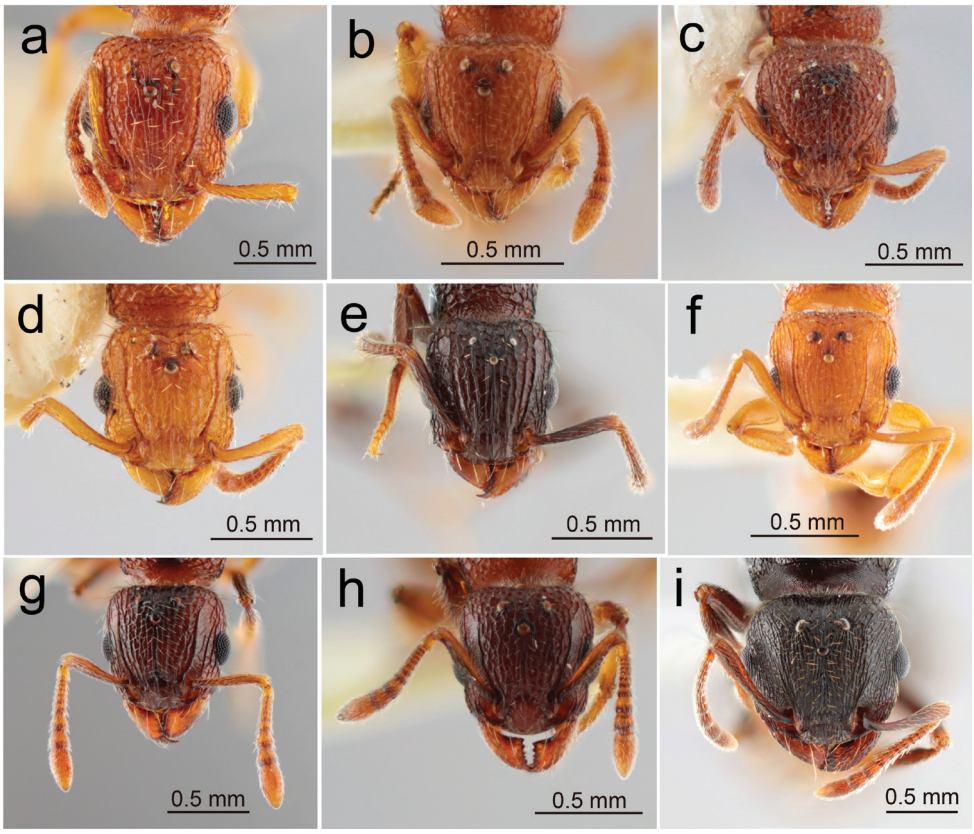


**Figure 4.** Japanese *Tetramorium* queens: head in full-face view **a** *T. bicarinatum* **b** *T.* cf. *kraepelini* **c** *T. lanuginosum* **d** *T. nipponense* **e** *T. pacificum* **f** *T. simillimum* **g** *T. smithi* **h** *T. tanakai* **i** *T. tsushimae*.

queens have widely separate posterior ocelli as in the queen from Yonaguni-jima. We consider the populations of Ishigaki-jima, Yonaguni-jima and Taiwan all belonging to the same species, *T. tanakai*. As species delimitation among the *T. kraepelini*-complex is very confusing, we need to have more colony series from various localities.

### *Tetramorium tonganum* Mayr, 1870

**Remarks.** This species is a well-known tramp distributed from New Caledonia through the Indo-Australian region to China and Japan and has been introduced to remote islands in the Pacific and Atlantic Oceans (AntWiki 2021). In Japan, it has been recorded from the Ogasawara Islands (Bolton 1977; Terayama et al. 2014). We have no queen specimen of this species from Japan or from any other country. Santschi (1924) described the queen caste, based on a single specimen collected in Samoa. However, this specimen has only one ocellus and, according to his drawing, the eye is located too posteriorly on the head for a queen of *Tetramorium*. Bharti and Kumar (2012) described

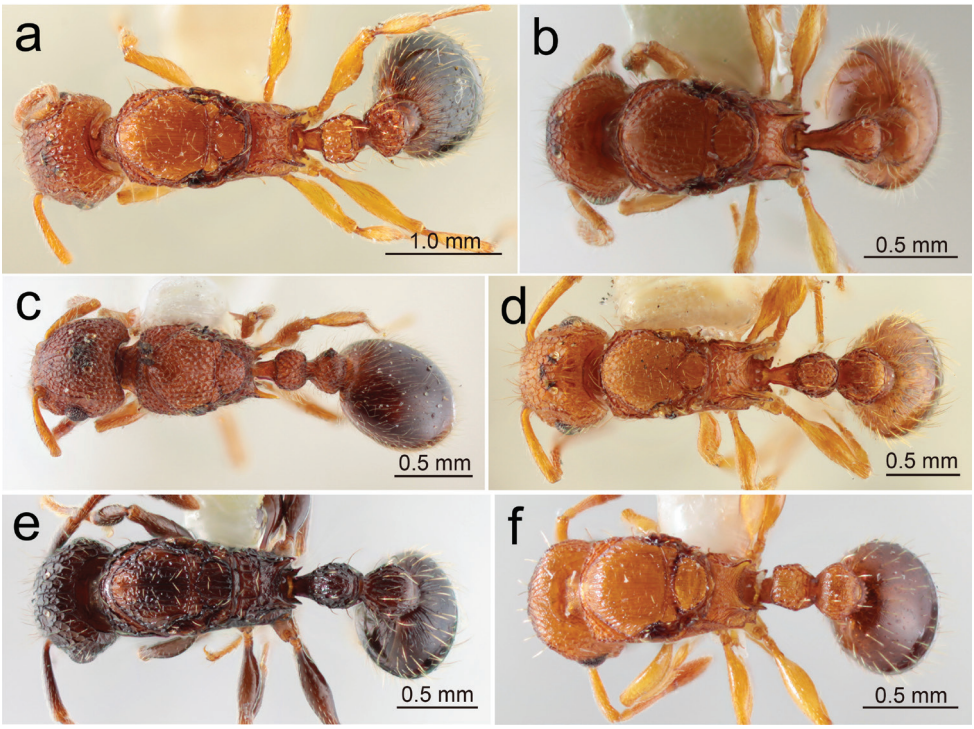


**Figure 5.** Japanese *Tetramorium* queens: habitus in dorsal view **a** *T. bicarinatum* **b** *T.* cf. *kraepelini* **c** *T. lanuginosum* **d** *T. nipponense* **e** *T. pacificum* **f** *T. simillimum*.

the queen caste of this species, based on material collected from Himachal Pradesh, India. According to their description (text and pictures), the queen of this species is recognised by the following combination of characteristics: i) anterior margin of clypeus entire, ii) no branched hairs present on body, iii) petiole in profile view with rounded anterodorsal and posterodorsal corners, iv) mid- and hind-tibiae without erect hairs, v) smooth lower portion of mesopleuron and vi) entirely smooth first gastral tergite.

### *Tetramorium tsushimae* Emery, 1925

Figs 1e, 3c, 4i, 6c

**Queen diagnosis.** Measurements (n = 5): TBL 5.9–7.0 (6.4), HL 1.14–1.18 (1.17), HW 1.24–1.31 (1.27), SL 0.79–0.90 (0.84), EL 0.33–0.35 (0.34), EW 0.25–0.28 (0.26), PtW 0.45–0.50 (0.47), PptW 0.68–0.77 (0.74), CI 108.5–110.2 (109.1), SI 62.3–70.3 (66.2), ELI 28.0–29.7 (28.9). Body dark reddish-brown to blackish-brown. Head distinctly broader than long (CI ca. 109); entire head densely and regularly striate, with reticulate area restricted. Frontal carina weak and antennal scrobe barely recognisable. Clypeus with around ten longitudinal carinae; anterior margin entire.

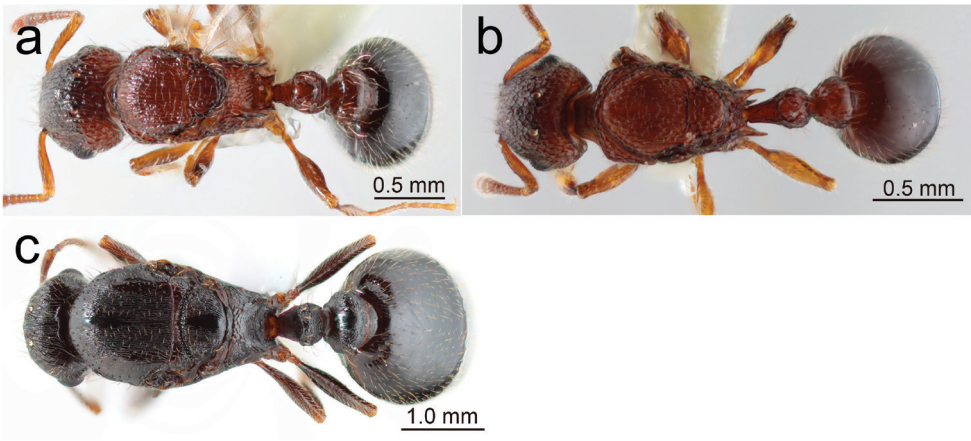


**Figure 6.** Japanese *Tetramorium* queens: habitus in dorsal view **a** *T. smithi* **b** *T. tanakai* **c** *T. tsushimae.*

Mesosoma extensively striate to rugose, with smooth areas in anteromedian portion and area along parapsidal line of mesoscutum and longitudinal median zone of mesoscutellum; sculpture on pronotum, metapleuron and lateral face of propodeum coarser than in other areas; propodeum with striation longitudinal and irregular on dorsum and dense and transverse on declivity; interspaces minutely punctate. Metapleural lobe low, generally with round apex. Petiole in dorsal view dorsum very short (often indistinct), 1/6 to 1/5 as long as broad; postpetiole very broad, 1.57× as broad as petiole. Gastral tergite 1 entirely smooth, but sometimes with very superficial sculpture near base. All erect hairs simple and more or less tapering apicad. Antennal scape and mid- and hind-tibia without erect hairs.

**Caste difference.** Worker measurements (n = 5): TBL 2.48–2.88 (2.71), HL 0.70–0.88 (0.77), HW 0.63–0.84 (0.71), SL 0.53–0.63 (0.57), EL 0.13–0.17 (0.15), EW 0.10–0.12 (0.11), PtW 0.18–0.28 (0.23), PptW 0.25–0.35 (0.29), CI 88.7–95.5 (92.1), SI 75.0–87.3 (81.1), ELI 18.1–18.3 (19.2). Worker very similar to the queen in colouration, structure, sculpture and pilosity, but differing in the following aspects: body much smaller; head longer than broad (CI ca. 92 vs. ca. 109 in the queen.); striation on mesonotum sparser and more irregular than in the queen; petiole more globular than in the queen, with rather distinct dorsum, which is in dorsal view only slightly broader than long; both petiole and postpetiole dorsally with smooth areas; in the queen almost entirely sculptured.

**Specimens examined.** Honshu: 1q (dealate), Mihagi-dai, Hagi-shi, Yamaguchi-ken, 12.x.2013, nest under stone, Sk. Yamane leg. (JP13-SKY-27); 1q (dealate), Niinohama, Heki, Nagato-shi, Yamaguchi-ken, 12.x.2013, nest under stone, Sk. Yamane leg. (JP13-SKY-28). Kyushu: 3q (dealate), Nokonoshima, Fukuoka-shi, Fukuoka-ken, 3.viii.2020, under stone, S. Hosoishi (SH20-Jpn-01) (Figs 3c, 4i, 6c); 2q (winged), Haruyama, Matsumoto-chô, Kagoshima-ken, 15.vi.2000, nest in soil, Sk. Yamane leg. (KG00-SKY-02).

**Distribution in Japan.** Hokkaido, Honshu, Shikoku, Kyushu, Ôsumi Islands, Tokara Islands. The southern limit lies in Suwanose-jima of the Tokara Islands (Yamane and Fukumoto 2017).

**Remarks.** *Tetramorium tsushimae* belongs to the *T. caespitum* species group. In the queen caste this species is easily distinguished from other Japanese congeners by the large and blackish-brown body, broad head, ill-defined antennal scrobe, presence of smooth areas on the mesonotum and very short petiole.

## Discussion

This paper is the first attempt to prepare a key to Japanese *Tetramorium* species, based on the queen and to give morphological diagnoses for them. Material is still very poor; only one or two queens were available for two species, i.e. *T.* cf. *kraepelini* and *T. tanakai*. This shortfall means that the results of this study are tentative, needing further material from colony series.

Nevertheless, we have a strong impression that *Tetramorium* queens can be sorted into species as for workers. We found some useful characters for identifying queens. For example, in the worker caste, *T. bicarinatum* is distinguished from *T. nipponense* mainly based on the relative length of erect hairs along the frontal carina (compared with maximum eye length) and the shape of the petiole. However, these characters are less reliable for the queen. The presence/absence of distinct transverse carinae between propodeal spines is more decisive, and, finally, this character has proved to be also useful for the worker caste (this has not been mentioned by previous authors including Bolton 1977). *Tetramorium tanakai* was resurrected from the synonymy with *T. kraepelini*; the worker characteristics mentioned by Bolton (1977), i.e. bicoloured body with very dark head and gaster and the long petiolar dorsum in *T. tanakai*, may be important, but in the queen caste, the configuration of the ocelli (very widely separated from each other) is quite distinctive amongst the *T. kraepelini*-complex. We have only two queens for *T. tanakai* (and one for the Japanese *T.* cf. *kraepelini*) so that our conclusion might remain tentative. However, our view would inspire further research on this difficult group over the entire Asian Region. Ocellar configuration can be a useful character for other *Tetramorium* species groups in the future when more material is amassed.

As mentioned earlier, there are many other useful queen characters. Some of them overlap with those traditionally used for workers. For example, the pilosity type on the antennal scape and mid- and hind-tibiae is generally common to both the worker and queen castes. On the other hand, the sculpture on the mesonotum in the queen is quite different from that of the worker. In most Japanese species the reticulation in the worker is replaced with longitudinal striae/rugae in the queen. Only in *T. lanuginosum* queens the rugae are irregular, mixed with reticulae. Rugose mesonotum in the worker caste is seen only in *T. smithi*. It is unknown which is more ancestral for *Tetramorium*,

reticulation or striation/rugosity. Another difference between the castes is seen in the sculpture type of the mesopleuron; in the queen it tends to be more feebly sculptured than in the worker or nearly smooth in some species.

In conclusion, we think all the Japanese species can be properly identified also in the queen caste. The difficulty is getting males of all species because we have rarely found males in colonies in the field. However, captive colonies can produce winged sexuals through laboratory rearing for a long period. Cooperation between taxonomists and behavioural ecologists is indispensable for obtaining a complete set of material for the taxonomic study of winged ants.

## Acknowledgements

We would like to thank Enago (www.enago.jp) for the English language review. This work was supported in part by JSPS KAKENHI (Grant-in-Aid for Scientific Research (C) Grant Number 21K05616, MEXT, Japan. Our cordial gratitude is extended to Mr. Ken'ichi Kanai (Amami-shi), Mr. Toshio Muroi (Shimizu Corporation), Prof. Kazuo Ogata (Kyushu University), Prof. Yôko Takematsu (Yamaguchi University) and many other friends of ours for their kind help in collecting the material.

## References

Agavekar G, Hita Garcia F, Economo EP (2017) Taxonomic overview of the hyperdiverse and genus *Tetramorium* Mayr (Hymenopter, Formicidae) in India with descriptions and X-ray microtomography of two new species from the Andaman Islands. PeerJ 2017, 5: e3800. https://doi.org/10.7717/peerj.3800

AntWiki (2021) *Tetramorium*. [online]. Available from antwiki org. [accessed 10 May 2021]

Bharti H, Kumar R (2012) Taxonomic studies on genus *Tetramorium* Mayr (Hymenoptera, Formicidae) with report of two new species and three new records including a tramp species from India with a revised key. ZooKeys 207: 11–35. https://doi.org/10.3897/zookeys.207.3040

Bolton B (1976) The ant tribe Tetramoriini (Hymenoptera: Formicidae). Constituent genera, review of smaller genera and revision of *Triglyphothrix* Forel. Bulletin of the British Museum (Natural History) Entomology Series 34: 283–379.

Bolton B (1977) The ant tribe Tetramoriini (Hymenoptera: Formicidae). The genus *Tetramorium* Mayr in the Oriental and Indo-Australian regions, and in Australia. Bulletin of the British Museum (Natural History) Entomology Series 36: 67–151.

Bolton B (1980) The ant tribe Tetramoriini (Hymenoptera: Formicidae). The genus *Tetramorium* Mayr in the Ethiopian zoogeographical region. Bulletin of the British Museum (Natural History) Entomology Series 40: 193–384.

Bolton B (1995) A New General Catalogue of the Ants of the World. Harvard University Press, Cambridge, Massachusetts & London, England, 512 pp.

Hita Garcia F, Fisher B (2012) The ant genus *Tetramorium* Mayr (Hymenoptera: Formicidae) in the Malagasy region-taxonomy of the *T. bessonii*, *T. bonibony*, *T. dysalum*, *T. marginatum*, *T. tsingy*, and *T. weitzeckeri* species groups. Zootaxa 3365: 1–133. https://doi.org/10.11646/zootaxa.3365.1.1

Japanese Ant Database Group (2003) Ants of Japan. Gakken, Tokyo, e136. [In Japanese]

Ogata K (1991) A generic synopsis of the poneroid complex of the family Formicidae (Hymenoptera), Part. II. Subfamily Myrmicinae. Bulletin of the Institute of Tropical Agriculture, Kyushu University 14: 61–149.

Onoyama K (1980) An introduction to the ant fauna of Japan, with a check list (Hymenoptera, Formicidae). Kontyû, Tokyo 48: 193–212.

Santschi F (1928) Insects of Samoa and Other Samoan Territorial Archipelagos 5. Hymenoptera, Formicidae: 41–58.

Steiner FM, Schlick-Steiner BC, Moder K (2006) Morphology-based cyber identification engine to identify ants of the *Tetramorium caespitum*/*impurum* complex (Hymenoptera: Formicidae). Myrmecologische Nachrichten 8: 175–180.

Terayama M (2020) Formicidae. In: Editorial Committee of Catalogue of the Insects of Japan (Ed.) Catalogue of the Insects of Japan. Hymenoptera Vol. 9, Part 3: 85–160 Apocrita, Aculeata. Entomological Society of Japan. [Distributed by Touka Shobo, Fukuoka]

Terayama M, Kubota S, Eguchi K (2014) Encyclopedia of Japanese Ants. Asakura-shoten, Tokyo, 278 pp. [In Japanese]

Yamane Sk, Fukumoto S (2017) Chapter 6. Tramp ant species in the Satsunan Islands, 108–131. In: Kagoshima University Biodiversity Study Group (Ed.) Alien Animals and Plants in the Amami Islands. Nanpô-shinsha, Kagoshima. [In Japanese]

Yamane Sk, Hosoishi S (2020) Identification of the Japanese species of the ant genus *Pheidole* based on queen characters. Japanese Journal of Entomology (New Series) 23: 37–53. [In Japanese with English abstract and keys to species]

Yoshimura M (2020) Chapter 4. Taxonomy of alien ants, 34–50. In: Hashimoto Y. (Ed.) Gairaiari no Hanashi. Asakura Shoten, Tokyo. [In Japanese]

ZooKeys 1084: 65–81 (2022)
doi: 10.3897/zookeys.1084.78883
https://zookeys.pensoft.net

RESEARCH ARTICLE

A peer-reviewed open-access journal
ZooKeys
Launched to accelerate biodiversity research

# Ultrastructure of androconia and surrounding scales of nine species of Hesperiidae (Lepidoptera)

Yue Pan[1], Zhuoshu Yu[2], Xiangqun Yuan[1]

**1** *Key Laboratory of Plant Protection Resources and Pest Management, Ministry of Education, Entomological Museum, College of Plant Protection, Northwest A&F University, Yangling, 712100, China* **2** *Key Laboratory of Bio-Resource and Eco-Environment of Ministry of Education, College of Life Sciences, Sichuan University, Chengdu, 610065, China*

Corresponding author: Xiangqun Yuan (yuanxq@nwsuaf.edu.cn)

Academic editor: Martin Wiemers | Received 6 December 2021 | Accepted 13 January 2022 | Published 27 January 2022

*http://zoobank.org/350DE328-CC81-4F0B-A22F-DE14FB9C9228*

Citation: Pan Y, Yu Z, Yuan X (2022) Ultrastructure of androconia and surrounding scales of nine species of Hesperiidae (Lepidoptera). ZooKeys 1084: 65–81. https://doi.org/10.3897/zookeys.1084.78883

## Abstract

The ultrastructure of androconia and their surrounding scales of nine species in nine genera across four subfamilies of Hesperiidae is studied. This provides a basis for the classification and identification of some genera and species. The wing surface of the scent glands patches was cut with scissors, observed and photographed under an S-4800 scanning electron microscope (at 10.0 kV accelerated pressure). There were significant differences in the types of scent glands patches across subfamilies. The scent glands patches of Pyrginae and Eudaminae are mainly in the costal fold of the forewing, while those of Coeliadinae and Hesperiinae are mainly in the line or circular stigma on the wing surface. The length, breadth and aperture of the androconia were further measured and the data are analysed by variance and multiple comparisons. There are significant differences amongst the subfamilies, except for Eudaminae and Pyrginae. In Hesperiinae, *Telicota colon* (Fabricius, 1775) and *Ampittia virgata* (Leech, 1890) have no significant difference in the aperture of the androconia, but are significantly different from *Thymelicus leoninus* (Butler, 1878). There are significant differences in the aperture between *Pyrgus alveus*'s (Hübner, 1803) androconium and the second androconium of *Lobocla bifasciata* (Bremer & Grey, 1853), but not with the first androconium of *Lobocla bifasciata*. The morphology of androconia in the scent glands patches is very similar in Hesperiinae; all are rod-shaped and paddle-like. The scale types around the scent glands patches are different, but there are one or two similar types. To a certain extent, the aperture of the androconia reflects the genetic relationships between subfamilies and species. The differences in scale type and structure of scent glands patches can be used as a reference for the classification of subfamilies and genera in Hesperiidae.

## Keywords

Androconia, Hesperiidae, scale, scanning electron microscope , scent glands patches

## Introduction

Sex signs are often used as the key morphological features of Lepidoptera to distinguish males from females outdoors, such as Danaidae and Nymphalidae males possessing ear-shaped pouches on the hindwings and brush-like odour sacs at the end of their abdomen (Boppre and Vane-Wright 1989; Chou 1998; Vane-Wright et al. 2002; Simonsen et al. 2012; de Oliveira Borges et al. 2020) or different markings on the wings of Pieridae males (Zhang 2008; Beserra Nobre et al. 2021). The male scent glands patches of Lycaenidae are marked on the abdomen dorsal plate (Ômura et al. 2015). Riodinidae scent glands patches are distributed on the wing surface, abdomen and tibia of the hind-feet of males (Hall and Harvey 2002). In Hesperiidae, the characteristics of the stigma, brand, costal fold and vein swelling on the wing surface are often used as the secondary sexual characteristics to distinguish males from females (Müller 1878; Pivnick et al. 1992; Hernández-Roldán et al. 2014; Yuan and Yuan 2015). The scent glands patches of Hesperiidae show obvious external morphological differences amongst subfamilies and genera and this has greatly attracted the attention of skipper researchers.

Previous studies have found that scent glands patches are not only obvious external morphological features, but are also closely involved in the release of pheromone. In the ultrastructure observation of the scent glands patches, it has been found that the release of pheromone is related to the special structural scales called "androconia" (Kuwahara 1979; Ômura et al. 2013; Okumura et al. 2016; Mann et al. 2017, 2020; Stamm et al. 2019). In recent years, studies of fossil scales have shown that scales had an earlier origin in the evolution of Lepidoptera and have significance in reflecting the relationships between species (Zhang et al. 2018). Many taxonomic studies, based on the morphological characteristics of the scale surface, have shown that the size, shape and surface ridges of the scales can accurately reflect the differences between species and genera. Scales have now been widely used in determining the classification, identification, evolutionary and genetic relationships of many species (Fang et al. 2007; Qiu and Han 2009).

In this paper, ultrastructural observations were made on the scales of nine representative species in four subfamilies of Hesperiidae. By comparing the types and morphological characteristics of scales that appear amongst subfamilies and genera, the differences between different taxa were analysed in order to provide a new morphological basis for studies of the classification of Hesperiidae.

## Materials and methods

### Insects

Voucher specimens representing all sampled species are deposited in the Entomological Museum of Northwest A&F University. Specimen information is presented in Table 1.

**Table 1.** Material localities and collection dates.

| Subfamily | Genus | Species | Locality | Quantity |
|---|---|---|---|---|
| Coeliadinae | *Burara* | *B. striata* | Yifeng County, Jiangxi Province | 10 |
| | *Hasora* | *H. taminata* | Ledong County, Hainan Province | 10 |
| Eudaminae | *Lobocla* | *L. bifasciata* | Lishui City, Zhejiang Province | 10 |
| Pyrginae | *Pyrgus* | *P. alveus* | Tianshui City, Gansu Province | 10 |
| | *Erynnis* | *E. montanus* | Fuping County, Shaanxi Province | 10 |
| Hesperiinae | *Ampittia* | *A. virgata* | Nanping City, Fujian Province | 10 |
| | *Baoris* | *B. leechi* | Sanjiang City, Zhejiang Province | 10 |
| | *Thymelicus* | *T. leoninus* | Nanping City, Fujian Province | 10 |
| | *Telicota* | *T. colon* | Sanming City, Fujian Province | 10 |

### Scanning electron microscopy

The dried wings of male skippers were selected. An appropriate size of wing surface containing the scent glands patches was cut using scissors. The samples were picked up by tweezers and were then stuck on to conductive adhesive. Each sample was given a number and its position was recorded. Samples were attached to a holder using electric adhesive tape, sputter coated with gold and observed and photographed with an S-4800 scanning electron microscope (at accelerated pressure 10.0 kV).

### Measurements and statistical analyses

Under the scanning electron microscope, the ultrastructure images of scent glands patches of nine species and their surrounding ordinary scales were obtained. Adobe Photoshop CS6 software was used to measure the length, breadth and aperture of androconia. All measurement data were analysed for variance and multiple comparisons using Excel and SPSS 24.0 software.

## Results

### Ultrastructure of androconia and surrounding scales

#### *Burara striata* (Hewitson, 1867)

The scent glands patches of *B. striata* are marked above the 2A vein on upperside of the forewing. There are three dark brown line stigmas on both sides of the Cu1 and Cu2 veins (Fig. 1). There are two main kinds of scales. One has wavy tooth cracks at the ends and the longitudinal ridges are thick and smooth, connected by tiny transverse ribs between the longitudinal ridges. The other has blunt ends without tooth cracks and the longitudinal ridges are smooth and connected by thicker transverse ribs. Two types of scales are observed around the scent glands patches. One is a slender hairy scale and the other is a flaky scale with 3–4 teeth at the ends.

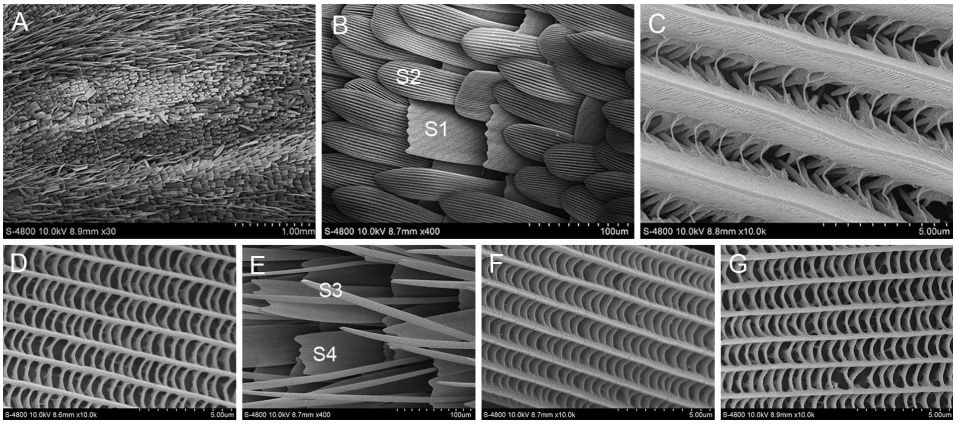


**Figure 1.** Ultrastructure of scales in and around the scent glands patches of *B. striata* **A** Scent glands patches **B** Scales in the scent glands patches (S1: The first scale; S2: The second scale) **C** Ultrastructure of the first scale **D** Ultrastructure of the second scale **E** Scales around the scent glands patches (S3: The third scale; S4: The fourth scale) **F** Ultrastructure of the third scale **G** Ultrastructure of the fourth scale.

### *Hasora taminata* (Hübner, 1818)

The scent glands patches of *H. taminata* are marked as a broken, discontinuous dark brown oval stigma on upperside of the forewing from the 2A vein to the Cu1 vein (Fig. 2). There are two kinds of scales in the scent glands patches. One is the rod-shaped androconia, which are connected by a band with constricted ends and hidden between another type of scale. The longitudinal ridges of androconia are smooth and parallel and the spacing between transverse ribs is different, forming a large number of rectangular and circular holes. The other type is neatly arranged in piles with blunt ends and narrow paddle-like scales in the middle and at the base. The longitudinal ridges of the scales are smooth and the small transverse ribs sometimes intersect similar to a pattern structure. Only one type of scales around the scent glands patches of *H. taminata* has contracted ends that are bluntly rounded.

### *Lobocla bifasciata* (Bremer & Grey, 1853)

The scent glands patches of *L. bifasciata* are in the costal fold on upperside of the forewing, dark brown in colour. The scent glands patches are divided into two distinct areas (Fig. 3). The lower area is scattered with short rod-shaped androconia, connected end to end in ribbons. The longitudinal ridges of the androconia are smooth and parallel. There is a row of holes with different sizes between the two longitudinal ridges and the transverse ribs are wider. The upper area has a long rod-shaped androconium with sharply contracted ends. The longitudinal ridges are connected by tiny transverse ribs, smooth without protrusions and the holes are scattered. There are two kinds of scales around the scent glands patches of *L. bifasciata*; one type has a long and narrow blade-like shape with two cleavages at the ends and another type has lateral flaky scales with broad scales and blunt ends without tooth cracks.

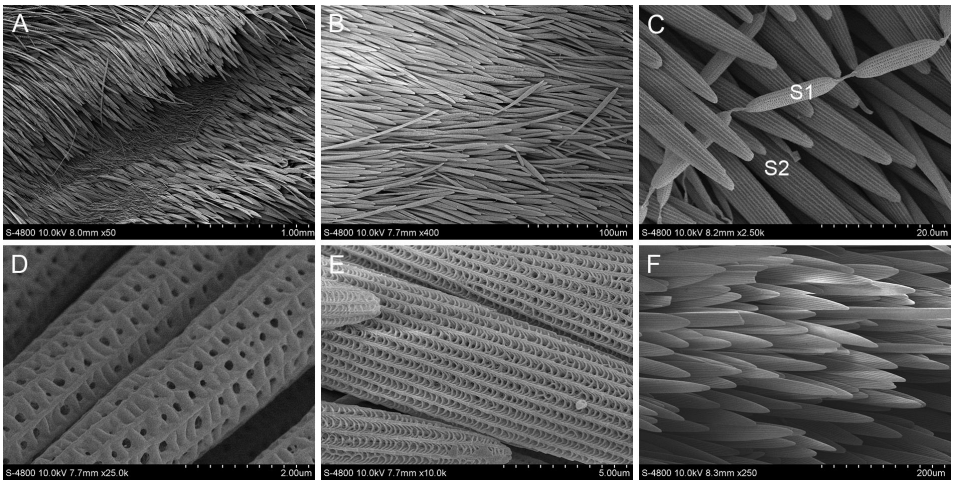


**Figure 2.** Ultrastructure of scales in and around the scent glands patches of *H. taminata* **A** Scent glands patches **B** and **C** Scales in the scent glands patches (S1: The first scale (androconium); S2: The second scale) **D** Ultrastructure of the first scale **E** Ultrastructure of the second scale **F** Scales around the scent glands patches.

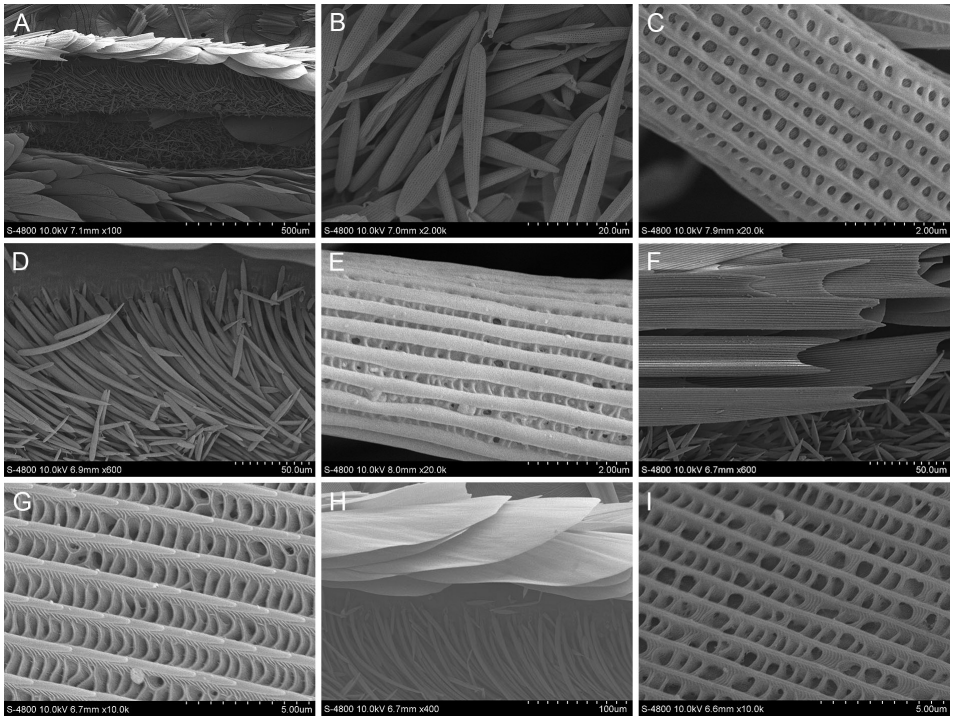


**Figure 3.** Ultrastructure of scales in and around the scent glands patches of *L. bifasciata* **A** Scent glands patches **B** Type 1 scales (androconia) in the scent glands patches **C** Ultrastructure of type 1 scale in the scent glands patches **D** Type 2 scales (androconia) in the scent glands patches **E** Ultrastructure of type 2 scale in the scent glands patches **F** Type 1 scales around the scent glands patches **G** Ultrastructure of type 1 scale around the scent glands patches **H** Type 2 scales around the scent glands patches **I** Ultrastructure of type 2 scale around the scent glands patches.

### *Pyrgus alveus* (Hübner, 1803)

The scent glands patches of *P. alveus* are marked in the costal fold on upperside of the forewing in ochre. There are mainly two kinds of scales distributed there (Fig. 4). One type is a bunch of paddle-shaped androconia. The androconia are wide at the end, narrow at the base and the longitudinal ridges are parallel. There are two rows of holes between the two longitudinal ridges. The androconia are connected by a ribbon structure. The other type is a lamellar scale with a blunt round end and no tooth cracks. There are two kinds of scales around the scent glands patches of *P. alveus*. One is a lateral flaky scale with a wide surface with blunt ends without tooth cracks and the longitudinal ridges are closely connected by flaky transverse ribs. There are holes of different sizes between the transverse ribs. The other is a long and narrow flaky scale with no or one tooth cracks at the ends. The transverse ribs have different degrees of convex ridges and the distribution density of the holes is greater than that of the other kind of scale.

### *Erynnis montanus* (Bremer, 1861)

The scent glands patches of *E. montanus* are in the costal fold on upperside of the forewing, are dark brown and composed of three kinds of scattered scales (Fig. 5). The first is a curved and upturned hairy scale around the mid-line of the scent glands patches area. The second is evenly distributed in the sex target area. The base is formed by the epidermis and there is a hole in the middle which is in the shape of a 2-leaf bud. The large leaf is like a 3-sided star and the small leaf is arc-shaped and curved. The third is young leaf-like scales with cracks. The base of the epidermis gathers in a bottle-like shape. There are

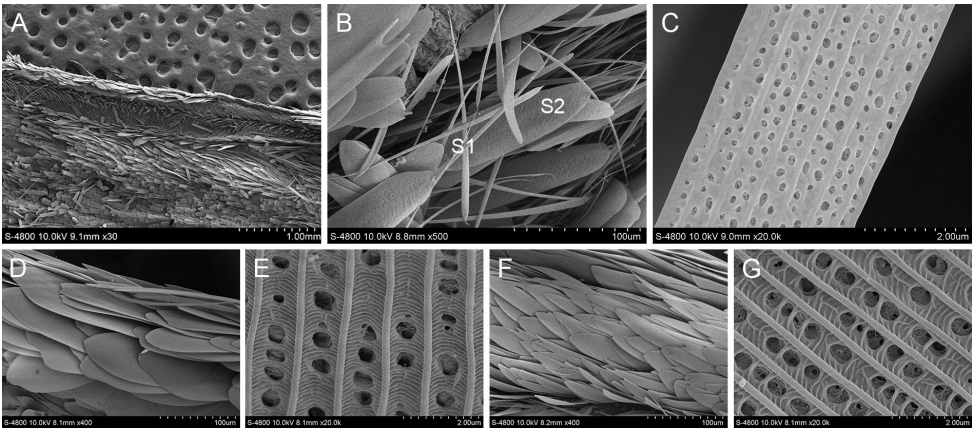


**Figure 4.** Ultrastructure of scales in and around the scent glands patches of *P. alveus* **A** Scent glands patches **B** Scales in the scent glands patches (S1: The first scale (androconium); S2: The second scale) **C** Ultrastructure of the first scale in the scent glands patches **D** Type 1 scales around the scent glands patches **E** Ultrastructure of type 1 scale around the scent glands patches **F** Type 2 scales around the scent glands patches **G** Ultrastructure of type 2 scale around the scent glands patches.

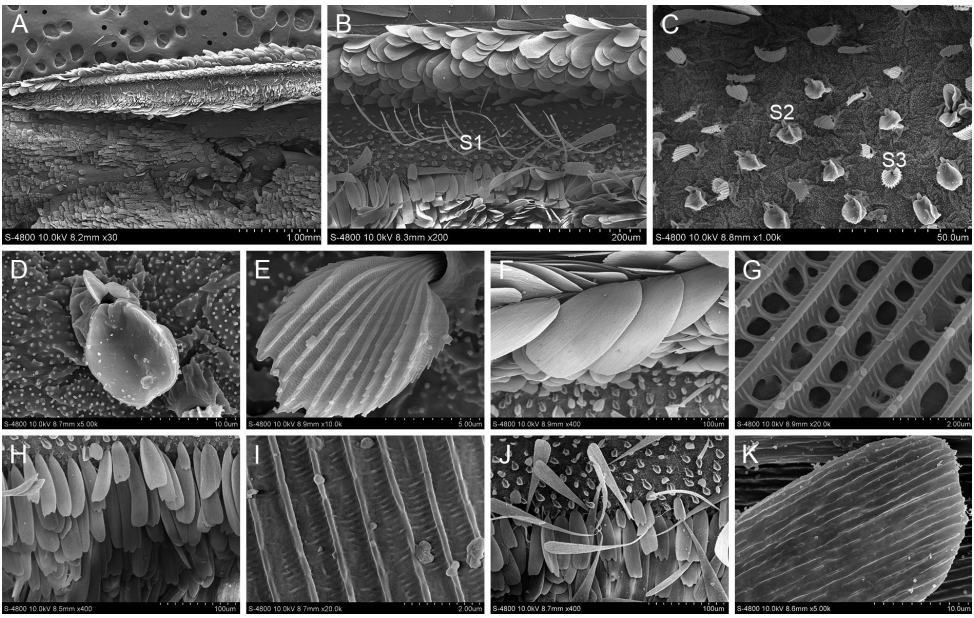


**Figure 5.** Ultrastructure of scales in and around the scent glands patches of *E. montanus* **A** Scent glands patches **B** and **C** Scales in the scent glands patches (S1: The first scale; S2: The second scale; S3: The third scale) **D** The second scale **E** The third scale **F** Type 1 scales around the scent glands patches **G** Ultrastructure of type 1 scale around the scent glands patches **H** Type 2 scales around the scent glands patches **I** Ultrastructure of type 2 scale around the scent glands patches **J** Type 3 scales around the scent glands patches **K** Ultrastructure of type 3 scale around the scent glands patches.

three kinds of scales around the scent glands patches of *E. montanus*. The first is adjacent to the outer edge of the scent glands patches with scales standing sideways, wide on the surface and the base of the transverse ribs is wide to form a row of holes between the longitudinal ridges. The second is long and narrow, with 0, 2 or 3 teeth cracks at the ends. The connection of the transverse ribs between the longitudinal ridges is not obvious and without holes. The third is narrow at the base and round at the end, with discontinuous longitudinal ridges and no transverse rib connection between longitudinal ridges.

### *Ampittia virgata* (Leech, 1890)

The scent glands patches of *A. virgata* form a grey line stigma on upperside of the forewing from the 2A vein to the base of the Cu2 vein (Fig. 6). There is a cluster of messy rod-shaped androconia. The longitudinal ridges are nearly parallel with holes arranged in a row. The androconia are connected in pairs. There are two types of scales around the scent glands patches of *A. virgata*. One kind of scale has ends that are blunt, flat, broad and flaky. The longitudinal ridges, parallel with protrusions, are connected by the transverse ribs in the middle, which are occasionally connected by tiny filaments. The other type has 2–3 teeth clefts at the ends.

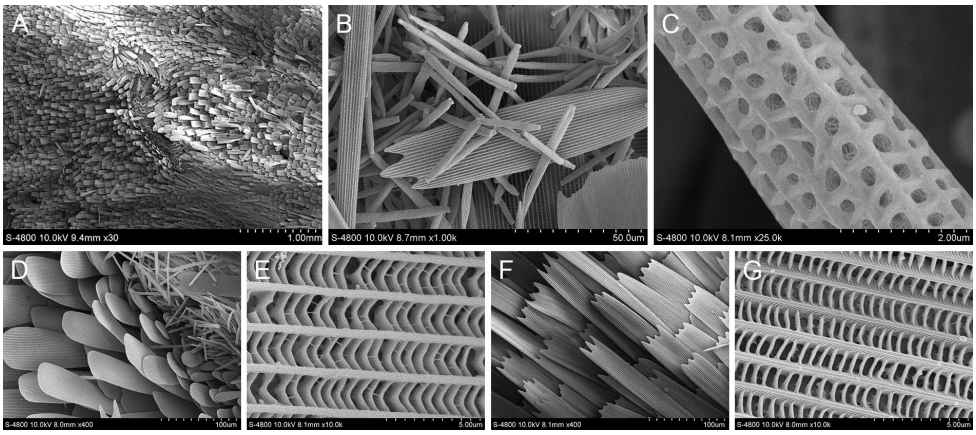


**Figure 6.** Ultrastructure of scales in and around the scent glands patches of *A. virgata* **A** Scent glands patches **B** Scales (androconia) in the scent glands patches **C** Ultrastructure of the androconium **D** Type 1 scales around the scent glands patches **E** Ultrastructure of type 1 scale around the scent glands patches **F** Type 2 scales around the scent glands patches **G** Ultrastructure of type 2 scale around the scent glands patches.

### *Baoris leechi* (Elwes & Edwards, 1897)

The scent glands patches of *B. leechi* are marked as an oval brand on underside of the forewing and two oval brands along the middle of vein 2A, dark brown in colour (Fig. 7). The scales at the brand are corrugated, neatly arranged on underside of the wing. The scales are short, erect on the wing surface, the ends are blunt and flat, the longitudinal ridges have protrusions and there are closely arranged horizontal stripes between the longitudinal ridges. Four types of scales were observed around the scent glands patches of *B. leechi*. The first has 3–4 teeth clefts at the ends. The longitudinal ridges are smooth, narrow flaky scales connected by tiny transverse ribs. The second is short with more than five teeth cracks at the ends. The structure of the transverse ribs is similar to that of the first type. The ends of the third are blunt and flat without tooth cracks and the longitudinal ridges are protruding and are connected by closely arranged transverse ribs. The fourth has longitudinal ridges with protrusions and the longitudinal ridges are connected by transverse ribs.

### *Thymelicus leoninus* (Butler, 1878)

The scent glands patches of *T. leoninus* are oblique black line stigmas from the 2A vein to the base of the Cu1 vein on upperside of the forewing. There are two kinds of scales distributed there (Fig. 8). The first is disorderly arranged rod-shaped androconia. The longitudinal ridges of the androconia are left helixes. The longitudinal ridges are connected by wider transverse ribs to form rows of holes. The second kind are paddle-like scales with smooth longitudinal ridges and holes between the longitudinal ridges. These holes vary in size, sometimes leaning to one side of the longitudinal ridge. There is one kind of scale around the scent glands patches of *T. leoninus*, long and narrow flaky scales with blunt ends.

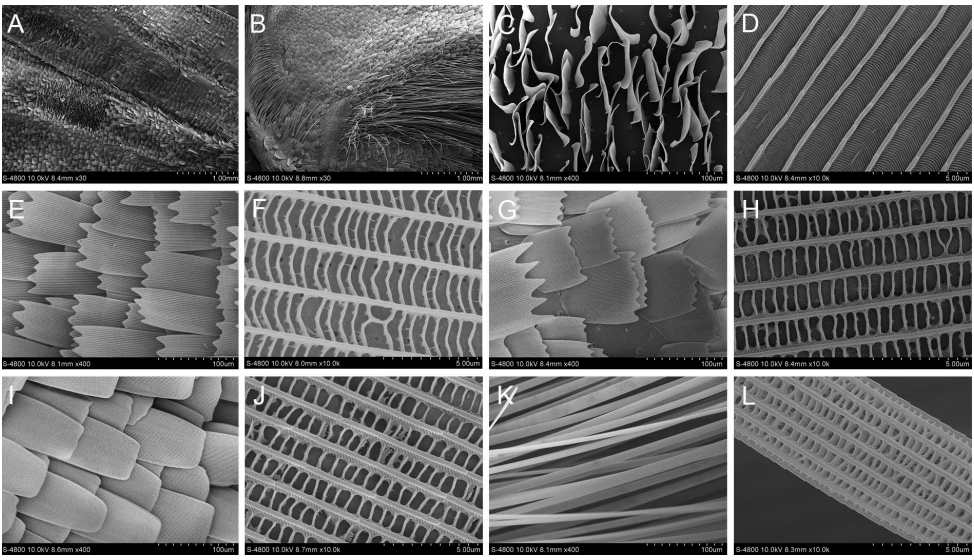


**Figure 7.** Ultrastructure of scales in and around the scent glands patches of *B. leechi* **A** and **B** Scent glands patches **C** Scales in the scent glands patches **D** Ultrastructure of scale in the scent glands patches **E** Type 1 scales around the scent glands patches **F** Ultrastructure of type 1 scale around the scent glands patches **G** Type 2 scales around the scent glands patches **H** Ultrastructure of type 2 scale around the scent glands patches **I** Type 3 scales around the scent glands patches **J** Ultrastructure of type 3 scale around the scent glands patches **K** Type 4 scales around the scent glands patches **L** Ultrastructure of type 4 scale around the scent glands patches.

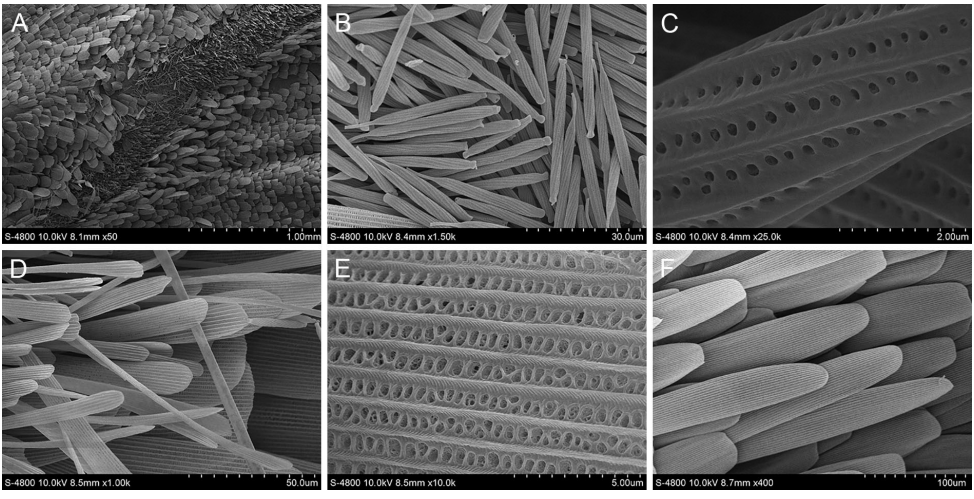


**Figure 8.** Ultrastructure of scales in and around the scent glands patches of *T. leoninus* **A** Scent glands patches **B** Scales (androconia) in the scent glands patches **C** Ultrastructure of androconium **D** Type 1 scales around the scent glands patches **E** Ultrastructure of type 1 scale around the scent glands patches **F** Type 2 scales around the scent glands patches.

### *Telicota colon* (Fabricius, 1775)

*T. colon* has a grey line stigma marked in the area medialis of upperside of the forewing. There are two kinds of scales distributed there (Fig. 9). The first are paddle-shaped androconia. The longitudinal ridges at the ends of the scales are connected by tiny transverse ribs. From the end to the middle of these scales, the rows of holes between the ribs gradually change from horizontal strips to round holes, resembling a rod-shaped androconial structure. The second has blunt ends without tooth cracks, wide and flaky scales, smooth longitudinal ridges and rows of transverse ribs between the longitudinal ridges and with some transverse ribs intersecting at the base. There is one type of scale around the scent glands patches of *T. colon*. The flaky scales have 4–6 teeth cracks at the ends. The longitudinal ridges are smooth and parallel without protrusions. They are connected by transverse ribs and some transverse ribs intersect in the middle.

## Androconia

Androconia were observed in seven of the nine species selected. The length, breadth, aperture, shape and longitudinal ridge direction of the androconia were observed and measured (Table 2). The androconia have been analysed by variance analysis amongst species and subfamilies.

In terms of length, the results of multiple comparisons of androconia show that there are significant differences amongst the subfamilies, except for Coeliadinae and Pyrginae. Except for the group of *T. colon*, *H. taminata* and *P. alveus* and another group of *A. virgata* and *T. leoninus*, there were significant differences amongst species ($\alpha = 0.05$).

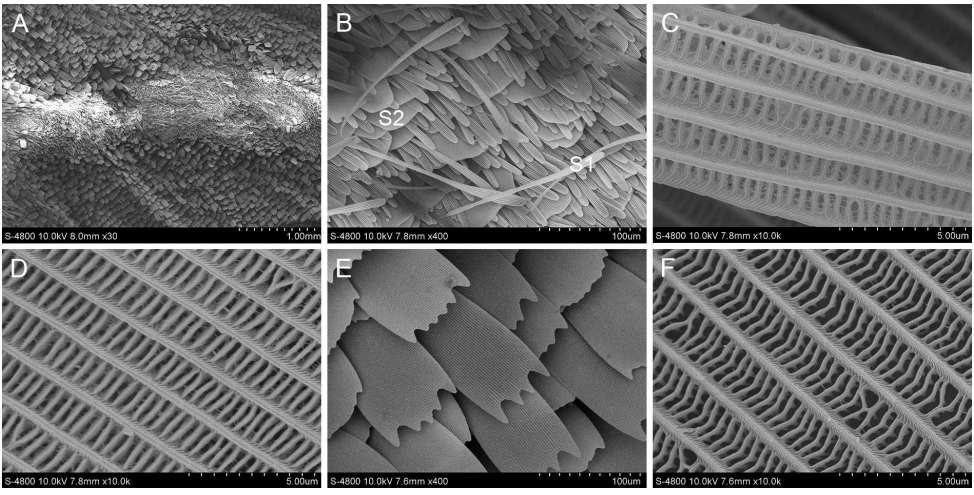


**Figure 9.** Ultrastructure of scales in and around the scent glands patches of *T. colon* **A** Scent glands patches **B** Scales in the scent glands patches (S1: The first scale (androconium); S2: The second scale) **C** Ultrastructure of the first scale **D** Ultrastructure of the second scale **E** Scales around the scent glands patches **F** Ultrastructure of the scale around the scent glands patches.

**Table 2.** The length, breadth, aperture, shape, longitudinal direction, number and multiple comparisons of the seven androconia.

| | Coeliadinae | Eudaminae | | Pyrginae | Hesperiinae | | |
|---|---|---|---|---|---|---|---|
| | *H. taminata* | *L. bifasciata* I | *L. bifasciata* II | *P. alveus* | *A. virgata* | *T. leoninus* | *T. colon* |
| Length/μm | 160.886 ± 17.517 (Aa) | 17.339 ± 0.728 (Dd) | 68.802 ± 3.502 (Bb) | 154.427 ± 6.985 (Aa) | 35.890 ± 1.172 (Cc) | 29.377 ± 1.319 (CDc) | 172.400 ± 5.208 (Aa) |
| Number | 33 | 56 | 18 | 21 | 66 | 92 | 32 |
| Breadth/μm | 2.459 ± 0.100 (Dd) | 2.928 ± 0.101 (CDc) | 2.841 ± 0.094 (CDcd) | 4.326 ± 0.211 (Bb) | 3.195 ± 0.082 (Cc) | 2.944 ± 0.039 (Cc) | 7.923 ± 0.128 (Aa) |
| Number | 44 | 43 | 40 | 59 | 73 | 96 | 94 |
| Aperture/μm | 0.200 ± 0.006 (Bb) | 0.166 ± 0.004 (CDc) | 0.140 ± 0.008 (Dd) | 0.172 ± 0.006 (Cc) | 0.318 ± 0.006 (Aa) | 0.204 ± 0.004 (Bb) | 0.323 ± 0.008 (Aa) |
| Number | 108 | 71 | 39 | 104 | 145 | 123 | 70 |
| Shape | rod | rod | rod | paddle | rod | rod | paddle |
| Longitudinal ridge direction | parallel | parallel | parallel | parallel | parallel | left helix | parallel |
| Length/μm | 160.886 ± 17.517 (Aa) | 29.857 ± 2.770 (Cc) | | 154.427 ± 6.985 (Aa) | | 55.727 ± 3.994 (Bb) | |
| Number | 33 | 190 | | 21 | | 190 | |
| Breadth/μm | 2.490 ± 0.096 (Bb) | 2.935 ± 0.085 (Bb) | | 4.521 ± 0.233 (Aa) | | 4.755 ± 0.154 (Aa) | |
| Number | 47 | 83 | | 59 | | 260 | |
| Aperture/μm | 0.200 ± 0.006 (Bb) | 0.157 ± 0.004 (Cc) | | 0.172 ± 0.006 (Cc) | | 0.277 ± 0.005 (Aa) | |
| Number | 108 | 110 | | 104 | | 338 | |

Each value retains 3 significant digits. Data are presented as Mean ± SE; Number: sample size. Different capital letters on the same line indicate extremely significant differences (α = 0.01). Different lower case letters on the same line indicate extremely significant differences (α = 0.05).

In terms of breadth, the results of comparing androconia show that there are significant differences amongst the subfamilies, except for Hesperiinae and Pyrginae, Coeliadinae and Eudaminae. There are no significant differences in the breadth of the two androconia of *L. bifasciata*, *A. virgata* and *T. leoninus*, *L. bifasciata* and *H. taminata*, but there are significant differences amongst species (α = 0.05).

In terms of aperture, the results of androconia comparisons show that there are significant differences amongst the subfamilies, except for Eudaminae and Pyrginae. There are no significant differences in the aperture of androconia of *T. colon* and *A. virgata*, *H. taminata* and *T. leoninus*, *L. bifasciata* I and *P. alveus*, but there are significant differences amongst species (α = 0.05).

## Discussion

### Scent organs

There are three main locations for scent organs on butterflies: a) Wings. There are different manifestations in different families of Lepidoptera. For example, the main scent glands patches of Danainae and Heliconiinae are in a small part of the central forewing and on the hindwing. Their location on the hindwing is obvious amongst different

genera. In addition, there is a specialised bag-like structure on the ventral surface of the hindwing (Boppre and Vane-Wright 1989; Vane-Wright et al. 2002; de Oliveira Borges et al. 2020). In Pieridae, the scent glands patches are mainly concentrated in the area where the forewings and hindwings overlap (Beserra Nobre et al. 2021). The scent glands patches of Riodinidae and Lycaenidae are located at the forewing tip (Hall and Harvey 2002; Ômura et al. 2015). b) Abdomen. These are characterised by specific plaques distributed in different areas of the abdomen and in tufts of hair at the end of the abdomen that can be turned out in Danaidae and Riodinidae (Hall and Harvey 2002; Simonsen et al. 2012; de Oliveira Borges et al. 2020). c) Appendages. This mainly refers to the upright hair tufts or hair pencils on the hind tibia, which have been reported in Riodinidae, *Pyrgus* and *Coladenia* in Hesperiidae (Hall and Harvey 2002; Hernández-Roldán et al. 2014).

The scent organs of Hesperiidae are mainly concentrated in the first type, especially the black, smooth and raised scars on upperside of the forewing, such as a brand formed after animal skin burns, with even a distortion of the veins where they are located. There are obvious differences in markings on the wing surface of other families (Yuan and Yuan 2015).

## Scales

Since people first became aware of butterflies, they have attracted the attention of researchers with their colourful appearance. The significance of the unique scales of butterflies lies not only in the appreciation of the external image of the butterfly, but also continues to promote the development of bionic technology, biogeography, paleontology and other fields (Ghiradella 1991; Zhong and Shen 2003; Han et al. 2008; Simonsen et al. 2012; Zhang et al. 2015; Yang and Chen 2021). Butterfly scales are divided into basal scales and cover scales. The basal scales are located on the surface of the wing's membrane and the cover scales cover the basal scales. Most of the basal scales have two to five cracks at the ends, while the brightly coloured surface scales without cracks are smooth, straight or curved (Fang et al. 2007; Han et al. 2008; Qiu and Han 2009; Simonsen et al. 2012; Parnell et al. 2018). The surrounding scales of the nine species of Hesperiidae are composed of more than two kinds of scales, except for *T. colon*, which has only one basal scale. *B. striata*, *H. taminata*, *L. bifasciata*, *P. alveus*, *A. virgata* and *T. leoninus* have one basal scale and one cover scale; *E. montanus* has one basal scale and two cover scales; and *B. leechi* has two basal scales and two cover scales. The scales of scent glands patches showed one type of androconia and one type of cover scale of *H. taminata*; two kinds of androconia with different shapes and different distributions of *L. bifasciata*; one kind of paddle-shaped androconia and one kind of cover scale of *P. alveus* and *T. colon*; *T. leoninus* with one kind of androconia and one kind of paddle-shaped cover scale; and *A. virgata* with one kind of paddle-shaped androconia. No androconia have been found in *B. striata*, *E. montanus* and *B. leechi*. *B. striata* has two kinds of ordinary scales: one type of basal scale and one kind of cover scale. *E. montanus* has three kinds of ordinary scales: one kind of basal scale (tender leaf with

tooth cracks) and two kinds of cover scales (hairy and bud-like). *B. leechi* has one kind of cover scale (tile-like).

The scales of Nymphalidae have similar shapes, structures and arrangements, especially the shape and size of the ultrastructure of the wing scales of the same genus which are small, indicating that the genetic relationship between them is close (Fang et al. 2007; Darragh et al. 2017; Stamm et al. 2019). Amongst the four subfamilies observed, *P. alveus* and *E. montanus* of Pyrginae; *A. virgata*, *B. leechi*, *T. leoninus* and *T. colon* of Hesperiinae; and Eudaminae and Pyrginae have one to two species with extremely similar scale types around the scent glands patches. However, this feature has not been found in *B. striata* and *H. taminata* of Coeliadinae.

## Androconia

In butterfly behavioural experiments, some studies have shown that the pheromone released from the scent organs plays a decisive role in the identification of related species (Andersson et al. 2007; Friberg et al. 2008; Ômura et al. 2013; Darragh et al. 2019). Previous studies have shown that the androconia are special glandular scales which are the main structural components of the male courtship pheromone system in Lepidoptera (Pivnick et al. 1992; Hall and Harvey 2002; Beserra Nobre et al. 2021).

The morphology of androconia is significantly distinctive amongst different families in Lepidoptera. For example, androconia are oval and flaky in Pieridae, fan-shaped in Lycaenidae, coronal-shaped in Nymphalidae and rod-shaped or paddle-shaped in Hesperiidae. It can be seen that the morphology of androconia can be used as an obvious morphological characteristic for family classification (Kuwahara 1979; Pivnick et al. 1992; Vane-Wright et al. 2002; Ômura et al. 2015; Darragh et al. 2017; Beserra Nobre et al. 2021). A study showed that the morphology of androconia in the same genus can be different, although 13 species of *Celastrina* (except *C. ladon*) have fan-shaped androconia. In this study, some species had differences in the size, lamellar microstructure and number of longitudinal ridges of androconia. In addition, the three subspecies of *C. argiolus* showed significant changes in androconia morphology (Ômura et al. 2015). In the study of the ultrastructure of androconia in Coliadinae, it was seen that the distribution density of androconia is significantly larger than that of the surrounding ordinary scales. This phenomenon is very obvious in Hesperiidae, which seems to alleviate the problem of insufficient wing surfaces. It is speculated that this morphological feature is closely related to the release of a pheromone (Pivnick et al. 1992; Beserra Nobre et al. 2021).

Analysing the observed morphological characteristics of the seven species of androconia in Hesperiidae, it is found that the aperture of androconia is the largest in Hesperiinae. Amongst them, the mean value for *T. colon* is 0.323 μm, *A. virgata* is 0.318 μm and *T. leoninus* is 0.204 μm, followed by *H. taminata* at 0.200 μm in Coeliadinae and *P. alveus* at 0.172 μm in Pyrginae. The mean values of apertures are 0.166 μm and 0.140 μm in *L. bifasciata*. Through multiple comparative analyses, the apertures were found to be extremely different amongst species and subfamilies and the

lengths and breadths of androconia were extremely different amongst subfamilies. The classification analysis of apertures is more consistent with existing domestic research in Hesperiidae: (Coeliadinae + (Pyrginae + (Eudaminae + (Heteropterinae + Hesperiinae)))) (Warren et al. 2008, 2009; Yuan 2010). The left helixes of the longitudinal ridge seem to be a unique feature. Is it unique to *T. leoninus*, to the genus *Thymelicus* or is it a feature possessed by a higher category? It can, thus, be seen that it is very important to extract the morphological characteristics of androconia insofar as it is of fundamental significance in reflecting our understanding of the phylogenetic relationships between species.

## Conclusions

Based on the above observation results, it is proposed that the types of scales around the scent glands patches, the presence of androconia in the scent glands patches and their types and morphological characteristics can be used as the basis for classification of different genera and species within the subfamily. Under further variance analysis and multiple comparisons of the length, breadth and aperture data of seven kinds of androconia, it is found that the data on androconial apertures fit the existing classification system better than the data on their length and breadth. This provides further knowledge of significance for phylogenetic research on Hesperiidae.

## Acknowledgements

We sincerely thank Dr. John Richard Schrock (Emporia State University, Emporia, KS, USA) for reviewing the manuscript. We also would like to express our appreciation to Xuan Zhang, Jintian Xiao and Ruitao Yu (Northwest A&F University, Yangling, China) for their assistance on methodology.

This study was supported by the National Natural Science Foundation of China (31772503, 31970448) and the National Key Research and Development Program of China (2017YFD0200900, 2017YFD0201800).

## References

Andersson J, Borg-Karlson AK, Vongvanich N, Wiklund C (2007) Male sex pheromone release and female mate choice in a butterfly. Journal of Experimental Biology 210: 964–970. https://doi.org/10.1242/jeb.02726

Beserra Nobre CE, da Silva Lucas LA, José Ribeiro Padilha R, do Amaral Ferraz Navarro DM, Carlos Alves L, Dália Maia AC (2021) Specialized androconial scales conceal species-specific semiochemicals of sympatric sulphur butterflies (Lepidoptera: Pieridae: Coliadinae). Organisms Diversity & Evolution 21: 93–105. https://doi.org/10.1007/s13127-020-00475-8

Boppre M, Vane-Wright RI (1989) Androconial systems in Danainae (Lepidoptera): functional morphology of *Amauris*, *Danaus*, *Tirumala* and *Euploea*. Zoological Journal of the Linnean Society 97: 101–133. https://doi.org/10.1111/j.1096-3642.1989.tb00549.x

Chou I (1998) Classification and identification of Chinese butterflies. Henan Scientific and Technological Publishing House.

Darragh K, Byers KJRP, Merrill RM, McMillan WO, Schulz S, Jiggins CD (2019) Male pheromone composition depends on larval but not adult diet in *Heliconius melpomene*. Ecological Entomology 44: 397–405. https://doi.org/10.1111/een.12716

Darragh K, Vanjari S, Mann F, Gonzalez-Rojas MF, Morrison CR, Salazar C, Pardo-Diaz C, Merrill RM, McMillan WO, Schulz S, Jiggins CD (2017) Male sex pheromone components in *Heliconius* butterflies released by the androconia affect female choice. PeerJ 2017. https://doi.org/10.7717/peerj.3953

Fang Y, Wang TQ, Sun G, Cong X (2007) Ultrastructure of wing scales of *Nymphalid* butterflies (Lepidoptera: Nymphalidae). Acta Entomologica Sinica 50: 313–317.

Friberg M, Vongvanich N, Borg-Karlson A-K, Kemp DJ, Merilaita S, Wiklund C (2008) Female mate choice determines reproductive isolation between sympatric butterflies. Behavioral Ecology and Sociobiology 62: 873–886. https://doi.org/10.1007/s00265-007-0511-2

Ghiradella H (1991) Light and color on the wing: structural colors in butterflies and moths. Applied Optics 30: 3492–3500. https://doi.org/10.1364/AO.30.003492

Hall JPW, Harvey DJ (2002) A survey of androconial organs in the Riodinidae (Lepidoptera). Zoological Journal of the Linnean Society 136: 171–197. https://doi.org/10.1046/j.1096-3642.2002.00003.x

Han ZW, Wu LY, Qiu ZM, Ren LQ (2008) The microstructure and structural color of the scales of *Thaumantis diores*. Science in China Press 53: 2692–2696.

Hernández-Roldán JL, Bofill R, Dapporto L, Munguira ML, Vila R (2014) Morphological and chemical analysis of male scent organs in the butterfly genus *Pyrgus* (Lepidoptera: Hesperiidae). Organisms Diversity and Evolution 14: 269–278. https://doi.org/10.1007/s13127-014-0170-x

Kuwahara Y (1979) Scent scale substances of male *Pieris melete* Ménétriès (Pieridae: Lepidoptera). Applied Entomology and Zoology 14: 350–355. https://doi.org/10.1303/aez.14.350

Mann F, Szczerbowski D, Silva L de, McClure M, Elias M, Schulz S (2020) 3-acetoxy-fatty acid isoprenyl esters from androconia of the ithomiine butterfly *Ithomia salapia*. Beilstein Journal of Organic Chemistry 16: 2776–2786. https://doi.org/10.3762/bjoc.16.228

Mann F, Vanjari S, Rosser N, Mann S, Dasmahapatra KK, Corbin C, Linares M, Pardo-Diaz C, Salazar C, Jiggins C, Schulz S (2017) The Scent Chemistry of *Heliconius* Wing Androconia. Journal of Chemical Ecology 43: 843–857. https://doi.org/10.1007/s10886-017-0867-3

Müller F (1878) A prega costal des Hesperideas. Archos del Museo Nacional de Rio de Janeiro 3: 41–45.

Okumura Y, Ozeki Y, Itoh T, Ohta S, Ômura H (2016) Volatile terpenoids from male wings lacking scent scales in *Anthocharis scolymus* (Lepidoptera: Pieridae). Applied Entomology and Zoology 51: 385–392. https://doi.org/10.1007/s13355-016-0410-y

de Oliveira Borges E, Bonfantti D, de Oliveira Ribeiro CA, Zarbin PHG (2020) Structures related to pheromone storage in alar androconia and the female abdominal scent gland

of *Heliconius erato phyllis*, *Heliconius ethilla narcaea*, and *Heliconius besckei* (Lepidoptera: Nymphalidae: Heliconiinae). Journal of Morphology 281: 388–401. https://doi.org/10.1002/jmor.21106

Ômura H, Yakumaru K, Honda K, Itoh T (2013) Two lactones in the androconial scent of the lycaenid butterfly *Celastrina argiolus ladonides*. Naturwissenschaften 100: 373–377. https://doi.org/10.1007/s00114-013-1030-9

Ômura H, Itoh T, Wright DM, Pavulaan H, Schröder S (2015) Morphological study of alar androconia in *Celastrina* butterflies. Entomological Science 18: 353–359. https://doi.org/10.1111/ens.12126

Parnell AJ, Bradford JE, Curran EV, Washington AL, Adams G, Brien MN, Burg SL, Morochz C, Fairclough JPA, Vukusic P, Martin SJ, Doak S, Nadeau NJ (2018) Wing scale ultrastructure underlying convergent and divergent iridescent colours in mimetic *Heliconius* butterflies. Journal of The Royal Society Interface 15. https://doi.org/10.1098/rsif.2017.0948

Pivnick K, Lavoie-Dornik J, Mcneil JN (1992) The role of the androconia in the mating behaviour of the European skipper, Thymelicus lineola, and evidence for a male sex pheromone. Physiological Entomology 17: 260–268. https://doi.org/10.1111/j.1365-3032.1992.tb01020.x

Qiu ZM, Han ZW (2009) Analysis of microstructure and model of butterfly scales. Transactions of the Chinese Society for Agricultural Machinery 40: 193–197.

Simonsen TJ, de Jong R, Heikkilä M, Kaila L (2012) Butterfly morphology in a molecular age–does it still matter in butterfly systematics? Arthropod Structure & Development 41: 307–322. https://doi.org/10.1016/j.asd.2012.04.006

Stamm P, Mann F, McClure M, Elias M, Schulz S (2019) Chemistry of the Androconial Secretion of the Ithomiine Butterfly *Oleria onega*. Journal of Chemical Ecology 45: 768–778. https://doi.org/10.1007/s10886-019-01100-5

Vane-Wright RI, Boppré M, Ackery PR (2002) *Miriamica*, a new genus of milkweed butterflies with unique androconial organs (Lepidoptera: Nymphalidae). Zoologischer Anzeiger 241: 255–267. https://doi.org/10.1078/0044-5231-00079

Warren AD, Ogawa JR, Brower AVZ (2008) Phylogenetic relationships of subfamilies and circumscription of tribes in the family Hesperiidae (Lepidoptera: Hesperioidea). Cladistics 24: 642–676. https://doi.org/10.1111/j.1096-0031.2008.00218.x

Warren AD, Ogawa JR, Brower AVZ (2009) Revised classification of the family Hesperiidae (Lepidoptera: Hesperioidea) based on combined molecular and morphological data. Systematic Entomology 34: 467–523. https://doi.org/10.1111/j.1365-3113.2008.00463.x

Yang S, Chen JY (2021) Structural color of butterflies wings living in temperate zone. Optical Technique 47: 339–343.

Yuan F, Yuan XQ (2015) 55 Fauna sinica insecta Vol.55 Lepidoptera Hesperiidae. Science Press, Beijing,China.

Yuan XQ (2010) Study on molecular systematics of Hesperiidae (Lepidoptera: Hesperiidae) from China. Northwest A & F University

Zhang D, Zhang W, Gu J, Fan T, Liu Q, Su H, Zhu S (2015) Inspiration from butterfly and moth wing scales: Characterization, modeling, and fabrication. Progress in Materials Science 68: 67–96. https://doi.org/10.1016/j.pmatsci.2014.10.003

Zhang Q, Mey W, Ansorge J, Starkey TA, Mcdonald LT, Mcnamara ME, Jarzembowski EA, Wichard W, Kelly R, Ren X, Chen J, Zhang H, Wang B (2018) Fossil scales illuminate the early evolution of lepidopterans and structural colors. Science Advances 4: 1–8. https://doi.org/10.1126/sciadv.1700988

Zhang TT (2008) Taxonomic study on the butterfly subfamily Coliadinae (Lepidoptera: Pieridae) from China.

Zhong M, Shen Z-R (2003) Scale structure and development of lepidopteran insects and their eyespot formation. Entomological Knowledge 40: 410–415.

ZooKeys 1084: 83–100 (2022)
doi: 10.3897/zookeys.1084.72868
https://zookeys.pensoft.net

RESEARCH ARTICLE

A peer-reviewed open-access journal
ZooKeys
Launched to accelerate biodiversity research

# A new species of *Cyrtodactylus* Gray, 1827 (Squamata, Gekkonidae) from southwestern Yunnan, China

Shuo Liu[1], Dingqi Rao[2]

**1** *Kunming Natural History Museum of Zoology, Kunming Institute of Zoology, Chinese Academy of Sciences, 32 Jiaochang Donglu, Kunming, Yunnan 650223, China* **2** *Kunming Institute of Zoology, Chinese Academy of Sciences, No.17 Longxin Road, Kunming, Yunnan, 650201, China*

Corresponding authors: Dingqi Rao (raodq@mail.kiz.ac.cn), Shuo Liu (liushuo@mail.kiz.ac.cn)

Academic editor: Thomas Ziegler | Received 11 August 2021 | Accepted 17 January 2022 | Published 27 January 2022

*http://zoobank.org/670EC7CC-90D3-4B2E-8EDE-7C34BF70FA0A*

Citation: Liu S, Rao D (2022) A new species of *Cyrtodactylus* Gray, 1827 (Squamata, Gekkonidae) from southwestern Yunnan, China. ZooKeys 1084: 83–100. https://doi.org/10.3897/zookeys.1084.72868

## Abstract

A new species of the *Cyrtodactylus chauquangensis* species group is described based on four specimens collected from the karst formations of Menglian County, Puer City, Yunnan Province, China. The new species can be separated from all other congeners by having a unique combination of morphological characters: a medium-sized body; ventrolateral folds present with interspersed small tubercles; seven precloacal pores in a continuous series in males, absent in females; enlarged femoral scales and femoral pores absent; two postcloacal tubercles on each side; and one or two rows of enlarged subcaudals. Genetically, the new species most closely related to *C. wayakonei* and the uncorrected sequence divergences of the ND2 gene and its flanking tRNAs between the new species and investigated congeners range from 7.2% to 18.4%.

## Keywords

Bent-toed gecko, *Cyrtodactylus chauquangensis* group, Menglian County, taxonomy

## Introduction

*Cyrtodactylus* Gray, 1827 is the most speciose and ecologically diverse gekkotan genus with more than 300 recognized species so far (Grismer et al. 2021a, b; Uetz et al. 2021). Grismer et al. (2021a) partitioned the species of *Cyrtodactylus* into 10 ecotypes according

to their habitat preferences. Of the 10 ecotypes, the karst ecotype is the second largest and contains the majority of the most recently described species (Grismer et al. 2021a).

The *Cyrtodactylus chauquangensis* Hoang, Orlov, Ananjeva, Johns, Hoang & Dau, 2007 species group, previously *C. wayakonei* Nguyen, Kingsada, Rösler, Auer & Ziegler, 2010 species group, is a karst ecotype species group, which is distributed in northern Indochina, ranging from northern Thailand and Laos to northwestern and central Vietnam, and to Yunnan Province in southern China (Grismer et al. 2021a, b). This species group contains 23 named species to date (Liu and Rao 2021a; Liu et al. 2021; Zhang et al. 2021).

During our fieldwork in southern Yunnan Province, China, in 2021, some specimens of *Cyrtodactylus* were collected from the karst formations of Menglian County, Puer City. Morphological and molecular phylogenetic analyses revealed that the new collection belonged to an unnamed species of the *C. chauquangensis* species group. We herein describe it as a new species.

## Materials and methods

### Sampling

Specimens were collected by hand. Photographs were taken to document the color pattern of specimens in life prior to their euthanization. Liver tissues were stored in 99% ethanol and specimens were preserved in 75% ethanol. Specimens were deposited at Kunming Natural History Museum of Zoology, Kunming Institute of Zoology, Chinese Academy of Sciences (**KIZ**).

### Morphological analyses

Measurements were taken with digital calipers to the nearest 0.1 mm. Bilateral scale counts were given as left/right. The methodology of measurements and meristic counts followed Liu and Rao (2021a, b):

**AG** axilla to groin distance;
**DTR** dorsal tubercle rows, number of dorsal, longitudinal rows of tubercles at midbody between ventrolateral folds;
**ED** ear diameter, greatest diameter of ear;
**EE** eye orbit to ear distance, from posterior corner of eye orbit to anterior margin of ear opening;
**EFS** enlarged femoral scales, number of enlarged femoral scale beneath each thigh;
**ForeaL** forearm length, from base of palm to elbow;
**FP** femoral pores;
**GSDT** granular scales surrounding dorsal midbody tubercles;
**HH** maximum head height, from occiput to underside of jaws;

**HL** head length, from tip of snout to posterior margin of retroarticular of lower jaw;
**HW** maximum head width;
**I** postrostrals or internasals;
**IFL** infralabials;
**IND** internarial distance, measured between inner borders of nostrils;
**IOD** interorbital distance, measured across narrowest point of frontal bone;
**LF4** subdigital lamellae under the fourth finger;
**LT4** subdigital lamellae under the fourth toe;
**ML** mental length;
**MW** mental width;
**OD** greatest diameter of orbit;
**PAT** postcloacal tubercles, number of tubercles on each side of postcloacal region;
**PM** postmentals, scales bordering mental shield, except infralabials;
**PP** precloacal pores;
**PVT** paravertebral tubercles, counted in a single paravertebral row from the level of the forelimb insertions to the level of the hind limb insertion;
**RH** rostral height;
**RW** rostral width;
**SE** snout to eye distance, from tip of snout to anterior corner of eye orbit;
**SL** shank length, from the base of heel to the knee;
**SPL** supralabials;
**SVL** snout–vent length, from tip of snout to anterior margin of cloaca;
**TaL** tail length, from posterior margin of cloaca to tip of tail;
**V** longitudinal ventral scale rows, counted across the belly between the ventrolateral folds at midbody.

Morphological comparisons were based on the original descriptions of each species (Hoang et al. 2007; Bauer et al. 2009, 2010; Ngo and Grismer 2010; Nguyen et al. 2010, 2015b, 2017; Sumontha et al. 2010; Luu et al. 2011; Ngo 2011; Ngo and Chan 2011; Kunya et al. 2014; Nazarov et al. 2014; Nguyen et al. 2014; Schneider et al. 2014, 2020; Le 2016; Pham et al. 2019; Liu and Rao 2021a; Liu et al. 2021; Zhang et al. 2021).

## Molecular analyses

Molecular data were generated for three specimens collected from Menglian County, Puer City, Yunnan Province, China, and available sequences of the *Cyrtodactylus chauquangensis* species group were obtained from GenBank; the new sequences have been deposited on GenBank under the accessions OM296042–OM296044. *Cyrtodactylus dattkyaikensis* Grismer, Wood, Quah, Grismer, Thura, Oaks & Lin, 2020 and *C. sinyineensis* Grismer, Wood Jr, Thura, Zin, Quah, Murdoch, Grismer, Lin, Kyaw & Lwin, 2017 were used as the outgroups according to Liu et al. (2021). Total genomic DNA was

extracted from liver tissue stored in 99% ethanol using a DNeasy blood and tissue kit, Qiagen (California, USA). A fragment of the NADH dehydrogenase subunit 2 (ND2) gene and its flanking tRNAs was amplified and sequenced using the primers L4437b and H5934 (Macey et al. 1997). The experiment protocols used in this study are the same as Liu et al. (2021). Sequences were edited and assembled using SeqMan in Lasergene 7.1 (DNASTAR Inc., Madison, WI, USA) and MEGA X (Kumar et al. 2018).

Sequences were aligned using ClustalW (Thompson et al. 1994) with default parameters. The best-fit substitution models were chosen using the Bayesian Information Criterion (BIC) in ModelFinder (Kalyaanamoorthy et al. 2017) for IQ-TREE and MrBayes, respectively. Maximum likelihood analysis was performed in IQ-TREE 1.6.12 (Nguyen et al. 2015a) used the TIM+F+I+G4 model for the first codon position, the second codon position, and the tRNAs; and the GTR+F+R2 model for the third codon position. One thousand bootstrap pseudoreplicates via the ultrafast bootstrap approximation algorithm were used to construct a final consensus tree. Nodes with ultrafast bootstrap values of 95 and above were considered significantly supported (Minh et al. 2013). Bayesian inference was performed in MrBayes 3.2.6 (Ronquist et al. 2012) used the GTR+F+I+G4 model of evolution for the first codon position, the second codon position, and the tRNAs; and GTR+F+G4 model for the third codon position. The chains were run for 1,000,000 generations and sampled every 100 generations. The first 25% of the sampled trees was discarded as burn-in and then the remaining trees were used to estimate Bayesian posterior probabilities. Nodes with Bayesian posterior probabilities of 0.95 or higher were considered well-supported (Huelsenbeck et al. 2001; Wilcox et al. 2002). Pairwise distances between species were calculated in MEGA X (Kumar et al. 2018).

## Results

The obtained sequence alignment is 1397 bp in length. The sequences of the three specimens collected from Menglian County, Yunnan, China, were nested within the *Cyrtodactylus chauquangensis* species group and represented a distinct clade sister to *C. wayakonei* Nguyen, Kingsada, Rösler, Auer & Ziegler, 2010 with strong support (Fig. 1). The interspecific pairwise distances between the newly collected specimens and other members of *C. chauquangensis* species group ranged from 7.2% to 18.4% (Table 1).

***Cyrtodactylus menglianensis* sp. nov.**
http://zoobank.org/6E8C0453-145B-4862-9A87-BC3F4F4344FD
Figures 2–5

**Type material.** ***Holotype*.** KIZ20210713, adult male, collected on 18 July 2021 by Shuo Liu from Menglian County, Puer City, Yunnan Province, China (22°20'11"N, 99°34'29"E, 980 m elevation).

**Table 1.** Mean uncorrected pairwise genetic distances (%) among the species of the *Cyrtodactylus chauquangensis* species group and outgroups based on the ND2 gene and its flanking tRNAs.

| | 1 | 2 | 3 | 4 | 5 | 6 | 7 | 8 | 9 | 10 | 11 | 12 | 13 | 14 | 15 | 16 | 17 | 18 | 19 | 20 | 21 | 22 | 23 |
|---|---|---|---|---|---|---|---|---|---|---|---|---|---|---|---|---|---|---|---|---|---|---|---|
| 1 *Cyrtodactylus menglianensis* sp. nov. | | | | | | | | | | | | | | | | | | | | | | | |
| 2 *Cyrtodactylus auribalteatus* | 12.2 | | | | | | | | | | | | | | | | | | | | | | |
| 3 *Cyrtodactylus bichnganae* | 18.4 | 18.3 | | | | | | | | | | | | | | | | | | | | | |
| 4 *Cyrtodactylus bobrovi* | 15.0 | 13.9 | 19.7 | | | | | | | | | | | | | | | | | | | | |
| 5 *Cyrtodactylus chauquangensis* | 12.6 | 13.3 | 18.1 | 8.6 | | | | | | | | | | | | | | | | | | | |
| 6 *Cyrtodactylus cucphuongensis* | 15.0 | 14.5 | 19.9 | 7.9 | 8.4 | | | | | | | | | | | | | | | | | | |
| 7 *Cyrtodactylus doisuthep* | 15.5 | 13.6 | 16.6 | 15.9 | 14.4 | 15.9 | | | | | | | | | | | | | | | | | |
| 8 *Cyrtodactylus dumnuii* | 11.4 | 11.9 | 17.0 | 13.7 | 12.3 | 14.4 | 14.3 | | | | | | | | | | | | | | | | |
| 9 *Cyrtodactylus erythrops* | 13.9 | 13.8 | 16.7 | 14.8 | 13.5 | 14.7 | 11.0 | 13.4 | | | | | | | | | | | | | | | |
| 10 *Cyrtodactylus gulinqingensis* | 14.3 | 13.2 | 18.1 | 13.8 | 14.0 | 14.0 | 14.1 | 12.9 | 13.8 | | | | | | | | | | | | | | |
| 11 *Cyrtodactylus houaphanensis* | 14.8 | 14.6 | 19.4 | 6.5 | 9.0 | 7.5 | 15.5 | 14.2 | 14.9 | 14.1 | | | | | | | | | | | | | |
| 12 *Cyrtodactylus huongsonensis* | 14.3 | 13.4 | 17.7 | 14.3 | 12.5 | 14.3 | 14.7 | 13.9 | 14.3 | 12.4 | 14.7 | | | | | | | | | | | | |
| 13 *Cyrtodactylus ngoiensis* | 13.1 | 13.2 | 18.2 | 11.1 | 10.5 | 10.7 | 14.9 | 12.0 | 14.2 | 13.1 | 11.3 | 13.1 | | | | | | | | | | | |
| 14 *Cyrtodactylus otai* | 15.2 | 14.6 | 19.1 | 3.6 | 9.1 | 8.4 | 16.3 | 15.6 | 16.4 | 15.6 | 6.8 | 14.7 | 12.2 | | | | | | | | | | |
| 15 *Cyrtodactylus puhuensis* | 14.2 | 13.4 | 18.9 | 5.7 | 8.0 | 7.1 | 14.7 | 12.9 | 14.2 | 13.6 | 2.8 | 13.8 | 10.5 | 6.2 | | | | | | | | | |
| 16 *Cyrtodactylus soni* | 13.4 | 13.0 | 18.2 | 14.3 | 13.6 | 14.4 | 14.2 | 13.1 | 14.2 | 13.0 | 15.3 | 6.7 | 14.0 | 14.7 | 14.2 | | | | | | | | |
| 17 *Cyrtodactylus sonlaensis* | 17.2 | 16.2 | 19.4 | 17.5 | 16.8 | 18.1 | 16.2 | 16.8 | 17.3 | 14.8 | 18.0 | 15.0 | 16.2 | 17.7 | 18.0 | 15.2 | | | | | | | |
| 18 *Cyrtodactylus spelaeus* | 14.6 | 13.9 | 18.3 | 10.0 | 9.2 | 10.4 | 15.7 | 13.4 | 15.0 | 13.9 | 10.4 | 14.3 | 11.1 | 11.3 | 9.1 | 14.3 | 17.7 | | | | | | |
| 19 *Cyrtodactylus taybacensis* | 16.8 | 15.6 | 9.3 | 17.1 | 15.5 | 17.3 | 15.7 | 14.9 | 16.4 | 16.3 | 17.3 | 16.1 | 16.6 | 18.3 | 16.7 | 15.6 | 18.9 | 16.5 | | | | | |
| 20 *Cyrtodactylus vilaphongi* | 14.1 | 13.4 | 17.8 | 8.1 | 7.3 | 8.2 | 14.2 | 13.3 | 14.0 | 13.5 | 8.2 | 14.2 | 9.5 | 9.1 | 7.0 | 13.5 | 16.9 | 9.6 | 16.5 | | | | |
| 21 *Cyrtodactylus wayakonei* | 7.2 | 13.1 | 18.0 | 15.5 | 13.1 | 15.5 | 16.3 | 12.7 | 15.6 | 15.3 | 14.7 | 15.1 | 12.2 | 15.4 | 14.2 | 13.9 | 16.4 | 15.2 | 17.5 | 13.7 | | | |
| 22 *Cyrtodactylus zhenkangensis* | 10.7 | 12.0 | 18.4 | 14.1 | 13.2 | 13.8 | 15.5 | 11.8 | 14.0 | 12.9 | 13.9 | 13.4 | 13.2 | 15.5 | 13.2 | 13.7 | 17.3 | 14.0 | 15.8 | 13.6 | 11.9 | | |
| 23 *Cyrtodactylus dattkyaikensis* | 18.3 | 17.2 | 21.4 | 18.8 | 18.0 | 19.4 | 18.0 | 17.0 | 16.8 | 16.8 | 19.9 | 17.2 | 18.0 | 21.5 | 18.8 | 17.9 | 21.8 | 19.3 | 18.4 | 17.8 | 19.9 | 17.9 | |
| 24 *Cyrtodactylus sinyineensis* | 18.8 | 17.8 | 18.9 | 18.7 | 17.5 | 18.1 | 18.2 | 17.0 | 18.7 | 18.9 | 18.9 | 19.1 | 17.5 | 20.9 | 18.1 | 18.7 | 21.9 | 18.9 | 17.9 | 18.1 | 19.4 | 18.4 | 13.1 |

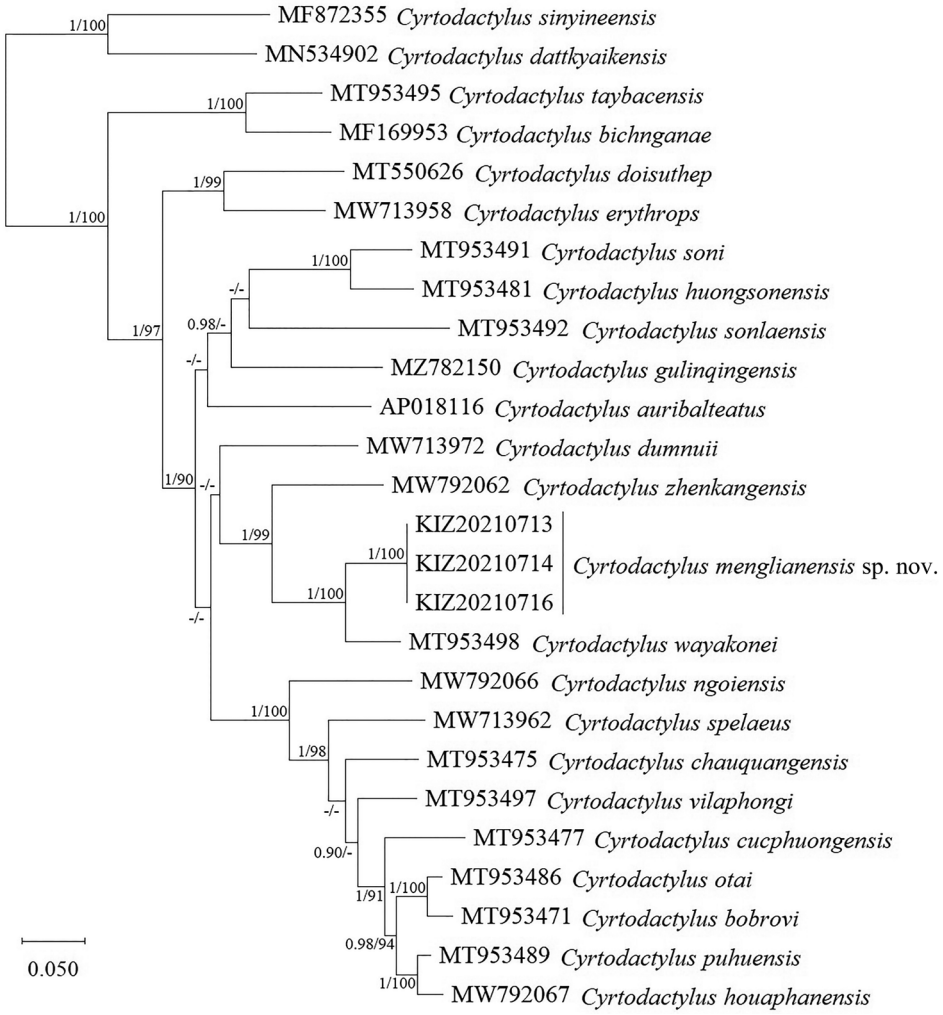


**Figure 1.** Bayesian phylogram of the *Cyrtodactylus chauquangensis* species group inferred from the ND2 gene and its flanking tRNAs. Numbers before slashes indicate Bayesian posterior probabilities and numbers after slashes indicate the ML ultrafast bootstrap. The symbol "–" represents the value below 0.90/90.

***Paratypes*.** KIZ20210714 and KIZ20210716, two adult females; KIZ20210715, adult male; all collected on 19 July 2021 by Shuo Liu from the same locality as the holotype.

**Etymology.** The specific epithet refers to Menglian County, the locality where the new species was found. We propose "Menglian Bent-toed Gecko" for the common English name and "孟连裸趾虎" (Mèng Lián Luǒ Zhǐ Hǔ) for the common Chinese name of the new species.

**Diagnosis.** Medium body size (SVL 67.7–78.1 mm in adults); ventrolateral folds present with interspersed small tubercles; seven precloacal pores in a continuous series in males, absent in females; femoral scales not enlarged; femoral pores absent; two

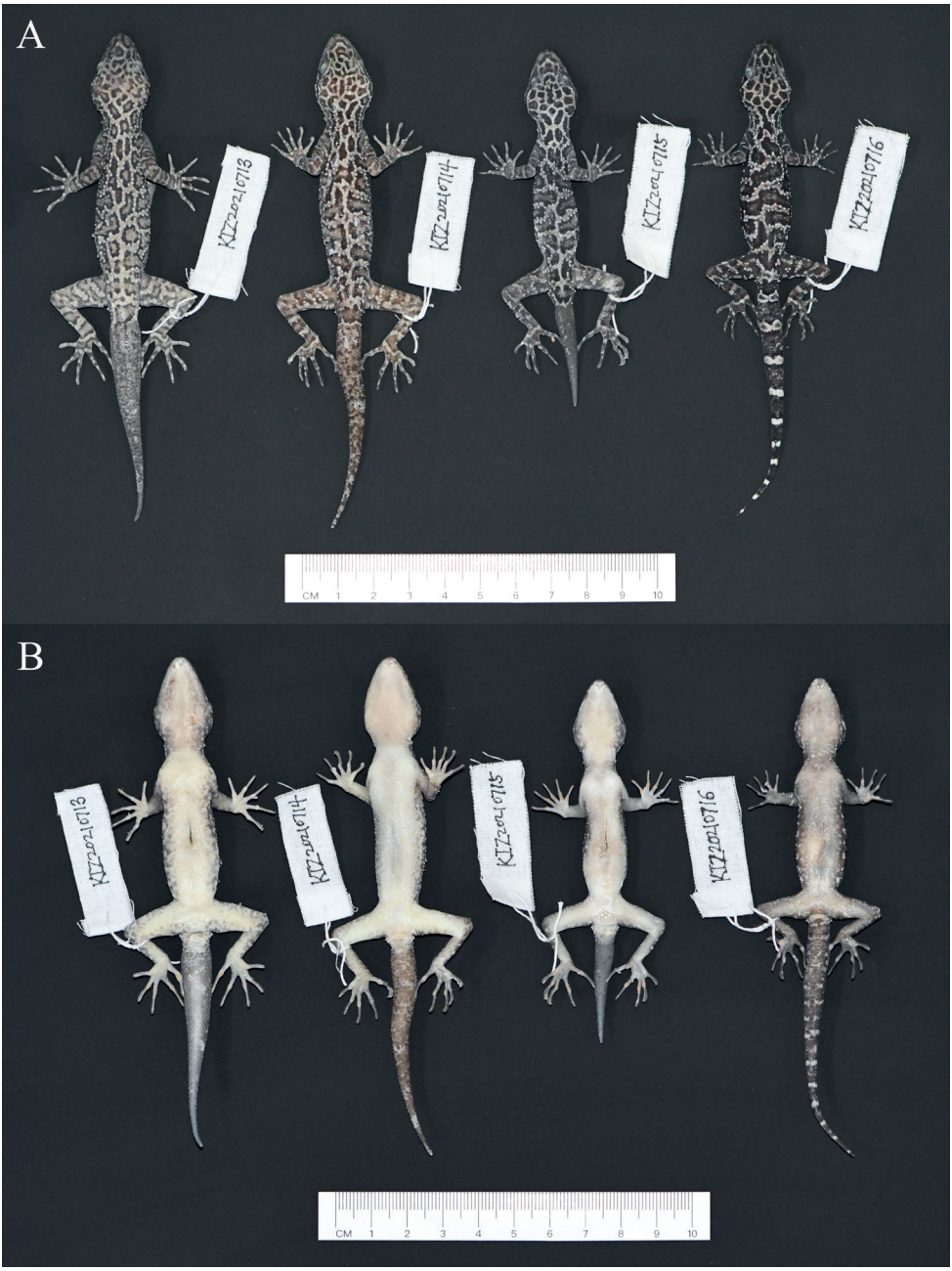


**Figure 2.** Type series of *Cyrtodactylus menglianensis* sp. nov. in preservative **A** dorsal views **B** ventral views.

postcloacal tubercles on each side; 17–22 lamellae under finger IV, 21–23 lamellae under toe IV; one or two rows of subcaudals enlarged; dark postocular streak and nuchal loop absent; six or seven dark irregular dorsal bands between limb insertions, most bands discontinuous.

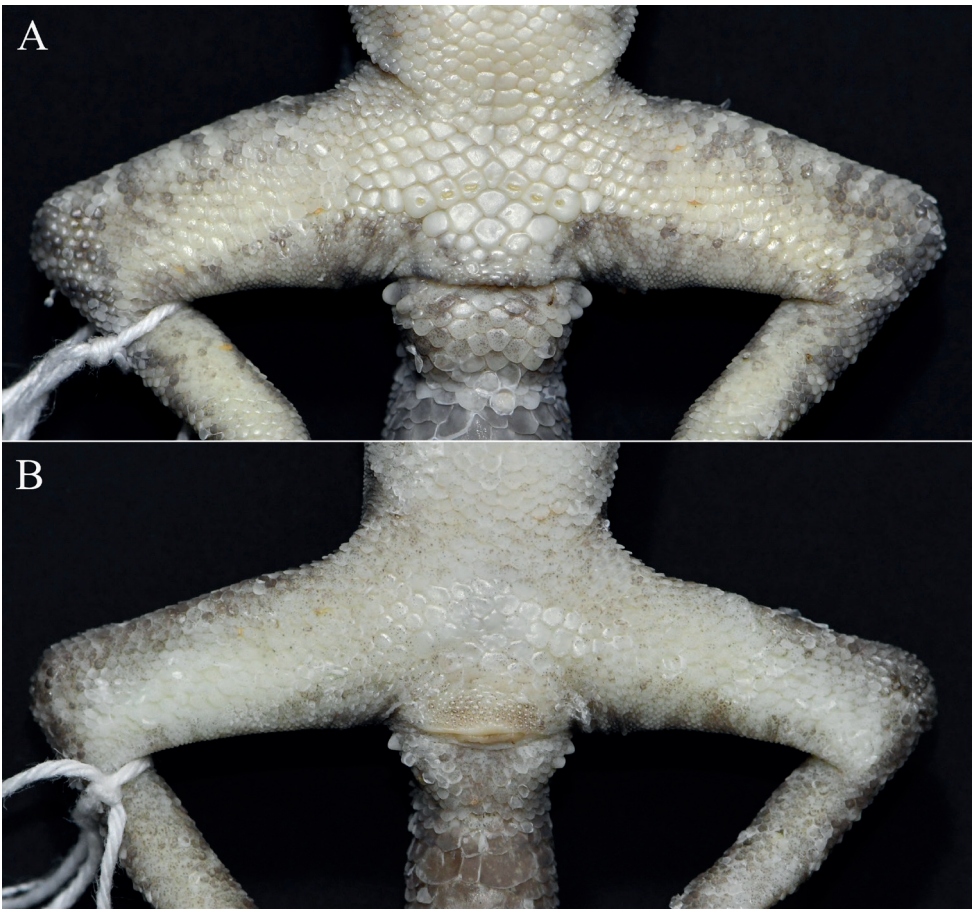


**Figure 3.** Close-up views of the femoral and precloacal regions of *Cyrtodactylus menglianensis* sp. nov. **A** male holotype (KIZ20210713) **B** female paratype (KIZ20210714).

**Description of holotype.** Adult male, SVL 77.8 mm; head distinguished from neck, moderately long (HL/SVL 0.28), relatively widened (HW/HL 0.76), slightly depressed (HH/HL 0.45); two supranasals separated by one internasal; nares oval, surrounded by supranasal, rostral, first supralabial, and three postnasals; loreal region concave; snout long (SE/HL 0.43), round anteriorly, longer than diameter of orbit (OD/SE 0.63); snout scales small, round, granular, larger than those in frontal and parietal regions; eye large (OD/HL 0.27), pupils vertical; upper eyelid fringe with spinous scales; ear opening oval, small (ED/HL 0.09); rostral wider than high (RH/RW 0.58), medially divided dorsally by a suture, reaching to approximately half down rostral, in contact with first supralabial and nostrils laterally, and supranasals and internasal dorsally; mental triangular, narrower than rostral (MW/RW 0.82), slightly wider than high (ML/MW 0.94); two postmentals, enlarged, in contact posteriorly, bordered by mental anteromedially, first infralabial anterolaterally, two enlarged chin scales posterolaterally, and small chin scales posteriorly; 10/12 supralabials; 9/9 infralabials.

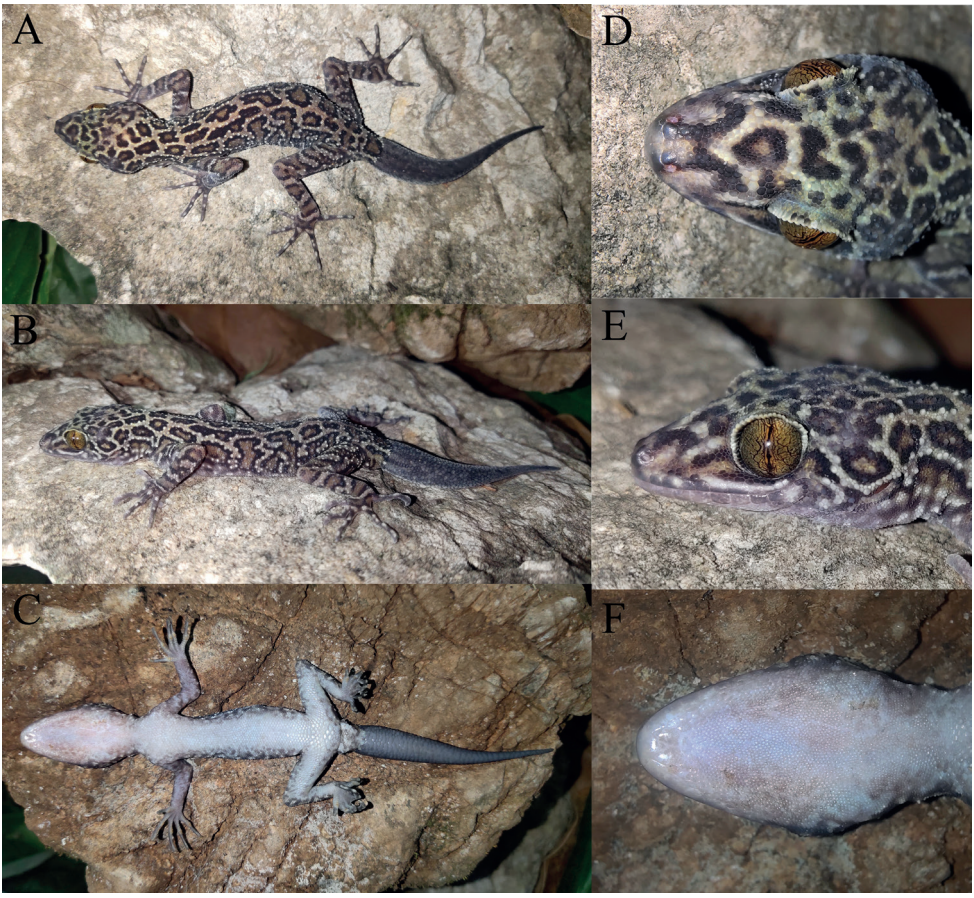


**Figure 4.** Holotype (KIZ20210713) of *Cyrtodactylus menglianensis* sp. nov. in life **A** dorsal view of whole body **B** lateral view of whole body **C** ventral view of whole body **D** dorsal view of head **E** lateral view of head **F** ventral view of head.

Body slender (AG/SVL 0.39), ventrolateral folds slightly developed with interspersed small tubercles; dorsal scales granular; dorsal tubercles round and weakly keeled, four or five times larger than the size of adjoining scales, conical, present on neck, back and tail base, each surrounded by 10 granular scales, in 19 irregular longitudinal rows at the midbody, 26 paravertebral tubercles; gular region with homogenous smooth scales; ventral scales smooth, larger than those of dorsum, round, subimbricate, largest posteriorly, in 29 longitudinal rows at midbody; precloacal groove absent; a patch of precloacal scales significantly enlarged; seven precloacal pores in a continuous series, the two on the edge round, the one in the middle pitted, others horizontally elongated; femoral scales not enlarged; femoral pore absent.

Fore and hind limbs moderately slender (ForeaL/SVL 0.17, SL/SVL 0.20); dorsal surface of forelimbs covered by a few weakly developed tubercles; interdigital webbing absent; lamellae under finger IV 22/21, under toe IV 23/22; relative length of fingers I < II < V < III < IV, relative length of toes I < II < III < V < IV.

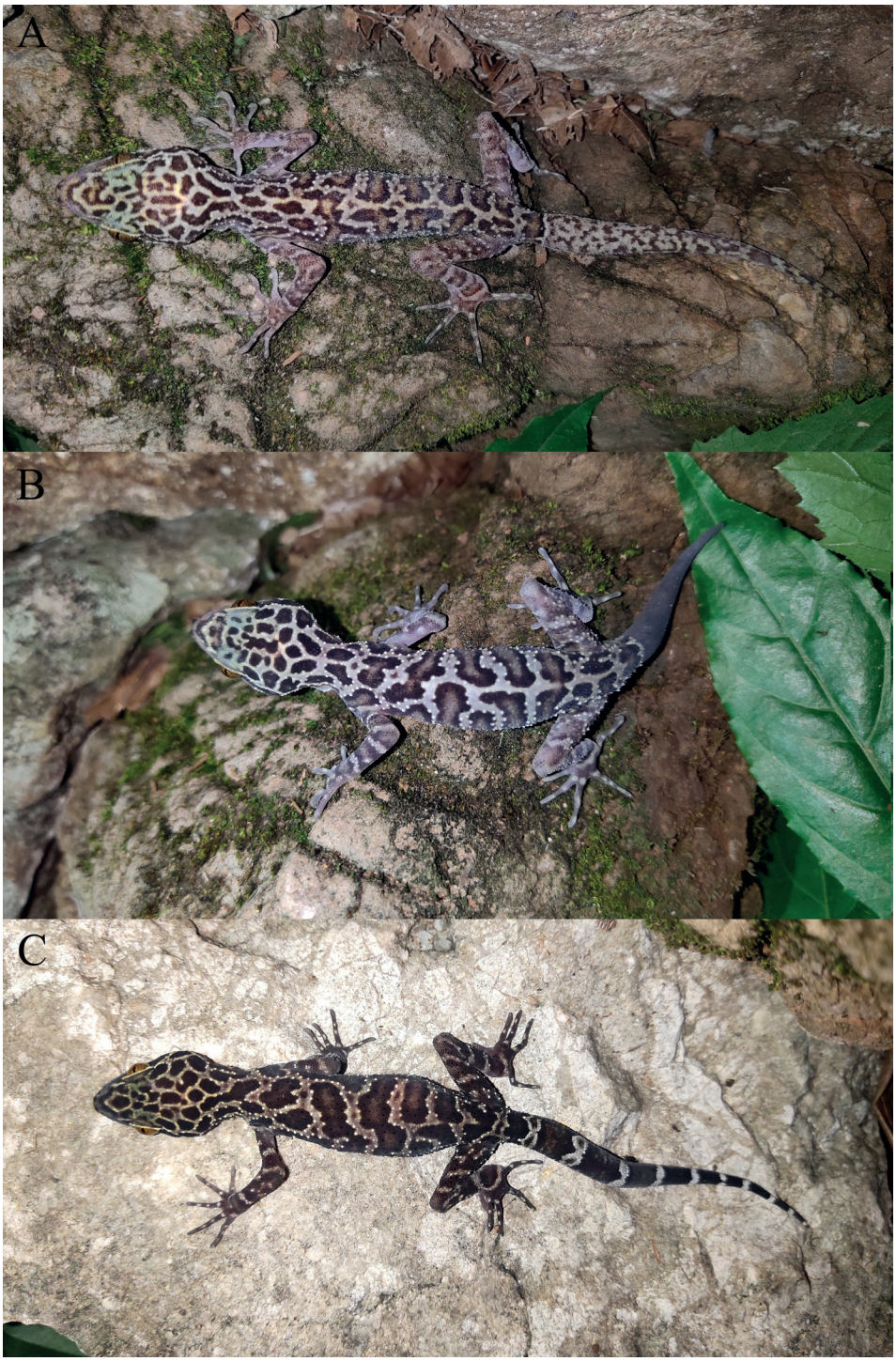


**Figure 5.** Paratypes of *Cyrtodactylus menglianensis* sp. nov. in life **A** female paratype (KIZ20210714) **B** male paratype (KIZ20210715) **C** female paratype (KIZ20210716).

Tail regenerated (TaL 60.8 mm); 2/2 postcloacal tubercles; dorsal tail base with tubercles; subcaudals smooth, enlarged but arranged irregularly.

**Color of holotype in life.** Dorsal ground color brownish yellow; dorsal surface of head with irregular brown blotches with black edges, largest at occiput; nuchal loop absent; dorsum with many irregular brownish black blotches with black edges, forming eight transverse discontinuous bands faintly, one on the neck, one between hind limbs, and six between fore and hind limb insertions; dorsal surfaces of limbs with brown bands with black edges; a brown band with black edge on dorsal tail base, dorsal surface of regenerated tail greyish black; ventral surface of head, limbs, and body greyish white; ventral surface of regenerated tail grey; iris bronze.

**Color of holotype in preservative.** The color pattern very much resembles that in life. Brownish yellow dorsal ground color turned to greyish white, the brown blotches and bands with black edges remained; ventral surface faded to pale white; iris became white.

**Variations.** The paratypes resemble the holotype except that the female KIZ20210714 has a longer regenerated tail, and the female KIZ20210716 has a longer original tail with one or two rows of subcaudals enlarged, and they both have no precloacal pores; the male KIZ20210715 has a smaller body size and much shorter regenerated tail; other morphometric and meristic differences are presented in Table 2. Color patterns of the paratypes also resemble the holotype except that the dark bands on the dorsum are relatively more distinct, and there are 10 black and white rings on the original tail of the female KIZ20210716.

**Distribution.** The new species is currently known only from the type locality (Fig. 6) in Menglian County, Puer City, Yunnan Province, China.

**Natural history.** All specimens were collected at night on large stones or cliffs of the karst formations in a park. The surrounding habitats was karst forest, there is a plank road and a river nearby.

**Comparisons.** *Cyrtodactylus menglianensis* sp. nov. is distinguishable from all other members of the *C. chauquangensis* species group by a unique combination of morphological characters. *Cyrtodactylus menglianensis* sp. nov. differs from *C. auribalteatus* Sumontha, Panitvong & Deein, 2010; *C. bichnganae* Ngo & Grismer, 2010; *C. doisuthep* Kunya, Panmongkol, Pauwels, Sumontha, Meewasana, Bunkhwamdi & Dangsri, 2014; *C. dumnuii* Bauer, Kunya, Sumontha, Niyomwan, Pauwels, Chanhome & Kunya, 2010; *C. erythrops* Bauer, Kunya, Sumontha, Niyomwan, Panitvong, Pauwels, Chanhome & Kunya, 2009; *C. gulinqingensis* Liu, Li, Hou, Orlov & Ananjeva, 2021; *C. hekouensis* Zhang, Liu, Bernstein, Wang & Yuan, 2021; *C. huongsonensis* Luu, Nguyen, Do & Ziegler, 2011; *C. ngoiensis* Schneider, Luu, Sitthivong, Teynié, Le, Nguyen & Ziegler, 2020; *C. soni* Le, Nguyen, Le & Ziegler, 2016; *C. sonlaensis* Nguyen, Pham, Ziegler, Ngo & Le, 2017; and *C. zhenkangensis* Liu & Rao, 2021 by not having enlarged femoral scales and femoral pores (vs having enlarged femoral scales and femoral pores).

*Cyrtodactylus menglianensis* sp. nov. differs from *C. puhuensis* Nguyen, Yang, Le, Nguyen, Orlov, Hoang, Nguyen, Jin, Rao, Hoang, Che, Murphy & Zhang, 2014 and *C. taybacensis* Pham, Le, Ngo, Ziegler & Nguyen, 2019 by not having enlarged femoral scales (vs having enlarged femoral scales). In addition, *C. menglianensis* sp. nov.

**Table 2.** Measurements (mm) and meristic data for the type series of *Cyrtodactylus menglianensis* sp. nov. Abbreviations defined in Materials and methods. "*" represents regenerated tail and "#" represents original tail.

| | KIZ20210713 Holotype | KIZ20210714 Paratype | KIZ20210715 Paratype | KIZ20210716 Paratype |
|---|---|---|---|---|
| | Male | Female | Male | Female |
| SVL | 77.8 | 78.1 | 69.1 | 67.7 |
| TaL | 60.8* | 62.9* | 33.2* | 70.6# |
| HH | 9.7 | 9.7 | 8.3 | 8.7 |
| HL | 21.7 | 21.8 | 19.4 | 19.2 |
| HW | 16.4 | 15.8 | 14.8 | 14.5 |
| OD | 5.9 | 6.9 | 5.1 | 5.3 |
| SE | 9.3 | 9.2 | 8.2 | 8.3 |
| EE | 6.3 | 5.9 | 5.6 | 5.6 |
| IND | 3.1 | 3.1 | 2.9 | 2.6 |
| IOD | 3.3 | 3.5 | 2.8 | 2.7 |
| ED | 1.9 | 1.3 | 1.3 | 1.2 |
| AG | 30.5 | 34.6 | 27.8 | 28.4 |
| ForeaL | 13.0 | 12.9 | 11.4 | 10.6 |
| SL | 15.7 | 15.6 | 14.0 | 13.1 |
| RW | 3.8 | 3.4 | 2.9 | 3.0 |
| RH | 2.2 | 2.1 | 1.9 | 1.8 |
| MW | 3.1 | 3.2 | 2.9 | 3.8 |
| ML | 2.9 | 2.6 | 2.6 | 2.0 |
| SPL | 10/12 | 9/10 | 8/9 | 10/9 |
| IFL | 9/9 | 9/9 | 9/8 | 9/7 |
| I | 1 | 1 | 1 | 1 |
| PM | 2 | 2 | 2 | 2 |
| GSDT | 10 | 10 | 10 | 10 |
| DTR | 19 | 21 | 20 | 18 |
| PVT | 26 | 27 | 25 | 29 |
| V | 29 | 26 | 26 | 28 |
| EFS | 0 | 0 | 0 | 0 |
| PP | 7 | 0 | 7 | 0 |
| FP | 0 | 0 | 0 | 0 |
| PAT | 2/2 | 2/2 | 2/2 | 2/2 |
| LF4 | 22/21 | 19/18 | 18/17 | 21/22 |
| LT4 | 23/22 | 22/22 | 22/21 | 23/23 |

differs from *C. puhuensis* by having more precloacal pores in males (seven vs five) and differs from *C. taybacensis* by having fewer precloacal pores in males (seven vs 11–13).

*Cyrtodactylus menglianensis* sp. nov. differs from *C. cucphuongensis* Ngo & Chan, 2011 by having precloacal pores in males (vs not having precloacal pores in males).

*Cyrtodactylus menglianensis* sp. nov. differs from *C. bobrovi* Nguyen, Le, Pham, Ngo, Hoang, Pham & Ziegler, 2015; *C. chauquangensis* Hoang, Orlov, Ananjeva, Johns, Hoang & Dau, 2007; *C. houaphanensis* Schneider, Luu, Sitthivong, Teynié, Le, Nguyen & Ziegler, 2020; *C. otai* Nguyen, Le, Pham, Ngo, Hoang, Pham & Ziegler, 2015; *C. spelaeus* Nazarov, Poyarkov, Orlov, Nguyen, Milto, Martynov, Konstantinov & Chulisov, 2014; and *C. vilaphongi* Schneider, Nguyen, Le, Nophaseud, Bonkowski & Ziegler, 2014 by not having dark postocular streak and nuchal loop (vs having very obvious dark postocular streak and not obvious nuchal loop).

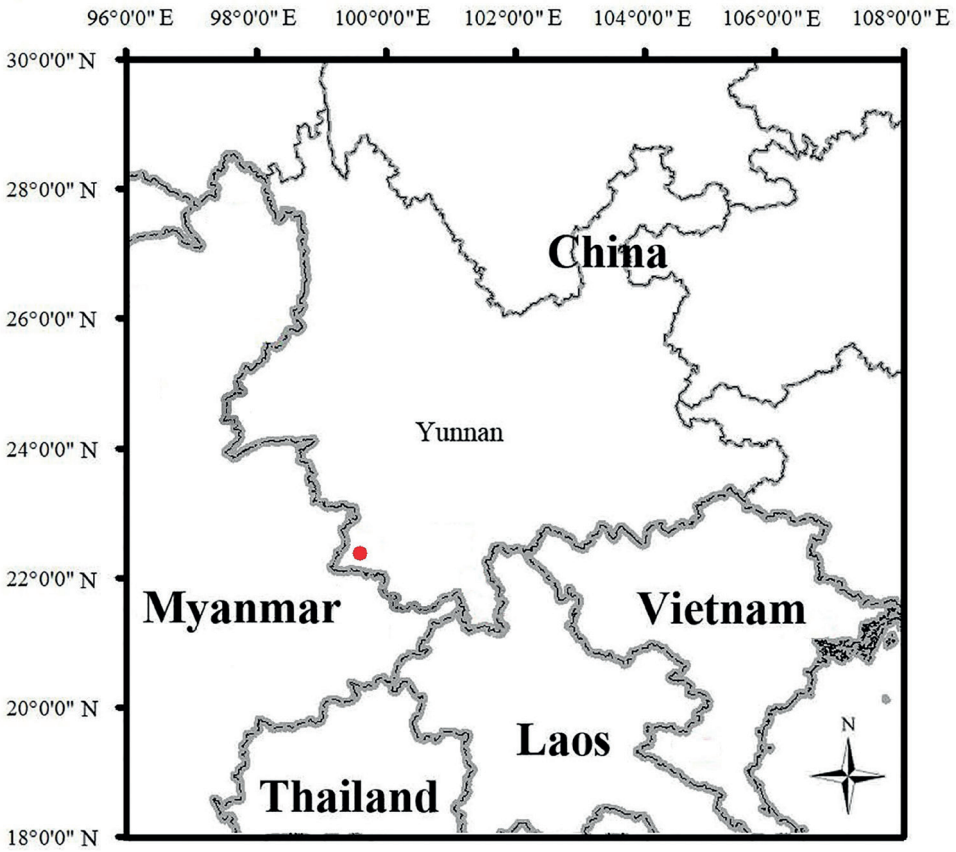


**Figure 6.** Map showing the type locality (red dot) of *Cyrtodactylus menglianensis* sp. nov. in Menglian County, Puer City, Yunnan Province, China.

*Cyrtodactylus menglianensis* sp. nov. differs from *C. martini* Ngo, 2011 by not having enlarged femoral scales (vs having indistinctly enlarged femoral scales), having fewer longitudinal ventral scale rows (26–29 vs 39–43), having more precloacal pores in males (seven vs four), and having more white rings on the original tail (10 vs 7).

*Cyrtodactylus menglianensis* sp. nov. differs from *C. wayakonei* Nguyen, Kingsada, Rösler, Auer & Ziegler, 2010 by having fewer longitudinal ventral scale rows (26–29 vs 31–35), not having precloacal pores in females (vs having precloacal pores in females), and having more white rings on the original tail (10 vs 6).

## Discussion

The new species was found in a park just beside the county seat. There is a plank road along the limestone cliffs in the park, and there are many lamps on the limestone cliffs along the plank road (Fig. 7). These lamps light up every night and have some influence on nocturnal animals. We found that the populations of nocturnal animals there

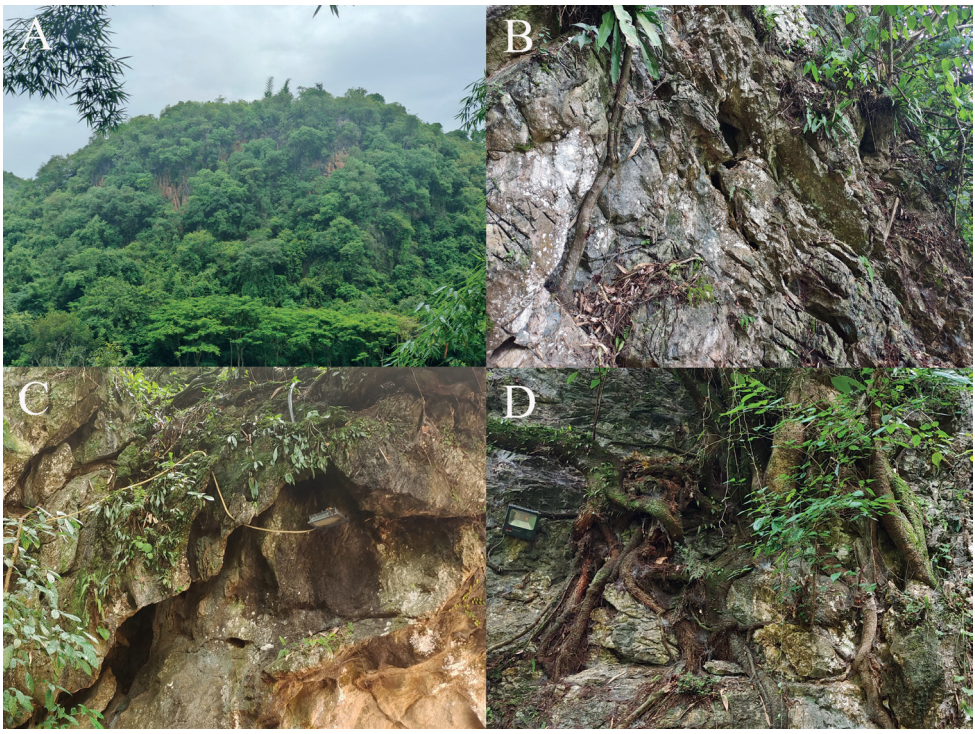


**Figure 7.** Habitat of *Cyrtodactylus menglianensis* sp. nov. at the type locality **A** distant view **B** close view **C, D** lamps on the limestone cliffs.

were very small, including that of the new species. Next to the park is a small nature reserve, which focuses only on the protection of several rare plants. We suggest that this nature reserve also include animals and the karst formations into their protection.

There are still many karst landforms in southern Yunnan which have not been surveyed in detail. Additional cryptic new species of *Cyrtodactylus* are likely to be found in these areas. It is necessary to strengthen the protection of these karst landforms and to survey these areas.

## Acknowledgements

We thank to our workmates for their help and advice. We also thank the editors and reviewers for their comments on the manuscript. This work was supported by Science-Technology Basic Condition Platform from the Ministry of Science and Technology of the People's Republic of China (grant no. 2005DKA21402), National Natural Science Foundation Project: Investigation and Classificatory and Phylogenetic Studies on the Lizards of Gekkonidae of China (grant no. NSFC-31970404), and the project of Ministry of Ecology and Environment of China: Investigation and assessment of amphibians and reptiles in southern Yunnan.

## References

Bauer AM, Kunya K, Sumontha M, Niyomwan P, Panitvong N, Pauwels OSG, Chanhome L, Kunya T (2009) *Cyrtodactylus erythrops* (Squamata: Gekkonidae), a new cave-dwelling gecko from Mae Hong Son Province, Thailand. Zootaxa 2142: 51–62. https://doi.org/10.11646/zootaxa.2124.1.4

Bauer AM, Kunya K, Sumontha M, Niyomwan P, Panitvong N, Pauwels OSG, Chanhome L, Kunya T (2010) *Cyrtodactylus dumnuii* (Squamata: Gekkonidae), a new cave-dwelling gecko from Chiang Mai Province, Thailand. Zootaxa 2570: 41–50. https://doi.org/10.11646/zootaxa.2570.1.2

Dring JCM (1979) Amphibians and reptiles from northern Trengganu, Malaysia, with descriptions of two new geckos: *Cnemaspis* and *Cyrtodactylus*. Bulletin of the British Museum (Natural History), Zoology 34: 181–241.

Grismer LL, Wood Jr PL, Thura MK, Thaw Zin, Quah ESH, Murdoch ML, Grismer MS, Lin A, Kyaw H, Lwin N (2017) Twelve new species of *Cyrtodactylus* Gray (Squamata: Gekkonidae) from isolated limestone habitats in east-central and southern Myanmar demonstrate high localized diversity and unprecedented microendemism. Zoological Journal of the Linnean Society 182(4): 862–959. https://doi.org/10.1093/zoolinnean/zlx057

Grismer LL, Wood Jr PL, Quah ESH, Grismer MS, Thura MK, Oaks JR, Lin A (2020) Two new species of *Cyrtodactylus* Gray, 1827 (Squamata: Gekkonidae) from a karstic archipelago in the Salween Basin of southern Myanmar (Burma). Zootaxa 4718(2): 151–183. https://doi.org/10.11646/zootaxa.4718.2.1

Grismer LL, Wood Jr PL, Poyarkov NA, Le MD, Karunarathna S, Chomdej S, Suwannapoom C, Qi S, Liu S, Che J, Quah ESH, Kraus F, Oliver PM, Riyanto A, Pauwels OSG, Grismer JL (2021a) Karstic landscapes are foci of species diversity in the world's third-largest vertebrate genus *Cyrtodactylus* Gray, 1827 (Reptilia: Squamata; Gekkonidae). Diversity 13(5): e183. https://doi.org/10.3390/d13050183

Gray JE (1827) A synopsis of the genera of saurian reptiles in which some new genera are indicated, and the others reviewed by actual examination. The Philosophical Magazine 2(7): 54–58. https://doi.org/10.1080/14786442708675620

Grismer LL, Wood Jr PL, Poyarkov NA, Le MD, Kraus F, Agarwal I, Oliver PM, Nguyen SN, Nguyen TQ, Karunarathna S, Welton LJ, Stuart BL, Luu VQ, Bauer AM, O'Connell KA, Quah ESH, Chan KO, Ziegler T, Ngo H, Nazarov RA, Aowphol A, Chomdej S, Suwannapoom C, Siler CD, Anuar S, Ngo TV, Grismer JL (2021b) Phylogenetic partitioning of the third-largest vertebrate genus in the world, *Cyrtodactylus* Gray, 1827 (Reptilia; Squamata; Gekkonidae) and its relevance to taxonomy and conservation. Vertebrate Zoology 71: 101–154. https://doi.org/10.3897/vz.71.e59307

Hoang QX, Orlov NL, Ananjeva NB, Johns AG, Hoang TN, Dau VQ (2007) Description of a new species of the genus *Cyrtodactylus* Gray, 1827 (Squamata: Sauria: Gekkonidae) from the karst of North Central Vietnam. Russian Journal of Herpetology 14: 98–106. https://doi.org/10.30906/1026-2296-2007-14-2-98-106

Huelsenbeck JP, Ronquist F, Nielsen R, Bollback JP (2001) Bayesian inference of phylogeny and its impact on evolutionary biology. Science 294(5550): 2310–2314. https://doi.org/10.1126/science.1065889

Ivanova NV, Dewaard JR, Hebert PDN (2006) An inexpensive, automation-friendly protocol for recovering high-quality DNA. Molecular Ecology Notes 6: 998–1002. https://doi.org/10.1111/j.1471-8286.2006.01428.x

Kalyaanamoorthy S, Minh BQ, Wong TKF, von Haeseler A, Jermiin LS (2017) ModelFinder: fast model selection for accurate phylogenetic estimates. Nature Methods 14: 587–589. https://doi.org/10.1038/nmeth.4285

Kumar S, Stecher G, Li M, Knyaz C, Tamura K (2018) MEGA X: Molecular Evolutionary Genetics Analysis across computing platforms. Molecular Biology and Evolution 35: 1547–1549. https://doi.org/10.1093/molbev/msy096

Kunya K, Panmongkol A, Pauwels OGS, Sumontha M, Meewasana J, Bunkhwamdi W, Dangsri S (2014) A new forest-dwelling bent-toed gecko (Squamata: Gekkonidae: *Cyrtodactylus*) from Doi Suthep, Chiang Mai Province, northern Thailand. Zootaxa 3811: 251–261. https://doi.org/10.11646/zootaxa.3811.2.6

Le DT, Nguyen TQ, Le MD, Ziegler T (2016) A new species of *Cyrtodactylus* (Squamata: Gekkonidae) from Ninh Binh Province, Vietnam. Zootaxa 4162(2): 268–282. https://doi.org/10.11646/zootaxa.4162.2.4

Liu S, Rao DQ (2021a) A new species of *Cyrtodactylus* Gray, 1827 (Squamata, Gekkonidae) from Yunnan, China. ZooKeys 1021: 109–126. https://doi.org/10.3897/zookeys.1021.60402

Liu S, Rao DQ (2021b) A new species of *Cyrtodactylus* Gray, 1827 (Squamata: Gekkonidae) from western Yunnan, China. Journal of Natural History 55: 713–731. https://doi.org/10.1080/00222933.2021.1921871

Liu S, Li QS, Hou M, Orlov NL, Ananjeva NB (2021) A new species of *Cyrtodactylus* Gray, 1827 (Squamata, Gekkonidae) from southern Yunnan, China. Russian Journal of Herpetology 28(4): 185–196. https://doi.org/10.30906/1026-2296-2021-28-4-185-196

Luu VQ, Nguyen TQ, Do HQ, Ziegler T (2011) A new *Cyrtodactylus* (Squamata: Gekkonidae) from Huong Son limestone forest, Hanoi, northern Vietnam. Zootaxa 3129: 39–50. https://doi.org/10.11646/zootaxa.3129.1.3

Minh Q, Nguyen MAT, von Haeseler A (2013) Ultrafast approximation for phylogenetic bootstrap. Molecular Biology and Evolution 30(5): 1188–1195. https://doi.org/10.1093/molbev/mst024

Nazarov RA, Poyarkov NA, Orlov NL, Nguyen SN, Milto KD, Martynov AA, Konstantinov EL, Chulisov AS (2014) A review of genus *Cyrtodactylus* (Reptilia: Sauria: Gekkonidae) in fauna of Laos with description of four new species. Proceedings of the Zoological Institute RAS 318: 391–423.

Ngo TV (2011) *Cyrtodactylus martini*, another new karst-dwelling *Cyrtodactylus* Gray, 1827 (Squamata: Gekkonidae) from Northwestern Vietnam. Zootaxa 2834: 33–46. https://doi.org/10.11646/zootaxa.2834.1.3

Ngo TV, Chan KO (2011) A new karstic cave-dwelling *Cyrtodactylus* Gray (Squamata: Gekkonidae) from Northern Vietnam. Zootaxa 3125: 51–63. https://doi.org/10.11646/zootaxa.3125.1.4

Ngo TV, Grismer LL (2010) A new karst dwelling *Cyrtodactylus* (Squamata: Gekkonidae) from Son La Province, northwestern Vietnam. Hamadryad 35: 84–95.

Nguyen LT, Schmidt HA, von Haeseler A, Minh BQ (2015a) IQ-TREE: a fast and effective stochastic algorithm for estimating maximum-likelihood phylogenies. Molecular Biology and Evolution 32: 268–274. https://doi.org/10.1093/molbev/msu300

Nguyen TQ, Kingsada P, Rösler H, Auer M, Ziegler T (2010) A new species of *Cyrtodactylus* (Squamata: Gekkonidae) from northern Laos. Zootaxa 2652(1): 1–16. https://doi.org/10.11646/zootaxa.2652.1.1

Nguyen TQ, Le MD, Pham AV, Ngo HN, Hoang CV, Pham CT, Ziegler T (2015b) Two new species of *Cyrtodactylus* (Squamata: Gekkonidae) from the karst forest of Hoa Binh Province, Vietnam. Zootaxa 3985(3): 375–390. https://doi.org/10.11646/zootaxa.3985.3.3

Nguyen TQ, Pham AV, Ziegler T, Ngo HT, Le MD (2017) A new species of *Cyrtodactylus* (Squamata: Gekkonidae) and the first record of *C. otai* from Son La Province, Vietnam. Zootaxa 4341(1): 25–40. https://doi.org/10.11646/zootaxa.4341.1.2

Nguyen SN, Yang JX, Le NT, Nguyen LT, Orlov NL, Hoang CV, Nguyen TQ, Jin JQ, Rao DQ, Hoang TN, Che J, Murphy RW, Zhang YP (2014) DNA barcoding of Vietnamese bent-toed geckos (Squamata: Gekkonidae: *Cyrtodactylus*) and the description of a new species. Zootaxa 3784(1): 48–66. https://doi.org/10.11646/zootaxa.3784.1.2

Pham AV, Le MD, Ziegler T, Nguyen TQ (2019) A new species of *Cyrtodactylus* (Squamata: Gekkonidae) from northwestern Vietnam. Zootaxa 4544(3): 360–380. https://doi.org/10.11646/zootaxa.4544.3.3

Ronquist F, Teslenko M, van der Mark P, Ayres DL, Darling A, Höhna S, Larget B, Liu L, Suchard MA, Huelsenbeck JP (2012) MrBayes 3.2: efficient Bayesian phylogenetic inference and model choice across a large model space. Systematic Biology 61: 539–542. https://doi.org/10.1093/sysbio/sys029

Schneider N, Luu VQ, Sitthivong S, Teynié A, Le MD, Nguyen TQ, Ziegler T (2020) Two new species of *Cyrtodactylus* (Squamata: Gekkonidae) from northern Laos, including new finding and expanded diagnosis of *C. bansocensis*. Zootaxa 4822(4): 503–530. https://doi.org/10.11646/zootaxa.4822.4.3

Schneider N, Nguyen TQ, Le MD, Nophaseud L, Bonkowski M, Ziegler T (2014) A new species of *Cyrtodactylus* (Squamata: Gekkonidae) from the karst forest of northern Laos. Zootaxa 3835(1): 80–96. https://doi.org/10.11646/zootaxa.3835.1.4

Sumontha M, Panitvong N, Deein G (2010) *Cyrtodactylus auribalteatus* (Squamata: Gekkonidae), a new cave-dwelling gecko from Phitsanulok Province, Thailand. Zootaxa 2370: 53–64. https://doi.org/10.11646/zootaxa.2370.1.3

Termprayoon K, Rujirawan A, Grismer LL, Wood Jr PL, Aowphol A (2021) Taxonomic reassessment and phylogenetic placement of *Cyrtodactylus phuketensis* (Reptilia, Gekkonidae) based on morphological and molecular evidence. ZooKeys 1040: 91–121. https://doi.org/10.3897/zookeys.1040.65750

Thompson JD, Higgins DG, Gibson TJ (1994) CLUSTAL W: improving the sensitivity of progressive multiple sequence alignment through sequence weighting, position-specific gap penalties and weight matrix choice. Nucleic Acids Research 22: 4673–4680. https://doi.org/10.1093/nar/22.22.4673

Uetz P (2021) The Reptile Database. http://www.reptile-database.org [accessed on: 2021-8-10]

Wilcox TP, Zwickl DJ, Heath TA, Hillis DM (2002) Phylogenetic relationships of the Dwarf Boas and a comparison of Bayesian and bootstrap measures of phylogenetic support. Molecular Phylogenetics and Evolution 25: 361–371. https://doi.org/10.1016/S1055-7903(02)00244-0

Zhang YP, Liu XL, Bernstein J, Wang J, Yuan ZY (2021) A New Species of *Cyrtodactylus* (Squamata: Gekkonidae) from the Karst Forests of Daweishan National Nature Reserve, Yunnan, China. Asian Herpetological Research 12(3): 1–11. https://doi.org/10.16373/j.cnki.ahr.200090

ZooKeys 1084: 101–117 (2022)
doi: 10.3897/zookeys.1084.77096
https://zookeys.pensoft.net

RESEARCH ARTICLE

A peer-reviewed open-access journal
ZooKeys
Launched to accelerate biodiversity research

# Taxonomy of *Landrevus* species group of *Velarifictorus* Randell, 1964 (Orthoptera, Gryllidae, Gryllinae) with one new species and morphological diversity of *Velarifictorus flavifrons* Chopard, 1966

Yan-Na Zheng[1], Xin-Ru Cai[1], Li-Bin Ma[1]

**1** *College of Life Sciences, Shaanxi Normal University, Xi'an, 710119, China*

Corresponding author: Li-Bin Ma (libinma@snnu.edu.cn)

Academic editor: T. Robillard | Received 26 October 2021 | Accepted 17 December 2021 | Published 28 January2022

*http://zoobank.org/96254C08-20EB-4F26-AB2E-DBC62983DA4E*

**Citation:** Zheng Y-N, Cai X-R, Ma L-B (2022) Taxonomy of *Landrevus* species group of *Velarifictorus* Randell, 1964 (Orthoptera, Gryllidae, Gryllinae) with one new species and morphological diversity of *Velarifictorus flavifrons* Chopard, 1966. ZooKeys 1084: 101–117. https://doi.org/10.3897/zookeys.1084.77096

## Abstract

The *Landrevus* species group includes four *Velarifictorus* species that are related to Landrevinae crickets (*Velarifictorus elephas* Gorochov, 1992, *Velarifictorus bubalus* Gorochov, 1992, *Velarifictorus gradifrons* Ingrisch, 1998, and *Velarifictorus landrevus* Ma, Qiao & Zhang, 2019). A new species of the group is discovered in the Yunnan Province of China, and it is described and illustrated here. *Velarifictorus yunnanensis* Liu & Yin, 1993 is recognized as a junior synonym of *Velarifictorus flavifrons* Chopard, 1966. The morphological variety of *V. flavifrons* ectoparamere is documented and studied.

## Keywords

Calling song, cricket, Grylloidea, Modicogryllini, new species group

## Introduction

There are 110 species of *Velarifictorus* Randell, 1964 (Orthoptera, Gryllidae, Gryllinae: Modicogryllini) in the world (Cigliano et al. 2021). Four members of the genus are closely related and look remarkably like crickets of the subfamily Landrevinae; they

are dark or chocolate brown, the tegmina are short, and they have a similar type of epiphallus. *Velarifictorus elephas* Gorochov, 1992, *Velarifictorus bubalus* Gorochov, 1992, *Velarifictorus gradifrons* Ingrisch, 1998 and *Velarifictorus landrevus* Ma, Qiao & Zhang, 2019 are the species that we recognize as belonging to the *Landrevus* species group. We identified a fifth species from Yunnan Province, China, which is similar to these, and we describe it as a new species for science.

Among the species of the genus *Velarifictorus*, *Velarifictorus yunnanensis* Liu & Yin, 1993 has been recorded from China. Gorochov (2001) designated it as a junior synonym of *Velarifictorus flavifrons* Chopard, 1966. We compared the illustrations in the original descriptions of both species and conclude that they are not the same. We analyzed many samples from Yunnan Province referred to as either *V. flavifrons* or *V. yunnanensis* to confirm the relationship between the two taxa. We also report on the morphological variation of the male genitalia of *V. flavifrons* and validate the synonymy as stated by Gorochov (2001).

## Materials and methods

The specimens were preserved in absolute analytical-grade ethanol during fieldwork and then pinned and dry-preserved in the laboratory. Identification of species is mainly based on male morphology. Illustrations of head and genitalia were taken with a ToupCam digital camera and bundled software (ToupTek, Hangzhou, China). Habitats and specimen photographs were obtained using a Keyence VHX-6000 super-high magnification lens zoom 3D microscope (Keyence, Japan). The details of ovipositor were obtained using JEC-6500 lon sputtering instrument (Hitachi, Japan) and TM3030Plus tabletop electron microscopy (Jeol, Japan). Genitalia were prepared by placing dissected genitalia into a solution of alkaline proteinase (0.2g/ml; AOBOX, Beijing, China) with water temperature of 40–50 °C for 48 h.

### Song recording and analyses

All the specimens were kept singly in a plastic box (diameter 20 mm, height 50 mm) with small holes in the laboratory. We recorded songs overnight by placing a Sony PCM-D50 (Sony, China) recorder near the box, and replayed songs in Raven Lite v. 2.0 (Bioacoustics Research Program, Cornell Lab of Ornithology).

### Measurements

All specimens were measured using ToupCam digital camera (E3ISPM05000KPA) and bundled software (ToupTek, Hangzhou, China). All measurements are in millimeters (mm).

## Abbreviations

**Measurements:**

**BL** body length (from head to tip of abdomen);
**HL** head length;
**HW** head width;
**PL** pronotum length;
**PW** pronotum width (maximum width of pronotum);
**FWL** tegmen (forewing) length;
**HFL** hind femur length;
**OL** ovipositor length.

**Male genitalia:**

**R** rami;
**G** guiding rod;
**Ect** ectoparamere;
**M. Ep** medial lobes of epiphallus;
**L. Ep** lateral lobes of epiphallus.

All specimens studied in the article are deposited in the museum of Flora and Fauna of Shaanxi Normal University, Xi'an, China (**SNNU**).

# Taxonomy

## Orthoptera, Grylloidea, Gryllidae, Gryllinae, Modicogryllini

**Genus *Velarifictorus* Randell, 1964**

**Type species.** *Scapsipedus micado* Saussure, 1877.

***Velarifictorus zhengi* Zheng & Ma, sp.nov.**
http://zoobank.org/160DF768-6BE9-4845-B8AE-AC1897B84F37
**Chinese name:** 郑氏斗蟋
Figures 1–4, 8A, D, 9A, D, 10A, D, 13A, D, 14A, B; Table 1

**Type material. *Holotype*.** Male. China: Yunnan, Pu'er, Meizihu Park, 22°74.6'N, 100°97.6'E, VIII–18–2021, Zhixin He, Ning Wang, and Wei Yuan leg. (SUUN); ***Paratypes*.** 4 males and 8 females. China: Yunnan, Pu'er, Meizihu Park, 22°74.6'N, 100°97.6'E, VIII–18–2021, Zhixin He, Ning Wang, and Wei Yuan leg. (SUUN). All specimens were found in leaf litter.

**Measurements. Male (*n* = 5):** BL 15.73±0.14, HL 3.63±0.31, HW 5.47±0.08, PL 3.09±0.03, PW 5.32±0.12, FWL 7.17±0.09, HTL 10.44±0.68; **Female (*n* = 8):**


**Figure 1.** *Velarifictorus zhengi* sp. nov. Habitus (alive) in field **A** male **B** female (photographed by Zhixin He).

BL 16.93±0.72, HL 3.11±0.53, HW 4.85±0.13, PL 3.14±0.03, PW 5.00±0.24, FWL 2.50±0.03, HTL 10.94±0.61, OL 13.00±0.09.

**Etymology.** Prof. Zhe-Min Zheng passed away on 16 September 2021. He was a well-known orthopterist in China, and he made outstanding contributions to the taxonomy of Chinese grasshoppers. To honor him, we named this new species after him.

**Description. Male:** vertex broad and flattened, rather inclined. Occiput bright, slightly convex and somewhat wider than pronotum. Frontal rostrum convex, inclined dorsally and ventrally, and nearly three times wider than antennal scape. Antennal scape shield-like. Ocelli transversely ovoid, almost equal in size. Eyes slightly convex, about 1/4 length of head. Postclypeus shaped as a narrow band, lower margin con-

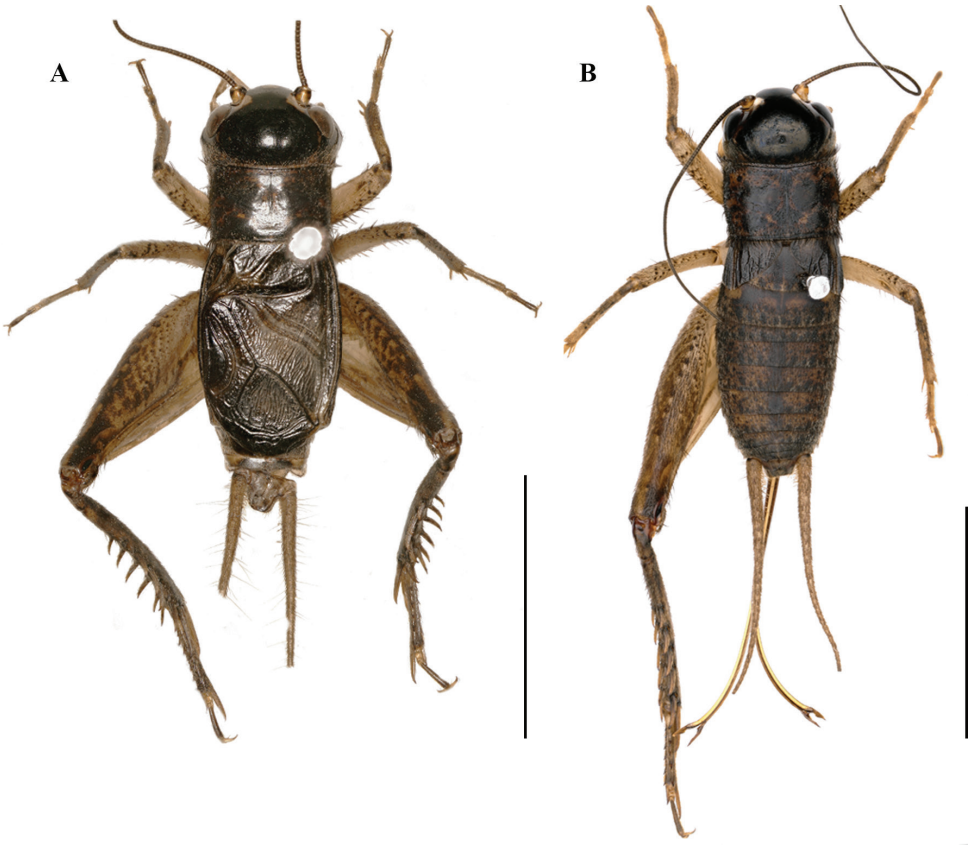


**Figure 2.** Bodies of *Velarifictorus zhengi* sp. nov. **A** male **B** female. Scale bars: 10 mm.

cave; anteclypeus shaped as a broad shield. Labrum shaped as rhombus, apical margin slightly round. End section of maxillary palpi is about 2/3 length of the third section; end section of labial palpi depressed and widened, almost equal to the total length of all other sections.

Pronotum broad and flattened. Median groove of pronotal disc distinct. Posterior margin straight and middle of anterior margin concaved inside, and both margins almost equal in width.

Tegmina reaching eighth abdominal tergite. Oblique veins bifurcated proximally, and each branch of them connected to CuA vein. Three chord veins, connecting to proximal part of mirror by two transverse veins. Mirror shield-like, about twice wider than basal field. Dividing vein absent. Apical field narrow and almost 1/4 length of mirror.

Outer tympanum larger than the inner, inner tympanum oval; outer tympanum elongate-oval. Hind tibiae armed with dorsal spurs (numbered 5:6) almost equal in length; and apical spurs outside three (the dorsal one longest and about two times longer than the dorsal spurs, ventral one about half length of the dorsal, the middle one slightly longer than the dorsal) and inner two (equal in length and about 2/3 length of the dorsal).

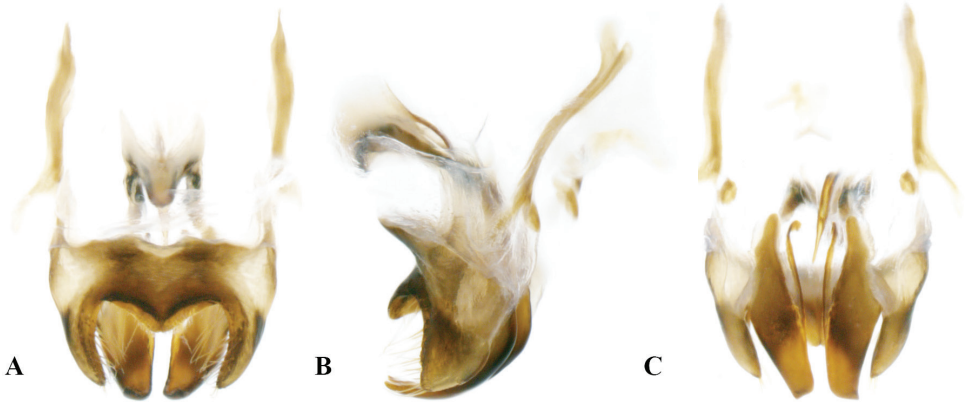


**Figure 3.** Genitalia of *Velarifictorus zhengi* sp. nov. **A** dorsal view **B** lateral view **C** ventral view.

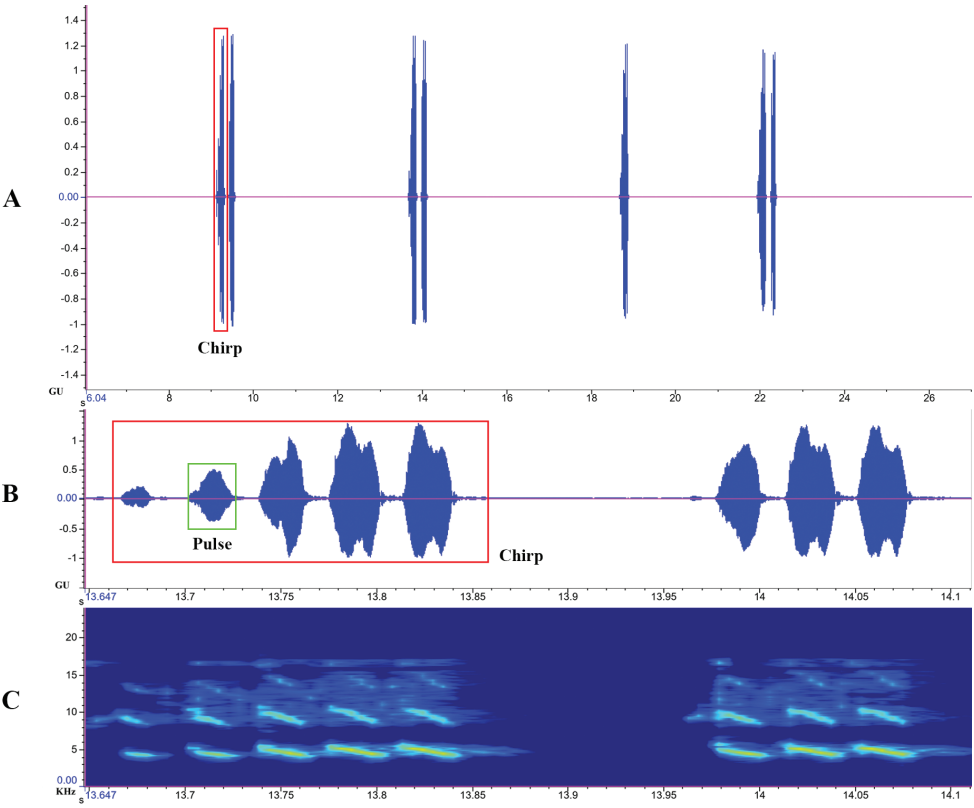


**Figure 4.** Calling song of *Velarifictorus zhengi* sp. nov. **A** oscillogram of chirp (amplitude versus time) **B** oscillogram of pulse (amplitude versus time) **C** spectrogram (frequency versus time).

**Genitalia.** Lateral lobes of epiphallus sheet-like, tapering, apically acute, and armed with pilose at the apex. Middle lobe of epiphallus angularity forming an obtuse angle and apically rounded, about 1/3 length of lateral lobes. Ectoparamere stripe-like, tapering, and about 2.5 times longer than epiphallic lateral lobes.

**Table 1.** Descriptive statistics of acoustic parameters in calling song samples of *Velarifictorus zhengi* sp. nov.

| | *n* | minimum | maximum | mean | std |
|---|---|---|---|---|---|
| Chirp interval | 26 | 0.181 | 3.289 | 1.735 | 1.554 |
| Chirp duration | 26 | 0.115 | 0.191 | 0.153 | 0.042 |
| Chirp period | 26 | 1.296 | 3.480 | 1.888 | 1.596 |
| Chirp elements | 26 | 3 | 5 | 4 | 1 |
| Pulse interval | 26 | 0.010 | 0.022 | 0.016 | 0.006 |
| Pulse duration | 26 | 0.031 | 0.029 | 0.030 | 0.001 |
| Pulse period | 26 | 0.041 | 0.051 | 0.046 | 0.007 |
| Peak frequency | 26 | 3.898 | 6.171 | 5.035 | 1.137 |

The time and frequency parameters are in seconds and kHz respectively. *n*= number of samples analyzed; std= standard deviation.

**Calling song.** Chirps lasting from 1.296 to 3.480 s (mean 1.888), and their duration vary from 0.115 to 0.191 s (mean 0.153). Each chirp equally contains four pulses (Fig. 4B). The peak frequency is between 3.898 and 6.171 kHz (mean 5.035), and the average temperature is 28.0 °C. In terms of spectro-temporal variation, its frequency modulation is inclined downward, which is obvious in the second harmonic.

**Female.** Resembles the male. Head almost as wide as pronotum. Tegmen extends anteriorly to the second abdominal tergite (Fig. 2B), which is shorter on the inside and progressively grows longer on the outside. Dorsally 3 or 4 longitudinal veins and laterally 6 Sc branches (the outermost of which is basally branched) arm the tegmen (Fig. 13D). Ovipositor smooth and slightly longer than the posterior femur. The dorsal ovipositor valve is hooked and has a sharp apex, whereas the apex of the ventral ovipositor valve is slightly rounded (Fig. 14 A, B).

**Coloration.** Body dark brown. Ocelli light yellow. Eyes brown; between eyes and anterior margin of pronotum marked with yellowish -brown band. Maxillary reddish brown. Cercus and legs yellowish brown.

**Remarks.** This species resembles species of the *Landrevus* group in features of the body and genitalia. In *V. gradifrons*, however, the inner tympanum is absent and the apical margin of epiphallic middle lobe is straight. In the new species, both tympana are present and the apical margin of epiphallic middle lobe is curved. The apical field of the tegmina of *V. bubalus* and *V. elephas* are longer than in *V. zhengi* sp. nov., and the apical margins of the epiphallic middle lobe are straighter than the new species. Furthermore, the new species is distinguished from *V. landrevus*, another Chinese species, in morphological and acoustical characters. *Velarifictorus zhengi* sp. nov. bears a longer epiphallic middle lobe, whose apex is partially pentagon-like in dorsal view and possesses more pulses (9–15) per chirp at a lower peak frequency. Finally, the absence of a dividing vein in the new species (observed in all type material) is distinct from all other species of the *Landrevus* group.

***Velarifictorus* (*Velarifictorus*) *landrevus* Ma, Qiao & Zhang, 2019**
**Chinese name:** 兰斗蟋
Figures 5–7, 8B, E, 9B, E, 10B, E, 13B, E, 14C, D, Table 2

*Velarifictorus* (*Velarifictorus*) *landrevus* Ma, Qiao & Zhang, 2019: 104

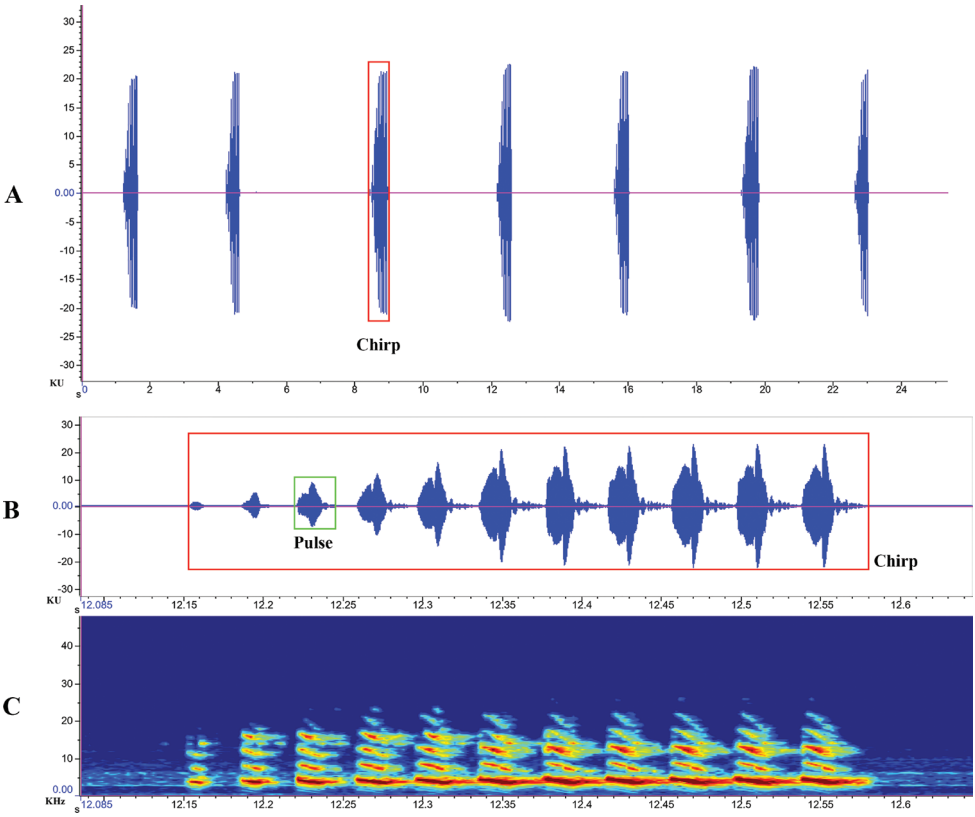


**Figure 5.** Calling song of *Velarifictorus landrevus* **A** oscillogram of chirp (amplitude versus time) **B** oscillogram of pulse (amplitude versus time) **C** spectrogram (frequency versus time).

**Examined material.** 5 males and 2 females, Yunnan, Mengla, Wangtianshu, 21°59.7'N, 101°58.8'E, X–12–23–2014, Zhang, Tao leg. The specimens were collected on grasses or leaf litter of a hillside.

**Measurements. Male (*n* = 5):** BL 19.49±0.60, HL 3.71±0.23, HW 6.52±0.31, PL 4.47±0.19, PW 6.20±0.23, FWL 9.32±0.98, MTL 5.42±0.22, HFL 13.82±0.26; **Female (*n* = 2):** BL 18.59±0.09, HL 3.71±0.56, HW 5.81±0.24, PL 4.61±0.02, PW 6.34±0.08, FWL 4.72±0.14, HFL 13.93±0.23, OL 13.68±0.41.

**Description. Male:** vertex broad and flattened, slightly inclined. Occiput slightly convex and almost as wide as pronotum. Frontal rostrum convex, inclined dorsally and ventrally, nearly1.5 times wider than antennal scape. Antennal scape shield-like. Ocelli transversely ovoid, almost equal in size. Eyes ovoid, about 1/5 length of head. Postclypeus shaped as narrow band, anteclypeus shaped as broad shield. Labrum shaped as rhombus, apical margin slightly round. End section of maxillary palpi almost as long as the third; end section of labial palpi depressed and widened, almost equal to the total length of remainder sections.

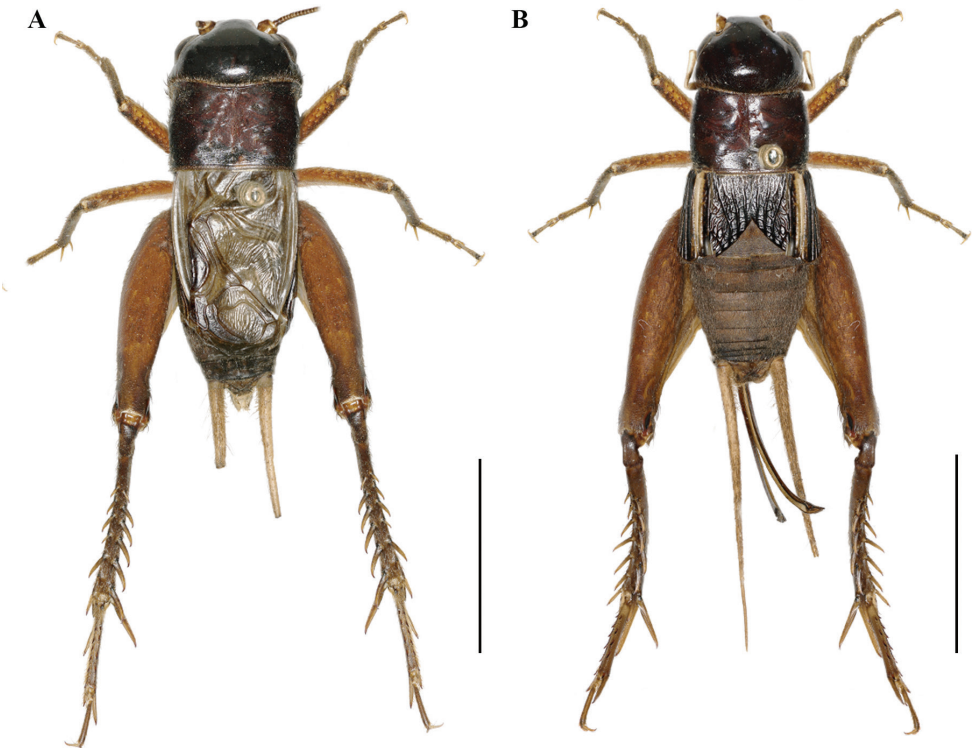


**Figure 6.** Bodies of *Velarifictorus landrevus* **A** male **B** female. Scale bars: 10 mm.

**Table 2.** Descriptive statistics of acoustic parameters in calling song samples of *Velarifictorus landrevus*.

| | *n* | minimum | maximum | mean | std |
|---|---|---|---|---|---|
| Chirp interval | 26 | 2.629 | 5.191 | 3.910 | 1.281 |
| Chirp duration | 26 | 0.394 | 0.553 | 0.474 | 0.080 |
| Chirp period | 23 | 3.023 | 6.463 | 4.384 | 1.361 |
| Chirp elements | 23 | 9 | 15 | 12 | 3 |
| Pulse interval | 23 | 0.021 | 0.028 | 0.024 | 0.03 |
| Pulse duration | 23 | 0.011 | 0.024 | 0.017 | 0.006 |
| Pulse period | 23 | 0.032 | 0.052 | 0.042 | 0.010 |
| Peak frequency | 23 | 2.383 | 5.347 | 3.865 | 1.482 |

The time and frequency parameters are in seconds and kHz respectively. *n*= number of samples analyzed; std= standard deviation.

Pronotum broad and flattened. Median groove of pronotal disc distinct. Posterior margin straight and middle of anterior margin concave, and both margins almost equal in width.

Tegmina not reaching apex of abdomen. Chord veins two. Diagonal vein proximally bifurcated, one branch of connected to the proximal of chord vein, while another branch connected to CuA vein. Mirror shield-like, anterior margin and the posterior

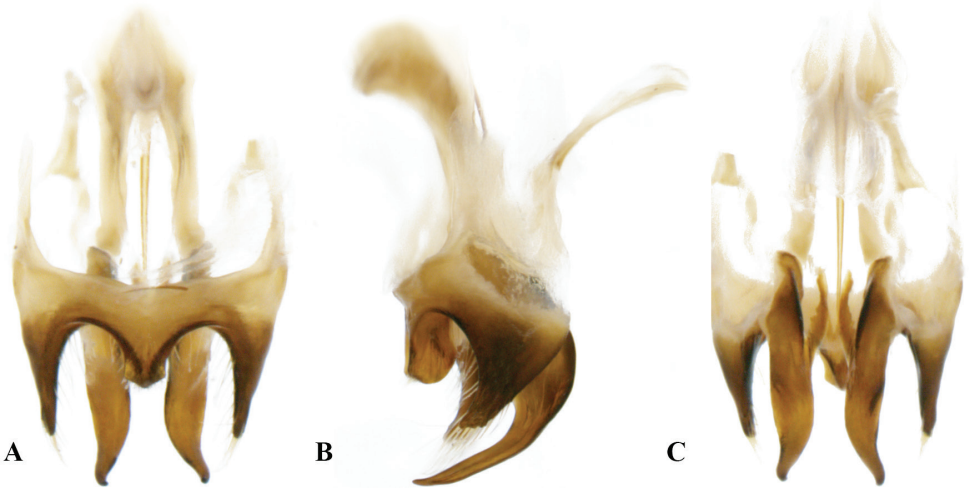


**Figure 7.** Genitalia of *Velarifictorus landrevus* **A** dorsal view **B** lateral view **C** ventral view.

almost equal in width. Apical field about 1/5 length of basal field, possessing two or three wing cells.

Inner tympanum absent; external tympanum elongate-oval. Hind tibiae armed with dorsal spurs (numbered 6:6) almost equal in length; and apical spurs three outside (the dorsal one slightly longer than the dorsal spurs, the ventral and middle almost equal in length and about half length of the dorsal) and inner two (equal in length and about two times longer than the dorsal).

**Genitalia.** Lateral lobes of epiphallus sheet-like, tapering, apically truncated, and pilose along margins. Middle lobe of epiphallus partially pentagon-like (dorsally viewed) and about half length of lateral lobes. Ectoparamere stripe-like, proximally broad, tapering, upward curved, and about twice as long as epiphallic lateral lobes.

**Calling song.** Chirps lasting from 3.023 to 6.463 s (mean 4.384) and their duration varying from 0.394 to 0.553 s (mean 0.474). Each chirp equally contains 12 pulses (Fig. 5B). The peak frequency is between 2.383 and 5.347 kHz (mean 3.865) and the mean temperature is 27.8 °C. Regarding spectro-temporal variation, the frequency modulation is inclined downward (Fig. 5C).

**Female.** Resembles the male. Tegmina reaches the apex of the second abdominal tergite (Fig. 6B) and is armed with longitudinal veins (inside shorter and progressively growing outward), dorsally four longitudinal veins, and laterally six Sc branches (the innermost of which medially and apically branched) (Fig. 13E). Ovipositor arrow-shaped, constricted, long, and with a somewhat sharp tip (Fig. 14 C, D).

**Coloration.** Body chocolate brown. Head dark brown. End section of maxillary palpi light yellow. Cercus and legs yellowish brown. CuA and Sc of female ornamented with yellowish band.

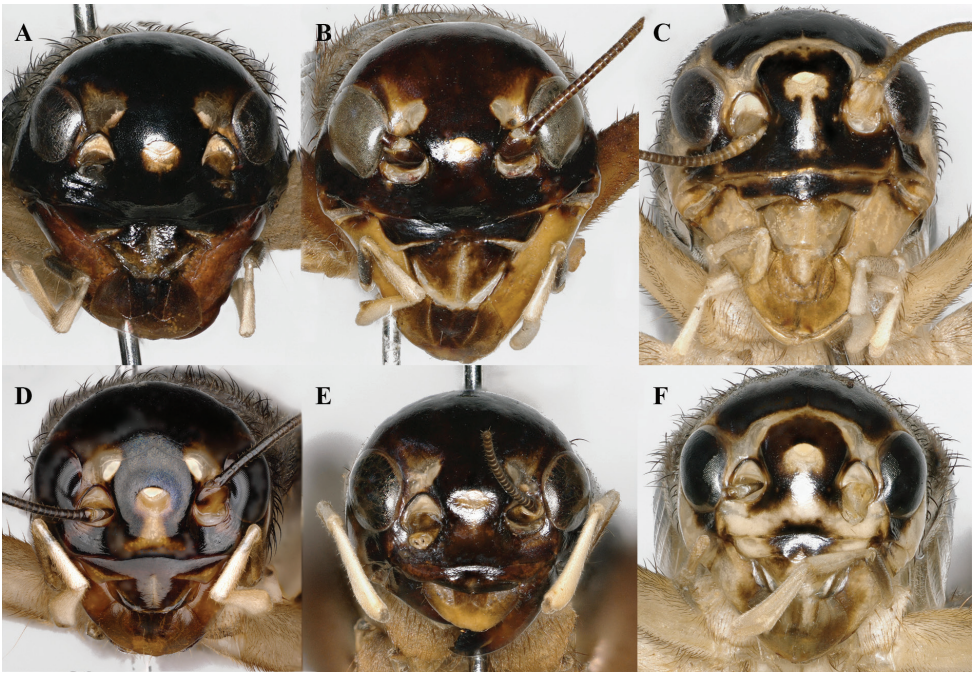


**Figure 8.** Front view of heads of *Velarifictorus* **A, D** *V. zhengi* sp. nov. **B, E** *V. landrevus* **C, F** *V. flavifrons* **A–C** male **D–F** female.

***Velarifictorus flavifrons* Chopard, 1966**
**Chinese name:** 黄额斗蟋
Figures 8C, F, 9C, F, 10C, F, 11, 12, 13C, F, 14E, F

*Velarifictorus flavifrons* Chopard, 1966: 607; Chopard, 1967: 124
*Velarifictorus* (*Velarifictorus*) *flavifrons*, Shishodia et al., 2010: 212; Kim and Hong 2014: 61; Zhang et al. 2017: 26; Chen et al. 2018: 502
*Scapsipedus arorai* Tandon & Shishodia, 1972: 281; synonymized by Vasanth 1993: 38
*Scapsipedus bhadurii* Bhowmik, 1967: 127; synonymized by Vasanth 1982: 123
*Velarifictorus dehradunensis* Tandon & Shishodia, 1974: 299; synonymized by Bhowmik 1985: 30
*Velarifictorus jaintianus* Biswas & Ghosh, 1975: 221; synonymized by Bhowmik 1985: 37
*Scapsipedus lohitensis* Tandon & Shishodia, 1972: 281; synonymized by Vasanth 1982: 123
*Scapsipedus sikkimensis* Bhowmik, 1967: 126; synonymized by Gorochov 2001:321
*Velarifictorus yunnanensis* Liu & Yin, 1993: 90, 93; synonymized by Gorochov 2001: 321

**Examined material.** 5 males and 2 females, Yunnan, Gongshan, 21°69.4'N, 101°57.3'E, VI–14–2019, Libin Ma leg.; 10 males and 2 females, Xizang, Motuo, Beibeng, 29°24.5'N, 95°17.6'E, V–31–2019, Libin Ma leg.; 5 males, Guangxi, Jingxi,

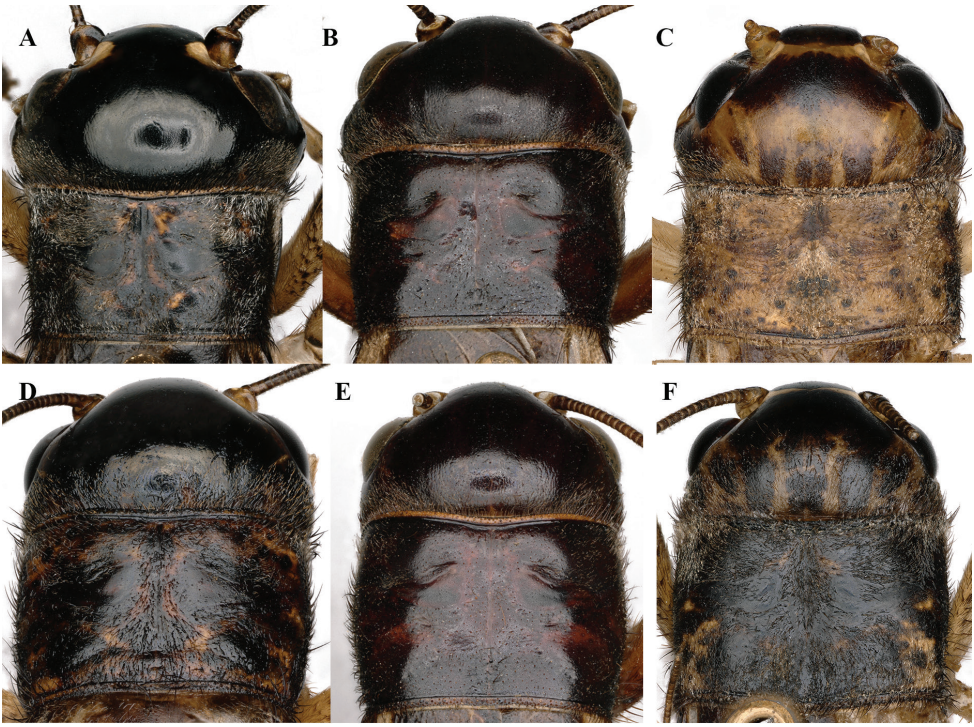


**Figure 9.** Dorsal view of heads and pronotum of *Velarifictorus* **A, D** *V. zhengi* sp. nov. **B, E** *V. landrevus* **C, F** *V. flavifrons* **A–C** male **D–F** female.

Longbang, 22°87.3'N, 106°32.8'E, V–1–2019, Libin and Tao Zhang leg. Specimens in grass and leaf litter.

**Measurements. Male (*n* = 15):** BL 16.7±0.53, HL 3.23±0.23, HW 5.13±0.23, PL 3.13±0.76, PW 4.98±0.03, FWL 8.98±0.64, MTL 5.18±0.22, HFL 9.23±0.26; **Female (*n* = 4):** BL 17.98±0.24, HL 3.87±0.54, HW 5.31±0.76, PL 4.43±0.03, PW 6.34±0.35, FWL 4.43±0.15, HFL 13.45±0.76, OL 13.63±0.18.

**Description. Male:** vertex broad and flattened, slightly inclined. Occiput slightly convex, almost in equal length with pronotum. Frontal rostrum convex, inclined dorsally and ventrally, and nearly twice wider than antennal scape. Antennal scape shield-like. Median ocellus transversely ovoid, lateral ocelli ovoid. Eyes ovoid, about 1/3 length of head. Postclypeus shaped as narrow band, lower margin convex; anteclypeus trapezoidal. Labrum rhomboid, apical margin slightly rounded. End section of maxillary palpi slightly longer than the third; end section of labial palpi depressed and widened, almost equal to the total length of all other sections.

Pronotum broad and flattened. Median groove of pronotal disc distinct and ornamented with symmetrical blade-pattern on both sides. Posterior margin straight and middle of anterior margin concave inside, and both margins almost equal in width.

Oblique veins three. Diagonal vein proximally bifurcate, each branch connected to CuA vein. Chord veins three. Mirror shield-like, posterior margin slightly rounded,

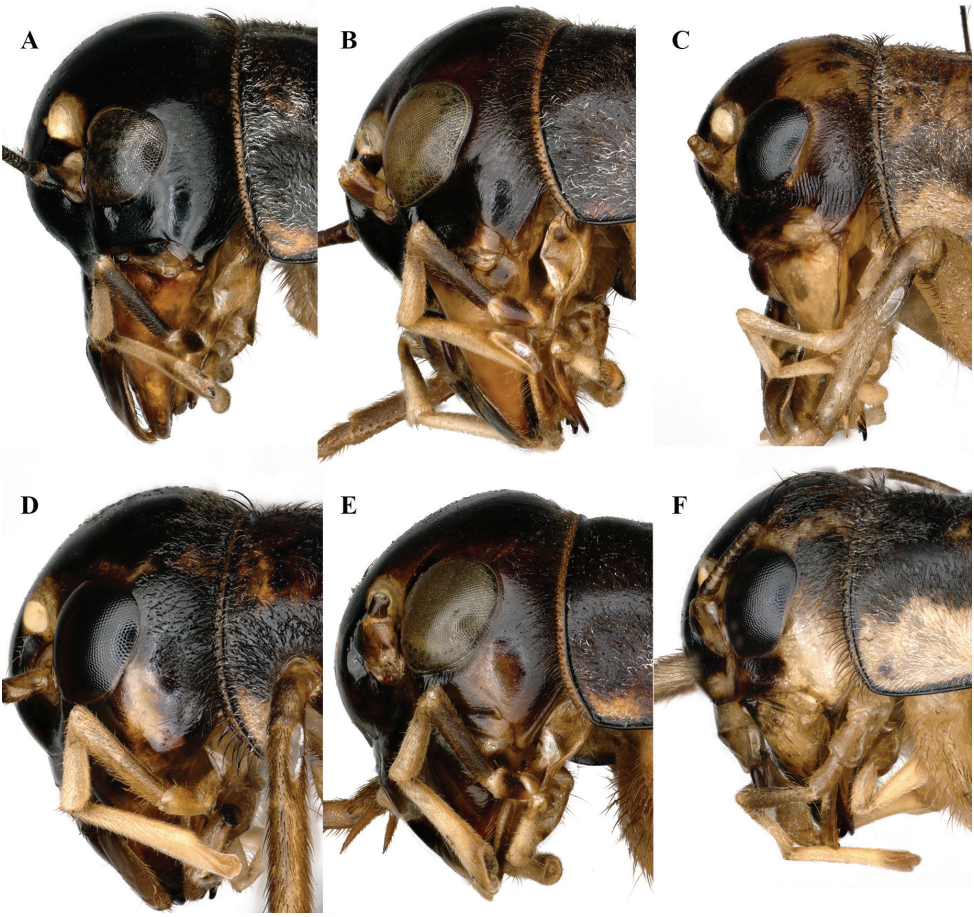


**Figure 10.** Lateral view of heads of *Velarifictorus* **A, D** *V. zhengi* sp. nov. **B, E** *V. landrevus* **C, F** *V. flavifrons* **A–C** male **D–F** female.

and dividing vein curved. The apical field almost as wide as mirror and armed with regular cells.

Inner tympanum relatively small or absent, and outer tympanum elongate-oval. Hind tibiae armed with dorsal spurs (numbered 5:6) almost equal in length; apical spurs external three (dorsal one about 3/2 length of dorsal spurs; ventral and middle nearly equal in length and almost equal to dorsal spurs) and inner two (equal in length and about 2/3 length of the dorsal).

**Genitalia.** Lateral lobes of epiphallus sheet-like, apically rounded, and pilose. Middle lobe of epiphallus about 1/2 length of epiphallic lateral lobes, ventrally possessing projections and about 1/3 length of epiphallic lateral lobes. Ectoparamere proximally rod-like and distally sheet-like. Ectoparamere curved dorsally (degree of curvature variable). Apex of ectoparamere bifurcate, outer branch rather long (slightly longer than epiphallic lateral lobes) and apically rounded, and the inner relatively short

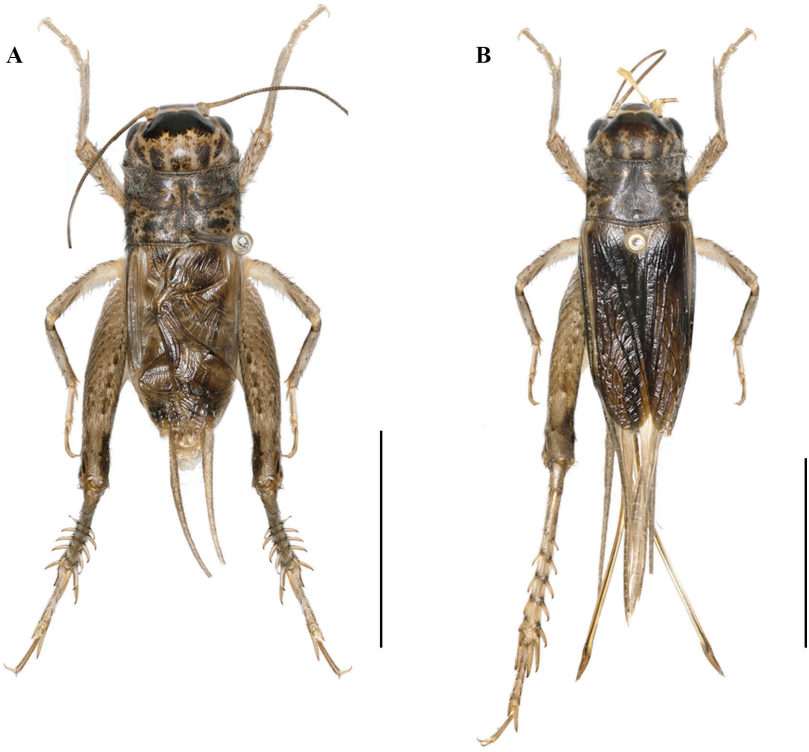


**Figure 11.** Bodies of *Velarifictorus flavifrons* **A** male **B** female. Scale bars: 10 mm.

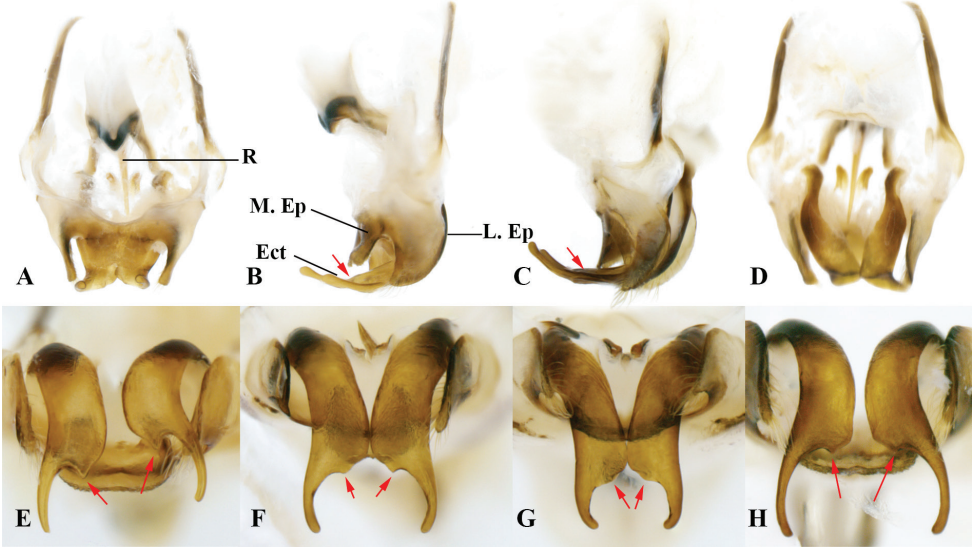


**Figure 12.** Genitalia of *Velarifictorus flavifrons* **A** dorsal view **B, C** lateral view (ectoparamerea are movable and may touch or be separated from middle epiphallic lobe in some material) **D** ventral view **E–H** caudal view **E** inner branch observable and apically acute **F** inner branch small and asymmetry (observed five samples), as evident here, the left apically rounded and the right somewhat acute **G** inner branch relatively weak **H** inner branch similarly placed as in F but different in details.

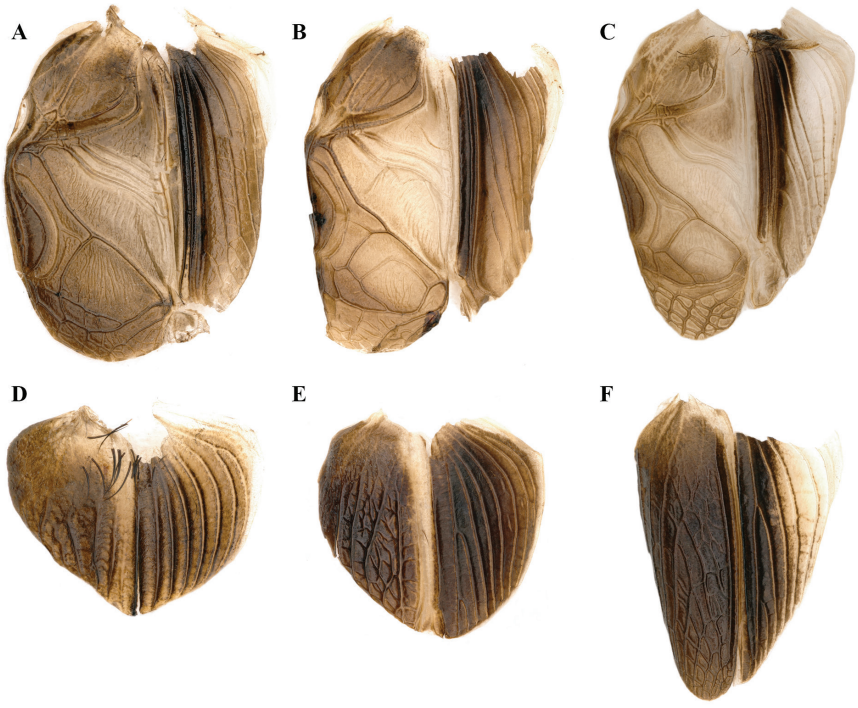


**Figure 13.** Right tegmina of *Velarifictorus* **A, D** *V. zhengi* sp. nov. **B, E** *V. landrevus* **C, F** *V. flavifrons* **A–C** male **D–F** female.

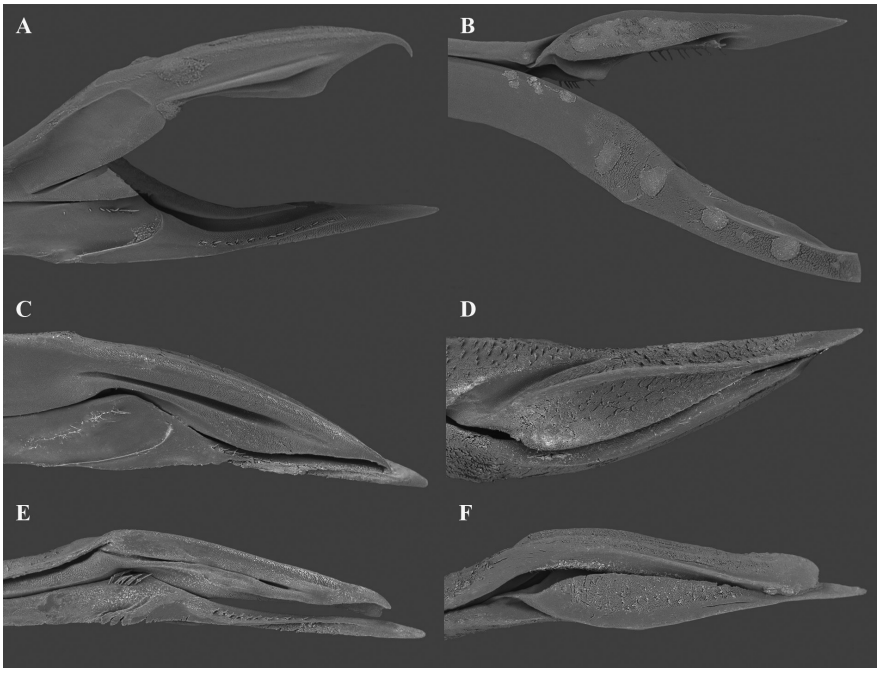


**Figure 14.** Ovipositor of *Velarifictorus* **A, B** *V. zhengi* sp. nov. **C, D** *V. landrevus* **E, F** *V. flavifrons* **A, C, E** inside of ovipositor **B, D, F** outside of ovipositor.

(only a small protrusion and varied in size and shape: round or acute, or asymmetry with one round while another acute) (Fig. 12E–H).

**Coloration.** Body brown. Occiput dark brown, vertex armed with six yellowish-brown strips. Anteclypeus dark brown, postclypeus light brown. With a broad yellowish-brown band between ocelli. End section of maxillary palpi dark brown and remainder sections light yellow.

**Female.** Resembles the male. Tegmen reaches apical abdominal tergite (Fig. 11B) and dorsally armed with irregular longitudinal veins and laterally with five Sc branches (innermost of which branches medially and apically) (Fig. 13F). Ovipositor brown, smooth, arrow-shaped, and slightly longer than posterior femur. The dorsal ovipositor valve apically truncated, whereas the ventral valve with apex slightly acute (Fig. 14E, F).

**Remarks.** Gorochov (2001) considered *V. yunnanensis* to be a junior synonym of *V. flavifrons.* We checked the original descriptions and found that the figures of these species differ. To confirm the relationship of these species, we studied material collected from Yunnan Province (seven individuals), which should either bear the name of *V. flavifrons* or *V. yunnanensis*. Most of these specimens were collected at the same time and in the same location. We conclude that morphological variation of is present in the male genitalial complex (Fig. 12), as follows: (1) ectoparamere dorsally curved and variable in its curvature; (2) ectoparamere bifurcate and inner branch variable in size (clearly or weakly observable); (3) inner branch of ectoparamere morphologically variable (round or acute, or asymmetry with one acute and the other rounded). Thus, our observations confirm the synonymy of *V. flavifrons* and *V. yunnanensis* as proposed by Gorochov (2001).

## Acknowledgements

We thank Zhixin He and Ning Wang of Shaanxi Normal University and Wei Yuan of Sichuan Agricultural University for their specimen collection and photography. This work is supported by National Natural Science Foundation of China (no. 32070474, 31750002) and the Fundamental Research Funds for the Central Universities (2021CSZL007, cx2021029).

## References

Bhowmik HK (1967) Five new species of crickets of the genus *Scapsipedus* Saussure (Orthoptera: Insecta) from India. Journal of the Zoological Society of India 20: 123–127.

Bhowmik H (1985) Contribution to the Gryllid fauna of the Western Himalayas (Orthoptera: Gryllidae). Records of the Zoological Survey of India, Miscellaneous Publication, Occasional Paper 73: 1–85.

Chopard L (1966) Contribution à l'étude des orthopteroides du Népal. Annales de la Société Entomologique de France, Nouvelle Série 2: 601–616.

Chopard L (1967) Gryllides. Fam. Gryllidae; Subfam. Gryllinae (Trib. Grymnogryllini, Gryllini, Gryllomorphini, Nemobiini). In: Beier M (Ed.) Orthopterorum Catalogus 10, 213 pp.

Cigliano MM, Braun H, Eades DC, Otte D (2021) Orthoptera species file online. Version 5.0/5.0. http://Orthoptera.SpeciesFile.org [Accessed 20 September 2021]

Gorochov AV (1992) Material on the fauna of Gryllinae (Orthoptera, Gryllidae) of Vietnam. Part 1. In: Gorochov AV, Korotiaev BA (Eds) News of systematics and faunistics of Vietnam insects Part 2. Trudy Zoologitscheskogo Instituta, Akademiia Nauk SSSR, Leningrad 240: 3–19.

Gorochov AV (2001) Additions to the revision of Itarinae (Orthoptera: Gryllidae). Zoosystematica Rossica 9(1): e36.

Ingrisch S (1998) The genera *Velarifictorus*, *Modicogryllus* and *Mitius* in Thailand (Ensifera: Gryllidae, Gryllinae). Entomologica Scandinavica 29(3): 315–359. https://doi.org/10.1163/187631298X00122

Liu ZB, Yin XC (1993) A survey of Grylloidea (Orthoptera) from Yunnan Province. Contributions from the Shanghai Institute of Entomology 11: 85–94.

Ma LB, Qiao M, Zhang T (2019) A new species of *Velarifictorus* Randell, 1964 (Orthoptera: Gryllidae: Gryllnae: Modicogryllini) bearing similarities to the Landrevinae from China. Zootaxa 4612(1): 103–108. https://doi.org/10.11646/zootaxa.4612.1.7

Otte D, Alexander RD (1983) The Australian crickets (Orthoptera: Gryllidae). Monographs of the Academy of Natural Sciences of Philadelphia 22: 1–477.

Randell RL (1964) The male genitalia in Gryllinae (Orthoptera: Gryllidae) and a tribal revision. Canadian Entomologist 96(12): 1565–1607. https://doi.org/10.4039/Ent961565-12

Tandon SK, Shishodia MS (1972) Notes on the collection of Grylloidea (Orthoptera) from NEFA, India. Oriental Insects 6: 281–292. https://doi.org/10.1080/00305316.1972.10434077

Tandon SK, Shishodia MS (1974) Descriptions of two new species of *Velarifictorus* (Orthoptera: Grylloidea) from India. Oriental Insects 8(3): 299–302. https://doi.org/10.1080/00305316.1974.10434863

Vasanth M (1982) Taxonomic studies on the gryllid fauna of northeast India (Insecta: Orthoptera: Gryllidae). PhD Thesis, University of Calcutta, Kolkata, India.

Vasanth M (1993) Studies on crickets (Insecta: Orthoptera: Gryllidae) of northeast India. Records of the Zoological Survey of India, Miscellaneous Publication, Occasional Paper 132(1–6): 1–178.

ZooKeys 1084: 119–137 (2022)
doi: 10.3897/zookeys.1084.73175
https://zookeys.pensoft.net

RESEARCH ARTICLE

A peer-reviewed open-access journal
ZooKeys
Launched to accelerate biodiversity research

# *Calotheca nigromaculata* species-group from sub-Saharan Africa with descriptions of two new species from KwaZulu-Natal (Chrysomelidae, Galerucinae, Alticini)

Paola D'Alessandro[1], Mattia Iannella[1], Elizabeth Grobbelaar[2], Maurizio Biondi[1]

**1** *Department of Health, Life and Environmental Sciences, University of L'Aquila, Via Vetoio, I-67100 L'Aquila, Italy* **2** *Biosystematics Division, ARC-Plant Protection Research Institute, Private Bag X134, Queenswood, Pretoria 0121, South Africa*

Corresponding author: Paola D'Alessandro (paola.dalessandro@univaq.it)

Academic editor: Ron Beenen | Received 18 August 2021 | Accepted 3 December 2021 | Published 28 January 2022

*http://zoobank.org/1CD83BDC-591D-40DB-8298-2E6E2F8F1CE5*

**Citation:** D'Alessandro P, Iannella M, Grobbelaar E, Biondi M (2022) *Calotheca nigromaculata* species-group from sub-Saharan Africa with descriptions of two new species from KwaZulu-Natal (Chrysomelidae, Galerucinae, Alticini). ZooKeys 1084: 119–137. https://doi.org/10.3897/zookeys.1084.73175

## Abstract

*Calotheca* Heyden is a flea beetle genus with a largely sub-Saharan distribution and currently comprising 34 species. The examination of new material is revealing an increase in species richness and intraspecific variability. *Calotheca carolineae* **sp. nov.** and *C. wanati* **sp. nov.**, both from KwaZulu-Natal in the Republic of South Africa, are here described and attributed to the *C. nigromaculata* (Jacoby) species group, mainly based on genitalic characters. Photographs of the main diagnostic characters are provided, including the habitus, median lobe of the aedeagus, and spermatheca. Information on the geographic distribution and host plants of these species is also provided.

## Keywords

Afrotropical region, *Calotheca carolineae* sp. nov., *C. nigromaculata*, *C. wanati* sp. nov., flea beetles, leaf beetles, Republic of South Africa

## Introduction

*Calotheca* Heyden, 1887 is a flea beetle genus (Chrysomelidae, Galerucinae, Alticini) that is widespread in sub-Saharan Africa where is particularly common in the eastern and southern parts, with some records from Israel and the Arabian Peninsula (Biondi and D'Alessandro 2010a, 2012; Biondi et al. 2017; D'Alessandro et al. 2018a). Up to now this genus comprised 32 species, mainly associated with plants in the family Anacardiaceae, particularly *Searsia* spp., which are distributed in several different forest and savannah environments (D'Alessandro et al. 2018a, 2020, 2021; Iannella et al. 2021). The new material under examination is revealing an increase in species richness and intraspecific variability. Since the knowledge of the Afrotropical flea beetle fauna is far from exhaustive, unexpected diversity is often discovered within genera (e.g. Biondi and D'Alessandro 2008, 2010b), new genera are recognized (e.g. Biondi and D'Alessandro 2013a), or genera are recorded for the first time from the Afrotropical region (e.g. Biondi and D'Alessandro 2013b). *Calotheca* was identified as a monophyletic group based on a phylogenetic analysis which included *Blepharida rhois* (Forster, 1771) from North America among the outgroups (Biondi et al. 2017). Even though the Afrotropical species of *Calotheca* are the most closely related to the North American *B. rhois*, they are significantly separated from it, and supported by two synapomorphies: frontal grooves sinuate and deeply impressed, extending approximately from the dorsal ocular margin to the interantennal space, and femora strongly punctured. The main diagnostic characters for *Calotheca*, compared to the closely related African genus *Blepharidina* Bechyné, 1968, are the sinuate and deeply impressed frontal grooves, extending approximately from the dorsal ocular margin to the inter-antennal space; and the punctate lateral striae on the pronotum, which run from the anterior margin onto the disc, and are straight, curved, or L- or C-shaped. Some species also have short lateral longitudinal furrows and/or small dimples close to the pronotal base (Biondi et al. 2017, 2019; D'Alessandro et al. 2018b, 2019). In this paper we review, based on newly examined material, the distribution and ecological data of *Calotheca nigromaculata* (Jacoby, 1888) from southern Africa. We also describe two new species, *Calotheca carolineae* sp. nov. and *C. wanati* sp. nov., both from KwaZulu-Natal in the Republic of South Africa. The three species are attributed to the *Calotheca nigromaculata* species group, based on the morphology of the pronotum and spermatheca.

## Materials and methods

Material examined consists of 212 dried pinned specimens, preserved in the institutions listed below in the "Abbreviations" section. The specimens were examined, measured, and dissected using a Leica M205C stereomicroscope. Photographs were taken using a Leica DFC500 camera and compiled using Zerene Stacker software, v. 1.04. Scanning electron micrographs were taken using a Hitachi TM-1000. Terminology follows D'Alessandro et al. (2016) for the median lobe of aedeagus and spermatheca.

Geographic coordinates for the localities were reported in degrees and minutes format using the WGS84 datum; information included in square brackets were added to the label data by the authors and using the Google Earth website for coordinates and geographic information. Abbreviations for the depositories follow the list on the following website: The Insect and Spider Collections of the World (Evenhuis 2021). Chorotypes follow Biondi and D'Alessandro (2006).

### Abbreviations

**Collections and depositories. BAQ**: Italy, University of L'Aquila, Collection of M. Biondi; **MNHN**: France, Paris, Muséum National d'Histoire Naturelle; **NHMUK**: United Kingdom, London, The Natural History Museum; **NMPC**: Czech Republic, Prague, National Museum (Natural History); **SANC**: South Africa, Pretoria, South African National Collection of Insects; **UWCP**: Poland, Wrocław, University of Wroclaw; and **ZSM**: Germany, München [= Munich], Zoologische Staatssammlung.

**Biometrics. LA**: numerical sequence from base to apex proportional to the length of each antennomere; **LAED**: length of aedeagus; **LAN**: length of antennae; **LB**: total body length (from apical margin of head to apex of elytra); **LE**: length of elytra; **LP**: medial length of pronotum; **LSP**: maximum length of spermatheca, including ductus; **WE**: maximum width of elytra combined; **WP**: maximum width of pronotum.

**Distribution. KZN**: KwaZulu-Natal; **LIM**: Limpopo; **MPU**: Mpumalanga; **WCape**: Western Cape; **[?]**: unknown locality.

## Results

***Calotheca carolineae* sp. nov.**
http://zoobank.org/73C82870-1A5C-43E0-A230-CC0B06C01A0D
Figures 1A–D, 4, 5

**Type material. *Holotype* ♂:** Republic Of South Africa: KZN: Kosi Bay Mouth Nature Reserve, 26°53'31"S, 32°52'39"E, c. 0 m, 24.i.2006, adults collected on *Allophylus natalensis* (Sapindaceae), C. Chaboo & E. Grobbelaar leg. (SANC). ***Paratypes*:** Republic Of South Africa: 1♂1♀, same data as for holotype (SANC); 1♂1♀, KZN: Kosi Bay Nature Reserve, 26°58'S, 32°48'E, 50 m, 08-11.ii.1990, E. Grobbelaar leg., beaten off *Ozoroa obovata* (Oliv.) R.&A. Fern. (Anacardiaceae) (SANC); 2♂5♀, Natal [KZN]: Sodwana Bay Park, 27°32'S, 32°41'E [27°32'25"S, 32°40'37"E], 9–11. xi.1986, D. D'Hotman & A. Nel leg. (SANC).

**Diagnosis.** *Calotheca carolineae* sp. nov. displays major similarities with *C. nigromaculata* and *C. wanati* sp. nov., more so than with other known *Calotheca* species. It is mainly characterized by the differently shaped median lobe of the aedeagus (Figs 1B, 2F, 3B) which is not sinuate in lateral view, and widely rounded in the apical part in ventral view (in *C. nigromaculata*, even though quite variable, it is curved in

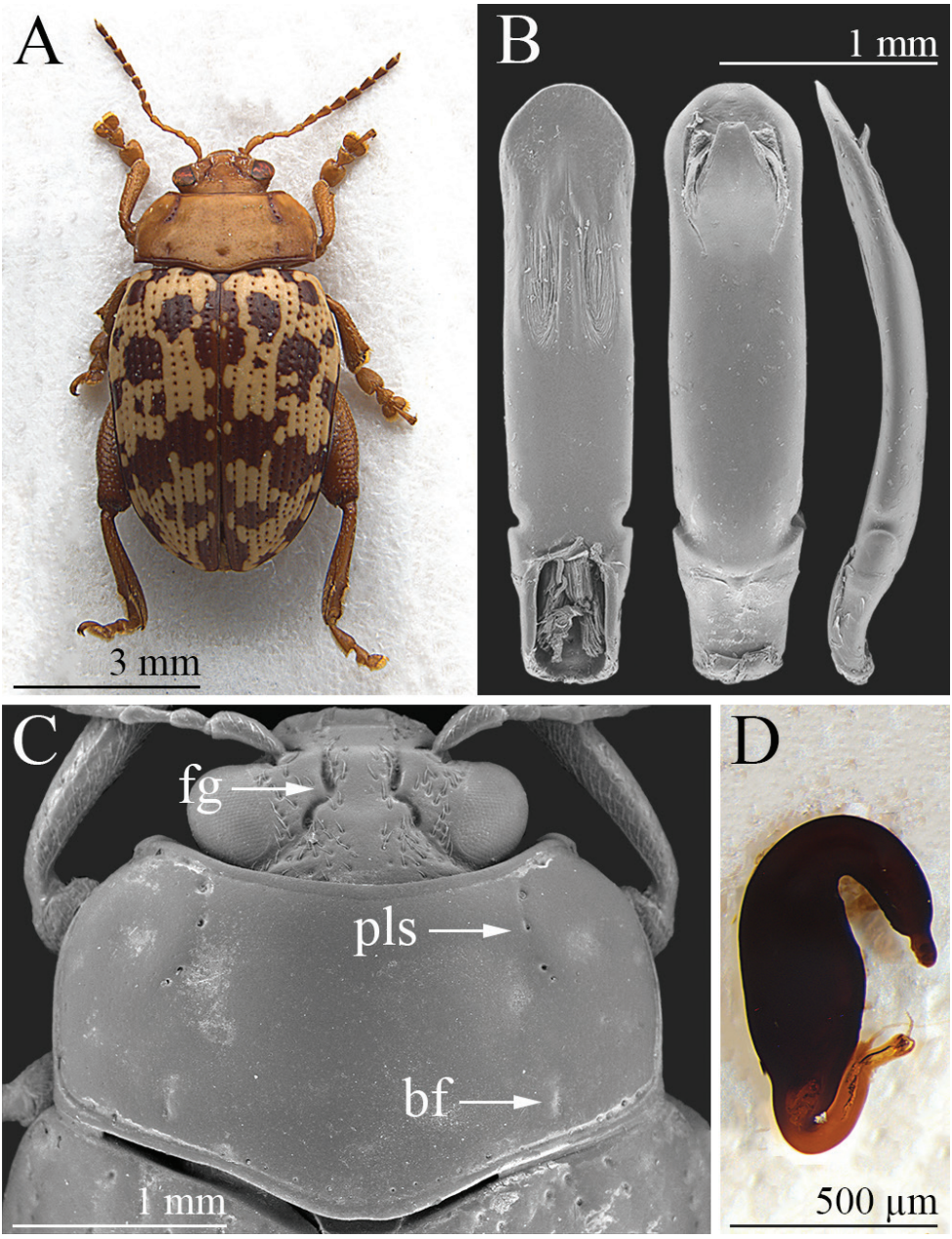


**Figure 1.** *Calotheca carolineae* sp. nov. **A** habitus, ♂ (holotype, KZN, Kosi Bay Nature Reserve) **B** median lobe of aedeagus, from left to right in ventral, dorsal, and lateral view (KZN, Sodwana Bay Park) **C** head, and pronotum, ♂ (KZN, Sodwana Bay Park) **D** spermatheca (KZN, Sodwana Bay Park). Abbreviations: bf = basal furrow; fg = frontal groove; pls = punctate lateral stria.

proximal 1/2 and distinctly sinuate in apical 1/2 in lateral view, and produced and sub-truncate apically in ventral view; in *C. wanati* sp. nov. it is curved in proximal 1/2 and more distinctly curved in apical 1/2 in lateral view, and produced and sub-rhomboidal in the apical 1/4, with prominent angulate lateral projections in ventral view). Other differences include: color of the dorsal integument with more clearly defined and generally larger colored elytral patches, reddish-brown on a yellow background (smaller and more confused, from brown to black, in *C. nigromaculata* and *C. wanati* sp. nov.) (Figs 1A, 2A–C, 3A); punctate lateral pronotal striae less dark (Figs 1A, 2A–C, 3A); antennae generally longer with LAN/(LE+LP) = 0.48 ± 0.01 in male, and = 0.41 ± 0.01 in female (in *C. nigromaculata* LAN/(LE+LP) = 0.42 ± 0.02 in male, and = 0.38 ± 0.02 in female; in *C. wanati* sp. nov. LAN/(LE+LP) = 0.42 ± 0.02 in male, and = 0.37 ± 0.02 in female) (Fig. 4A); shape of the pronotum, straight laterally in basal 2/3 and abruptly incurved in apical 1/3 (slightly curved in basal 2/3 and distinctly incurved in apical 1/3 in *C. nigromaculata* and *C. wanati* sp. nov.) (Figs 1C, 2D, 3C).

**Description of the holotype (♂).** Body elliptical in dorsal view (Fig. 1A), rather convex in lateral view; total body length (LB) = 7.00 mm; maximum pronotal width in the apical third (WP = 3.05 mm); maximum width of elytra in the basal 1/3 (WE = 3.85 mm). Head and antennae pale brown, with antennomeres 6–11 slightly darker (Fig. 1A); head surface microreticulate, with evident setiferous punctures on most of the vertex and part of the frons (Fig. 1C); frontal grooves sinuate, deeply impressed, extending approximately from the dorsal ocular margin to the inter-antennal space (Fig. 1C); eyes elliptical, clearly elongate; antennae slightly shorter than half the body length (LAN = 3.15 mm; LAN/LB = 0.45); LA: 100:44:61:63:73:68:73:68:73:63:88. Pronotum (Fig. 1A, C) slightly convex, pale brown; punctate lateral stria, basal dimples and margins slightly darker; distinctly transverse in dorsal view (LP = 1.53 mm; WP/LP = 2.00), sub-rectangular, distinctly incurved laterally in the anterior third only; surface microreticulate, with minute punctation; anterolateral surface with very shallow depressions; lateral punctate striae distinctly impressed, C-shaped and slightly curved on the disc; some additional sparse punctures along the pronotal margins; basal furrows short and moderately incised; anterior and basal margins finely bordered, lateral margins thickened slightly, poorly visible in dorsal view; anterior angles distinctly prominent, moderately swollen; posterior angles obtuse. Scutellum brown, sub-triangular. Elytra (Fig. 1A) pale yellow, with irregular wide brown patches and dark punctation; elytra moderately elongate (LE = 5.10 mm; WE/LE = 0.75; LE/LP = 3.34), distinctly sinuate laterally, jointly rounded apically; lateral margin narrow, visible in dorsal view; elytral punctation arranged in single regular rows formed by distinctly impressed punctures; interstriae flat on the elytral disc, with finely microreticulate and sparsely micropunctate surface; humeral calli indistinctly raised. Macropterous. Basal pro- and mesotarsomeres clearly enlarged (Fig. 1A). Underside pale brown; apical abdominal ventrite without preapical sculptures or impressions. Median lobe of the aedeagus (LAED = 2.65 mm; LE/LAED = 1.92) (Fig. 1B) with subparallel sides in ventral view, widely rounded in the apical part; ventral surface with a pair of lateral U-shaped depressions with a wrinkled surface in the distal half, and evident punctation apically; moderately and

evenly curved up to the apex in lateral view; dorsal ligula short, formed by a wide subtriangular, apically truncate median lobe, and two narrow lateral lobes.

**Variability.** Males (*n* = 5; mean ± standard deviation, range): LE = 5.21 ± 0.17 mm (5.05 ≤ LE ≤ 5.50 mm); WE = 3.89 ± 0.14 mm (3.70 ≤ WE ≤ 4.10 mm); LP = 1.57 ± 0.04 mm (1.55 ≤ LP ≤ 1.63 mm); WP = 3.14 ± 0.09 mm (3.05 ≤ WP ≤ 3.25 mm); LAN = 3.25 ± 0.9 mm (3.15 ≤ LAN ≤ 3.35 mm); LAED = 2.70 ± 0.08 mm (2.60 ≤ LAED ≤ 2.80 mm); LB = 6.83 ± 0.31 mm (6.45 ≤ LB ≤ 7.15 mm); LE/LP = 3.32 ± 0.09 (3.20 ≤ LE/LP ≤ 3.44); WE/WP = 1.24 ± 0.02 (1.21 ≤ WE/WP ≤ 1.26); WP/LP = 2.00 ± 0.03 (1.97 ≤ WP/LP ≤ 2.03); WE/LE = 0.75 ± 0.01 (0.73 ≤ WE/LE ≤ 0.75); LAN/LB = 0.48 ± 0.02 (0.45 ≤ LAN/LB ≤ 0.51); LE/LAED = 1.93 ± 0.05 (1.89 ≤ LE/LAED ≤ 2.00). Females (n = 7; mean ± standard deviation; range): LE = 5.40 ± 0.31 mm (4.80 ≤ LE ≤ 5.70 mm); WE = 4.23 ± 0.24 mm (3.95 ≤ WE ≤ 4.60 mm); LP = 1.57 ± 0.08 mm (1.45 ≤ LP ≤ 1.70 mm); WP = 3.18 ± 0.15 mm (2.90 ≤ WP ≤ 3.38 mm); LAN = 2.87 ± 0.14 mm (2.70 ≤ LAN ≤ 3.05 mm); LSP = 0.74 ± 0.05 mm (0.68 ≤ LSP ≤ 0.80 mm); LB = 6.79 ± 0.51 mm (5.85 ≤ LB ≤ 7.25 mm); LE/LP = 3.43 ± 0.09 (3.31 ≤ LE/LP ≤ 3.55); WE/WP = 1.33 ± 0.04 (1.29 ≤ WE/WP ≤ 1.36); WP/LP = 2.03 ± 0.03 (1.99 ≤ WP/LP ≤ 2.06); WE/LE = 0.78 ± 0.02 (0.76 ≤ WE/LE ≤ 0.82); LAN/LB = 0.42 ± 0.03 (0.39 ≤ LAN/LB ≤ 0.47); LE/LSP = 7.28 ± 0.29 (6.94 ≤ LE/LSP ≤ 7.85). Paratypes very similar in shape, sculpture, and color to the holotype. Basal furrows and punctate lateral striae weakly to distinctly impressed. Female with basal pro- and mesotarsomeres less enlarged than in male. Spermatheca (Fig. 1D) sub-fusiform and elongate basally, narrowing towards the ductus attachment; distal part distinctly curved and about 2/3 the basal part in length, with a distinct appendix; ductus basally inserted, thickset, short, uncoiled, roughly U-shaped.

**Etymology.** The specific epithet is a noun in the genitive case after our friend Caroline S. Chaboo (University of Nebraska-Lincoln, Nebraska, USA), one of its collectors and appreciated expert of chrysomelid Coleoptera.

**Distribution.** Republic of South Africa (KZN) (Fig. 5). Chorotype: Southern-Eastern African (SEA).

**Ecological notes.** Adults were collected in November, January, and February, between 0–50 m a.s.l., on *Allophylus natalensis* (Sapindaceae) and *Ozoroa obovata* (Anacardiaceae).

### ***Calotheca nigromaculata*** **(Jacoby)**

Figures 2A–F, 4, 5

*Blepharida nigromaculata* Jacoby, 1888: 194
*Calotheca nigromaculata* (Jacoby) Biondi et al. 2017: 121 (pars)

**Type material examined.** ***Lectotype*** ♂: [Mozambique]: Delagoa B[ay] [Maputo Bay, 25°53'31"S, 32°36'18"E], [R.] Monteiro [leg.], Jacoby Coll., 1909-28a (NHMUK) (M. Biondi des. 2017). ***Paralectotype*****:** 1♂; same data as for lectotype (NHMUK).

**Additional material examined.** Mozambique: 10 specimens, Delagoa Bay [Maputo Bay, 25°53'31"S, 32°36'18"E], [R.] Monteiro [leg.], ex. coll. R. Oberthur

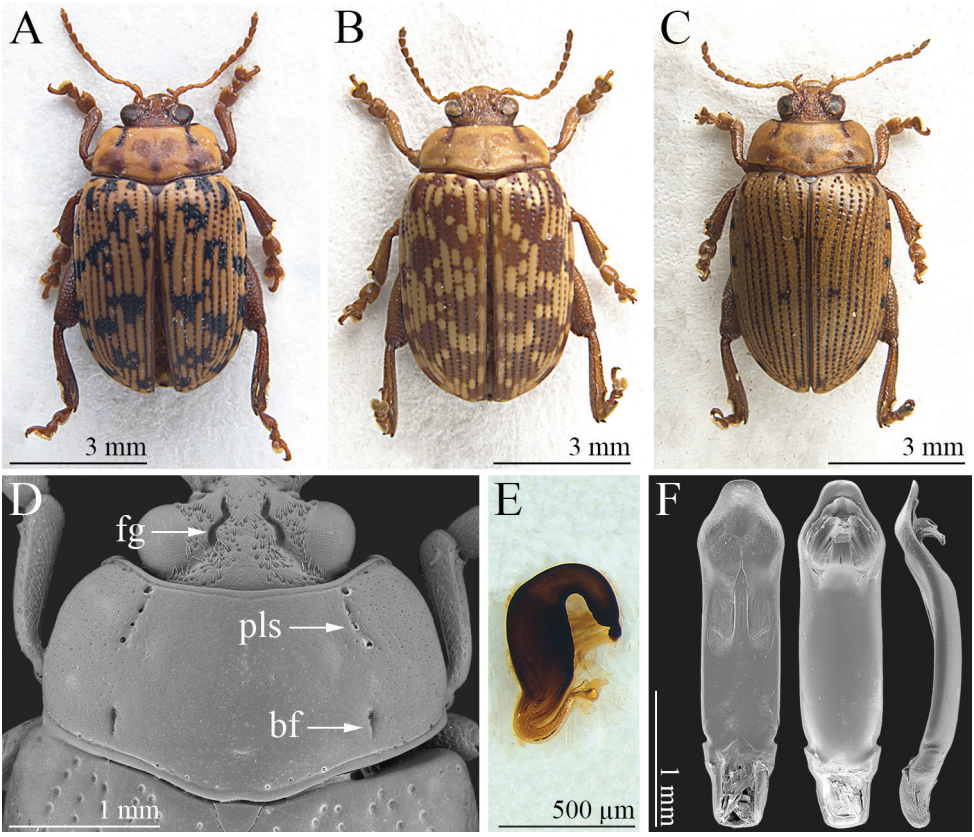


**Figure 2.** *Calotheca nigromaculata*. **A** habitus, ♂ (KZN, Tembe Elephant Park, Research Camp) **B** ibid, ♂ (MPU, Mapoch's Caves) **C** ibid, ♂ (KZN, Vryheid Hill Nature Reserve) **D** head, and pronotum, ♂ (MPU, Mariepskop base Picnic Site at Blyde River) **E** spermatheca (KZN, Estcourt) **F** median lobe of aedeagus, from left to right in ventral, dorsal, and lateral view (MPU, Pretoriuskop). Abbreviations: bf = basal furrow; bfg = frontal groove; pls = punctate lateral stria.

(MNHN); 2 specimens, ibid, 1885 (MNHN). Republic Of South Africa: [KZN]: 3 specimens, Hluhluwe Game Reserve, 28°02'S, 32°05'E, 4–6.ii.1994, U. Göllner leg. (ZSM); 1 specimen, ibid, 4–7.ii.1994 (ZSM); 3 specimens, Natal [KZN]: Itala Game Reserve, Thalu River, 27°30'S, 31°20'E, 27.i.1994, U. Göllner leg. (ZSM); 1 specimen, Natal [KZN]: Itala Game Reserve, Louwsburg, 27°35'S, 31°17'E, 10–23.xii.1992, F. Koch leg. (BAQ); 1 specimen, Natal [KZN]: Santa Lucia [28°22'21"S, 32°24'51"E], 29.x.1981, Klapperich leg. (BAQ); 1 specimen, [KZN]: St. Lucia Estuary, 22.x.[19]66, G. du Plessis leg., (SANC); 1 specimen, ibid, 24.x.[19]66 (SANC); 1 specimen, KwaZulu-Natal: Mkuze Natural Reserve, 27°37'S, 32°03'E, 100 m, 16.xi.1988, Colonnelli leg. (BAQ); 1 specimen, Zululand [KZN]: Mkuzi [Mkuze, 27°36'24"S, 32°02'53"E], xii.1945, DDT Killed, DDT No. 153; 7/15; Imp. Inst. Ent. Coll.No. 10519 (SANC); 7 specimens, KZN: Mkuzi Game Res.[erve], c. 2 km NE Mantuma

Rest Camp, 27°35'06"S, 32°14'14"E, c. 69 m, 21.i.2006, adults beaten off cf. *Rhus gueinzii* (Anacardiaceae), C. Chaboo & E. Grobbelaar leg. (SANC); 2 specimens, [KZN]: King[s]burgh, 18km S, 30°05'S, 30°47'E, 24.ii.1989, B.[=E.] Grobbelaar & E. v.d. Linde leg. (SANC); 1 specimen, Natal [KZN]: Cape Vidal, 28°10'S, 32°32'E, 15.xi.1986, D. D'Hotman & A. Nel leg. (SANC); 2 specimens, ibid, 13.i.1981, I.M. Millar leg. (SANC); 3 specimens, KZN: Tembe Elephant Park, Research Camp, 27°02'40"S, 32°25'17"E, c. 100 m, 25-26.i.2006, adults beaten off cf. *Allophylus decipiens* (Sapindaceae), C. Chaboo & E. Grobbelaar leg. (SANC); 3 specimens, KZN: Tembe Elephant Park, Sihangwane Area, 27°02'S, 32°25'E, 100 m, 01.ii–04.ii.1996, collected from *Rhus* sp. (Anacardiaceae), E. Grobbelaar leg. (SANC); 8 specimens, Natal [KZN]: Estcourt, 29°00'S, 29°53'E, 25.ii.1984, R. Oberprieler & C.G.E. Moolman leg. (SANC); 1 specimen, Natal [KZN]: Pietermaritzburg, Ukulinga Station [29°40'27"S, 30°24'31"E], 3.x.1983, A. Freidberg leg. (DG Furth coll) (BAQ); 1 specimen, Natal [KZN]: S Coast, Umkomaas [30°12'06"S, 30°46'57"E], 11.x.1983, A. Freidberg leg. (DG Furth coll) (BAQ); 1 specimen, [KZN]: Isipingo, Nat., [29°58'58"S, 30°55'20"E], ii.1896 (NHMUK); 2 specimens, KZN: Ndumo Game Reserve, c. 1 km NE Rest Camp, 26°54'07"S, 32°18'20"E, c. 80 m, 28.i.2006, collected by beating, C. Chaboo & E. Grobbelaar leg. (SANC); 4 specimens, KZN: Ndumo Game Reserve, Fig Tree Forest, 26°51'39"S, 32°15'32"E, c. 42 m, 29.i.2006, adults beaten off *Rhus gueinzii* (Anacardiaceae), C. Chaboo & E. Grobbelaar leg. (SANC); 6 specimens, KZN: Vryheid Hill Nature Res.[erve], Ntinginono Eco Centre, 27°45'14"S, 30°47'11"E, c. 1259 m, 30.i–02.ii.2007, E. Grobbelaar leg. (SANC); 6 specimens, ibid, adults beaten off *Rhus* sp. (Anacardiaceae) (SANC); 1 specimen, KZN: Empangeni, 28°45'S, 31°54'E, 152 m, xii.1999, P.E. Reavell leg. (SANC); 1 specimen, KZN: Lewomba, SE 28 31 Da [Lewomba Miss., Empangeni, 28°44'54"S, 31°53'53"E], 20.iv.1979, R. Oberprieler leg. (SANC); 1 specimen, KZN: Lugwavana [?], SE 27 31 Bb, 1.i.1980, on forest vegetation, R. Oberprieler leg. (SANC); 1 specimen, KZN: Ingwavuma, Mac's Pass, SE 27 31 Bb [28°44'54"S, 31°53'53"E], 13.i.1980, on vegetation, R. Oberprieler leg. (SANC); 1 specimen, Natal [KZN]: Lynnfield Park, 13km SE Pietermaritzburg, 29°41'S, 30°29'E, 28–30.iii.1989, A.E. Whittington leg. (SANC); 1 specimen, NTL [KZN]: Kuleni Farm, Hluhluwe, 27°54'S, 32°22'E, 13–14. ii.1990, N. Verheijen leg. (SANC); 1 specimen, Natal [KZN]: Balgowan, 29°23'S, 30°02'E, 26.ii.1984, R. Oberprieler & C.G.E. Moolman leg. (SANC); 1 specimen, KZN: Ntinini Nature Reserve, 28°17'S, 30°56'E, 1015 m, 16.xi.2010, collected by sweeping through very short grass with various forbs, some flowering, R. Stals leg. (SANC); 2 specimens, KZN: Nyala Game Ranch [28°42'S, 31°46'E], 16.xii.1980, R. Oberprieler leg. (SANC); 1 specimen, KZN: Intendele Game Ranch, nr Bayala, 27°50'S, 32°12'E, 07.i.2000, ex *Rhus* sp.1 (Anacardiaceae), C.N. Duckett leg. (SANC); 4 specimens, Natal [KZN]: Dr. Martin (NMPC); 6 specimens, ibid (MNHN); 1 specimen, ibid (NHMUK); 1 specimen, ibid, Zululand (NMPC); 1 specimen, ibid (SANC); 1 specimen, [KZN]: Howick [29°29'21"S, 30°12'60"E], 1901, J.P. Cregoe leg. (NHMUK); 2 specimens, [KZN]: Durban [29°51'31"S, 31°01'18"E], x.1896, J.P. Cregoe leg. (NHMUK); 2 specimens, ibid, viii.[19]20, A.F.J. Gedye leg. (NHMUK);

1 specimen, [KZN]: Durban, The Bluff [29°56'08"S, 31°00'07"E], 15.x.1931, Mrs L. Ogilvie leg. (NHMUK); 1 specimen, Natal [KZN]: Weenen [28°51'31"S, 30°00'12"E], xii.1926, H.P. Thomasset leg. (NHMUK); 4 specimens, ibid, i.1927 (NHMUK); 1 specimen, ibid, xi.1927 (NHMUK); 2 specimens, ibid, iii-iv.1925 (NHMUK); 1 specimen, Zululand [KZN]: Gingindhlovu [29°01'S, 31°35'E], 9.vi.1926, R.E. Turner leg. (NHMUK); 2 specimens, Natal [KZN]: Lower Tugela [29°09'50"S, 31°26'16"E], E. Reynolds leg. (NHMUK); 1 specimen, Natal [KZN]: Malvern [Malvern, Queensburgh, 29°53'S, 30°55'18"E] iii.1897, G.A.K. Marshall leg. (NHMUK); 1 specimen, ibid, xii.1899, J.P. Cregoe leg. (NHMUK); 4 specimens, KwaZulu-Natal: between Colenso and Weenen Game Reserve, 28.48S, 29.57E [28°28'48"S, 29°34'12"E], 900 m, 4.iii.1998, P. Audisio, M. Biondi & M. Zapparoli leg. (BAQ); 19 specimens Natal [KZN]: Ulundi [28°19'S, 31°25'E], 22.i.1994, A. Poll leg. (ZSM); 1 specimen (NE), KwaZulu-Natal: Ubombo Mountain Nat. Res., –27.6100S/32.0802E [27°36'36"S, 32°04'49"E], 110 m, beating, 30.xi.2012, M. Wanat leg. (UWCP); 2 specimens, Tvl. [LIM]: Hans Merensky Nat.[ure] Res.[erve], 23°42'S, 30°44'E, 23–25.i.1987, collected by beating, B.[=E.] Grobbelaar leg. (SANC); 1 specimen, Limpopo: Strydpoortberge Pass, hill slope, S24 02.741 E29 52.198, [24°02'44"S, 29°52'12"E], 1650 m, 21.ii.2007, P. Audisio & M. Biondi leg. (BAQ); 1 specimen, [LIM]: Pietersburg [Polokwane], 24°14'40"S, 29°15'30"E [23°53'55"S, 29°27'01"E], 18.ii.1989, F.J. Joubert leg. (SANC); 5 specimens, [LIM]: Mathlari, Nas. K.W. [Kruger National Park], 17.iii.1970, H.A.D. van Schalkwyk leg. (SANC); 4 specimens, NProv [LIM]: Thabaphaswa (Groenkom Farm), near Potgietersrus, 24°03'S, 29°02'E, 21–23.ii.2001, adults and larvae collected from *Rhus leptodictya* (Anacardiaceae), E. Grobbelaar leg. (SANC); 1 specimen, LIM: Orrie, The Downs, Baragwanath Pass, forest edge, 24°08'S, 29°57'E, 900–1370 m, 14.iii.1998, M. Biondi & M. Zapparoli leg. (BAQ); 2 specimens, Mpumalanga: Mariepskop base Picnic Site at Blyde River, –24.5931S/30.8249E [24°35'35"S, 30°49'29"E], 780 m, night collecting, 26.xi.2012, R. Ruta leg. (UWCP); 1 specimen, Transvaal [MPU]: Blydepoort [24°34'51"S, 30°46'20"E], 20.xi.1981, Klapperich leg. (BAQ); 1 specimen, Transvaal [MPU]: Pretoriuskop, 25°10'S, 31°16'E, 500 m, 12.xi.1988, E. Colonnelli leg. (BAQ); 7 specimens, Transvaal [MPU]: Badplaas, 26°03'S, 30°33'E, 1250 m, 25.xi.1988, E. Colonnelli leg. (BAQ); 2 specimens, MPU: Mapoch's Caves, c. 4 km ENE Roossenekal, 25°11'S, 29°58'E, 16.i.1989, collected from *Rhus* sp. (Anacardiaceae), E. Grobbelaar leg. (SANC); 10 specimens, Tvl. [MPU]: 20 km NE of Barberton, 25°41'S, 31°09'E, 21.iii.1993, collected from *Rhus pentheri* Zahlbr. (Anacardiaceae), E. Grobbelaar leg. (SANC); 5 specimens, Tvl. [MPU]: Sudwala Caves, [N]W of Nelspruit, 25°22'S, 30°42'E, 21.iii.1993, E. Grobbelaar leg. (SANC); 12 specimens, MPU: Paddadors Farm, Nelspruit, 22 km SE, 25°37'02"S, 31°07'56"E, 28.i.1984, E. de Wet, A. Nel & E. Grobbelaar leg. (SANC); 1 specimen, [MPU]: Marloth Park, 25°21'S, 31°47'E, 04.iv.1989, F.J. Joubert leg. (SANC); 1 specimen, Tvl. [MPU]: Swadini, Blydepoort Nat.[ure] Res.[erve], 24°32'S, 30°54'E, 26–29.i.1987, collected by beating, B.[=E.] Grobbelaar leg. (SANC); 1 specimen, Tvl. [MPU]: Barberton, 25°48'S, 31°03'E, 26–29.iii.1979, C. Moolman leg. (SANC); 1 specimen, ibid, iii.1979, C. Kok leg. (SANC); 1 specimen, MPU: Gustav Klingbiel

Nature Reserve, 25°06'S, 30°00'E, 17.i.1989, collected by sweeping, E. Grobbelaar leg. (SANC); 5 specimens, TVL [MPU]: Blyderivierpoortdam Nat.[ure] Reserve, 24°32'S, 30°47'E, 25–26.x.1984, G.L. Prinsloo leg. (SANC); 1 specimen, Tvl [MPU]: between Baberton & Kaap Muiden, 24°29'S, 28°35'E, 25.ii.1991, V.M. Uys leg. (SANC).

**Taxonomic remarks.** *Calotheca nigromaculata* displays much variation in the number, shape, and color of the elytral patches (Fig. 2A–C), and in some biometric ratios (e.g., LE/LP) (Fig. 4). However, pronotal shape, sculpture, and color are consistent and useful for identification (Fig. 2A–D): lateral margins barely or not visible in dorsal view, more incurved in the anterior third; punctate lateral striae and basal furrows distinctly impressed and generally darker than the rest of the pronotal surface; pronotal margins mostly darkened. Median lobe of the aedeagus (Fig. 2F) in ventral view: lateral margins sinuate, but prominently rounded in apical 1/4, subtruncate apically; ventral surface with a pair of rounded lateral U-shaped depressions with a wrinkled surface in the apical half; surface clearly punctate in the apical 1/4; in lateral view, aedeagus curved in the basal 1/2 and distinctly sinuate in the apical 1/2; dorsal ligula short but clearly visible in lateral view, formed by a subtriangular, apically truncate median lobe, and two lateral lobes. The apical part of the median lobe shows considerable variability: in ventral view it is more or less sinuate laterally and more or less prominently rounded in apical 1/4, and more or less sinuate in lateral view. Spermatheca (Fig. 2E) globosely fusiform basally, sub-conical and generally dorsally orientated at the ductus attachment; distal part distinctly curved, generally about as long as the basal part, with a distinct appendix; ductus basally inserted, thickset, short, uncoiled, roughly U-shaped.

**Biometrics.** Males ($n$ = 10; mean ± standard deviation, range): LE = 5.04 ± 0.37 mm (4.25 ≤ LE ≤ 5.30 mm); WE = 3.73 ± 0.25 mm (3.18 ≤ WE ≤ 4.10 mm); LP = 1.46 ± 0.07 mm (1.35 ≤ LP ≤ 1.55 mm); WP = 2.88 ± 0.20 mm (2.45 ≤ WP ≤ 3.10 mm); LAN = 2.74 ± 0.15 mm (2.45 ≤ LAN ≤ 3.00 mm); LAED = 2.62 ± 0.10 mm (2.45 ≤ LAED ≤ 2.83 mm); LB = 6.36 ± 0.53 mm (5.15 ≤ LB ≤ 7.15 mm); LE/LP = 3.45 ± 0.21 (3.19 ≤ LE/LP ≤ 3.79); WE/WP = 1.30 ± 0.03 (1.24 ≤ WE/WP ≤ 1.36); WP/LP = 1.97 ± 0.08 (1.81 ≤ WP/LP ≤ 2.07); WE/LE = 0.74 ± 0.02 (0.71 ≤ WE/LE ≤ 0.78); LAN/LB = 0.43 ± 0.03 (0.39 ≤ LAN/LB ≤ 0.48); LE/LAED = 1.92 ± 0.09 (1.73 ≤ LE/LAED ≤ 2.00). Females ($n$ = 10; mean ± standard deviation; range): LE = 5.41 ± 0.37 mm (4.75 ≤ LE ≤ 6.00 mm); WE = 3.96 ± 0.28 mm (3.40 ≤ WE ≤ 4.30 mm); LP = 1.42 ± 0.12 mm (1.23 ≤ LP ≤ 1.55 mm); WP = 3.01 ± 0.25 mm (2.70 ≤ WP ≤ 3.25 mm); LAN = 2.60 ± 0.21 mm (2.20 ≤ LAN ≤ 2.93 mm); LSP = 0.70 ± 0.06 mm (0.63 ≤ LSP ≤ 0.85 mm); LB = 6.48 ± 0.48 mm (5.60 ≤ LB ≤ 7.25 mm); LE/LP = 3.81 ± 0.17 (3.57 ≤ LE/LP ≤ 4.00); WE/WP = 1.32 ± 0.03 (1.26 ≤ WE/WP ≤ 1.37); WP/LP = 2.12 ± 0.06 (2.03 ≤ WP/LP ≤ 2.25); WE/LE = 0.73 ± 0.01 (0.72 ≤ WE/LE ≤ 0.77); LAN/LB = 0.40 ± 0.02 (0.38 ≤ LAN/LB ≤ 0.44); LE/LSP = 7.71 ± 0.33 (7.48 ≤ LE/LSP ≤ 8.23).

**Distribution.** Mozambique and the Republic of South Africa (KZN, LIM, MPU). Records from Namibia (1 specimen, Fish River Canyon, Ai-Ais, 27°55'S, 17°29'E, 250 m, 13.ii.1994, F. Koch leg. (ZSM)), WCape Province (RSA) (3 specimens, Knysna, [34°02'S, 23°03'E], i.1979, C.D. Eardley leg. (SANC)), and Tanzania (Biondi et al. 2017) need additional confirmation (Fig. 5). Chorotype: probably Southern-Eastern Afrotropical (SEA).

**Ecological notes.** Adults were collected from October to March, between 42–1650 m a.s.l., on *Searsia* sp. [= *Rhus* pars, cf. Moffett (2007)], *S. leptodictya* (along with larvae), *S.* cf. *gueinzii*, *S. pentheri* (Anacardiaceae), and on *Allophylus decipiens* (Sapindaceae), in forest or habitat with very short grass.

***Calotheca wanati* sp. nov.**

http://zoobank.org/36AF9FD0-098F-4444-ABF5-AF7CEA799A5D

Figures 3A–D, 4, 5

**Type material.** ***Holotype*** ♂**:** Republic Of South Africa: KZN: Ubombo Mountain Nat. Res., –27.6100S/32.0802E [27°36'36"S, 32°04'49"E], 110 m, beating, 30.xi.2012, M. Wanat leg. (SANC). ***Paratypes*:** Republic Of South Africa: 3♂8♀, same data as for holotype (UWCP); 1♀, ibid, R. Ruta leg. (UWCP); 1♂1♀, KZN: Jozini, 10 km SW, W slope of Ubombo Mts, 27°28'S, 32°01'E, 500 m, 23.i.2006, adults beaten off *Allophylus natalensis* (Sapindaceae), E. Grobbelaar leg. (SANC); 2♂2♀, KwaZulu-Natal: Mkhuze Game Res., –27.6392S/32.1583E [27°38'21"S, 32°09'29"E], 100 m, camping site, beating, 1.xii.2012, M. Wanat leg. (UWCP); 1♀, KwaZulu-Natal, Sodwana Bay, –27.5315S/32.6699E [27°31'53"S, 32°40'12"E], 5 m, swamp forest, site 1, 3.xii.2012, M. Wanat leg. (UWCP).

**Diagnosis.** *Calotheca wanati* sp. nov. is very similar to *C. nigromaculata*, both in external morphology and shape of the aedeagus and spermatheca. It is mainly distinguishable by: the almost invariable elytral color pattern, with quite small, irregular, light brown patches (*C. nigromaculata* is very variable in number, shape, and color of elytral patches, but the color pattern is generally different from *C. wanati* sp. nov.) (Figs 2A–C, 3A); the first pro- and metatarsomeres in male less enlarged, slightly larger than the distal part of the tibia (distinctly larger than the distal part of the tibia in *C. nigromaculata*) (Figs 2A–C, 3A); and the female has enlarged elytra (WE/LE = 0.76 ± 0.01 in *C. wanati* sp. nov.) (WE/LE = 0.73 ± 0.01 in *C. nigromaculata*) (Fig. 4B). The aedeagus is relatively short in *C. wanati* sp. nov. (LE/LAED = 2.16 ± 0.01) (Fig. 4C), in ventral view it has a sub-rhomboidal apical 1/4, and the prominent lateral expansions are angulate; in lateral view the median lobe is more distinctly curved apically (in *C. nigromaculata*, it is more elongate–LE/LAED = 1.92 ± 0.09, with indistict or very indistinct rounded lateral expansions in apical 1/4 in ventral view, and only slightly curved apically in lateral view) (Figs 2F, 3B).

**Description of the holotype (♂).** Body elliptical in dorsal view (Fig. 3A), rather convex in lateral view; total length of the body (LB) = 6.40 mm; maximum pronotal width in the middle (WP = 2.98 mm); maximum width of elytra in the basal third (WE = 3.80 mm). Head pale brown, slightly darker along the frontal grooves; antennae pale brown, with antennomeres 6–11 slightly darkened (Fig. 3A); surface microreticulate and densely micropunctate, with evident setiferous punctures on most of the vertex and part of the frons; frontal grooves sinuate, very deeply impressed, extending from approximately the dorsal ocular margin to the inter-antennal space (Fig. 3C); eyes elliptical, clearly elongate; antennae shorter than half the body length (LAN = 2.75 mm;

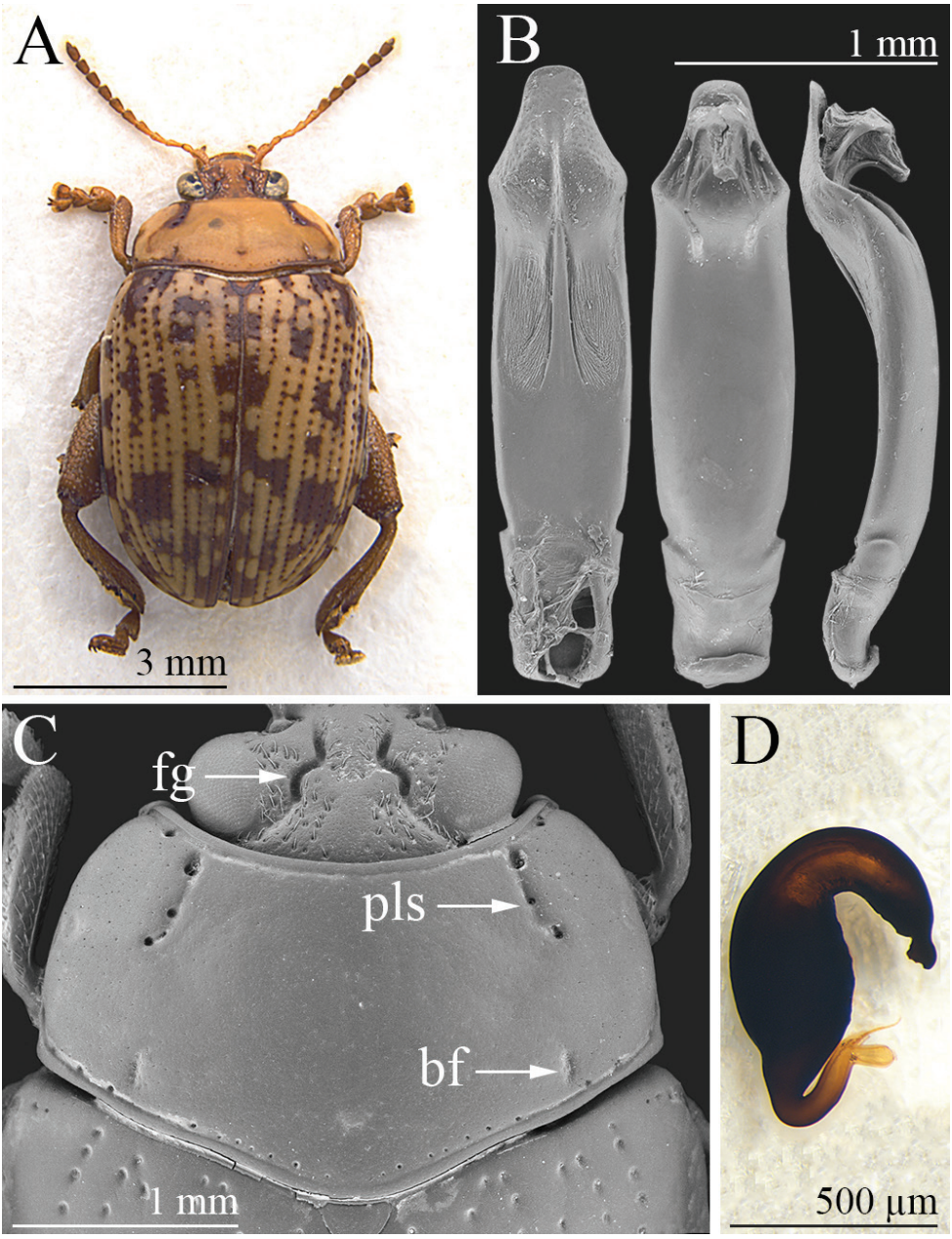


**Figure 3.** *Calotheca wanati* sp. nov. **A** habitus, ♂ (holotype, KZN, Ubombo Mountain Nature Reserve) **B** median lobe of aedeagus, from left to right in ventral, dorsal, and lateral view (KZN, Ubombo Mountain Nature Reserve) **C** head, and pronotum, ♂ (KZN, Ubombo Mountain Nature Reserve) **D** spermatheca (KZN, Ubombo Mountain Nature Reserve). Abbreviations: bf = basal furrow; fg = frontal groove; pls = punctate lateral stria.

LAN/LB = 0.43); LA: 100:50:61:61:67:67:61:61:64:61:100. Pronotum (Fig. 3A, C) slightly convex, pale brown, punctate lateral stria and part of the margins darkened; distinctly transverse in dorsal view (LP = 1.40 mm; WP/LP = 2.13), sub-rectangular, with sides more distinctly incurved in the anterior third; surface microreticulate and micropunctate, with minute punctation; anterolateral surface with very shallow depressions; punctate lateral striae distinctly impressed, C-shaped, and slightly curved on the disc; some additional sparse punctures along the pronotal margins; basal furrows short and moderately incised; anterior, basal, and lateral margins evenly and finely bordered; lateral margins barely visible in dorsal view; anterior angles distinctly prominent, indistinctly swollen; posterior angles obtuse. Scutellum brown, sub-triangular. Elytra (Fig. 3A) elongate (LE = 4.90 mm; WE/LE = 0.78; LE/LP = 3.50), moderately rounded and indistinctly sinuate laterally, jointly rounded apically; slightly paler than pronotum, with irregular brown patches and brown punctation; lateral margin narrow, barely visible in dorsal view; elytral punctation arranged in single regular rows formed by distinctly impressed punctures; interstriae flat on the elytral disc, with finely microreticulate and sparsely micropunctate surface; humeral calli indistinctly raised. Macropterous. Basal pro- and mesotarsomeres clearly enlarged (Fig. 3A). Underside brown; apical abdominal ventrite without preapical sculptures or impressions. Median lobe of the aedeagus (LAED = 2.28 mm; LE/LAED = 2.15) (Fig. 3B) distinctly sinuate laterally in ventral view; in ventral view it has a sub-rhomboidal apical 1/4 truncate apically, and the prominent lateral projections are angulate; ventral surface with a pair of elongate lateral U-shaped depressions with a wrinkled surface in the apical half; surface distinctly punctate in the apical 1/4; aedeagus curved in the basal 1/2 and distinctly sinuate in the apical 1/2; dorsal ligula short but clearly visible in lateral view, formed by a subtriangular apically truncate median lobe, and two narrower lateral lobes.

**Variability.** Males ($n$ = 7; mean ± standard deviation, range): LE = 4.94 ± 0.12 mm (4.75 ≤ LE ≤ 5.10 mm); WE = 3.80 ± 0.09 mm (3.65 ≤ WE ≤ 3.90 mm); LP = 1.45 ± 0.05 mm (1.38 ≤ LP ≤ 1.50 mm); WP = 2.95 ± 0.06 mm (2.85 ≤ WP ≤ 3.03 mm); LAN = 2.66 ± 0.10 mm (2.50 ≤ LAN ≤ 2.75 mm); LAED = 2.28 ± 0.06 mm (2.20 ≤ LAED ≤ 2.35 mm); LB = 6.25 ± 0.22 mm (6.00 ≤ LB ≤ 6.60 mm); LE/LP = 3.40 ± 0.11 (3.27 ≤ LE/LP ≤ 3.53); WE/WP = 1.29 ± 0.01 (1.28 ≤ WE/WP ≤ 1.31); WP/LP = 2.03 ± 0.06 (1.97 ≤ WP/LP ≤ 2.13); WE/LE = 0.77 ± 0.01 (0.75 ≤ WE/LE ≤ 0.79); LAN/LB = 0.43 ± 0.02 (0.38 ≤ LAN/LB ≤ 0.45); LE/LAED = 2.16 ± 0.07 (2.02 ≤ LE/LAED ≤ 2.22). Females ($n$ = 10; mean ± standard deviation; range): LE = 5.43 ± 0.25 mm (5.20 ≤ LE ≤ 5.70 mm); WE = 4.13 ± 0.19 mm (3.75 ≤ WE ≤ 4.30 mm); LP = 1.54 ± 0.08 mm (1.40 ≤ LP ≤ 1.55 mm); WP = 3.14 ± 0.13 mm (2.88 ≤ WP ≤ 3.28 mm); LAN = 2.61 ± 0.18 mm (2.40 ≤ LAN ≤ 3.05 mm); LSP = 0.66 ± 0.04 mm (0.60 ≤ LSP ≤ 0.75 mm); LB = 6.68 ± 0.34 mm (6.05 ≤ LB ≤ 7.10 mm); LE/LP = 3.53 ± 0.11 (3.35 ≤ LE/LP ≤ 3.70); WE/WP = 1.31 ± 0.02 (1.30 ≤ WE/WP ≤ 1.36); WP/LP = 2.04 ± 0.07 (1.88 ≤ WP/LP ≤ 2.13); WE/LE = 0.76 ± 0.01 (0.74 ≤ WE/LE ≤ 0.78); LAN/LB = 0.39 ± 0.02 (0.36 ≤ LAN/LB ≤ 0.45); LE/LSP = 8.21 ± 0.28 (7.93 ≤ LE/LSP ≤ 8.54). Paratypes very similar in shape, sculpture, and color to the holotype. Maximum pronotal width close to the

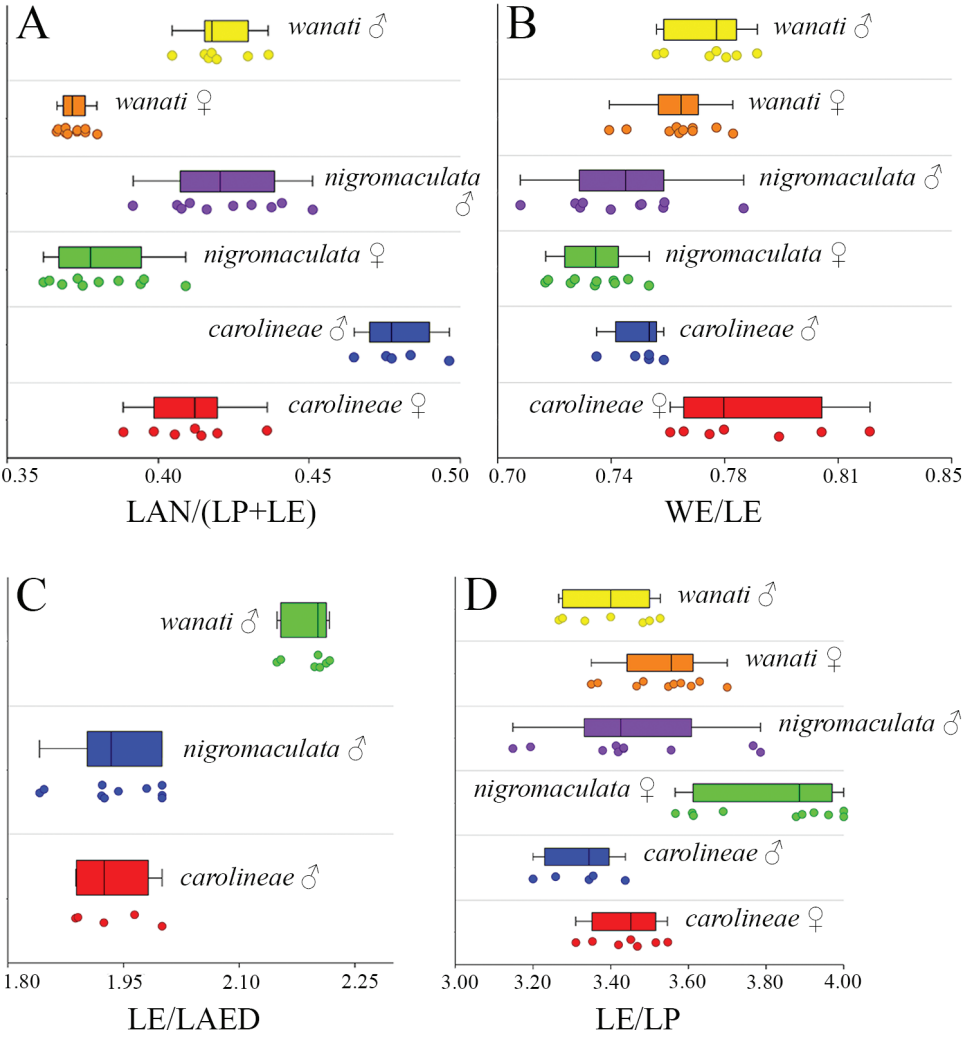


**Figure 4.** Histograms of morphometric variables in the *Calotheca nigromaculata* species group. Abbreviations: LAED = length of aedeagus; LAN = length of antennae; LE = length of elytra; LP = medial length of pronotum; WE = maximum width of elytra combined; WP =maximum width of pronotum.

pronotal base in some specimens. Female with basal pro- and mesotarsomeres less enlarged than in male. Spermatheca (Fig. 3D) globosely fusiform basally, subconical at the ductus attachment; distal part distinctly curved and slightly shorter than the basal part, with a distinct, irregularly enlarged appendix; ductus basally inserted, thickset, short, uncoiled, roughly U-shaped.

**Etymology.** The specific epithet is a noun in the genitive case after Dr Marek Wanat (University of Wrocław, Poland), one of its collectors and esteemed expert of Coleoptera Curculionoidea.

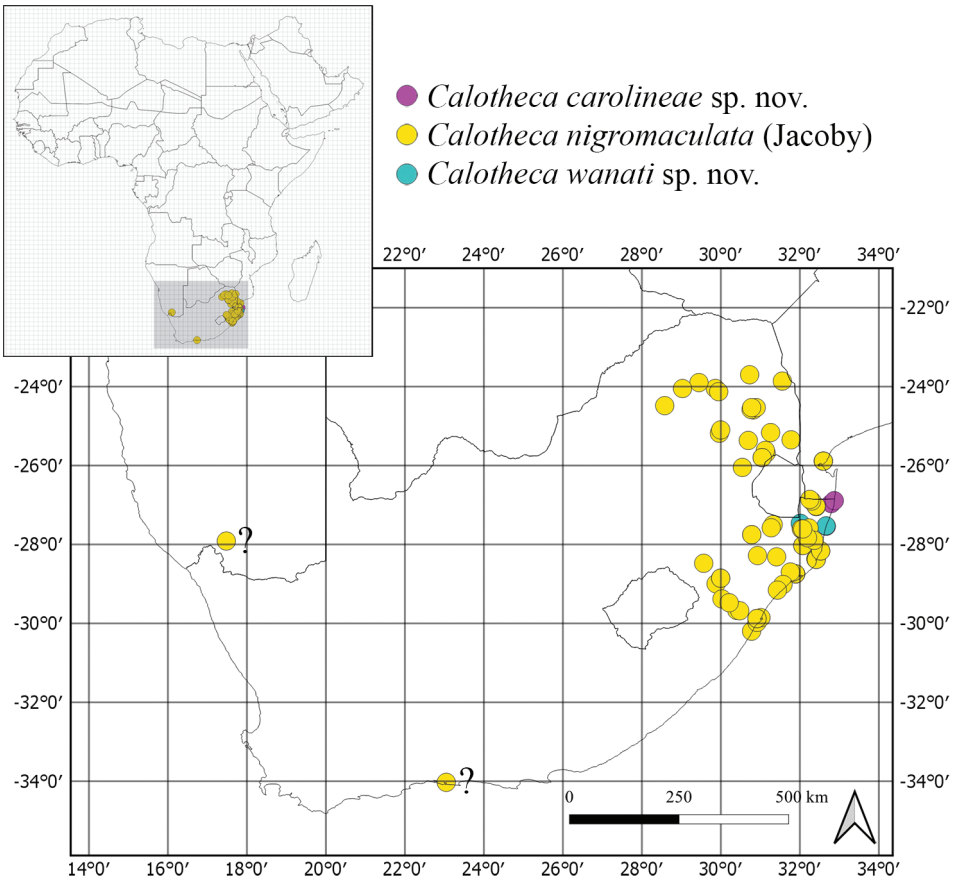


**Figure 5.** Distribution of the *Calotheca nigromaculata* species group.

**Distribution.** Republic of South Africa (KZN) (Fig. 5). Chorotype: Southern-Eastern African (SEA).

**Ecological notes.** Adults were collected in November, December, and January, between 5–500 m a.s.l., on *Allophylus natalensis* (Sapindaceae) on one occasion and in swamp forest during a different collecting event.

## Discussion

*Calotheca carolineae* sp. nov., *C. nigromaculata* and *C. wanati* sp. nov. differ from the other known *Calotheca* species in that they share a combination of morphological characters, which are listed below. The basal part of the spermatheca is sub-fusiform; the area where the ductus is attached is roughly conical; the distal part is distinctly curved, elongate and about 2/3 or sub-equal to the basal part in length, with a distinct appendix; the ductus is

basally inserted, quite thickset, short, uncoiled, and roughly U-shaped (Figs 1D, 2E, 3D). Ventrally the aedeagus has a pair of elongate to sub-rounded U-shaped depressions with a wrinkled surface in the distal 1/2, and distinct punctation towards the apex (Figs 1B, 2F, 3B). The pronotum shows distinct, but not expanded, lateral margins which are not thicker than the basal margin, barely or not visible in dorsal view, and more distinctly incurved in the anterior third; the punctate lateral striae, and sometimes the basal furrows, are darker in color than the rest of the pronotal surface (Figs 1C, 2D, 3C). The head has evident setiferous punctures on most of the surface of the vertex and at least on part of the frons (Figs 1C, 2D, 3C). Clear similarity in the shape of the median lobe of the aedeagus of *C. nigromaculata* and *C. wanati* sp. nov. reveals a closer affinity between these species than with *C. carolineae* sp. nov. In these two species, the aedeagus shows (Figs 2F, 3B): in ventral view the apical 1/4 sub-rhomboidal, truncate, or slightly rounded apically, with a strongly punctate surface; two lateral U-shaped depressions with a wrinkled surface in the distal half; in dorsal view a short ligula, with a slender median lobe and lateral lobes; in lateral view the apical part clearly sinuate. The main characters discussed above are reported below in the form of a key to species to facilitate the identification of the specimens.

Based on the available data, *C. nigromaculata* displays a wider distribution, that includes those of *C. carolineae* sp. nov. and *C. wanati* sp. nov. The species are even syntopic in some areas (*C. nigromaculata* with *C. wanati* sp. nov. in Ubombo Mountain Nature Reserve, and *C. wanati* sp. nov. with *C. carolineae* sp. nov. in Sodwana Bay), and they are associated with the same plant genus *Allophylus* (Sapindaceae), with *C. nigromaculata* also collected on *Searsia* (Anacardiaceae). Sapindaceae represents the first record of a host plant family other than Anacardiaceae. The two families belong to the same order Sapindales (The Angiosperm Phylogeny Group 2016), indicating a possible phylogenetically constrained host-use for *Calotheca*.

## Key to species of the *Calotheca nigromaculata* group

The three species are distinguishable mainly by the characters of the median lobe of the aedeagus. Females can be identified by evaluating the combination of: color pattern, which is consistent within *Calotheca carolineae* sp. nov. and *C. wanati* sp. nov. but variable in *C. nigromaculata*; pronotal shape; some biometric features, such as LAN/LB and WE/LE.

1 Apical part of the median lobe of the aedeagus widely rounded in ventral view, and not sinuate in lateral view (Fig. 1B). Pronotum straight laterally in basal 2/3 and abruptly incurved in the apical 1/3 (Fig. 1C). Dorsal integuments with clearly defined and generally larger elytral patches, reddish-brown on yellow surface (Fig. 1A). Antennae generally longer: LAN/LB > 0.45 in male and > 0.40 in female..... ***Calotheca carolineae* sp. nov.**

– Apical part of the median lobe of the aedeagus sub-rhomboidal, and sub-truncate apically in ventral view; clearly sinuate towards apex in lateral view (Figs 2F, 3B). Pronotum slightly curved laterally in basal 2/3 and more distinctly incurved

in the apical 1/3 (Figs 2D, 3C). Dorsal integument generally with smaller and more confused patches, from brown to black (Figs 2A–C, 3A). Antennae generally shorter: LAN/LB ≤ 0.45 in male and ≤ 0.40 in female ..... **2**

2 Median lobe of aedeagus shorter (LE/LAED > 2) (Fig. 4C), sub-rhomboidal apical 1/4 with prominent angulate lateral projections in ventral view; in lateral view, median lobe more distinctly curved apically (Fig. 3B). First pro- and metatarsomeres in male less enlarged, slightly larger than the distal part of the tibia. Female with more enlarged elytra (WE/LE generally > 0.74). Elytral patches quite small, irregular, light brown (Fig. 3A) ..... ***C. wanati* sp. nov.**

– Median lobe of aedeagus longer (LE/LAED ≤ 2) (Fig. 4C), sub-rhomboidal apical 1/4 with rounded, indistict or very indistinct lateral projections in ventral view; in lateral view, median lobe slightly curved apically (Fig. 2F). First pro- and metatarsomeres in male distinctly larger than the distal part of the tibia. Female with less enlarged elytra (WE/LE ≤ 0.74). Elytral patches variable in number, shape, and color, but generally larger or darker (Fig. 2A–C) ..... ..... ***C. nigromaculata* (Jacoby)**

## Conclusion

The genus *Calotheca* currently comprises 34 species, including the two new species here described. Diagnostic characters at species level, based on morphology, are mainly found on the median lobe of the aedeagus, the pronotum, and in the color of the dorsal integument. The identification of particular species groups relies mainly on the characteristics of the spermatheca and pronotum (D'Alessandro et al. 2020, 2021; Biondi unpublished data). Based on these characteristics *C. carolineae* sp. nov., *C. nigromaculata*, and *C. wanati* sp. nov. are here attributed to the *C. nigromaculata* species group. While the geographic distribution of the new species and the new distributional data of *C. nigromaculata* do not expand the geographic range of the genus, data on the association of the three species with the genus *Allophylus* (Sapindaceae) widen the range of its trophic spectrum, previously known as being limited to the family Anacardiaceae. However, due to the affinity between Anacardiaceae and Sapindaceae (The Angiosperm Phylogeny Group 2016), *Calotheca* species feeding on both the plant families cannot be considered as polyphagous.

## Acknowledgements

We are grateful to the collection managers and curators from the institutions listed above, who enabled us to study their material: Michael Balke (ZSM), Michael Geiser (NHMUK), Antoine Mantilleri (MNHN), Lukas Sekerka (NMPC), and Marek Wanat (UWCP).

## References

Bechyné J (1968) Contribution à la faune du Congo (Brazzaville). Mission A. Villiers et A. Descarpentries. LXXXI. Coléoptères Alticidae. Bulletin de l'Institut Français d'Afrique Noire (série A) 30: 1687–1728.

Biondi M, D'Alessandro P (2006) Biogeographical analysis of the flea beetle genus *Chaetocnema* in the Afrotropical Region: distribution patterns and areas of endemism. Journal of Biogeography 33: 720–730. https://doi.org/10.1111/j.1365–2699.2006.01446.x

Biondi M, D'Alessandro P (2008) Taxonomical revision of the *Longitarsus capensis* species-group: an example of Mediterranean-southern African disjunct distributions (Coleoptera: Chrysomelidae). European Journal of Entomology 105: 719–736. https://doi.org/10.14411/eje.2008.099

Biondi M, D'Alessandro P (2010a) Genus-group names of Afrotropical flea beetles (Coleoptera: Chrysomelidae: Alticinae): annotated catalogue and biogeographical notes. European Journal of Entomology 107: 401–424. https://doi.org/10.14411/eje.2010.049

Biondi M, D'Alessandro P (2010b) Revision of the Afrotropical flea beetle genus *Serraphula* Jacoby and description of *Bechynella*, a new genus from Western and Central Africa (Coleoptera: Chrysomelidae: Alticinae). Zootaxa 2444: 1–44. https://doi.org/10.11646/zootaxa.2444.1.1

Biondi M, D'Alessandro P (2012) Afrotropical flea beetle genera: a key to their identification, updated catalogue and biogeographical analysis (Coleoptera, Chrysomelidae, Galerucinae, Alticini). ZooKeys 253: 1–158. https://doi.org/10.3897/zookeys.253.3414

Biondi M, D'Alessandro P (2013a) *Ntaolaltica* and *Pseudophygasia*, two new flea beetle genera from Madagascar (Coleoptera: Chrysomelidae: Galerucinae: Alticini). Insect Systematics & Evolution 44: 93–106. https://doi.org/10.1163/1876312X-04401004

Biondi M, D'Alessandro P (2013b) The genus *Chabria* Jacoby: first records in the Afrotropical region with description of three new species from Madagascar and annotated worldwide species catalogue (Coleoptera, Chrysomelidae, Galerucinae, Alticini). Zoologischer Anzeiger 252: 88–100. https://doi.org/10.1016/j.jcz.2012.03.005

Biondi M, Frasca R, Grobbelaar E, D'Alessandro P (2017) Supraspecific taxonomy of the flea beetle genus *Blepharida* Chevrolat, 1836 (Coleoptera: Chrysomelidae) in the Afrotropical Region and description of *Afroblepharida* subgen. nov. Insect Systematics & Evolution 48: 97–155. https://doi.org/10.1163/1876312X-48022152

Biondi M, Iannella M, D'Alessandro P (2019) Unravelling the taxonomic assessment of an interesting new species from Socotra Island: *Blepharidina socotrana* sp. nov. (Coleoptera: Chrysomelidae). Acta Entomologica Musei Nationalis Pragae 59: 499–505. https://doi.org/10.2478/aemnp-2019-0040

D'Alessandro P, Samuelson A, Biondi M (2016) Taxonomic revision of the genus *Arsipoda* Erichson, 1842 (Coleoptera, Chrysomelidae) in New Caledonia. European Journal of Taxonomy 230: 1–61. https://doi.org/10.5852/ejt.2016.230

D'Alessandro P, Iannella M, Frasca R, Biondi M (2018a) Distribution patterns and habitat preference for the genera-group *Blepharida* s.l. in Sub-Saharan Africa (Coleoptera: Chrysomelidae: Galerucinae: Alticini). Zoologischer Anzeiger 277: 23–32. https://doi.org/10.1016/j.jcz.2018.08.001

D'Alessandro P, Frasca R, Grobbelaar E, Iannella M, Biondi M (2018b) Systematics and biogeography of the Afrotropical flea beetle subgenus *Blepharidina* (*Afroblepharida*) Biondi & D'Alessandro, with description of seven new species (Coleoptera, Chrysomelidae, Galerucinae, Alticini). Insect Systematics & Evolution 49: 443–480. https://doi.org/10.1163/1876312X-00002182

D'Alessandro P, Iannella M, Biondi M (2019) Revision of the Afrotropical flea beetle subgenus *Blepharidina* s. str. Bechyné (Coleoptera, Chrysomelidae). Zootaxa 4545: 32–60. https://doi.org/10.11646/zootaxa.4545.1.2

D'Alessandro P, Iannella M, Grobbelaar E, Biondi M (2020) Revision of the *Calotheca nigrotessellata* species group from southern Africa, with description of two new species (Coleoptera: Chrysomelidae, Galerucinae, Alticini). Fragmenta Entomologica 52: 169–182. https://doi.org/10.4081/fe.2020.457

D'Alessandro P, Iannella M, Grobbelaar E, Biondi M (2021) Taxonomic revision of the *Calotheca parvula* species group from southern Africa, with descriptions of three new species (Coleoptera, Chrysomelidae). African Invertebrates 62(1): 315–337. https://doi.org/10.3897/AfrInvertebr.62.62426

Evenhuis NL (2021) The insect and spider collections of the world website. http://hbs.bishopmuseum.org/codens/ [accessed 25 July 2020]

Forster JR (1771) Novae Species Insectorum. Centuria I. Davies and White, London, [viii +] 100 pp. https://doi.org/10.5962/bhl.title.152194

Heyden von L (1887) Kleine coleopterologische Mitteilungen. Wiener Entomologische Zeitung 6: e98. https://doi.org/10.5962/bhl.part.17738

Iannella M, D'Alessandro P, De Simone W, Biondi M (2021) Habitat specificity, host plants and areas of endemism for the genera-group *Blepharida* s.l. in the Afrotropical Region (Coleoptera, Chrysomelidae, Galerucinae, Alticini). Insects 12(299): 1–16. https://doi.org/10.3390/insects12040299

Jacoby M (1888) Descriptions of new or little-known species of phytophagous Coleoptera from Africa and Madagascar. Transactions of the Entomological Society of London 1888: 189–206. https://doi.org/10.1111/j.1365-2311.1888.tb01308.x

Moffett RO (2007) Name changes in the Old World *Rhus* and recognition of *Searsia* (Anacardiaceae). Bothalia 37(2): 165–175.

The Angiosperm Phylogeny Group (2016) An update of the Angiosperm Phylogeny Group classification for the orders and families of flowering plants: APG IV. Botanical Journal of the Linnean Society 181: 1–20. https://doi.org/10.1111/boj.12385

ZooKeys 1084: 139–150 (2022)
doi: 10.3897/zookeys.1084.78664
https://zookeys.pensoft.net

RESEARCH ARTICLE

A peer-reviewed open-access journal
ZooKeys
Launched to accelerate biodiversity research

# Mini-exon gene reveals circulation of TcI *Trypanosoma cruzi* (Chagas, 1909) (Kinetoplastida, Trypanosomatidae) in bats and small mammals in an ecological reserve in southeastern Mexico

Eliza F. Gómez-Sánchez[1], Héctor Ochoa-Díaz-López[2], Eduardo E. Espinoza-Medinilla[1], D. Daniel Velázquez-Ramírez[2], Nancy G. Santos-Hernández[1], Christian Ruiz-Castillejos[1], Dolores G. Vidal-López[3], Adriana Moreno-Rodríguez[4], Any Laura Flores-Villegas[5], Eduardo López-Argueta[1], José A. De Fuentes-Vicente[1]

**1** *Laboratorio de Investigación y Diagnóstico Molecular, Instituto de Ciencias Biológicas, Universidad de Ciencias y Artes de Chiapas, Tuxtla Gutierrez, Mexico* **2** *Departamento de Salud, El Colegio de la Frontera Sur, Tuxtla Gutierrez, Chiapas, Mexico* **3** *Laboratorio Multidisciplinario Experimental y Bioterio, Instituto de Ciencias Biológicas, Universidad de Ciencias y Artes de Chiapas, Tuxtla Gutierrez, Mexico* **4** *Laboratorio 16, Facultad de Ciencias Químicas, Universidad Autónoma Benito Juárez de Oaxaca, Oaxaca, Mexico* **5** *Laboratorio de Biología de Parásitos, Facultad de Medicina, Universidad Nacional Autónoma de Mexico, Ciudad de México, Mexico*

Corresponding authors: José A. De Fuentes-Vicente (jose.defuentes@unicach.mx), Nancy G. Santos-Hernández (nancy.santos@unicach.mx)

Academic editor: Jader Oliveira | Received 1 December 2021 | Accepted 14 January 2022 | Published 28 January 2022

*http://zoobank.org/0F466EA7-AC18-4268-AF7D-8F7925341282*

**Citation:** Gómez-Sánchez EF, Ochoa-Díaz-López H, Espinoza-Medinilla EE, Velázquez-Ramírez DD, Santos-Hernández NG, Ruiz-Castillejos C, Vidal-López DG, Moreno-Rodríguez A, Flores-Villegas AL, López-Argueta E, De Fuentes-Vicente JA (2022) Mini-exon gene reveals circulation of TcI *Trypanosoma cruzi* (Chagas, 1909) (Kinetoplastida, Trypanosomatidae) in bats and small mammals in an ecological reserve in southeastern Mexico. ZooKeys 1084: 139–150. https://doi.org/10.3897/zookeys.1084.78664

## Abstract

A wide variety of mammals are involved in the sylvatic cycle of *Trypanosoma cruzi*, the causative agent of Chagas disease. In many areas in Latin America where *T. cruzi* is endemic, this cycle is poorly known, and its main reservoirs have not been identified. In this study we analyzed *T. cruzi* infection in bats and other small mammals from an Ecological Reserve in southeastern Mexico. From January through March 2021, we captured wild individuals to extract cardiac and peripheral blood, and infection was detected by PCR of the mini-exon gene. In bats, the prevalence of infection was 16.36%, while in small mammals the prevalence was 28.57%. All of the samples that were positive for *T. cruzi* were identified as the

TCI genotype. Our findings suggest that this zone, situated at the periphery of urban zones might have epidemiological relevance in the sylvatic cycle of *T. cruzi* and needs to be monitored. The infection of bats in this area is particularly concerning since the flight pattern of this populations overlaps with human settlements. Despite being subject to conservation protections, there continue to be anthropogenic actions that disturb the study area, which could exacerbate risks to public health.

**Keywords**
Chagas disease, molecular epidemiology, reservoirs, sylvatic cycle

## Introduction

The protozoan *Trypanosoma cruzi* (Chagas, 1909) (Kinetoplastida, Trypanosomatidae) is the causative agent of Chagas disease, a neglected tropical infection affecting ~6 million people (Krats 2019). This disease typically occurs in rural areas of Central and South America, but urban areas are not exempt. In humans, chronic *T. cruzi* infection leads to heart failure and death in 20–30% of infected patients (WHO 2014; Krats 2019). Chagas disease is difficult to diagnosis, and only two drugs, Nifurtimox and Benznidazole, are currently available to treat it, both of which have severe side effects (Vallejo et al. 2020).

*Trypanosoma cruzi* exhibits high genetic variability and has recently been classified into six discrete typing units (DTUs; TCI–TCVI) and an additional unit named TC Bat (see Zingales et al. 2018). Under natural conditions, *T. cruzi* is transmitted by blood-sucking insects of the subfamily Triatominae (Hemiptera, Reduviidae) known as kissing bugs (De Fuentes-Vicente and Gutiérrez-Cabrera 2020). *Trypanosoma cruzi* transmission cycles are well defined into domestic, peridomestic, and sylvatic cycles, each with epidemiological and ecological differences. The domestic and peridomestic cycles involve humans, pets (dogs and cats), and farmyard animals. In sylvatic cycles in wild habitats, marsupials, edentates, and rodents are important reservoirs, but *T. cruzi* can infect more than 100 different species of wild mammals (Noireau et al. 2009; Alvarado-Otegui et al. 2012). This heterogeneity suggests a highly variable ecology of *T. cruzi*, and each area may have a unique set of conditions underlying the occurrence of the parasite (Moreira-Alves et al. 2016).

Historically, the domestic and peridomestic cycles have been the most studied, and little is known about the sylvatic cycle, especially in the southeastern region of Mexico (e.g., Jimenez-Coello et al. 2012). The climatic and biodiversity conditions of this region, in addition to poverty and marginalization, create scenarios for increased occurrence of Chagas disease (see Cruz-Reyes and Pickering-López 2006). In the current study, we sought to determine the infection by *T. cruzi* in wild mammals from the "El Zapotal" Ecological Reserve using multiplex PCR amplification of the mini-exon gene. "El Zapotal" is located in the state of Chiapas in southeastern Mexico, and we believe that this area may have epidemiological importance in the sylvatic cycle of *T. cruzi* in the region and that the proximity of human settlements may make it relevant to public health. In fact, the circulation of *T. cruzi* in small mammals in this area has previously been reported (Domínguez-Vázquez et al. 1990; Solís-Franco et al. 1997; Camacho-

Sierra 2016). In addition, this area has high bat species richness, including synanthropic species (Velazquez-Pérez et al. 2010; López-Argueta 2021). Although bats have played a key role in the evolution of *T. cruzi* (Hamilton et al. 2012), their importance in the transmission dynamics has been poorly studied in many regions.

Although "El Zapotal" is subject to conservation protections, anthropogenic actions may have already caused irreversible damage (Fernández-Moreno 2010). Large-scale changes in land use and habitat fragmentation can affect wild transmission cycles of *T. cruzi* (Vaz et al. 2007), mostly because habitat loss restricts the area and food resources available to wild mammals, which can increase their contact with humans. All these factors support the need to conduct new studies to better understand the dynamics of *T. cruzi* transmission in wild ecotopes.

## Methods

### Study site

The "El Zapotal" Ecological Reserve, decreed as an Ecological and Recreational Park, is located 2 km southeast of Tuxtla Gutiérrez, Chiapas (Fig. 1). It is a natural protected area measuring approximately 200 ha. The geology is largely karstic,

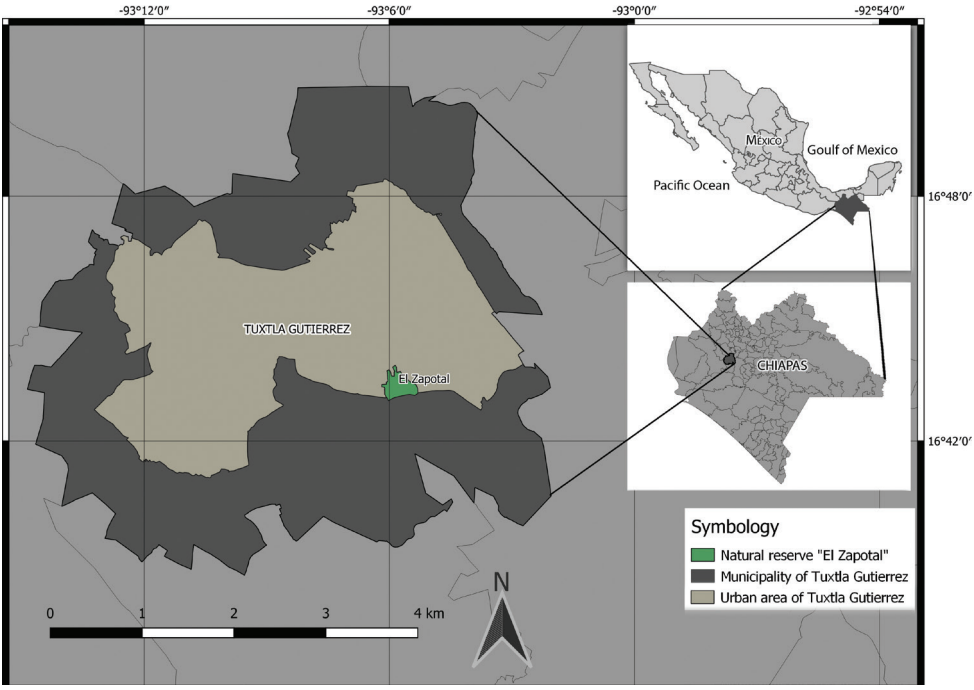


**Figure 1.** Location of the "El Zapotal" Ecological Reserve in southeastern Mexico, note the border of the reserve with the urban area.

with abundant caves and springs. The altitudinal range is from 600 to 850 m above sea level and the vegetation is medium sub-evergreen forest and low deciduous forest.

## Mammal capture and blood sampling

Wild mammals were captured from January through March 2021 in areas of the "El Zapotal" Ecological Reserve near bodies of water and fruit trees. To capture bats, we deployed three 12 × 2.5 m mist nets from dusk to dawn (eight sampling hours per net) for five consecutive nights. The captured specimens were deposited in canvas bags for identification and blood sampling. The identification was performed as described by Díaz (2021). Meanwhile, the blood sample was obtained by intracardiac puncture (100 µL) and deposited in microcentrifuge tubes with 500 µL 3.8% sodium citrate pH 7.2 for their transportation to the laboratory. Finally, the bats were marked on the wings with ink and released on site.

For the capture of smalls mammals 20 Tomahawk type traps and 15 Sherman traps were used (Romero-Almaraz et al. 2000). As bait, a mixture of oats with vanilla extract was used. The traps were set at dusk and removed eight hours later for five nights. Captured individuals were marked and identified as described by Reid (2009), and a blood sample was taken by puncture in the tail vein, after disinfecting the area with 70% alcohol. The samples obtained (100 µL) were treated as mentioned above.

## Bioethical guidelines

Animal handling was carried out in accordance with the provisions of Mexican Animal Welfare Law. The capture of animals was approved by the Mexican Secretariat of the Environment and Natural Resources (Secretaría de Medio Ambiente y Recursos Naturales, SEMARNAT (minute 07 / K6-0095 / 10/189)). No individuals were sacrificed or removed from the site.

## Extraction of DNA and mini-exon gene amplification

Total DNA was extracted using a modified phenol-chloroform isoamyl alcohol protocol (Espinoza and García 2003). For the amplification of the mini-exon gene, we used a pool of three oligonucleotides reported by Souto et al. (1996): [5'-GTGTCCGCCACCTCCTTCGGGCC (TCI, group 1-specific), 5'-CCTGCAGGCACACGTGTGTGTG (TCII, group 2-specific), and 5'-CCCCCCTCCCAGGCCAC ACTG (TC, common to groups TCI and TCI)]. We used the previously characterized strains Querétaro (TCI) and strain Y (TCII), which amplify at 350 and 300 base pairs (bp), respectively, as controls (Espinoza et al. 2010). Amplification reactions were performed in a final volume of 25 µL, containing 12 µL of Go Taq Green Master Mix 2X, 10 µL of nuclease-free water, 0.4 µM of each primer, and 20 ng of Trypanosoma DNA. Cycle amplification was performed using a MyGene MG96G thermal cycler (Hangzhou

LongGene Scientific Instruments Co. Ltd, Hangzhou, China) under the following conditions: 5 min at 94 °C, followed by 27 cycles of 40 s at 94 °C, 40 s at 61 °C, and 1 min at 72 °C, and a final elongation of 5 min at 72 °C. Amplified products were visualized on 2% W/V agarose gels stained with ethidium bromide under UV light.

## Results

A total of 152 mammals were captured: 110 bats and 42 small mammals. Among bats, eight species were identified, and *Artibeus jamaicensis* Leach, 1821 (Chiroptera, Phyllostomidae) was the most common species. Only two hematophagous individuals (*Desmodus rotundus* É. Geoffroy, 1810) (Phyllostomidae) were captured. We captured four species of small mammals, of which *Didelphis marsupialis* Linnaeus, 1758 (Didelphimorphia, Didelphidae) was the most common (Table 1).

**Table 1.** Bats and smalls mammals captured in "El Zapotal" ecological reserve and infected individuals.

| **Bats** | | | |
|---|---|---|---|
| **Family** | **Species** | **# individuals** | **Infected indivuals (% prevalence)** |
| Phyllostomidae | *Artibeus jamaicensis* | 64 | 10 (15.6) |
| | *Artibeus lituratus* | 16 | 3 (18.7) |
| | *Sturnira lillium* | 3 | 2 (66.6) |
| | *Centurio senex* | 2 | 0 |
| | *Leptonycteris yebabuenae* | 2 | 0 |
| | *Carollia perspicillata* | 7 | 2 (28.5) |
| | *Desmodus rotundus* | 2 | 0 |
| | *Glossophaga soricina* | 8 | 1 (12.5) |
| | *Pteronotus davyi* | 1 | 0 |
| Mormoopidae | *Pteronotus parnelli* | 3 | 0 |
| | *Mormoops megallophyla* | 2 | 0 |
| **Total** | | **110** | **18 (16.3)** |
| **Small mammals** | | | |
| Didelphidae | *Didelphis marsupialis* | 18 | 6 (33.3) |
| Cricetidae | *Peromyscus mexicanus* | 7 | 4 (57.1) |
| Heteromyidae | *Heteromys desmarestianus* | 10 | 1 (10) |
| Dasyproctidae | *Dasyprocta mexicana* | 7 | 1 (14.2) |
| **Total** | | **42** | **12 (28.5)** |

Of the total bat samples examined, 18 were positive for *T. cruzi* infection (16.36%). *Sturnira lilium* É. Geoffroy, 1810 had the highest prevalence among the bat species (66.6%), though only three individuals were captured. Meanwhile, the most commonly captured bat species, *A. jamaicensis*, had a prevalence of 15.62% (10/64) (Table 1). All PCR products amplified at 350 bp, indicating that they belonged to the TCI group (Fig. 2).

For smalls mammals there was an overall prevalence of 28.57% (12/42), when combining all four mammal species. *Peromyscus mexicanus* (Saussure, 1860) (Rodentia,

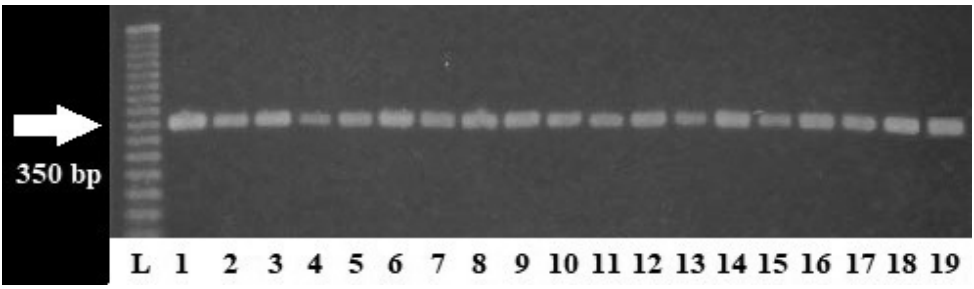


**Figure 2.** PCR products of the mini-exon gene in blood of bats from the "El Zapotal" Ecological Reserve. Amplification resulted in a PCR product of 350 bp and this confirms that these parasites belong to the TCI group. L: Ladder; Samples: 1 positive control (Qro. strain); 2–11 *A. jamaicensis*; 12–14 *A. lituratus*; 15–16 *C. perspicillata*; 17–18 *S. lilium*; 19 *G. soricina*.

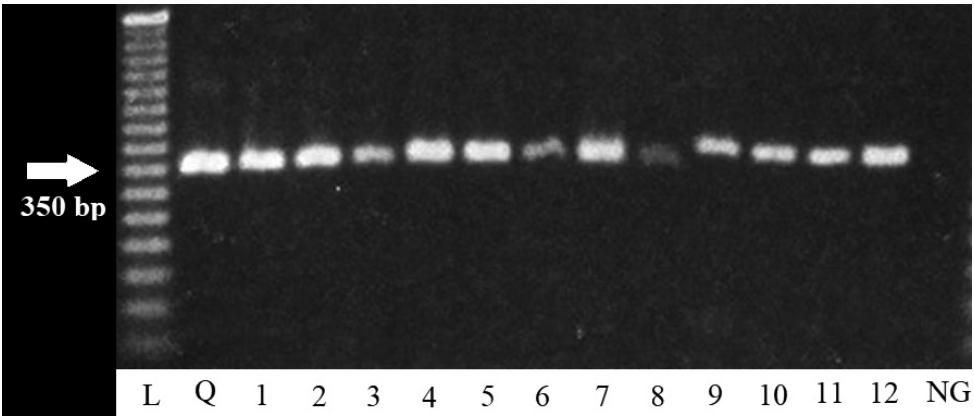


**Figure 3.** PCR products of the mini-exon gene in blood of smalls mammals from the "El Zapotal" Ecological Reserve. Amplification resulted in a PCR product of 350 bp and this confirms that these parasites belong to the TCI group. L: ladder; samples: Q positive control (Qro. strain); 1–6 *D. marsupialis*; 7–10 *P. mexicanus*; 11 *H. desmarestianus*; 12 *D. mexicana*.

Cricetidae) presented the highest prevalence with 57.14% (4/7), while the most commonly captured species, *D. marsupialis*, had a prevalence of 33.33% (6/18) (Table 1). Here too, all PCR products amplified at 350 bp indicating the TCI group of *T. cruzi* (Fig. 3).

## Discussion

We show evidence of the circulation of *T. cruzi* in wild mammals from an ecological reserve in southeastern Mexico. Although other studies have demonstrated the presence of the parasite in small mammals from "El Zapotal" (Domínguez-Vázquez et al. 1990; Solís-Franco et al. 1997; Camacho-Sierra 2016), the present study is the first to report infection in bats. TCI was the only genetic group detected. This genetic group is

the most prevalent in Mexico (Bosseno et al. 2002; Dorn et al. 2017) and is associated with *Triatoma dimidiata* Latreille, 1811 (Hemiptera, Triatominae), the main *T. cruzi* vector in Central and North America (López-Cancino et al. 2015). Some *T. cruzi* genotypes have close evolutionary relationships with specific triatomine species, possibly favoring parasite transmission (De Fuentes-Vicente et al. 2019).

Overall, the prevalence of *T. cruzi* infection was 19.73% in all captured individuals (30/152). The overall infection prevalence in small mammals (28.57%) was similar to previous findings in a recent study (26.66%) in the same area (Camacho-Sierra 2016) and higher than in bats. We found a higher prevalence of infection in *P. mexicanus* (Mexican mouse) than in *D. marsupialis* (common opossum). The fact that small rodents are an important food source for several predators could maintain the transmission of *T. cruzi* among mammals through predation. In addition, vertical or congenital transmission has been demonstrated in these animals (Alarcón et al. 2009). Other studies in southern Mexico have also reported high prevalence of *T. cruzi* circulation in terrestrial mammals (e.g., Ruiz-Piña and Cruz-Reyes 2002; Martínez-Hernández et al. 2014), including in livestock (sheep, pigs, and horses) and urban and rural dogs in Yucatán (Jiménez-Coello et al. 2008; Ruiz-Piña et al. 2018).

To date, it is largely unknown how the sylvatic cycle interacts with the peridomestic and domestic cycles, but it is inferred that some synanthropic animals may be the link between them. For example, some synanthropic rodents captured in Yucatán have shown histological lesions associated with *T. cruzi* infection (Torres-Castro et al. 2016; Ucan-Euan et al. 2019). "El Zapotal" is surrounded by urbanized human settlements, and infected rodents might represent a public health risk due to their ability to invade and colonize human dwellings, where they could interact with domestic animals and parasite transmission could occur. For example, in the neighboring city of Tuxtla Gutiérrez, a prevalence of 4.5% of *T. cruzi* infection in stray dogs has been reported (Jiménez-Coello et al. 2010), and recently the first report of an infected triatomine bug in the urban area was published (De Fuentes-Vicente et al. 2020).

In Mexico, the dynamics of *T. cruzi* in bats in the sylvatic cycle has been little studied, even though bats have wide distributions that may overlap with urbanized environments (Krauel and Lee Buhn 2016), as occurs in the populations analyzed here (López-Argueta 2022). The synanthropic condition of bats has made them the transmitters of several pathogens including Ebola virus, rabies, and hantaviruses (Calisher et al. 2006; Kasso and Balakrishnan 2013). Currently, they are the focus of increased attention because of their possible relationship with the origin of the novel SARS-COV-2 coronavirus that causes COVID-19 (Lau et al. 2020; Córdoba-Aguilar et al. 2021). In particular, bats play a role of interest in the evolution of *T. cruzi* because, according to some hypotheses, *T. cruzi* evolved from a larger clade of bat trypanosomes (Hamilton et al. 2012). The importance of bats as reservoirs of *T. cruzi* may be enhanced by their ability to fly, gregarious social structure, and longevity (Luis et al. 2013). In bats, we found a prevalence of infection of 16.36%, a value much higher than that found in the only previous study in Chiapas, which sampled bats from the Selva Lacandona (1.60%) (Víquez-Rodríguez 2015). Interestingly, they reported a higher prevalence of

infection by *Leishmania mexicana* in the same individuals (8.84%) and only one bat infected by both (Víquez-Rodríguez 2015). Although bats are known to be associated with a wide range of zoonotic pathogens, the effects of competition between parasites in the same reservoir remains virtually unknown (Bashey 2015).

High prevalence of *T. cruzi* infection in bats have been previously reported in southern Mexico: Torres-Castro et al. (2021) reported a 30.2% prevalence of infection in bats from Campeche and Yucatan, mostly in non-hematophagous species. We only collected two hematophagous individuals (*D. rotundus*), neither of which was infected. Non-hematophagous species may acquire the parasite by ingesting infected insects or by vector transmission, but we did not find any triatomine insects at the study sites. Vertical transmission of *T. cruzi* has also been demonstrated in bats (Añez et al. 2009), so this mechanism may also favor the permanence of the parasite in these animals. Another interesting fact in this group is that *T. cruzi* was detected in the salivary glands of a hematophagous bat specimen in Peru (Villena et al. 2018), suggesting that the importance of bats in the dynamics of *T. cruzi* may be greater than previously thought, since they may be able to transmit the parasite directly through biting.

Maintaining biodiversity has been shown to be an important – if not the most important – action to prevent the spread of zoonotic parasites (Córdoba-Aguilar et al. 2021), and *T. cruzi* is no exception (Keesing and Ostfeld 2021). As such, we must continue to explore how ecosystem fragmentation affects sylvatic transmission cycles of *T. cruzi*, a topic which is further complicated by heterogeneity in the reservoirs, vectors, and genetic structure of the parasites. Further studies of all of these topics are necessary in order to construct effective interventions that prevent the sylvatic cycle from connecting with the peridomestic or domestic cycle and further exposing humans. Finally, future research should emphasize the role of bats in the dynamics of *T. cruzi* to determine their role in the epidemiology of Chagas disease and to inform health authorities about this potential danger.

## Acknowledgements

We thank the Miguel Alvarez del Toro Zoo (ZOOMAT) for its support in the logistics of animal captures. Funding for our study was contributed by the Consejo Nacional de Ciencia y Tecnología (CONACyT) (SEP-CONACYT A1-S-47901). We are grateful to the reviewers and academic editor for their comments.

## References

Alarcón M, Pérez MC, Villarreal J, Araujo S, Goncalves L, González A, Lugo-Yarbuh A (2009) Detección de ADN de *Trypanosoma cruzi* en la placenta y fetos de ratones con infección chagásica aguda. Investigación Clínica 50: 335–345.

Alvarado-Otegui JA, Ceballos LA, Orozco MM, Enriquez GF, Cardinal MV, Cura C, Schijman AG, Kitron U, Gurtler RE (2012) The sylvatic transmission cycle of *Trypanosoma cruzi* in a rural area in the humid Chaco of Argentina. Acta Tropica 124: 79–86. https://doi.org/10.1016/j.actatropica.2012.06.010

Añez N, Crisante G, Soriano PJ (2009) *Trypanosoma cruzi* congenital transmission in wild bats. Acta Tropica 109: 78–80. https://doi.org/10.1016/j.actatropica.2008.08.009

Bashey F (2015) Within-host competitive interactions as a mechanism for the maintenance of parasite diversity. Philosophical Transactions of the Royal Society B 370(1675): e20140301. https://doi.org/10.1098/rstb.2014.0301

Bosseno M, Barnabe C, Magallón E, Lozano F, Ramsey J, Espinoza B, Frédérique S (2002) Predominance of *Trypanosoma cruzi* Lineage I in México. Journal of Clinical Microbiology 40: 627–632. https://doi.org/10.1128/JCM.40.2.627-632.2002

Calisher CH, Childs JE, Field HE, Holmes KV, Schountz T (2006) Bats: important reservoir hosts of emerging viruses. Clinical Microbiology Reviews 19: 531–545. https://doi.org/10.1128/CMR.00017-06

Camacho-Sierra V (2016) Identificación de unidades discretas de tipificación (DTU's) de *Trypanosoma cruzi* en marsupiales (*Didelphis marsupialis*, *Didelphis virginianus*, *Philander oposum*) presentes en la Reserva Ecológica "El Zapotal" en el estado de Chiapas. Master's thesis, Universidad Autónoma del estado de México, México.

Córdoba-Aguilar A, Ibarra-Cerdeña CN, Castro-Arellano I, Suzan G (2021) Tackling zoonoses in a crowded world: lessons to be learned from the COVID-19 pandemic. Acta Tropica 214: 105780. https://doi.org/10.1016/j.actatropica.2020.105780

Cruz-Reyes A, Pickering-López JM (2006) Chagas disease in Mexico: an analysis of geographical distribution during the past 76 years—a review. Memorias do Instituto Oswaldo Cruz 101: 345–354. https://doi.org/10.1590/S0074-02762006000400001

De Fuentes-Vicente JA, Gómez-Gómez A, Santos-Hernández NG, Ruiz-Castillejos C, Gómez-Sánchez EF, Vidal-López DG, Flores-Villegas L, Gutiérrez-Jiménez J, Moreno-Rodríguez A (2021) First report of an infected triatomine bug in an urban area of Tuxtla Gutierrez, Chiapas, México. Biocyt: Biología, Ciencia y Tecnología 14: 1009–1020.

De Fuentes-Vicente JA, Gutiérrez-Cabrera AE (2020) Kissing bugs (triatominae). References Module in Biomedical Sciences. Elsevier. https://doi.org/10.1016/B978-0-12-818731-9.00010-0

De Fuentes-Vicente JA, Vidal-López DG, Flores-Villegas AL, Moreno-Rodríguez A, De Alba-Alvarado MC, Salazar-Schettino PM, Gutiérrez-Cabrera AE (2019) *Trypanosoma cruzi*: a review of biological and methodological factors in Mexican strains. Acta Tropica 195: 51–57. https://doi.org/10.1016/j.actatropica.2019.04.024

Díaz M, Solari S, Gregorin R, Aguirre L, Barquez R (2021) Clave de identificación de los murciélagos neotropicales. Primera edición. Ed Programa de Conservación de los Murciélagos de Argentina, Tucumán, 211 pp.

Domínguez A, Ricárdez J, Espinoza E (1990) Study of *Trypanosoma cruzi* in wild reservoirs in the ecological reserve of El Zapotal, Chiapas, México. Boletín Chileno de Parasitología 45: 3–8.

Dorn PL, McClure AG, Gallaspy MD, Waleckx E, Woods AS, Monroy M, Stevens L (2017) The diversity of the Chagas parasite, *Trypanosoma cruzi*, infecting the main Central American vector, *Triatoma dimidiata*, from Mexico to Colombia. PLoS Neglected Tropical Diseases 11: e0005878. https://doi.org/10.1371/journal.pntd.0005878

Espinoza B, Rico T, Sosa S, Oaxaca E, Vizcaino-Castillo A, Caballero ML, Satoskar AR (2010) Mexican *Trypanosoma cruz*i (TCI) strains with different degrees of virulence induce diverse humoral and cellular immune responses in a murine experimental infection model. Journal of Biomedicine and Biotechnology 2010: e890672. https://doi.org/10.1155/2010/890672

Espinoza E, García E (2003) Manual de laboratorio de genética. ECOSUR-San Cristóbal de las Casas. El Colegio de la Frontera Sur, Tapachula, 37 pp.

Fernández-Moreno Y (2010) Percepciones ambientales sobre una Reserva Ecológica Urbana, El Zapotal, Tuxtla Gutiérrez, Chiapas. El Colegio de la Frontera Sur, San Cristóbal de las Casas, 170 pp.

Hamilton PB, Teixeira MM, Stevens JR (2012) The evolution of *Trypanosoma cruzi*: the 'bat seeding' hypothesis. Trends in Parasitology 28: 136–141. https://doi.org/10.1016/j.pt.2012.01.006

Jiménez-Coello M, Acosta-Viana KY, Guzman-Marin E, Gomez-Rios A, Ortega-Pacheco A (2012) Epidemiological survey of *Trypanosoma cruzi* infection in domestic owned cats from the tropical southeast of Mexico. Zoonoses Public Health 59: 102–109. https://doi.org/10.1111/j.1863-2378.2012.01463.x

Jimenez-Coello M, Ortega-Pacheco A, Guzman-Marin E, Guiris-Andrade DM, Martinez-Figueroa L, Acosta-Viana KY (2010) Stray dogs as reservoirs of the zoonotic agents *Leptospira interrogans*, *Trypanosoma cruzi*, and *Aspergillus* spp. in an urban area of Chiapas in southern Mexico. Vector-borne and Zoonotic Diseases 10: 135–141. https://doi.org/10.1089/vbz.2008.0170

Jimenez-Coello M, Poot-Cob M, Ortega-Pacheco A, Guzman-Marin E, Ramos-Ligonio A, Sauri-Arceo C, Acosta-Viana K (2008) American trypanosomiasis in dogs from an urban and rural Area of Yucatan, Mexico. Vector-Borne and Zoonotic Diseases 10: 755–762. https://doi.org/10.1089/vbz.2007.0224

Kasso M, Balakrishnan M (2013) Ecological and economic importance of bats (order Chiroptera). International Scholarly Research Notices 2013: e187415. https://doi.org/10.1155/2013/187415

Keesing F, Ostfeld R (2021) Impacts of biodiversity and biodiversity loss on zoonotic diseases. Proceedings of the National Academy of Sciences of the United States of America 118: e2023540118. https://doi.org/10.1073/pnas.2023540118

Kratz JM (2019) Drug discovery for chagas disease: a viewpoint. Acta Tropica 198: 105107. https://doi.org/10.1016/j.actatropica.2019.105107

Krauel JJ, LeBuhn G (2016) Patterns of bat distribution and foraging activity in a highly urbanized temperate environment. PLoS ONE 11(12): e0168927. https://doi.org/10.1371/journal.pone.0168927

Lau SKP, Luk HKH, Wong ACP, Li KSM, Zhu L, He Z, Fung J, Chan TTY, Fung KSC, Woo PCY (2020) Possible bat origin of Severe Acute Respiratory Syndrome Coronavirus 2. Emerging Infectious Diseases 26: 1542–1547. https://doi.org/10.3201/eid2607.200092

López-Argueta E (2022) Diversidad y gremios alimenticios de los murciélagos en el ambiente urbano de Tuxtla Gutiérrez, Chiapas. Bachelor's thesis, Universidad de Ciencias y Artes de Chiapas, México.

López-Cancino SA, Tun-Ku E, De la Cruz-Felix HK, Ibarra-Cerdeña CN, Izeta-Alberdi A, Pech-May A, Mazariegos-Hidalgo CJ, Valdez-Tah A, Ramsey JM (2015) Landscape ecology of *Trypanosoma cruzi* in the southern Yucatan Peninsula. Acta Tropica 151: 58–72. https://doi.org/10.1016/j.actatropica.2015.07.021

Luis AD, Hayman DT, O'Shea TJ, Cryan PM, Gilbert AT, Pulliam JR, Webb CT (2013) A comparison of bats and rodents as reservoirs of zoonotic viruses: are bats special? Proceedings of the Royal Society B: Biological Sciences 280: e20122753. https://doi.org/10.1098/rspb.2012.2753

Martínez-Hernández F, Rendon-Franco E, Gama-Campillo L, Villanueva-García C, Romero-Valdovinos M, Maravilla P, Villalobos G (2014) Follow up of natural infection with *Trypanosoma cruzi* in two mammals species, *Nasua narica* and *Procyon lotor* (Carnivora: Procyonidae): evidence of infection control? Parasites & Vectors 7: e405. https://doi.org/10.1186/1756-3305-7-405

Moreira-Alves F, De Lima JS, Rocha FL, Herrera HM, Mourao GD, Jansen AM (2016) Complexity and multi-factoriality of *Trypanosoma cruzi* sylvatic cycle in coatis, *Nasua nasua* (Procyonidae), and triatomine bugs in the Brazilian Pantanal. Parasites & Vectors 9: e378. https://doi.org/10.1186/s13071-016-1649-4

Noireau F, Diosque P, Jansen AM (2009) *Trypanosoma cruzi*: adaptation to its vectors and its hosts. Veterinary Research 40: e26. https://doi.org/10.1051/vetres/2009009

Reid F (2009) A Field Guide of the Mammals of Central America and Southeast México, Second Edition. Oxford University Press, New York, 238 pp.

Romero-Almaraz ML, Sánchez-Hernández C, García-Estrada C, Owen RD (2000) Mamíferos pequeños: manual de técnicas de captura, preparación, preservación y estudio. Editorial Las prensas de ciencias UNAM, México, 324 pp.

Ruiz-Piña HA, Cruz-Reyes A (2002) The opossum *Didelphis virginiana* as a synanthropic reservoir of *Trypanosoma cruzi* in Dzidzilché, Yucatán, México. Memórias do Instituto Oswaldo Cruz 97: 613–620. https://doi.org/10.1590/S0074-02762002000500003

Ruiz-Piña HA, Gutiérrez-Ruiz E, Escobedo-Ortegón FJ, Rodríguez-Vivas RI, Bolio-González M, Ucan-Leal D (2018) Prevalence of *Trypanosoma cruzi* in backyard mammals from a rural community of Yucatan, Mexico. Tropical and Subtropical Agroecosystems 21: 367–371.

Solís-Franco R, Romo-Zapata A, Martínez-Ibarra J (1997) Wild reservoirs infected by *Trypanosoma cruzi* in the ecological park "El Zapotal", Tuxtla Gutiérrez, Chiapas, México. Memorias do Instituto Oswaldo Cruz 92: 163–164. https://doi.org/10.1590/S0074-02761997000200006

Souto RP, Fernandes O, Macedo AM, Campbell DA, Zingales B (1996) DNA markers define two major phylogenetic lineages of *Trypanosoma cruzi*. Molecular and Biochemical Parasitology 83: 141–152. https://doi.org/10.1016/S0166-6851(96)02755-7

Torres-Castro M, Cuevas-Koh N, Hernández-Betancourt S, Noh-Pech H, Estrella E, Herrera-Flores B, Peláez-Sánchez R (2021) Natural infection with *Trypanosoma cruzi* in bats captured in Campeche and Yucatán, México. Biomédica 41: 131–140. https://doi.org/10.7705/biomedica.5450

Torres-Castro M, Hernández-Betancourt S, Puerto FI, Torres-León M (2016) Lesiones histológicas asociadas a la posible infección por *Trypanosoma cruzi* (Chagas, 1909) en corazones de roedores sinantrópicos capturados en Yucatán, México. Anales de Biología 38: 29–35. https://doi.org/10.6018/analesbio.38.03

Ucan-Euan F, Hernández-Betancourt S, Arjona-Torres M, Panti-May A, Torres-Castro M (2019) Estudio histopatológico de tejido cardiaco de roedores infectados con *Trypanosoma cruzi* capturados en barrios suburbanos de Mérida, México. Biomédica 39: 32–43. https://doi.org/10.7705/biomedica.v39i3.4192

Vallejo M, Reyes PP, García MM, Garay AG (2020) Trypanocidal drugs for late-stage, symptomatic Chagas disease (*Trypanosoma cruzi* infection). Cochrane Database of Systematic Reviews 12: CD004102. https://doi.org/10.1002/14651858.CD004102.pub3

Vaz VC, D'Andrea PS, Jansen AM (2007) Effects of habitat fragmentation on wild mammal infection by *Trypanosoma cruzi*. Parasitology 134: 1785–1793. https://doi.org/10.1017/S003118200700323X

Vázquez-Pérez EU, Roque-Velázquez JA, Velázquez-Velázquez E (2010) Diversidad alfa y beta en murciélagos cavernícolas de la Depresión Central, Chiapas, México. Lacandonia 4: 47–54.

Villena FE, Gómez-Puerta LA, Jhonston EJ, Del Alcazar OM, Maguiña JL, Albujar C, Ampuero JS (2018) First report of *Trypanosoma cruzi* infection in salivary gland of bats from the Peruvian Amazon. The American Journal of Tropical Medicine and Hygiene 99: 723–728. https://doi.org/10.4269/ajtmh.17-0816

Vízquez-Rodríguez LR (2015) Prevalencia de *Leishmania* y *Trypanosoma cruzi* en los murciélagos *Carollia sowelli* y *Sturnira lilum* bajo dos condiciones distintas de perturbación antropogénica en la Selva Lacandona, Chiapas. Master's thesis, Universidad Nacional Autónoma de México, México.

WHO (2014) A Global Brief on Vector-Borne Disease. World Health Organization, Geneva, 54 pp. https://apps.who.int/iris/handle/10665/111008

Zingales B (2018) *Trypanosoma cruzi* genetic diversity: something new for something known about Chagas disease manifestations, serodiagnosis and drug sensitivity. Acta Tropica 184: 38–52. https://doi.org/10.1016/j.actatropica.2017.09.017

ZooKeys 1084: 151–164 (2022)
doi: 10.3897/zookeys.1084.79415
https://zookeys.pensoft.net

RESEARCH ARTICLE

A peer-reviewed open-access journal
ZooKeys
Launched to accelerate biodiversity research

# A striking color variation is detected in *Ponera testacea* Emery, 1895 (Hymenoptera, Formicidae) across its Western Palaearctic geographic range

Sándor Csősz[1,2], Kadri Kiran[3], Celal Karaman[3], Albena Lapeva-Gjonova[4]

**1** *Evolutionary Ecology Research Group, Institute of Ecology and Botany, Centre for Ecological Research, Alkotmány út 2-4, Vácrátót H-2163, Hungary* **2** *MTA-ELTE-MTM Ecology Research Group, Pázmány Péter sétány 1/C, Budapest H-1117, Hungary* **3** *Trakya University, Faculty of Science, Department of Biology, Edirne, Turkey* **4** *Sofia University, Faculty of Biology, Department of Zoology and Anthropology, Bulgaria*

Corresponding author: Sándor Csősz (sandorcsosz2@gmail.com)

Academic editor: Matthew Prebus | Received 15 December 2021 | Accepted 12 January 2022 | Published 1 February 2022

*http://zoobank.org/B75F07C9-A892-4963-B81E-147192B71929*

Citation: Csősz S, Kiran K, Karaman C, Lapeva-Gjonova A (2022) A striking color variation is detected in *Ponera testacea* Emery, 1895 (Hymenoptera, Formicidae) across its Western Palaearctic geographic range. ZooKeys 1084: 151–164. https://doi.org/10.3897/zookeys.1084.79415

## Abstract

In this paper, we provide numeric morphology-based evidence that the dark-colored *Ponera coarctata* var. *lucida* Emery, 1898, formerly considered a synonym of *P. coarctata* (Latreille, 1802), is conspecific with the lighter-colored *Ponera testacea* Emery, 1895. Species hypotheses are developed via NC-PART clustering, combined with Partitioning Algorithm based on Recursive Thresholding (PART), and via PCA combined with gap statistics. We obtained our results from an extensive dataset from the 10 continuous morphometric traits measured on 165 workers belonging to 73 nest samples. Linear discriminant analysis (LDA) confirmed the grouping of hypotheses generated by exploratory analyses with 100% classification success when all ten morphometric traits were involved. The Anatolian Turkish black and the predominantly European yellow samples, did not separate based on their morphometric characteristics. These two color variations broadly overlap in their geographic range in Anatolian Turkey. The investigated type series of *Ponera coarctata* var. *lucida* Emery, 1898 (collected from Kazakhstan) fell within the *P. testacea* cluster instead of *P. coarctata* and is also classified with high certainty as *P. testacea* by confirmatory LDA. Therefore, we propose the synonymy of *Ponera coarctata* var. *lucida* Emery, 1898 with *Ponera testacea* Emery, 1895. As no other morphological differences than color patterns were detected between the "black" and "pale" *P. testacea* samples, we hold that these populations constitute geographically occurring color variations of the same species. Finally, our quantitative morphology-based results show that relying on color patterns is not a robust approach in identifying European *Ponera* samples, particularly in the east, but using multivariate analyses of morphometric traits is advised instead.

**Keywords**
Biogeography, exploratory analyses, gap statistic, morphometry, species delimitation

## Introduction

The taxonomy of the European representatives of the tiny hypogeic genus *Ponera* has for several decades been apparently unambiguous. The two European species belonging to this genus, *P. coarctata* (Latreille, 1802) and *P. testacea* Emery, 1895 constitute one of the continent's most easily distinguishable species pairs (Csősz and Seifert 2003; Scupola 2006; Czechowski and Radchenko 2010; Attewell et al. 2011). Conspicuous size and color features help to tell these species apart. *Ponera coarctata* is larger, generally black, and has a higher petiole, while its typically lighter yellow congener, *P. testacea*, is significantly smaller, having a low and thick petiolar node (Csősz and Seifert 2003). In addition, these species differ in habitat preferences; *P. testacea* prefers more xerothermous biotopes than its sister species, *P. coarctata*. Based on several environmental variables measured in 25 study plots in Central Europe (Seifert 2017), *P. testacea* sites can be characterized as having higher maximum calibrated soil temperatures and lower soil moisture values. These previously considered European species extend their distribution to Turkey (Kiran and Karaman 2021), and *P. coarctata* has been known to occur north of the Black Sea coastline and reach the Caucasus range (Kiran and Karaman 2020). However, the most recent investigations revealed that a third morph, with a mixed combination of traits, also appears to occur in this region. This form is similar to *P. coarctata* in its shiny black or dark brown color. At the same time, the lower petiole node, dense pilosity, and multivariate analyses on their morphometric data place representatives of this particular group in *P. testacea*. Therefore, the normal morphological approaches that help to separate these *Ponera* species in the rest of the European part of the Western Palaearctic region seemed to fail in accurately identifying them in Turkey.

This problem prompted us to examine the possibility of whether a third *Ponera* species appeared in this region and, if so, to describe it appropriately. Ant taxonomists have often considered color traits unreliable as species-level traits due to the high intraspecific color polymorphism (Seifert 2003a,b, 2019; Seifert et al. 2017) that may reportedly lead to taxonomic errors. Therefore, we analyzed an extensive set of continuous morphometric data via robust multivariate statistic procedures, NC-clustering and principal component analysis (PCA) to infer species boundaries. Both these approaches were used in combination with Gap statistic algorithms that estimate the number of clusters in the data and assign observations (i.e. specimens or samples) into partitions. We tested the validity of the recognized pattern via confirmatory linear discriminant analysis (LDA).

We compared the morphologically recognized clusters with the color patterns of the samples. As a result, the third *Ponera* morph found in Turkey broadly overlaps with the cluster of European *P. testacea* via the complex morphometric protocol. The Anatolian Turkish black and the predominantly European yellow samples did not separate on

the basis of their morphometric characteristics, and these two color variations broadly overlap in their geographic range in Anatolian Turkey. The investigated type series of *Ponera coarctata* var. *lucida* Emery, 1898 (collected from Azerbaijan) fell within the *P. testacea* cluster instead of *P. coarctata* and is also classified with high certainty as *P. testacea* by confirmatory LDA. Therefore, we propose the synonymy of *Ponera lucida* with *Ponera testacea*. As no other morphological differences than color patterns were detected between the "black" and "pale" *P. testacea* samples, we hold that these populations constitute geographically occurring color variations of the same species. Thus, making *P. lucida* a subspecies of *P. testacea* is proven unnecessary.

## Material and methods

In this research 10 continuous morphometric traits were measured on 165 workers belonging to 73 nest samples. The material is deposited in the following institutions: Entomological Museum of Trakya University (EMTU), Hungarian Natural History Museum, Budapest, Hungary (HNHM), Muséum d'histoire naturelle, Genève (MHNG), Natural History Museum, Genoa (MSNG), private collection of Sándor Csősz (PCSC). The full list of material investigated is listed below:

### Material examined

**Type material**

***Ponera coarctata* var. *testacea* Emery, 1895**

**Lectotype**: "Bonifacio, leg. REVEL 1872" (1 w, MCSN); paralectotypes (3 workers) Rapallo / Liguria / Mai 1891" (1 w, MHNG); and two other specimens (on one pin) labelled by Emery "Gallia merid." and with a blue label "Cotypus" (2 ww, MHNG)

***Ponera coarctata* var. *lucida* Emery, 1898**

**Syntypes**: "Lenkoran / (next line) Korb / next label Syntypus *Ponera coarctata* var. lucida Emery, 1898" (3 ww), MCSN) [1st and 3rd measured, 2nd not measurable due to glue obstructing the view]

**Other material**

***Ponera coarctata***

Austria: **AUT:Felsolovo**: Felsőlövő, 1911.04.03, N47.35, E16.20, (3, HNHM); Croatia: **CRO:Buccari**: Buccari, 1927.04.21, N45.30, E14.53, (3, HNHM); **CRO:Orehovica**: Orehovica, 1885.06.04, N46.33, E16.50, (5, HNHM); Hungary: **HUN:Badacsony**:

Badacsony, 1929.08.24, N46.79, E17.50, (9, HNHM); **HUN:Batorliget**: Bátorliget, 1948.06.17, N47.76, E22.27, (6, HNHM); **HUN:Kolked**: Kölked, 1924.05.23, N45.95, E18.70, (3, HNHM); **HUN:Mezokovacshaza**: Mezőkovácsháza, 1886.07.15, N46.40, E20.90, (2, HNHM); **HUN:Nagyvazsony**: Nagyvázsony, Kab-hegy, 1924.05.06, N47.046, E17.65, (5, HNHM); **HUN:Simontornya**: Simontornya, 1913.06.18, N46.75, E18.55, (6, HNHM); Montenegro: **MNE:Zlatitca**: Zlatitca, 1886.06.07, N 42.46, E 19.29, (5, HNHM); Romania: **ROM:O.Sebeshely**: O.Sebeshely, 1913.07.03, N45.75, E23.25, (1, HNHM); **ROM:Tasnad-Szarvad**: Tasnád Szarvad, 1882.12.12, N47.47, E22.58, (3, HNHM); Slovakia: **SLO:Baan**: Baán [Bánovce], 1881.08.22, N48.72, E18.26, (3, HNHM); Switzerland: **SWI:Enge**: Enge, 1880.04.12, N47.36, E8.53, (1, MHNG); **SWI:Neuveville**: Neuveville, N47.063, E7.091, (7, MHNG); Turkey: **TUR:10/1520**:**Çorum:** Uğurludağ, 2010.06.15, N40.3864, E35.4650, (2, EMTU); **TUR:06/035**: **Edirne**: 2006.09.13, N41.67, E26.55, (2, EMTU); **TUR:12/719a**:**Giresun:** Bulancak-Tekmezar Vill., 2012.06.12, N40.8556, E38.2403, (1, EMTU); **TUR:12/721**: Bulancak-Tekmezar Vill., 2012.06.12, N40.8556, E38.2403, (1, EMTU); **TUR:12/931a**: Espiye-Çepni Vill., 2012.06.15, N40.8575, E38.7314, (2, EMTU); **TUR:12/615b**: Piraziz-Armutçukuru Vill., 2012.06.11, N40.8367, E38.08001, (2, EMTU); **TUR:12/626**: Piraziz-Armutçukuru Vill., 2012.06.11, N40.8367, E38.0800, (2, EMTU); **TUR:11/197b**:**Kırklareli:** Demirköy-Sivriler Vill., 2011.05.24, N41.78, E27.86, (2, EMTU); **TUR:11/199a**: Demirköy-Sivriler Vill., 2011.05.24, N41.7839, E27.8651, (2, EMTU); **TUR:11/0203**: Demirköy-Sivriler Vill., 2011.05.24, N41.78, E27.86, (2, EMTU); **TUR:11/0253**: Pınarhisar-Yenice Vill., 2011.05.25, N41.7408, E27.7114, (2, EMTU); **TUR:11/157a**: Vize-Kıyıköy, 2011.05.22, N41.6345, E28.0697, (2, EMTU); **TUR:12/0539a**:**Ordu:** Şenocak Vill., 2012.06.10, N40.8867, E37.9567, (2, EMTU); **TUR:12/542b**: Şenocak Vill., 2012.06.10, N40.8867, E37.9567, (2, EMTU); **TUR:12/553a**: Kabadüz-Harami Vill., 2012.06.10, N40.8242, E37.9258, (2, EMTU); Ukraine: **UKR:Beregszasz**: Beregszász, 1883.10.15, N48.20, E22.63, (1, HNHM);

***Ponera testacea***

"BLACK MORPH"

**AZE:Lenkaran-lucida-ST**: Lenkoran [Lankaran, syntype series], Korb, N38.75, E48.85, (2, MSNG); **TUR:07/2463**:**Balıkesir:** Bayramiç-Adalı Vill., 2007.09.07, N39.3697, E28.2811, (1, EMTU); **TUR:10/726:Çankırı:** Yapraklı-Ayseki Vill., 2010.06.01, N40.7925, E33.9014, (2, EMTU); **TUR:12/1109b**:**Gümüşhane:** Kürtün-Taşlıca Vill., 2012.06.17, N40.7187, E39.0344, (2, EMTU); **TUR:K98/483a**:**İzmit:** Karamürsel-Tahtalı Vill., 1998.08.05, N40.5775, E29.6441, (1, EMTU); **TUR:04/914a**: Derbent-Sultaniye Vill., 2004.08.29, N40.6106, E30.0867, (2, EMTU); **TUR:04/915b**: Derbent-Sultaniye Vill., 2004.08.29, N40.6106, E30.0867, (2, EMTU); **TUR:04/796**:**Konya:** Altınopa Dam Lake, 2006.08.27, N37.88, E32.29, (1, EMTU); **TUR:11/680**: Akşehir-Engili Vill., 2011.06.27, N38.3031, E31.4467, (2, EMTU); **TUR:12/553b**:**Ordu:** Kabadüz-Harami Vill., 2012.06.10, N40.8242, E37.9258, (2, EMTU); **TUR:12/1941a**:**Rize:** Çamlıhemşin-Topluca Vill., 2012.08.05, N41.0603,

E41.0158, (1, EMTU); **TUR:12/2352:** Ardeşen-Sinan Vill., 2012.08.07, N41.0930, E41.0895, (2, EMTU); **TUR:10/1754a**:**Sivas:** Gürün-Reşadiye Vill., 2010.08.14, N38.8214, E37.1892, (2, EMTU); **TUR:12/1326**:**Trabzon:** Düzköy-Aykut, 2012.06.20, N40.9122, E39.4581, (2, EMTU); **TUR:12/1415b**: Maçka-Acısu Vill., 2012.06.21, N40.7125, E39.5920, (2, EMTU); **TUR:12/1416**: Maçka-Acısu Vill., 2012.06.21, N40.7125, E39.5919, (2, EMTU); **TUR: 12/1421b**: Maçka-Akmescit Vill., 2012.06.21, N40.8405, E39.6547, (2, EMTU); **TUR:K98/656**:**Yalova:** Armutlu-Hayriye Vill., 1998.08.14, N40.5008, E28.9664, (2, EMTU).

"PALE MORPH"

**CRO:Senj**: Zengg [Senj], N44.9893, E14.9037, (1, HNHM); **FRA:Corse-Bonifacio(LT)**: Bonifacio [lectotype], 1972, N41.39, E9.159, (1, MSNG); **FRA:Gallia meridionale (PLT)**: Gallia Meridionale [paralectotype], (2, MSNG); **HUN:Pusztapoo**: Pusztapoó, 1929.02.11, N47.093, E20.4556, (6, HNHM); **HUN:Rimaszombat**: Rimaszombat, 1909.07.10, N48.382, E20.021, (2, HNHM); **HUN:Szigetszentmiklos**: Szigetszentmiklós, 1912.10.16, N47.34, E19.035, (2, HNHM); **ITA:Rapallo (PLT)**: Rapallo [paralectotype], 1891.05, N4435, E9.23, (1, MHNG); **TUR:12/2674**:**Artvin:** Şavşat-Maden Vill., 2012.08.11, N41.3781, E42.1333, (2, EMTU); **TUR:K98/0689a**:**Bilecik:** Osmaneli-Yeşilçimen Vill., 1998.08.17, N40.4475, E29.8881, (2, EMTU); **TUR:10/1515b**:**Çorum:** Uğurludağ, 2010.06.15, N40.3863, E35.465, (2, EMTU); **TUR:10/1520b**: Uğurludağ, 2010.06.15, N40.3863, E35.4650, (2, EMTU); **TUR:12/929**:**Giresun:** Espiye-Çepni Vill., 2012.06.15, N40.8575, E38.7314, (1, EMTU); **TUR:12/1071**: Tirebolu, 2012.06.16, N41.0217, E38.8942, (1, EMTU); **TUR:10/1269b**:**Kayseri:** Pınarbaşı-Cinliyurt Vill., 2010.06.09, N38.5019, E36.1909, (2, EMTU); **TUR:10/1278b**: Pınarbaşı-Cinliyurt Vill., 2010.06.09, N38.5019, E36.1908, (2, EMTU); **TUR:10/1285**: Melikgazi, 2010.06.09, N38.7195, E36.2142, (1, EMTU); **TUR:10/1286**: Melikgazi, 2010.06.09, N38.7195, E36.2141, (1, EMTU); **TUR:11/231a**:**Kırklareli:** Vize, 2011.05.25, N41.5837, E27.2703, (1, EMTU); **TUR:11/232a**: Vize, 2011.05.25, N41.5836, E27.7102, (2, EMTU); **TUR:12/1831a**:**Rize:** Pazar-Örnek Vill., 2012.08.03, N41.1464, E40.7978, (2, EMTU); **TUR:10/766**:**Yozgat:** Sungurlu-Çingirler Vill., 2010.06.02, N40.2814, E34.37, (2, EMTU).

Distribution map for all species discussed in this revisionary work is generated via SimpleMappr (Shorthouse 2010).

## Protocol for color-coding

Pigmentation scaling was performed via a subjective evaluation of body coloration ranging from whitish yellow (score 1) to black (score 5). The specimens were illuminated via Photonic Optics 2-arms Illuminator with neutral white color temperature, 5900 K (equivalent to halogen, 4000 K). Specimens with light pigmentation (score 2 and score 3) were classified as "pale morph" (Fig. 1.), darker (score 4 and score 5) specimens were considered "black morph" (Fig. 2). Very light, whitish-yellow (score 1) specimens have not been found.


**Figure 1.** Light-colored (score 2) *Ponera testacea* worker from Hungary. Specimen: CASENT0906719, from www.antweb.org.


**Figure 2.** A syntype worker of *Ponera coarctata* var. *lucida* representing a dark-colored (score 4) *P. testacea* worker from Azerbaijan. Specimen: CASENT0903905, from www.antweb.org.

## Protocol for morphometric character recording

Morphometric characters are defined as in Seifert (2018). All measurements were made in an Olympus SZX9 stereomicroscope at a magnification of 150× for each character. Morphometric data are given in μm throughout the paper. All worker individuals were measured by SC. Definitions of morphometric characters are listed below (for details see Csősz and Seifert 2003: 202–204):

CL Cephalic length;
CW Cephalic width;
FL Maximum width of frontal lobes;
FR Minimum distance between frontal carinae;
ML Mesosoma length;
PEH The maximum height of petiole;
PEL Petiole length;
PH Height of petiole node;
PW Petiole width;
SL Scape length.

## Statistical framework on morphometric data–hypothesis formation and testing

### Exploratory analyses through NC-PART clustering

The statistical procedure has been done on worker caste only. The prior species hypothesis was generated based on workers through the combined application of NC clustering (Seifert et al. 2014) and Partitioning Algorithm based on Recursive Thresholding (PART) (Nilsen et al. 2013; see also Csősz and Fisher 2016). The optimal number of clusters and the partitioning of samples are accepted as the preliminary species hypothesis in every case in which the two clustering methods, 'hclust' and 'kmeans' through PART, have yielded the same conclusion.

### Exploratory analyses through sPCA in combination with Gap statistics

Structure in morphometric data was also displayed in a scatterplot via a principal component analysis (sPCA; Baur and Leuenberger 2011). The sPCA does not return an estimate on the number of clusters, hence an iterative gap statistic algorithm (function 'gap') implemented in package clusterGenomics (Tibshirani et al. 2001; Nilsen et al. 2013), was employed to determine the optimal number of clusters within data and also assigned observations (i.e. specimens, or samples) into partitions.

### Hypothesis testing by confirmatory analyses

The validity of the prior species hypothesis imposed by the two exploratory processes was tested via a cross-validated linear discriminant analysis (CV-LDA), and the best fitting simple ratio is found via multivariate ratio analysis (MRA). Statistical analyses have been done in R (R Core Team 2019).

## Results

### Finding biodiversity patterns through numeric morphology

Altogether two clusters were revealed to be the most parsimonious solution by both NC-PART clustering (Fig. 3.) and by the gap statistic based on PC scores (Figs 4, 5.). The grouping hypotheses generated by hypothesis-free exploratory analyses is confirmed by LDA with 100% classification success when all 10 morphometric traits were involved. This pattern is also supported by the examination of external morphological traits (e.g. shape of petiolar node, and density of pilosity on the first gaster tegite). *Ponera coarctata* appears to exhibit uniform color patterns throughout the whole distributional area, but *P. testacea* has a rather bimodal coloration; the western (European) population has a pale brown, or yellow appearance, whilst the eastern, Anatolian samples are black. This geography driven shift does not appear in other morphological features and the multivariate analyses of continuous traits do not support separateness.

### Taxonomic acts

We hold *P. testacea* does not split into separate subspecies and the "pale morph" and the "black morph" of *P. testacea* belong to the same species. Therefore, we synonymize *Ponera coarctata* var. *lucida* Emery, 1898, which was formerly considered a junior synonym of *P. coarctata* (see Taylor 1967), with *P. testacea* Emery, 1895.

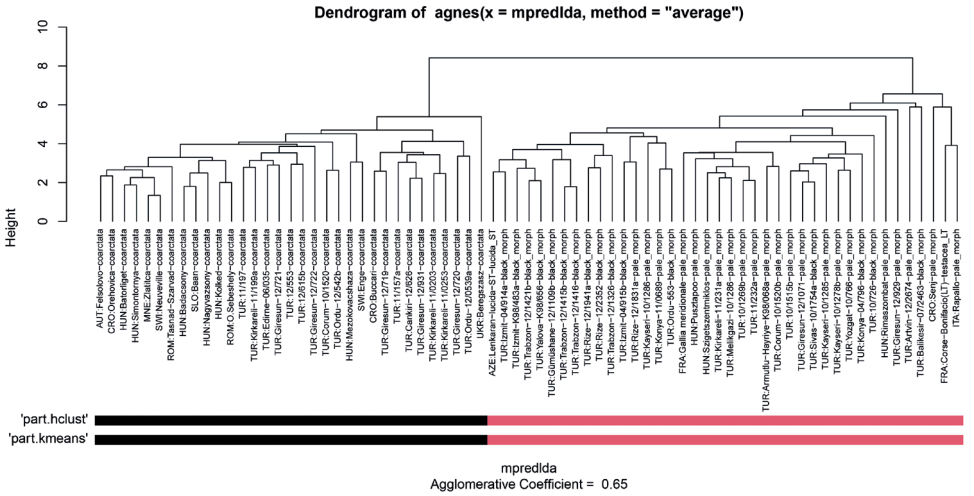


**Figure 3.** Dendrogram solution for the Western Palaearctic representatives of *Ponera*. Sample information in the dendrogram follows this format: abbreviated country code, locality name, and/or a special collection code followed by final species hypothesis separated by underscore. Two columns of rectangles represent results of partitioning resulted by method PART using two cluster methods 'hclust' and 'kmeans'.

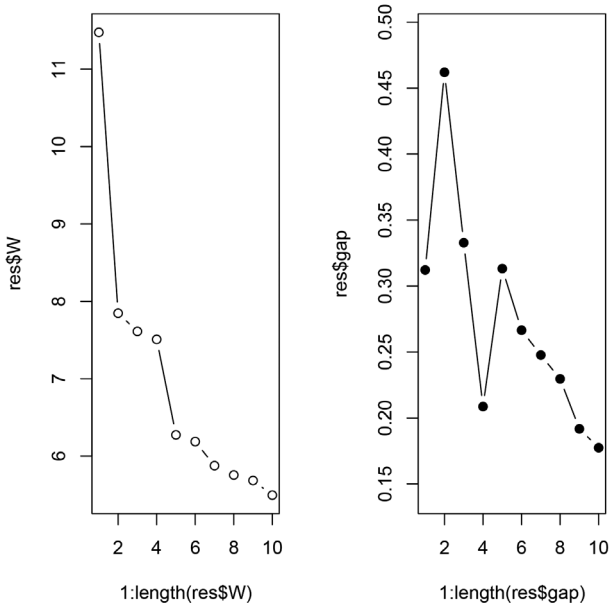


**Figure 4.** Gap statistic for dataset of Western Palaearctic *Ponera* samples. Two-cluster solution is highly supported by the elbow at 2 components by the dispersion curve (left) and by the peak at cluster number four by the gap curve (right). Number of clusters in the data (X axis), the total within-cluster dispersion for each evaluated partition (Y axis for the left plot) and the vector of length Kmax giving the Gap statistic for each evaluated partition (Y axis for the right plot) is illustrated.

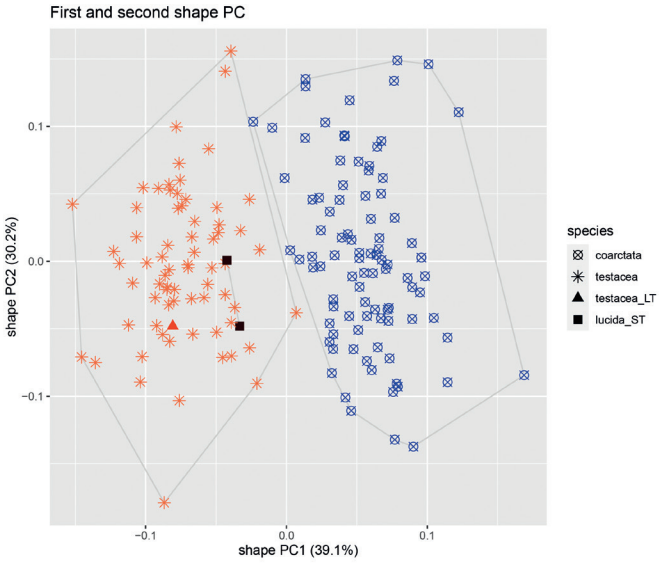


**Figure 5.** Ordination biplot for shape principal component analysis (sPCA) based on species identity. Color codes represent: *Ponera coarctata*: blue circles, *P. testacea*: orange asterisks, *P. testacea* lectotype: orange triangle, *P. lucida* syntypes: dark brown rectangles.

## The spatial distribution pattern

Geographic distribution of *Ponera coarctata* and *P. testacea* (including the "pale morph" and the "black morph") broadly overlap in Europe and in Anatolian Turkey, where *P. coarctata* occupies significantly ($p$ = 0.046) lower altitudes (519 m [5 m, 743 m]) than *P. testacea* (900 m [0 m, 1900 m]). The two color variations of *P. testacea* does not show significant differences ($p$ = 0.92) in their vertical distribution ("black morph" ($n$ = 14) 896 m [442 m, 1791 m], "pale morph" ($n$ = 10) 919 m [0 m, 1900 m]).

## Species delimitation

The distinctive morphology of these species allows for considerable reduction of morphological characters, so that workers of the two taxa *Ponera coarctata* and *P. testacea* can be separated based on the combination of three continuous morphometric traits (CW, PEL, and PH; Fig. 6) with 99.4% (a single misclassified case out of the total 165 individuals).

Coefficients of linear discriminants help to place and identify samples via placing workers in the discriminant space using the linear discriminant function (LD) as follows (morphometric traits are in micrometers):

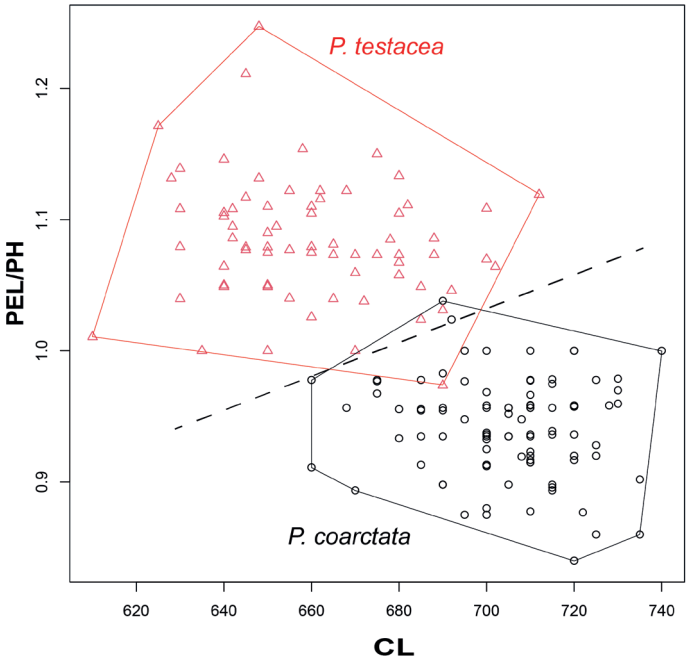


**Figure 6.** The best morphometric ratio (petiole length / petiole height; PEL/PH) is illustrated on the head length (CL). Scatterplots of the most discriminating ratio on the head length between workers of Western Palaearctic representatives of *Ponera*; *P. coarctata*: black circles, *P. testacea*: red triangles. The thin dashed line illustrates best separation.

$$LD = 0.0449*CW - 0.0893 * PEL + 0.0750 * PH - 21.4786$$

*Ponera coarctata* ($n$ = 93) = +1.99 (+0.22, +5.02)

*Ponera testacea* ($n$ = 72) = −2.57 (−5.05, +0.27)
(including both "pale morph" and "black morph")

A simple morphometric ratio of two petiole characters (petiole length / height of petiolar node, PEL/PH) appears an excellent numeric key to tell these species apart but is slightly affected by allometry. Therefore, a graphical display of this ratio on the head length (CL) is also provided as an easy-to-use asset aiding routine determinations (Fig. 6). This key yields a 98.18% classification success ($n$ = 165).

## Discussion

The yellow and black *Ponera testacea* morphs do not differ via multivariate analyses of continuous morphometric traits based on an extensive material collected in a wide geographic range. Furthermore, no other shape characteristics support their separation. The investigated type series of *Ponera coarctata* var. *lucida* (the "black" morph) fell within the *P. testacea* cluster instead of *P. coarctata* in both exploratory analyses (NC-clustering and PCA) and is also classified with high certainty as *P. testacea* by confirmatory LDA. Therefore, we propose synonymy of *Ponera lucida* with *Ponera testacea* instead of *P. coarctata*.

Although the yellowish phenotype of *Ponera testacea* is dominant in the Western Palaearctic (western Turkey and Europe), the black *P. testacea* morph is prevalent in Turkey; distribution of these color variations broadly overlaps in Anatolia (Fig. 7). The sympatric pattern might indicate a subspecific rank. However, due to the lack of morphological differences other than the color of *P. testacea* morphs, we hold that these populations constitute geographically occurring color variations of the same species, making *P. lucida* a subspecies of *P. testacea* unnecessary.

In conclusion, relying solely on color patterns is not a robust approach in identifying European *Ponera* samples, but using multivariate analyses of morphometric traits or the presented numeric key is advised to distinguish these species. Straightforward pigmentation patterns, such as variation of light versus dark, red versus brown, or red versus black on the whole body or specific body parts, are frequently unreliable taxonomic characters in insects and other animals. A minor point mutation may change pigmentation profoundly, whereas complex morphological structures are less easily changed. Many textbook examples demonstrate relatively simple pigmentation genetics (e.g. Lus 1932; Barrion and Saxena 1987; Majerus 1998; Andrés and Cordero 1999; Majumdar et al. 2008). Taxonomic failures or pitfalls resulting from pigmentation in ants have been repeatedly reported. Seifert (1997, 2018, 2020) described color dimorphism as superimposed by an allometric change in the *Formica rufibarbis* group and *Lasius* species. Intraspecific color polymorphism superimposed by geographic


**Figure 7.** Geographic map of *Ponera* species in Europe and Turkey. Color codes for species are as follows: *Ponera coarctata*: red circles, *P. testacea* "black morphs": blue triangles, *P. testacea* "yellow morphs": yellow rectangles.

clines has also been shown for species of the *Formica cinerea* group (Seifert 2003a). Furthermore, extreme intraspecific color polymorphism is reported in several species of *Cardiocondyla* (Seifert 2003b; Seifert et al. 2017) and in *Camponotus* (Seifert 2019) that reportedly leads to taxonomic errors.

## Acknowledgements

This study was partially supported by the National Research, Development, and Innovation Fund under grant no. K 135795 (S.C) and the Scientific and Technological Research Council of Turkey (TÜBİTAK) projects no. 109T088 and 111T811 (K.K.). Special thanks are due to Phil Attewell for kindly improving the language of the manuscript. We also wish to thank the three reviewers, J.J. Longino, B. Seifert, and H.C. Wagner, for their constructive critiques that helped to improve the manuscript's quality.

## References

Andrés JA, Cordero A (1999) The inheritance of female color morphs in the damselfly *Ceriagrion tenellum* (Odonata, Coenagrionidae). Heredity 82: 328–335. https://doi.org/10.1038/sj.hdy.6884930

AntWeb (2020) AntWeb. Version 8.68.7. California Academy of Science. Accessed on: 2022-1-5. https://www.antweb.org

Attewell PJ, Collingwood CA, Godfrey A (2010) *Ponera testacea* (Emery, 1895) (Hym.: Formicidae) new to Britain from Dungeness, East Kent. Entomologist's Record and Journal of Variation 122: 113–119.

Barrion AA, Saxena RC (1987) Inheritance of body color in the brown planthopper, *Nilaparvata lugens*. Entomologia Experimentalis et Applicata 43: 267–270. https://doi.org/10.1111/j.1570-7458.1987.tb02220.x

Baur H, Leuenberger C (2011) Analysis of ratios in multivariate morphometry. Systematic Biology 60(6): 813–825. https://doi.org/10.1093/sysbio/syr061

Csősz S, Fisher BL (2016) Taxonomic revision of the Malagasy members of the *Nesomyrmex angulatus* species group using the automated morphological species delineation protocol NC-PART-clustering. PeerJ 4: e1796. https://doi.org/10.7717/peerj.1796

Csősz S, Seifert B (2003) *Ponera testacea* Emery, 1895 stat. n.—a sister species of *P. coarctata* (Latreille, 1802) (Hymenoptera: Formicidae). Acta Zoologica Academiae Scientiarum Hungaricae 49(3): 211–223.

Czechowski W, Radchenko A (2010) *Ponera testacea* Emery, 1895 (Hymenoptera: Formicidae) in Poland. Polish Journal of Entomology 79: 327–337.

Kiran K, Karaman C (2020) Additions to the ant fauna of Turkey (Hymenoptera, Formicidae). Zoosystema 42(18): 285–329. https://doi.org/10.5252/zoosystema2020v42a18

Kiran K, Karaman C (2021) Ant fauna (Hymenoptera: Formicidae) of Central Anatolian Region of Turkey. Turkish Journal of Zoology 45(3): 161–196. https://doi.org/10.3906/zoo-2008-6

Lus JJ (1932) An analysis of the dominance phenomenon in the inheritance of the elytra and pronotum color in *Adalia bipunctata*. Trudy Labroratorii Genetiki, Leningrad 9: 135–162.

Majerus M (1998) Melanism: Evolution in Action. Blackwell, Oxford, 338 pp.

Majumdar KC, Nasuruddin K, Ravinder K (2008) Pink body color in *Tilapia* shows single gene inheritance. Aquaculture Research 28 (8): 581–589. https://doi.org/10.1046/j.1365-2109.1997.00898.x

Nilsen G, Borgan Ø, LiestØl K, Lingjaerde OC (2013) Identifying clusters in genomics data by recursive partitioning. R package version 1.0. https://doi.org/10.1515/sagmb-2013-0016

R Core Team (2019) R: A language and environment for statistical computing. R Foundation for Statistical Computing, Vienna, Austria. https://www.R-project.org/

Scupola A (2006) *Ponera coarctata* var. *crassisquama* Emery, 1916 a new synonym of *P. testacea* Emery, 1895 (Hymenoptera, Formicidae). Bollettino del Museo Civico di Storia Naturale di Verona Botanica Zoologia 30: 161–164.

Seifert B (1997) *Formica lusatica* n. sp.—a sympatric sibling species of *Formica cunicularia* and *Formica rufibarbis* (Hymenoptera Formicidae). Abhandlungen und Berichte des Naturkundemuseums Görlitz 69(5): 3–16.

Seifert B (2003a) A taxonomic revision of the *Formica cinerea* group (Hymenoptera: Formicidae). Abhandlungen und Berichte des Naturkundemuseums Görlitz 74(2): 245–272.

Seifert B (2003b) The ant genus *Cardiocondyla* (Insecta: Hymenoptera: Formicidae)—a taxonomic revision of the *C. elegans*, *C. bulgarica*, *C. batesii*, *C. nuda*, *C. shuckardi*, *C. stambuloffii*, *C. wroughtonii*, *C. emeryi*, and *C. minutior* species groups. Annalen des Naturhistorischen Museums Wien, Serie B 104: 203–338.

Seifert B (2017) The ecology of Central European non-arboreal ants—37 years of a broad-spectrum analysis under permanent taxonomic control. Soil Organisms 89(1): 1–69.

Seifert B (2018) The Ants of Central and North Europe. Lutra Verlags- und Vertriebsgesellschaft, Tauer, 408 pp.

Seifert B (2019) A taxonomic revision of the members of the *Camponotus lateralis* species group (Hymenoptera: Formicidae) from Europe, Asia Minor and Caucasia. Soil Organisms 91(1): 7–32. https://doi.org/10.25674/so-91-1-02

Seifert B (2020) A taxonomic revision of the Palaearctic members of the subgenus *Lasius* s.str. (Hymenoptera, Formicidae). Soil Organisms 92(1): 15–86. https://doi.org/10.25674/so92iss1pp15

Seifert B, Okita I, Heinze J (2017) A taxonomic revision of the *Cardiocondyla nuda* group (Hymenoptera: Formicidae). Zootaxa 4290(2): 324–356. https://doi.org/10.11646/zootaxa.4290.2.4

Seifert B, Ritz M, Csősz S (2014) Application of exploratory data analyses opens a new perspective in morphology-based alpha-taxonomy of eusocial organisms. Myrmecological News 19: 1–15.

Shorthouse DP (2010) SimpleMappr, an online tool to produce publication-quality point maps. Accessed on: 2021-11-18. https://www.simplemappr.net

Taylor RW (1967) A monographic revision of the ant genus *Ponera* Latreille (Hymenoptera: Formicidae). Pacific Insects Monograph 13: 1–112.

Tibshirani R, Walther G, Hastie T (2001) Estimating the number of clusters in a data set via the gap statistic. Journal of the Royal Statistical Society: Series B (Statistical Methodology) 63(2): 411–423. https://doi.org/10.1111/1467-9868.00293

ZooKeys 1084: 165–182 (2022)
doi: 10.3897/zookeys.1084.78405
https://zookeys.pensoft.net

RESEARCH ARTICLE

A peer-reviewed open-access journal
ZooKeys
Launched to accelerate biodiversity research

# First report of the genus *Tenuibaetis* (Ephemeroptera, Baetidae) from Thailand revealing a complex of cryptic species

Chanaporn Suttinun[1], Jean-Luc Gattolliat[2,3], Boonsatien Boonsoong[1]

**1** *Animal Systematics and Ecology Speciality Research Unit (ASESRU), Department of Zoology, Faculty of Science, Kasetsart University, Bangkok 10900, Thailand* **2** *Museum of Zoology, Palais de Rumine, Place Riponne 6, CH-1005 Lausanne, Switzerland* **3** *University of Lausanne (UNIL), Department of Ecology and Evolution, CH-1015 Lausanne, Switzerland*

Corresponding author: Boonsatien Boonsoong (fscibtb@ku.ac.th)

Academic editor: L. Pereira-da-Conceicoa | Received 24 November 2021 | Accepted 18 January 2022 | Published 1 February 2022

*http://zoobank.org/1F7A3F8B-31D9-481D-B7EC-4357CADC4D2D*

**Citation:** Suttinun C, Gattolliat J-L, Boonsoong B (2022) First report of the genus *Tenuibaetis* (Ephemeroptera, Baetidae) from Thailand revealing a complex of cryptic species. ZooKeys 1084: 165–182. https://doi.org/10.3897/zookeys.1084.78405

## Abstract

A new species of the genus *Tenuibaetis* Kang & Yang, 1994 is described from Thailand and the genus is reported for the first time from this country. *Tenuibaetis panhai* **sp. nov.** is easily distinguished from other known *Tenuibaetis* by the complete absence of hindwing pads. Molecular evidence based on COI confirmed the validity of the new species. Additional putative species of *Tenuibaetis* based on molecular evidence only are considered as Molecular Operational Taxonomic Units (MOTUs) without description. The morphological characters of the new species and its closely related species are discussed; a key to the Oriental species is provided.

## Keywords

COI, mayflies, MOTUs, new species, Southeast Asia, *Tenuibaetis panhai* sp. nov.

## Introduction

Kang et al. (1994) established the subgenus *Tenuibaetis*, and *Baetis* (*Tenuibaetis*) *pseudofrequentus* Müller-Liebenau, 1985 from Taiwan was considered as the type species. This subgenus originally included three species (*B.* (*T.*) *pseudofrequentus* Müller-Liebenau, 1985, *B.* (*T.*) *arduus* Kang & Yang, 1994 and *B.* (*T.*) *inornatus* Kang & Yang, 1994) and was characterized by the following larval characters: mandibles with margin between

prostheca and mola without setae, spines or serration, apex of labial palps somewhat acute, femoral villopore present and paraproct with a patch of notched scales. Waltz and McCafferty (1997) synonymized *Tenuibaetis* with *Baetiella* based on the shape of the labial palp. Fujitani et al. (2003b, 2011) questioned this transfer by stating that the larvae of *Tenuibaetis*, significantly differ from those of *Baetiella* and related genera by the inner margins of cerci fringed with setae in *Tenuibaetis* but glabrous in *Baetiella*, and the robust setae with medial ridges on the dorsomedian surface of the larval femur. Therefore, they revalidated *Tenuibaetis* and raised it to the generic rank.

The genus *Tenuibaetis* currently contains seven species: *T. flexifemora* (Gose, 1980) from Japan (Gose 1980); *T. pseudofrequentus* (Müller-Liebenau, 1985) from Taiwan, Japan and Hong Kong (Müller-Liebenau 1985; Tong and Dudgeon 2000; Fujitani et al. 2003a, 2003b, 2011); *T. frequentus* (Müller-Liebenau & Hubbard, 1985) from Sri Lanka and India (Müller-Liebenau and Hubbard 1985; Balaji et al. 1990; Sivaramakrishman and Venkataraman 1990; Kubendran et al. 2015); *T. arduus* (Kang & Yang, 1994) and *T. inornatus* (Kang & Yang, 1994) from Taiwan (Kang et al. 1994), *T. parviptera* Fujitani, 2011 from Japan (Fujitani et al. 2011), and *T. fujitanii* Kaltenbach & Gattolliat, 2019 from Indonesia (Kaltenbach and Gattolliat 2019). Two additional species, *Baetis ursinus* Kazlauskas, 1963 and *B. hissaricus* Novikova, 1991, were considered to belong to this genus by Kluge (2021), but they were never formally transferred to this genus. The distribution of this genus is encompassing the whole oriental realm and the most Eastern part of Palearctic realm.

In the last decade, knowledge of the diversity of the Baetidae in Thailand has grown, as seven genera were reported for the first time from this area: *Procloeon* Bengtsson, 1915 (Tungpairojwong and Bae 2015; Kluge 2016), *Anafroptilum* Kluge, 2012 (Kluge and Novikova 2017), *Platybaetis* Müller-Liebenau, 1980 (Sutthinun et al. 2018), *Centroptella* Braasch & Soldán, 1980 (Kluge et al. 2020), *Indocloeon* Müller-Liebenau, 1982 (Kluge and Suttinun 2020), and *Procerobaetis* Kaltenbach & Gattolliat, 2019 (Suttinun et al. 2021). The newest genus, *Cymbalcloeon* Suttinun, Gattolliat & Boonsoong, 2020, is for the moment only known from Thailand (Suttinun et al. 2020). We describe a new species of *Tenuibaetis* from Thailand, based on material collected during the first mass survey of the family Baetidae in this country (Suttinun 2021). Additionally, we also present cryptic diversity within this genus treated as Molecular Operational Taxonomic Units (MOTUs) based on molecular evidence only (COI), without formal description of the species (Floyd et al. 2002; Blaxter et al. 2005; Morard et al. 2016; Kaltenbach et al. 2020). As Thailand is in the middle of the Oriental realm, our study will provide a better understanding of the distribution of this genus.

## Materials and methods

The specimens were collected from headwater streams in different parts of North, West and South of Thailand (Table 1, GPS map versatile navigator (Garmin eTrex 10)). They are preserved in 95% ethanol. Larval dissection was performed in Cellosolve, with subsequent mounting on slides with Euparal. Measurements (given in mm) and photographs were taken using a Visionary LK System (Dun, Inc., USA). All drawings were made with

**Table 1.** GPS coordinates of locations of examined specimens.

| Species | Locality | GPS coordinates |
|---|---|---|
| *T. panhai* sp. nov. | Kanchanaburi (KN) | 14°34'57.9"N, 98°34'52.0"E |
| | | 14°33'10.8"N, 98°33'94.3"E |
| | | 14°58'21.0"N, 98°53'50.3"E |
| | Ratchaburi (RB) | 13°31'45.6"N, 99°14'65.6"E |
| | Petchaburi (PC) | 12°38'14.5"N, 99°30'59.5"E |
| | Loei (LE) | 17°06'40.7"N, 101°28'72.0"E |
| | Chiang Rai (CR) | 19°51'76.8"N, 99°39'07.8"E |
| | | 20°03'15.8"N, 99°49'28.2"E |
| | | 20°05'36.0"N, 99°46'79.7"E |

a camera lucida attached to a compound microscope and scanned for editing in Procreate 5X (iOS application). Final plates were prepared with Adobe Photoshop CC 2020.

DNA was extracted using non-destructive methods to allow subsequent morphological analysis (see Vuataz et al. 2011 for details). Part of the COI (a 658 bp fragment of the mitochondrial gene cytochrome oxidase subunit 1) was amplified using the primers LCO1490 and HCO2198 (Folmer et al. 1994). The polymerase chain reaction (PCR) conditions and procedure were performed as described by Kaltenbach et al. (2020). Sequencing was done using Sanger's method (Sanger et al. 1977). The genetic distances between species were calculated using Kimura 2-parameter distances (K2P, Kimura 1980), using MEGA X (Kumar et al. 2018). Sequence alignment and editing were performed using ClustalW. The phylogenetic tree was analysed by Bayesian inference using MrBayes. The best evolution model obtained was Hasegawa-Kishino-Yano and proportion of invariable sites (HKY+I). The GenBank accession numbers are given in Table 2, nomenclature of gene sequences follows Chakrabarty et al. (2013). Other analyzed

**Table 2.** Sequenced specimens of *Tenuibaetis*.

| Species | Locality | Code | Genbank # | GenSeq Nomenclature |
|---|---|---|---|---|
| *T. panhai* sp. nov. | Kanchanaburi | TEKN01 | OM264189 | genseq-1 COI |
| | | TEKN06 | OM319584 | genseq-3 COI |
| | Ratchaburi | TERB01 | OM302269 | genseq-3 COI |
| | Petchaburi | TEPC02 | OM302305 | genseq-3 COI |
| | | TEPC03 | OM319569 | genseq-3 COI |
| | Loei | TELE01 | OM302308 | genseq-3 COI |
| | | TELE02 | OM303507 | genseq-3 COI |
| | Chiang Rai | TECR01 | OM302358 | genseq-3 COI |
| | | TECR02 | OM303508 | genseq-3 COI |
| *T.* cf. *panhai* sp. I | Patthaluang | TEPT01 | OM320557 | genseq-4 COI |
| | Nakhon Sri Thammarat | TENT01 | OM320559 | genseq-4 COI |
| | Surat Thani | TEST01 | OM320558 | genseq-4 COI |
| | Narathiwat | TENW01 | OM320563 | genseq-4 COI |
| *T.* cf. *panhai* sp. II | Chiang Mai | TECM02 | OM320576 | genseq-4 COI |
| | | TECM03 | OM320587 | genseq-4 COI |
| | | TECM04 | OM320571 | genseq-4 COI |
| | | TECM05 | OM320562 | genseq-4 COI |
| *T. frequentus* | India | | LC056074 | – |
| *T. flexifemorus* | Japan | | KX824012 | – |
| | | | KP970712 | – |

*Tenuibaetis* sequences were obtained from GenBank: *T. frequentus* (LC056074.1) and *T. flexifemora* (KX824012.1; KP970712.1). *Liebebiella vera* (LC056071.1) was used as an outgroup. The nomenclature used for Molecular Operational Taxonomic Units (MOTUs) broadly follows Morard et al. (2016) original proposal.

The distribution map was generated with the SimpleMappr software (https://simplemappr.net; Shorthouse 2010).

The material was deposited in the collection of the Zoological Museum at Kasetsart University in Bangkok, Thailand (**ZMKU**) and at the Museum of Zoology in Lausanne, Switzerland (**MZL**).

We followed all guidelines of the Animal Ethics Committee of Kasetsart University (approval no. ACKU61-SCI-029) for collecting the mayfly specimens.

## Taxonomy

***Tenuibaetis panhai* sp. nov.**
http://zoobank.org/B39C17B1-A135-4DEC-8172-CB6C497F89AD
Figs 1–4

**Type material.** ***Holotype.*** Thailand • larva; Kanchanaburi, Thong Pha Phumi District, Pra Chum Mai; 14°34'58"N, 98°34'52"E; 269 m; 31 Jan. 2019; leg. C. Suttinun; on slide; Genbank OM264189; TEKN01; ZMKU. ***Paratypes.*** Thailand • 7 larvae; same data as holotype; 1 on slide TEKN03; 4 in alcohol; ZMKU; 1 on slide GBIFCH00829251; 1 in alcohol; TEKN02; GBIFCH00673241; MZL. ***Other material.*** Thailand • 1 larva; Kanchanaburi, Thong Pha Phumi District, Pat Sadu Klang; 14°33'11"N, 98°33'94"E; 349 m; 1 Feb. 2019; leg. C. Suttinun; in alcohol; ZMKU. • 6 larvae; Kanchanaburi, Thong Pha Phumi District, Huai Pak Kok; 14°39'57"N, 98°32'04"E; 175 m; 1 Feb. 2019; leg. C. Suttinun; in alcohol; ZMKU. • 2 larvae; Kanchanaburi, Thong Pha Phumi District, Huai Pheung Ban Lung Yee; 14°58'21"N, 98°53'50"E; 709 m; 1 Feb. 2018; leg. C. Auychinda; 1 in alcohol (mouthpart); Genbank OM319584; TEKN05; TEKN06; ZMKU. • 1 larva; Ratchaburi, Suan Phueng District, Bo Klueng; 13°31'46"N, 99°14'66"E; 180 m; 25 Nov. 2018; leg. C. Suttinun; in alcohol (mouthpart); Genbank OM302269; TERB01; ZMKU. • 5 larvae; Petchaburi, Kaeng Krachan District, Huai Sat Lek; 12°38'15"N, 99°30'60"E; 166 m; 25 Feb. 2018; leg. C. Suttinun; 4 in alcohol; 1 on slide; Genbank OM302305, OM319569; TEPC02; ZMKU. • 14 larvae; Loei, Phu Luang District, Ban Non Pattana; 17°06'41"N, 101°28'72"E; 527 m; 18 Dec. 2018; leg. C. Suttinun; 10 in alcohol; 3 on slides; Genbank OM302308, OM303507; TELE01; TELE03; TELE04; ZMKU; 1 on slide; TELE02; GBIFCH00829259; MZL • 2 larvae; Chiang Rai, Mueng District, Mae Korn Stream; 19°51'77"N, 99°39'08"E; 534 m; 6 May. 2019; leg. C. Suttinun; in alcohol; ZMKU. • 2 larvae; Chiang Rai, Mueng District, Nang Lae Nai waterfall; 20°03'16"N, 99°49'28"E; 529 m; 7 May. 2019; leg. C. Suttinun; 1 in alcohol; 1 on slide; Genbank OM303508; TECR02; ZMKU. • 3 larvae; Chiang Rai, Mae Chan

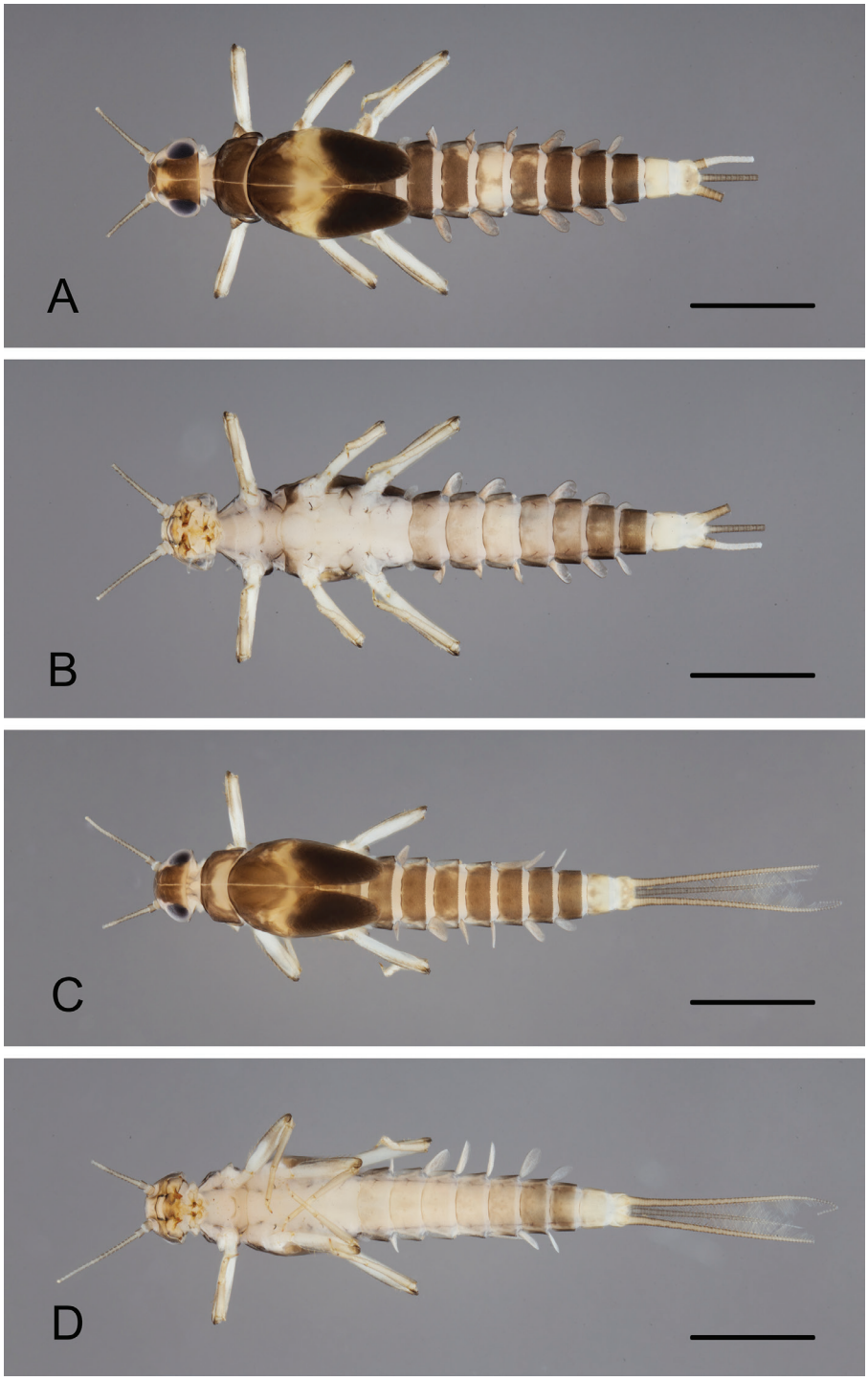


**Figure 1.** *Tenuibaetis panhai* sp. nov., larval habitus. Kanchanaburi province **A** dorsal view **B** ventral view; Loei province: **C** dorsal view **D** ventral view. Scale bar: 1 mm.

District, Huai Kang Pla waterfall; 20°05'36"N, 99°46'80"E; 519 m; 7 May. 2019; leg. C. Suttinun; 2 in alcohol; 1 on slide; Genbank OM302358; TECR01; ZMKU.

**Description.** ***Coloration*** (Fig. 1). Head dorsally brown and yellow, with a yellow marking between ocelli. Thorax dorsally brown, pronotum with (Fig. 1C) or without (Fig. 1A) posterior yellow marking; mesonotum medially with a yellow transverse band. Abdomen dorsally brown; tergite III with (Fig. 1A) or without (Fig. 1C) a pair of yellow markings on lateral sides; tergite IV yellowish with or without median brown marking; tergite V with or without anterior yellow marking; tergite VIII with or without posterior yellow marking; tergites IX–X yellow. Head and thorax ventrally whitish; abdomen ventrally light brown; sternites VI–VIII darker brown; sternites IX–X yellow. Legs light brown; dorsal, ventral, and apical femur margins darker brown with brown stripes distomedially; claws distally dark brown. Caudal filaments light brown without darker band or pattern.

**Head.** ***Antenna.*** Flagellum with lanceolate spines at apex of each segment.

***Labrum*** (Fig. 2A). Subrounded, length 0.66–0.74 × maximum width. Distal margin with medial emargination. Dorsally with submarginal arc composed of one long, pointed, simple seta medially plus two long, pointed, simple setae laterally and four long, pointed, simple setae decreasing in size along margin; dorsal surface with short, fine, simple setae scattered medially toward the basal area. Ventrally with submarginal row of setae composed of about 20 lateral long, feathery setae equal in size and a row of stout, simple setae laterally near margin.

***Right mandible*** (Fig. 2B, C). Incisors fused. Outer set with 4 denticles composed of two pointed denticles plus one larger, blunt denticle and one pointed denticle; inner sets with 4 pointed denticles; each denticle separated by a deep groove. Inner margin of innermost denticle with a row of minute teeth. Prostheca robust, apicolaterally denticulate. Margin between prostheca and mola straight, without setae. Tuft of setae at apex of mola present.

***Left mandible*** (Fig. 2D, E). Incisors fused. Outer and inner sets of pointed denticles with 3 + 3 denticles; each denticle separated by a deep groove, plus a minute intermediate denticle between sets. Inner margin of innermost denticle with minute denticles. Prostheca slightly shorter than incisor, robust, apically denticulate, with a comb-shaped structure. Margin between prostheca and mola straight without setae. Tuft of spine-like setae absent at base of mola. Subtriangular process long and wide, above level of area between prostheca and mola. Denticles of mola apically as wide as basal. Setae present at apex of mola.

Both mandibles with lateral margin almost straight. Basal half with fine, simple setae scattered over dorsal surface.

***Hypopharynx*** (Fig. 2F). Lingua slightly shorter than superlingua, longer than broad, with medial tuft of long, thin setae. Superlingua distally with a concave margin, with long, fine setae along distal margin; lateral margin rounded with simple setae along lateral margin.

***Maxilla*** (Fig. 2G). Galea-lacinia with two long, fine, simple setae under crown. Inner dorsal row of setae with three denti-setae; distal denti-seta tooth-like, middle denti-seta slender and pectinate, proximal denti-seta very long, slender, simple setae.

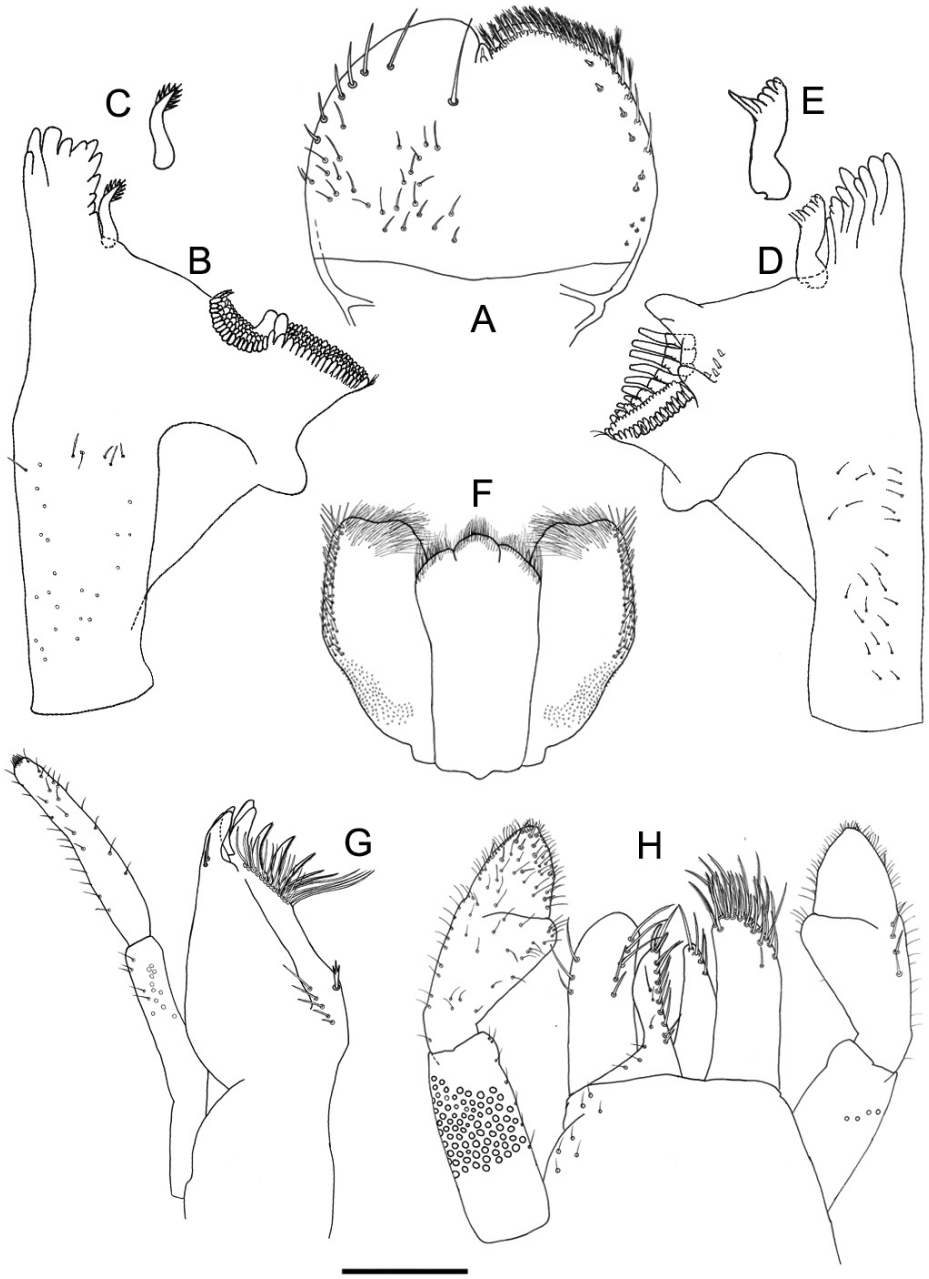


**Figure 2.** *Tenuibaetis panhai* sp. nov., larval morphology **A** labrum **B** right mandible **C** right prostheca **D** left mandible **E** left prostheca **F** hypopharynx **G** maxilla **H** labium. Scale bar: 0.1 mm.

Medially with one trifid, stout seta and five short to long, simple setae. Maxillary palp 1.4–1.5 × as long as length of galea-lacinia, 2-segmented; fine, simple setae scattered over surface of maxillary palp. Palp segment II 1.3 × length of segment I. Apex of last segment conical.

***Labium*** (Fig. 2H). Glossae basally broad, narrowing toward apex, shorter than paraglossae; inner margin with nine long, simple setae; apex with one long, simple seta and two medium, robust, pectinate setae; outer margin with four long, simple setae; dorsal surface with a long, simple seta medially; basal area with fine scattered setae. Paraglossae sub-rectangular, apically rounded, with three rows of setae, distal row of very long, pectinate, simple setae, other rows of pectinate long and medium setae; one curved, blunt, simple seta at inner apical margin; two long, simple setae in outer margin near three rows of setae; dorsal surface with one medium, simple seta anteromedially; dorsally with row of five long, simple setae parallel to inner margin, with an arc of three long, simple setae at outer margin; basal area with medium, spine-like setae scattered. Labial palp with segment I 0.8 × length of segments II and III combined. Segment I covered with micropores and few fine, simple setae. Segment II with poorly developed, apically rounded, distomedial protuberance; tuft of medium, fine, simple setae present at apex of protuberance; inner margin with medium, fine, simple setae; outer margin with short, fine, simple setae; dorsally with medium, fine, simple, scattered setae; dorsally with row of 4–6 medium, simple setae. Segment III conical, slightly asymmetrical; length subequal to width; covered with medium simple setae and stout simple setae anterolaterally.

**Thorax.** ***Hindwing pads*** (Fig. 3A). Absent.

***Foreleg*** (Fig. 3B–D). Ratio of foreleg segments 2.1:1.5:1:0.4. ***Femur.*** Length 2.9 × maximum width; dorsal margin with a row of 18–25 apically rounded, simple setae; length of setae 0.2 × maximum width of femur; anterior surface with 5–10 spatulate setae medially and about 28 acute, lanceolate setae close to ventral margin; apex rounded, with one pair of apically rounded, simple seta and two rows of stout, apically rounded, simple setae along apical margin; posterior surface with one row of stout, spatulate setae transverse anteromedially; femoral patch strongly developed. ***Tibia.*** Dorsal margin with a few short, spine-like setae and a pair of short, spine-like seta apically; ventral margin with a row of 7–13 acute, spine-like, curved setae and three long, spine-like apical setae; tibio-patella suture on basal 2/3 area with a row of eight stout, spatulate setae along suture. ***Tarsus*** (Fig. 3B, C). Dorsal margin nearly bare, with a few acute, simple setae on proximal area; ventral margin with one row of acute, curved, spine-like setae increasing apically; apex with one short, spine-like seta; claw curved, apically pointed, with one row of 11–13 denticles increasing apically; subapical setae absent.

**Abdomen.** ***Terga*** (Fig. 3H). Surface with scattered scales or scale-bases and micropores. Posterior margin of terga with row of apically, blunt, triangular spines.

***Gills*** (Fig. 3E–G). Present on segments I–VII; oval shaped. Margins serrate with small spines. Tracheation (Fig. 3F) extending from main trunk to inner and outer margins. Gill I (Fig. 3E) reduced, 0.3 × length of segment II; gills II–VI 1.2 × length of following segment; gill VII (Fig. 3G) 0.8 × length of segment VIII.

***Paraproct*** (Fig. 3I, J). Posterior margin with 5–7 pointed spines; surface with U-shaped scale base, micropores and fine, simple setae, and with a patch of notched scales (Fig. 3J); posterolateral extension (cercotractor) with 9–12 marginal spines.

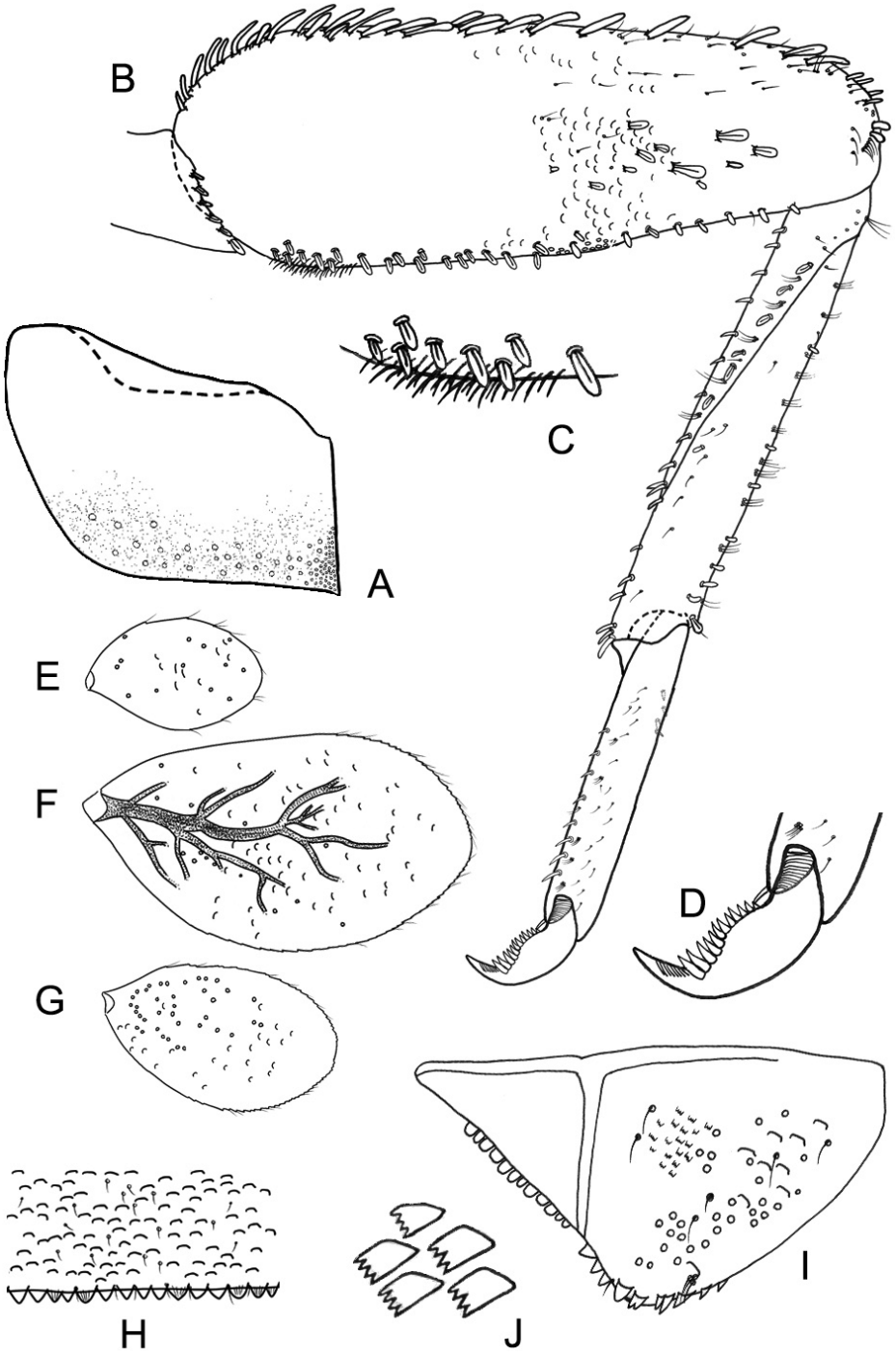


**Figure 3.** *Tenuibaetis panhai* sp. nov., larval morphology **A** metathorax without hindwing pad **B** foreleg **C** femoral patch **D** claw **E** gill I **F** gill V **G** gill VII **H** distal margin of tergite IV **I** paraproct **J** notched scales on paraproct.

***Caudal filaments*** (Fig. 1). Cerci ca. 0.5 × body length. Paracercus ca. 0.4 × body length.

**Diagnostic characters. Larva.** The main diagnosis character is the absence of hindwing pads, followed by a combination of characters: A) distinct pattern on thorax and abdomen or "Zebra form," as in Fig. 1; B) labrum dorsal submarginal arc composed of one long, pointed, simple seta medially plus two long, pointed, simple setae laterally and four long, pointed, simple setae decreasing in size along margin; C) right mandible: incisors with 4 + 4 pointed denticles, each denticle separated by a deep groove; D) left mandible: incisors with 3 + 3 pointed denticles plus a minute intermediate denticle between sets; E) hypopharynx: lingua with medial tuft of long, fine setae; superlingua lateral margin with long, simple setae; F) maxillary palp longer than galea-lacinia, apex conical; G) femur: dorsal margin with 15–25 apical rounded, simple seta, anterior surface with 5–10 spatulate setae; H) claw with a row of 11–13 denticles; I) paraproct: distal margin with 5–7 spines, surface with a patch of notched scales.

**Winged stages.** Unknown.

**Etymology.** *Tenuibaetis panhai* sp. nov. is dedicated to Professor Dr. Somsak Panha (Animal Systematics Research Unit, Department of Biology, Faculty of Science, Chulalongkorn University, Bangkok, Thailand) for his outstanding contributions to the systematics study of the fauna in Thailand.

**Distribution.** Kanchanaburi (KN), Ratchaburi (RB), Petchaburi (PC), Chiang Rai (CR), and Loei (LE) provinces of Thailand.

**Biological aspects.** The specimens were collected in headwater streams (Fig. 4A) and above waterfalls at different altitudes (150–700 m a.s.l.). The streams were mostly located in forest areas with a partly complete canopy; the substrate was dominated by pebbles, gravel, and sand. The larvae were found on the undersides of pebbles in fast-flowing water (Fig. 4B). The waterfalls were located in areas with human disturbing activity as tourist attractions. They were collected together with other mayfly species: *Cymbalcloeon sartorii* Suttinun, Gattolliat & Boonsatien, 2020 (Baetidae), *Liebebiella vera* (Baetidae), and *Afronurus* spp. (Heptageniidae).

**Molecular analysis.** COI sequences were obtained from specimens for each locality (Table 2). The K2P analysis revealed interspecific distances between *T. panhai* sp. nov. and the available *Tenuibaetis* species ranging between 17% and 27% (Table 3). The intraspecific distance was very limited within the nine sequences of *T. panhai* sp. nov. (0% to 4%).

**Table 3.** Genetic distances (COI) between sequenced specimens and MOTUs, using the Kimura 2-parameter.

| | Species | 1 | 2 | 3 | 4 | 5 |
|---|---|---|---|---|---|---|
| 1 | *T. panhai* sp. nov. | 0.00–0.05 | | | | |
| 2 | *T.* cf. *panhai* sp. I | 0.15–0.19 | 0.00–0.03 | | | |
| 3 | *T.* cf. *panhai* sp. II | 0.18–0.20 | 0.22–0.24 | 0.00 | | |
| 4 | *T. frequentus* | 0.16–0.19 | 0.18–0.19 | 0.16 | – | |
| 5 | *T. flexifemora* | 0.24–0.27 | 0.24–0.26 | 0.23 | 0.23 | 0.00 |


**Figure 4.** Type locality and larval habitats of *Tenuibaetis panhai* sp. nov. **A, B** fast-flowing water with bottom sand, pebble and gravel (Pa Chum Mai, Mae Klong headwater stream).

Sequences of eight specimens, morphologically indistinct from *T. panhai* sp. nov. present genetic distance ranging between 15% and 20% to *T. panhai* sp. nov. These eight sequences are separated into two distinct groups. To depict the genetic diversity of *Tenuibaetis* in Thailand, we propose to consider these two groups as Molecular Operational Taxonomic Units (MOTUs) corresponding respectively to *T.* cf. *panhai* sp. I (Southern) and *T.* cf. *panhai* sp. II (Chiang Dao), based on genetic evidence only (COI; Table 2). The K2P distances of *T.* cf. *panhai* sp. I and *T.* cf. *panhai* sp. II range between 22% and 24% (Table 3). The intraspecific distances within MOTUs are limited (0% to 3%).

The COI reconstruction was built by the Bayesian Interference (BI) using MrBayes (Fig. 5). Seventeen sequences of *Tenuibaetis* in Thailand are separated into two main distinct clades: the first clade includes *T. panhai* sp.nov. and *T.* cf. *panhai* sp. I while the second clade includes *T.* cf. *panhai* sp. II and *T. frequentus*.

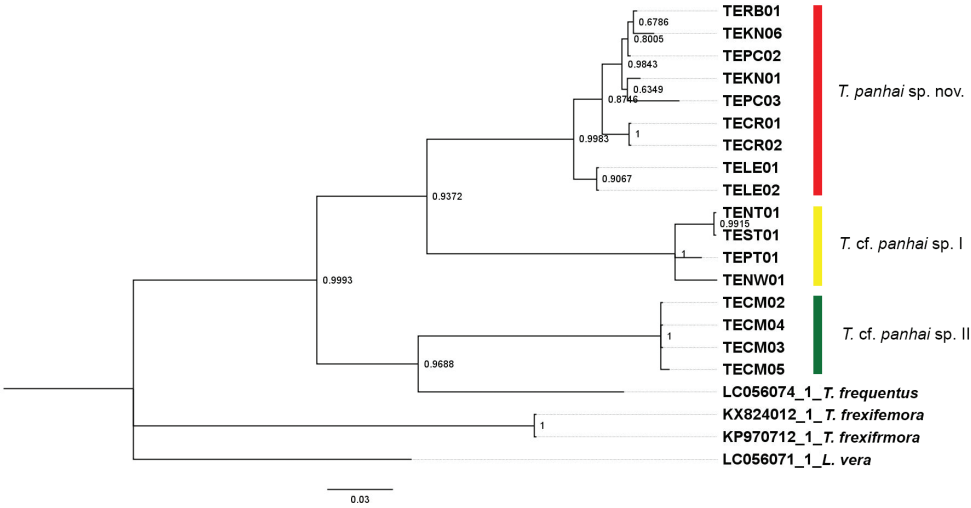


**Figure 5.** The Bayesian COI reconstruction of *Tenuibaetis* from the Oriental region. *Tenuibaetis panhai* sp. nov. (Red). *T.* cf. *panhai* sp. I (Yellow). *T.* cf. *panhai* sp. II (Green). *Liebebiella vera* (genbank accession no. LC056071) as an outgroup. The posterior probability was represented for each node.

## Discussion

*Tenuibaetis panhai* sp. nov. belongs to the genus *Tenuibaetis* based on the following characters defined by Kang et al. (1994) and Fujitani et al. (2003): mandible with a margin between the mola and prostheca without setae; a pointed apex of labial palp segment III, with segment II poorly expanded at the inner distal margin; villopore on the anteromedial corner of each femur; paraproct with a patch of notched scales medially; and robust setae with median ridge on the dorsomedian surface of the larval femur. The new species can be easily distinguished from all the other species of *Tenuibaetis* by the lack of hindwing pads. The combinations of characters commonly used

to differentiate Oriental species of *Tenuibaetis* (Kaltenbach and Gattolliat 2019) are listed in Table 4. A comparison between the new species and the other known species of *Tenuibaetis* indicates a close morphological similarity between the new species and *T. flexifemora* (from Japan) in terms of the dorsal pattern coloration, the ratio of the length vs. the width of labrum, the shape of the spines on the distal margin of terga, the ratio of the length of gill IV to gill I, and the ratio of the terminal filament to the cerci. The new species also shows similarities with *T. frequentus* (from Sri Lanka, and India) regarding the dorsal pattern coloration, the ratio of the length vs. width of the labrum and the lack of patterning, and the ratio of the length of the maxillary palp versus the galea-lacinia.

The genetic distances between the new species and MOTUs are unexpected, with a range between 15% and 20% (K2P, Table 3), which is similar to the inter-specific distance between the available *Tenuibaetis* species. Ball et al. (2005) also reported in a few cases a mean interspecific distance of 18% for congeneric mayflies

**Table 4.** Larval character states of Oriental *Tenuibaetis* species (modified from Table 1 in Kaltenbach and Gattolliat 2019, p. 21).

| | | ***T. panhai* sp. nov.** | ***T. fujitanii*** | ***T. pseudofrequentus*** | ***T. arduus*** | ***T. inornatus*** | ***T. frequentus*** |
|---|---|---|---|---|---|---|---|
| **Colouration** | Dorsal pattern | distinct pattern | rather uniform brown | distinct pattern | distinct pattern | distinct pattern | distinct pattern |
| | | (Figs 1–2 in this study) | (fig. 1a in Kaltenbach and Gattolliat 2019) | (fig. 9 in Müller-Liebenau 1985) | (fig. 27 in Kang et al. 1994) | (figs 12, 26 in Kang et al. 1994) | (fig. 10 in Müller-Liebenau and Hubbard 1985; fig. 1 in Kubendran et al. 2015) |
| **Labrum** | Length vs. width | 0.7× | 0.7× | 0.8× | 0.8× | 0.8× | 0.7× |
| | Pattern | absent | absent | Absent | absent | U-shaped dark marking | absent |
| **Maxillary palp** | Length vs. galea-lacinia | 1.45× | 1.1× | 1.3× | 1.2× | 1.15× | 1.4× |
| **Forefemur** | Number of dorsal setae | 15–23 | 19–24 | about 14 | about 13 | ? | about 15 |
| **Terga** | Spines at posterior margin | triangular, blunt; wider than long or about as wide as long | mostly rounded; wider than long | triangular, pointed; longer than wide | triangular, blunt; wider than long | triangular, blunt; wider than long | triangular, pointed; longer than wide |
| **Gills** | Tracheation | distinct, till margins | basal part of trunk | Obscure | obscure | distinct, till margins | obscure |
| | Length Gill IV / Gill I | 2.7× | 2.3× | 2.7×–3.1× | 2.3× | 1.5× | 2.0× |
| **Paraproct** | Number of marginal spines | 5–7 | about 15 | about 10 | about 14 | about 11 | about 20 |
| **Terminal filament** | Length paracerus vs. cerci | 0.7× | 0.7×–0.8× | 0.5×–0.6× | 0.76× | 0.65× | 0.6× |
| **Distribution** | | Thailand | Indonesia | Taiwan | Taiwan | Taiwan | Taiwan, Sri lanka, India |
| **References** | | Present study | Kaltenbach and Gattolliat (2019) | Müller-Liebenau (1985) | Kang et al. (1994) | Kang et al. (1994) | Müller-Liebenau and Hubbard (1985); Kubendran et al. (2015) |

in the USA and Canada. The intraspecific distances of each new species (including MOTUs) are very low, as expected, ranging from 0% to 4% (K2P). MOTUs were used for mayflies of the genus *Labiobaetis* from the Phillipines in Kaltenbach et al. (2020). This approach was originally defined and used to solve the enormous diversity of small organisms like nematodes and foraminifera (Floyd et al. 2002; Blaxter et al. 2005; Morard et al. 2016). All identified MOTUs of *Tenuibaetis* of Thailand are morphologically indistinct from *T. panhai* sp. nov., but present all the differences with the other known species of *Tenuibaetis* especially the lack of hindwing pads. We may assume the geographical and ecological factors to be the main drivers of the molecular evolution as *T.* cf. *panhai* sp. I is distributed in South of Thailand only (allopatric distribution) while *T.* cf. *panhai* sp. II was only collected in a waterfall from Chiang Dao Mountain Range, Chiang Mai province. Additional material and investigations will be necessary to confirm their status in the future. Because of the interspecific genetic distance between MOTUs and *T. panhai* sp. nov., but without morphological support, *T.* cf. *panhai* sp. I and *T.* cf. *panhai* sp. II remain considered as species hypotheses for now without further treatment in this paper.

In conclusion, the genus *Tenuibaetis* is widespread and common in Thailand. Due to its pattern (the "Zebra form"), it can be easily recognized even in the field. The distribution should be used for taxa delimitation. However, definitive species attributions of additional populations will require molecular confirmation. We propose two MOTUs; they will be considered or not as valid species in the future.

The results of this study provide a better understanding of the distribution of this genus, as Thailand is located in the middle of the distribution of other known Oriental species, but the genus was not reported from this area until this study (Fig. 6). We expect a broader distribution of the genus in Thailand, especially in the southern and eastern parts, as well as in rather poorly sampled areas, such as Myanmar, continental Malaysia, Laos, Cambodia, and Vietnam.

## Key to Oriental species of the genus *Tenuibaetis*

1 Hindwing pads present (Müller-Liebenau and Hubbard 1985, fig. 1, p. 540) ..... **2**

– Hindwing pads absent (Fig. 3A). Denticles on both mandibles pointed, with deep groove between denticle; Length of maxillary palp vs. galea-lacinia about 1.4–1.5×; about 8 setae along tibia-patella suture on tibia (Figs 2B, 2D, 2G, 3B) ..... ***T. panhai* sp. nov.**

2 Labrum without U-shaped dark brown pattern, Gills without or with poorly developed tracheation (Kang et al. 1994, fig. 11A, L, p. 27; Kubendran et al. 2015, figs 4 (p. 190), 13–14 (p. 191)) ..... **3**

– Labrum with U-shaped dark brown pattern; Gills with developed tracheation (Kang et al. 1994, fig. 13A, K, p. 30) ..... ***T. inornatus***

3 Abdominal tergites with distinct pattern coloration (Kang et al. 1994, figs 25, 27, p. 42; Kubendran et al. 2015, figs 1–2, p. 190); spines at posterior margin of terga mostly triangular (Kang et al. 1994, figs 11K, 14L, p. 27; Kubendran et al. 2015, fig. 16, p. 191) ..... **4**

– Abdominal tergites rather uniform brown; spines at posterior margin terga mostly rounded (Kaltenbach and Gattolliat 2019, figs 1 (p. 16), 3c (p. 19)) . ..... ***T. fujitanii***

4 Dorsal margin of tibiae and tarsi with short spine-like setae (Müller-Liebenau and Hubbard 1985, fig. 1g, 540). Spines at posterior margin of terga mostly triangular pointed, longer than wide (Kang et al. 1994, fig. 11K, p. 27; Kubendran et al. 2015, fig. 16, p. 191); Length of terminal filament vs. cerci about 0.6× (Müller-Liebenau and Hubbard 1985, fig. 1i, p. 540; Kubendran et al. 2015, figs 1–2, p. 190) ..... **5**

– Dorsal margin of tibiae and tarsi with only thin setae. Spines at posterior margin of terga mostly triangular blunt, wider than long (Kang et al. 1994, fig. 14L, p. 31); Length of terminal filament vs. cerci 0.75×..... ***T. arduus***

5 Length of gill IV 2.0× of gill I; posterior margin of paraproct with about 20 spines (Müller-Liebenau and Hubbard 1985, fig. 1h, j, p. 540; Kubendran et al. 2015, fig. 15, p. 191) ..... ***T. frequentus***

– Length of gill IV 2.7–3.0× of gill I; posterior margin of paraproct with about 10 spines (Kang et al. 1994, fig. 11I, L, p. 27) ..... ***T. pseudofrequentus***

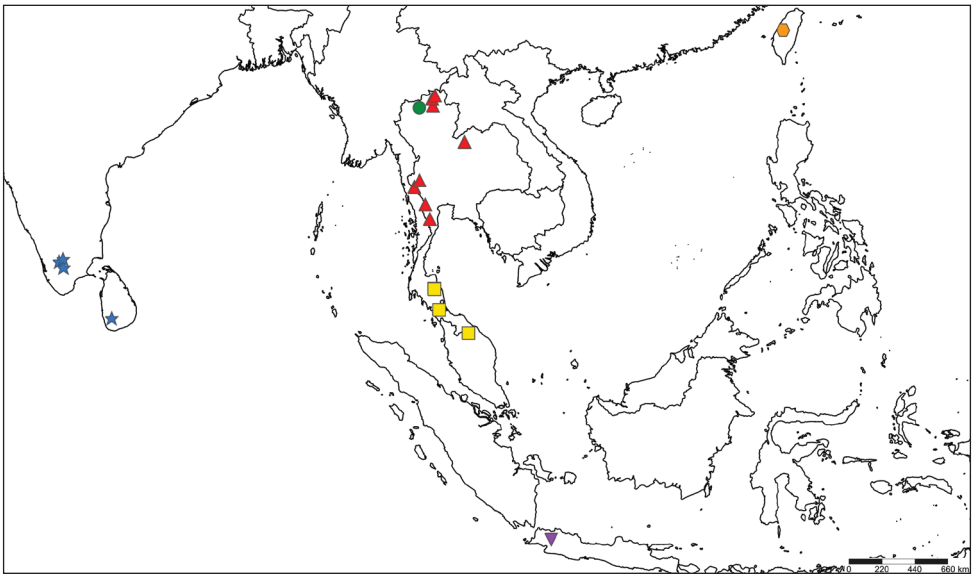


**Figure 6.** Distribution of the genus *Tenuibaetis* in the Oriental region. *Tenuibaetis panhai* sp. nov. (Triangular: Red). *T.* cf. *panhai* sp. I (Square: Yellow). *T.* cf. *panhai* sp. II (Circle: Green). *T. fujitanii* (Inverse triangular: Purple). *T. arduus*, *T. inornatus*, *T. pseudofrequentus* (Hexagon: Orange). *T. frequentus* (Star: Blue).

## Acknowledgements

The project was funded by a Science Achievement Scholarship of Thailand (SAST). This research has been supported by the Centre of Excellence on Biodiversity (BDC) Office of Higher Education Commission (BDC-PG2-161004). This research was approved by the Institutional Animal Care and Use Committee, Faculty of Science, Kasetsart University, Thailand under Project number ACKU63-SCI-006. We are most grateful to our colleagues for assistance during field trips. We would like to thank the MZL team (Museum of Zoology, Lausanne), the Department of Zoology and the Faculty of Science at Kasetsart University in Bangkok for their assistance and use of their facilities.

## References

Balaji A, Vatheeswaran M, Venkataraman K (1990) Laboratory observations on the life cycle patterns of two *Baetis* spp. Geobios 17: 15–17.

Ball SL, Hebert PDN, Burian SK, Webb JM (2005) Biological identifications of mayflies (Ephemeroptera) using DNA barcodes. Journal of the North American Benthological Society 24: 508–524. https://doi.org/10.1899/04-142.1

Chakrabarty P, Warren M, Page L (2013) GenSeq: An updated nomenclature and ranking for genetic sequences from type and non-type sources. ZooKeys 346: 29–41. https://doi.org/10.3897/zookeys.346.5753

Folmer O, Black M, Hoeh W, Lutz R, Vrijenhoek R (1994) DNA primers for amplification of mitochondrial cytochrome c oxidase subunit I from diverse metazoan invertebrates. Molecular Marine Biology and Biotechnology 3: 294–299.

Fujitani T, Hirowatari T, Tanida K (2003a) Genera and species of Baetidae in Japan: *Nigrobaetis*, *Alainites*, *Labiobaetis*, and *Tenuibaetis* n. stat. (Ephemeroptera). Limnology 4: 121–129. https://doi.org/10.1007/s10201-003-0105-2

Fujitani T, Hirowatari T, Tanida K (2003b) Nymphs of *Nigrobaetis*, *Alainites*, *Labiobaetis*, *Tenuibaetis* and *Baetis* from Japan (Ephemeroptera: Baetidae): diagnosis and keys for genera and species. In: Gaino E (Ed.) Research update on Ephemeroptera & Plecoptera, University of Perugia, Perugia, 127–133.

Fujitani T, Kobayashi N, Hirowatari T, Tanida K (2011) Three species of a genus *Tenuibaetis* (Ephemeroptera: Baetidae) from Japan, with description of a new species. Limnology 12: 213–223. https://doi.org/10.1007/s10201-010-0342-0

Gose (1980) The mayflies of Japan 7. Aquabiology 2: 122–123. [In Japanese]

Kaltenbach T, Gattolliat J-L (2019) A new species of *Tenuibaetis* Kang & Yang, 1994 from Indonesia (Ephemeroptera, Baetidae). ZooKeys 820: 13–23. https://doi.org/10.3897/zookeys.820.31487

Kaltenbach T, Garces JM, Gattolliat J-L (2020) A new genus of Baetidae (Insecta, Ephemeroptera) from Southeast Asia. European Journal of Taxonomy 612: 1–32. https://doi.org/10.5852/ejt.2020.612

Kang S-C, Chang H-C, Yang C-T (1994) A revision of the genus *Baetis* in Taiwan (Ephemeroptera, Baetidae). Journal of Taiwan Museum 47: 9–44.

Kimura M (1980) A simple method for estimating evolutionary rates of base substitutions through comparative studies of nucleotide sequences. Journal of Molecular Evolution 16: 111–120. https://doi.org/10.1007/BF01731581

Kluge NJ (2016) A new subgenus *Oculogaster* subgen. n. for viviparous representatives of *Procloeon* s. l., with discussion about status of the generic name *Austrocloeon* Barnard 1932 and the species name *africanum* Esben-Petersen 1913 [*Cloeon*] (Ephemeroptera, Baetidae). Zootaxa 4107: 491–516. https://doi.org/10.11646/zootaxa.4107.4.2

Kluge NJ (2021) Ephemeroptera of the world. www.insecta.bio.spbu.ru/z/Eph-spp/Contents.htm [Retrieved 28.08.2021]

Kluge NJ, Novikova EA (2017) Occurrence of *Anafroptilum* Kluge 2012 (Ephemeroptera: Baetidae) in Oriental Region. Zootaxa 4282: 453–472. https://doi.org/10.11646/zootaxa.4282.3.2

Kluge NJ, Godunko RJ, Svitok (2020) Nomenclatural changes in *Centroptella* Braasch & Soldán, 1980 (Ephemeroptera, Baetidae). ZooKeys 914: 81–125. https://doi.org/10.3897/zookeys.914.46652

Kluge NJ, Suttinun C (2020) Review of the Oriental genus *Indocloeon* Müller-Liebenau 1982 (Ephemeroptera: Baetidae) with descriptions of two new species. Zootaxa 4779: 451–484. https://doi.org/10.11646/zootaxa.4779.4.1

Kubendran T, Balasubramanian C, Selvakumar C, Gattolliat J-L, Sivaramakrishnan KG (2015) Contribution to the knowledge of *Tenuibaetis* Kang & Yang 1994, *Nigrobaetis* Novikova & Kluge, 1987 and *Labiobaetis* Novikova & Kluge (Ephemeroptera: Baetidae) from the Western Ghats (India). Zootaxa 3957: 188–200. https://doi.org/10.11646/zootaxa.3957.2.3

Kumar S, Stecher G, Li M, Knyaz C, Tamura K (2018) MEGA X: Molecular Evolutionary Genetics Analysis across computing platforms. Molecular Biology and Evolution 35: 1547–1549. https://doi.org/10.1093/molbev/msy096

Müller-Liebenau I (1985) Baetidae from Taiwan with remarks on *Baetiella* Ueno, 1931 (Insecta, Ephemeroptera). Archive of Hydrobiology 104: 93–110.

Müller-Liebenau I, Hubbard MD (1985) Baetidae from Sri Lanka with some general remarks on the Baetidae of the Oriental region (Insecta: Ephemeroptera). Florida Entomologist 68: 537–561. https://doi.org/10.2307/3494855

Tong X, Dudgeon D (2000) *Baetiella* (Ephemeroptera: Baetidae) in Hong Kong, with description of a new species. Entomological News 111: 143–148.

Tungpairojwong N, Bae YJ (2015) Three new species of *Procloeon* (Ephemeroptera: Baetidae) from Thailand. Animal Systematics, Evolution and Diversity 31: 22–30. https://doi.org/10.5635/ASED.2015.31.1.022

Sanger F, Nicklen S, Coulson AR (1977) DNA sequencing with chain-terminating inhibitors. Proceedings of the National Academy of Sciences 74: 5463–5467. https://doi.org/10.1073/pnas.74.12.5463

Shorthouse DP (2010) SimpleMappr, an online tool to produce publication-quality point maps. https://www.simplemappr.net [Retrieved 28.08.2021]

Sivaramakrishnan KG, Venkataraman K (1990) Abundance, altitudinal distribution and swarming of Ephemeroptera in Palani hills, South India. In: Campbell IC (Ed.) Mayflies and Stoneflies: Life Histories and Biology. Series Entomologica Vol. 44, Kluwer Academic Publishers, Dordrecht, 209–213. https://doi.org/10.1007/978-94-009-2397-3_24

Suttinun C (2021) Systematics of the family Baetidae (Order Ephemeroptera) in Southern and Western of Thailand. Doctoral dissertation, Kasetsart University, Bangkok.

Sutthinun C, Gattolliat JL, Boonsoong B (2018) A new species of *Platybaetis* Müller-Liebenau, 1980 (Ephemeroptera: Baetidae) from Thailand, with description of the imago of *Platybaetis bishopi* Müller-Liebenau, 1980. Zootaxa 4378: 85–97. https://doi.org/10.11646/zootaxa.4378.1.5

Suttinun C, Gattolliat JL, Boonsoong B (2020) *Cymbalcloeon* gen. nov., an incredible new mayfly genus (Ephemeroptera: Baetidae) from Thailand. PLoS ONE 15: e0240635. https://doi.org/10.1371/journal.pone.0240635

Suttinun C, Kaltenbach T, Gattolliat J-L, Boonsoong B (2021) A new species and first record of the genus *Procerobaetis* Kaltenbach & Gattolliat, 2020 (Ephemeroptera, Baetidae) from Thailand. ZooKeys 1023: 13–28. https://doi.org/10.3897/zookeys.1023.61081

Vuataz L, Sartori M, Wagner A, Monaghan MT (2011) Toward a DNA taxonomy of Alpine *Rhithrogena* (Ephemeroptera: Heptagenidae) using a mixed Yule-coalescent analysis of mitochondrial and nuclear DNA. PLoS ONE 6: 1–11. https://doi.org/10.1371/journal.pone.0019728

Waltz RD, McCafferty WP (1997) New generic synonymies in Baetidae (Ephemeroptera). Entomological News 108: 134–140.

ZooKeys 1084: 183–199 (2022)
doi: 10.3897/zookeys.1084.78744
https://zookeys.pensoft.net

RESEARCH ARTICLE

A peer-reviewed open-access journal
ZooKeys
Launched to accelerate biodiversity research

# The Oriental millipede genus *Nepalella* Shear, 1979, with the description of a new species from Thailand and an updated key (Diplopoda, Chordeumatida, Megalotylidae)

Natdanai Likhitrakarn[1,2], Sergei I. Golovatch[3], Somsak Panha[4,5]

**1** *Division of Plant Protection, Faculty of Agricultural Production, Maejo University, Chiang Mai, 50290, Thailand* **2** *Biodiversity and Utilization Research Center of Maejo University, Maejo University, Chiang Mai, 50290, Thailand* **3** *Institute for Problems of Ecology and Evolution, Russian Academy of Sciences, Leninsky pr. 33, Moscow 119071, Russia* **4** *Animal Systematics Research Unit, Department of Biology, Faculty of Science, Chulalongkorn University, Bangkok, 10330, Thailand* **5** *Academy of Science, The Royal Society of Thailand, Bangkok 10300, Thailand*

Corresponding author: Somsak Panha (somsak.pan@chula.ac.th)

Academic editor: Dragan Antić | Received 1 December 2021 | Accepted 10 January 2022 | Published 1 February 2022

*http://zoobank.org/42DE4083-042B-4F1B-ACDD-D126C67ACC87*

**Citation:** Likhitrakarn N, Golovatch SI, Panha S (2022) The Oriental millipede genus *Nepalella* Shear, 1979, with the description of a new species from Thailand and an updated key (Diplopoda, Chordeumatida, Megalotylidae). ZooKeys 1084: 183–199. https://doi.org/10.3897/zookeys.1084.78744

## Abstract

The Oriental genus *Nepalella* is reviewed, rediagnosed and shown to comprise 28 species, including *N. siamensis* **sp. nov.** from southeastern Thailand. All *Nepalella* species are keyed, and their distributions mapped, being highly localized and mainly allopatric. Unlike most congeners, which are largely confined to subtropical environments (including montane to high-montane conditions, up to 3800 m a.s.l.) or karst caves (eight species, all in southern China alone), the new species is the southernmost in the distribution area of the entire genus, also being among the very few (four) that are restricted to lowland, purely tropical habitats.

## Keywords

Distribution, Indochina, key, taxonomy

## Introduction

*Nepalella* Shear, 1979 is one of the relatively few Indo-Malayan genera of the millipede order Chordeunatida and only the second in the small family Megalotylidae (Enghoff et al. 2015). Unlike the oligotypic, more boreal, East Asian *Megalotyla* Golovatch, in Golovatch and Mikhaljova 1978, represented by only two species from the Russian Far East or North Korea, *Nepalella* is far more southerly in distribution, being also regarded as one of the most species-rich diplopod genera in the entire Oriental Realm (Golovatch et al. 2006b).

*Nepalella* is presently known to comprise 27 described species ranging from Nepal (10 species) in the west, southern China (12 species) in the north, through Myanmar and northern Thailand in the south (2 species each), to northern Vietnam (1 species) in the east (Liu et al. 2017b; Fig. 1). Most species of *Nepalella* are only known from a single locality, being highly localized in distribution (Table 1, Fig. 1). This concerns not only the rather numerous cavernicoles (eight species, largely presumed troglobionts confined to karst caves in southern China), but also epigean congeners, among which most are montane (>800 m a.s.l.) to high-montane (2200–3800 m a.s.l.) and allopatric (Table 1), with only two pairs that have been found to occur syntopically (Shear 2002; Liu et al. 2017b). Some *Nepalella* species are among the largest Chordeumatida globally and they mainly appear to be restricted to subtropical rather than purely tropical environments, all lying between 23.5° and 34°N (Fig. 1), whereas lowland, typically tropical encounters are only very few.

Therefore, the discovery of another lowland, tropical species of *Nepalella*, this time in southeastern Thailand, is noteworthy, especially as it represents both the southernmost and the most lowland congener reported to date. The new species was collected in a dipterocarp forest in the Ta Phraya National Park, Sa Kaeo Province, Thailand (Fig. 1). The opportunity is also taken to update the previous key to *Nepalella* spp. (Golovatch et al. 2006b) and to revisit its taxonomy and distribution.

## Materials and methods

Material was euthanized using a two-step method following Guidelines for the Euthanasia of Animals (AVMA 2013). Specimens were then preserved in 75% ethanol for morphological observations which were carried out in the laboratory. The specimens were examined, measured and photographed under a Nikon SMZ 745T trinocular stereo microscope, equipped with a Canon EOS 5DS R digital SLR camera. Digital images obtained were processed and edited with Adobe Photoshop CS5. Line drawings were based on photographs and examined under a stereo microscope equipped with a digital SLR camera. Scanning electron micrographs (**SEM**) of gonopods coated with a 8 nm gold layer using a CCU-010 high vacuum sputter and a carbon coater (Safematic) were imaged with a TESCAN VEGA3 scanning electron microscope operated at 5 keV of acceleration voltage and returned to alcohol after SEM examination. The images were enhanced and arranged in plates with Adobe Photoshop CS6 software. Collecting sites were located by GPS WGS84 datum using a Garmin GPSMAP 60

**Table 1.** Checklist of all described *Nepalella* species, arranged in alphabetic order and supplied with geographic details (Shear 1979, 1987, 1999, 2002; Golovatch 1983; Mauriès 1988; Golovatch et al. 2006a, 2006b; Liu et al. 2017b).

| No. | Species | Locality |
|---|---|---|
| 1 | *Nepalella birmanica* Mauriès, 1988 | Myanmar, Kambaiti (2270 m) |
| 2 | *Nepalella caeca* Shear, 1999 | China, Guizhou Province, Shuicheng County, Cave Anjia Yan; same County, Cave Shendongmigong (26°35'15"N, 104°59'47"E, 1900 m) |
| 3 | *Nepalella deharvengi* Mauriès, 1988 | Nepal, Sagarmatha Province, trace of the Tomba-Kosi in Namche Bazar: Sété (2900–3250 m); same locality (2900 m); same locality, above Sété (3000–3300 m); same locality, Sété pass (Abies) (3000–3400 m); same locality (3300–3500 m) |
| 4 | *Nepalella gairiensis* Mauriès, 1988 | Nepal, Sagarmatha Province, trace of the Tomba-Kosi in Namche Bazar: Gairi; same locality, chasse à vue |
| 5 | *Nepalella grandis* Golovatch, Geoffroy & Mauriès, 2006a | China, Yunnan Province, Zheng Xiong County, Cave Bai Yin Dong |
| 6 | *Nepalella grandoides* Golovatch, Geoffroy & Mauriès, 2006b | China, Sichuan Province, Beichuan County, Cave Yuan Dong; same County Cave Black Wind Dong |
| 7 | *Nepalella griswoldi* Shear, 2002 | China, Yunnan Province, Baoshan Prefecture, Mountain Gaoligong, Luoshuidong, 28 air km East of Teng Chong, (24°57'N, 98°45'E, 2300 m); same Prefecture, Mountain Gaoligong, Namkang, 36 air km Southeast of Teng Chong (24°50'N, 98°47'E, 2100 m) |
| 8 | *Nepalella gunsa* Shear, 1987 | Nepal, Taplejung District, south of Gunsa (=Ghunsa), (3800–3600 m) |
| 9 | *Nepalella inthanonae* Mauriès, 1988 | Thailand, Chiang Mai Province, Doi Inthanon National Park (2000–2540 m) |
| 10 | *Nepalella jaljalae* Mauriès, 1988 | Nepal, Kosi Province, Jaljale Himal, forest in south of Mangsingma, 2200 m (Mauriès 1988) |
| 11 | *Nepalella jinfoshan* Liu, in Liu et al. 2017b | China, Chongqin Province, Jinfoshan, Cave Houshan Dong (28°58'44"N, 107°11'20"E, 1500 m); same locality, Cave Lingguan Dong (29°01'10"N, 107°10'28"E, 2100 m) |
| 12 | *Nepalella kavanaughi* Shear, 2002 | China, Yunnan Province, Nujiang Prefecture, Pianma, Mountain Gaoligong, native forest (25°59'N, 98°40'E, 2500 m) |
| 13 | *Nepalella khumbua* Shear, 1979 | Nepal, Kumbu, Mt. Everest region, confluence of Phunki and Imja Drangka, northeast of Kumjung (3250–3300 m) |
| 14 | *Nepalella lobata* Liu, in Liu et al. 2017b | China, Sichuan Province, Mianyang City, Beichuan County, Cave Liangshui Dong (31°55'30"N, 104°40'56"E, 1000 m) |
| 15 | *Nepalella magna* Shear, 2002 | China, Yunnan Province, Baoshan Prefecture, Mountain Gaoligong, Luoshuidong, 28 air km East of Teng Chong (24°57'N, 98°45'E, 2300 m) |
| 16 | *Nepalella marmorata* Golovatch, Geoffroy & Mauriès, 2006a | China, Sichuan Province, Zin Long County, Snake Mouth Cave; same County, Cave Three Eyes (Trois Yeux) (AKL) |
| 17 | *Nepalella pallida* Mauriès, 1988 | Myanmar, Kambaiti (2270 m) |
| 18 | *Nepalella phulcokia* Mauriès, 1988 | Nepal, Kathmandu District, Phulcoki (2250 m); same locality (2650 m) |
| 19 | *Nepalella pianma* Shear, 2002 | China, Yunnan Province, Nujiang Prefecture, Pianma, Mountain Gaoligong, native forest (25°59'N, 98°40'E, 2500 m) |
| 20 | *Nepalella ringmoensis* Mauriès, 1988 | Nepal, Sagarmatha Province, trace of the Tomba-Kosi in Namche Bazar: Gonda (before Ringmo) (2750–3000 m) |
| 21 | *Nepalella siamensis* sp. nov. | Thailand, Sa Kaeo Province, Ta Phraya District, Ta Phraya National Park (14°08'22"N, 102°40'11"E, 183 m) |
| 22 | *Nepalella taiensis* Mauriès, 1988 | Thailand, Chiang Mai Province, Doi Pha Hom Pok, northwest of Fang (1550–1750 m) |
| 23 | *Nepalella taplejunga* Shear, 1987 | Nepal, Taplejung District, ridge Lasse Dhara and pasture Lassetham (3000–3300 m) |
| 24 | *Nepalella thodunga* Shear, 1979 | Nepal, Thodung near Jiri and Those (3200 m) |
| 25 | *Nepalella tragsindola* Mauriès, 1988 | Nepal, Sagarmatha Province, trace of the Tomba-Kosi in Namche Bazar: east of Tragsindo-La (2450–2650 m) |
| 26 | *Nepalella troglodytes* Liu, in Liu et al. 2017b | China, Guizhou Province, Guiyang City, Xifeng County, Hejiadong Village, Cave Hejia Dong (27°02'31"N, 106°31'40"E, 1200 m); same county, Mushan Village, Cave Zhangkou Dong (27°04'10"N, 106°32'55"E, 1300 m); same province, Qiannan Zizhizhou, Longli County, Cave Feilong Dong (26°27'11"N, 106°58'46"E, 1200 m); same province, Qiannan Zizhizhou, Fuquan County, Cave Sanlou Dong (26°56'46"N, 107°18'47"E, 1280 m) |
| 27 | *Nepalella vietnamica* Golovatch, 1983 | Vietnam, Yen Bai Province, Chay valley, Lục Yên (300 m) |
| 28 | *Nepalella wangi* Liu, in Liu et al. 2017b | China, Chongqin Province, Wulong County, Huangying Town, Qimenxia, Cave I Dong (29°10'33"N, 107°42'12"E, 1300 m) |

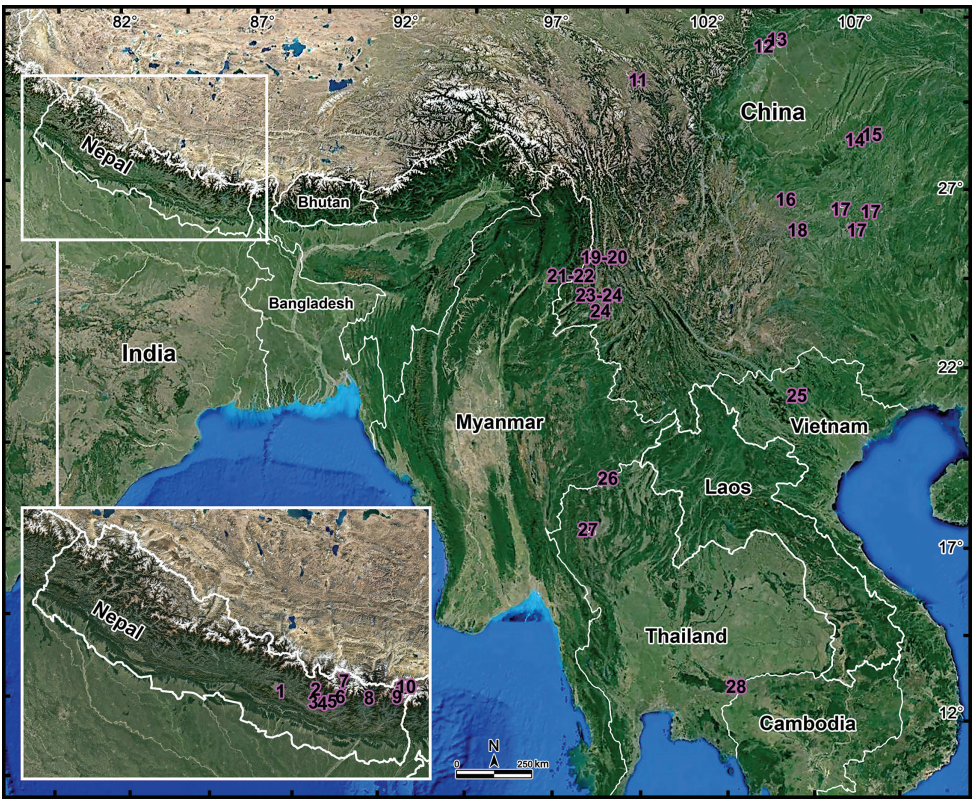


**Figure 1.** Distributions of *Nepalella* species (28 species), arranged from northwest to southeast **1** *N. phulcokia* Mauriès, 1988 **2** *N. gairiensis* Mauriès, 1988 **3** *N. thodunga* Shear, 1979 **4** *N. deharvengi* Mauriès, 1988 **5** *N. ringmoensis* Mauriès, 1988 **6** *N. tragsindola* Mauriès, 1988 **7** *N. khumbua* Shear, 1979 **8** *N. jaljalae* Mauriès, 1988 **9** *N. taplejunga* Shear, 1987 **10** *N. gunsa* Shear, 1987 **11** *N. marmorata* Golovatch, Geoffroy & Mauriès, 2006 **12** *N. grandoides* Golovatch, Geoffroy & Mauriès, 2006 **13** *N. lobata* Liu, in Liu et al. 2017 **14** *N. jinfoshan* Liu, in Liu et al. 2017 **15** *N. wangi* Liu, in Liu et al. 2017 **16** *N. grandis* Golovatch, Geoffroy & Mauriès, 2006 **17** *N. troglodytes* Liu, in Liu et al. 2017 **18** *N. caeca* Shear, 1999 **19** *N. kavanaughi* Shear, 2002 **20** *N. pianma* Shear, 2002 **21** *N. pallida* Mauriès, 1988 **22** *N. birmanica* Mauriès, 1988 **23** *N. magna* Shear, 2002 **24** *N. griswoldi* Shear, 2002 **25** *N. vietnamica* Golovatch, 1983 **26** *N. taiensis* Mauriès, 1988 **27** *N. inthanonae* Mauriès, 1988 **28** *N. siamensis* sp. nov.

CSx, and all coordinates and elevations were checked with Google Earth. The holotype of *Nepalella siamensis* sp. nov. is housed in the Museum of Zoology, Chulalongkorn University (**CUMZ**), Bangkok, Thailand. The Animal Care and Use Protocol Review No. 1723018 was applied.

In the synonymy sections, D stands for the original description and/or subsequent descriptive notes, K for the appearance in a key, L for the appearance in a species list, and M for a mention.

Terminology concerning gonopodal and somatic structures, including the following abbreviations used in the text, mostly follows Spelda (2001), Golovatch et al. (2006a) and Liu et al. (2017b).

Abbreviations of certain gonopodal structures in the figures are explained both in the text and figure captions.

**CIX** macrochaetal index; distance between the exterior and median macrochaeta divided by the distance between the interior and median macrocheata;

**MA** macrochaetal angle; formed between the arm from the median and exterior macrochaetae and that between the median and interior macrochaetae;

**MIX** median index; distance between the interior macrochaeta and axial (longitudinal) suture divided by the distance between the interior and median macrochaeta;

**PIX** paraterga index; distance between the edges of both pataterga and the edges of the prozonite divided by double the length of a paratergum.

## Taxonomy

### Family Megalotylidae Golovatch, in Golovatch and Mikhaljova 1978

#### Genus *Nepalella* Shear, 1979

*Nepalella* Shear, 1979: 126, D, K.

*Nepalella* – Golovatch 1983: 126, D; Shear 1987: 237, D; 1999: 2, D; 2002: 65, D; Mauriès 1988: 26, D; Golovatch et al. 2006a: 83, M, K; 2006b: 84, M; Liu et al. 2017b: 455, M, K; Golovatch and Liu 2020, L, M.

**Diagnosis.** The millipede genus *Nepalella* Shear, 1979 as a member of the family Megalotylidae is mainly distinguished from *Megalotyla*, the only other component genus of the family, by the anterior gonopods still showing weakly developed coxites placed on a relatively small, central sternum (versus coxites completely absent from a larger sternal plate in *Megalotyla*) (Enghoff et al. 2015).

**Brief description.** Body medium- to large-sized (ca 10–42 mm long, ca 0.64–3.2 mm wide), with 28 or 30 segments. Mentum not divided. Paraterga either distinct keels or small bulges, or missing. ♂ legs 3–7 often distinctly and increasingly crassate, some with femoral knobs. ♂ legs 10 with coxal glands, but ♂ legs 11 either with or without coxal glands. Female genitalia often species-characteristic.

Anterior gonopods strongly reduced, consisting of only a small sternal (coxosternal?) plate with a median lamellate process and two lateral spikes (coxites). Posterior gonopods with large and bipartite coxites, divisions being clearly visible when seen in anterior view, either branching or simple; lateral division often in the form of a broad, flat plate turned with its axis parallel to body midline. Posteriorly, at least one branch covered with fine cuticular fimbriae present, entire posterior surface of coxite may appear densely hairy. Telopodites may be quite small, typically reduced to a prefemur and a femur, the latter turned sharply dorsad.

**Type species.** *Nepalella khumbua* Shear, 1979, by original designation.

**Other species included.** *Nepalella birmanica* Mauriès, 1988, *N. caeca* Shear, 1999, *N. deharvengi* Mauriès, 1988, *N. gairiensis* Mauriès, 1988, *N. grandis* Golovatch, Geoffroy & Mauriès, 2006, *N. grandoides* Golovatch, Geoffroy & Mauriès, 2006, *N. griswoldi* Shear, 2002, *N. gunsa* Shear, 1987, *N. inthanonae* Mauriès, 1988, *N. jaljalae* Mauriès, 1988, *N. jinfoshan* Liu, in Liu et al. 2017b, *N. kavanaughi* Shear, 2002, *N. lobata* Liu in Liu et al. 2017b, *N. magna* Shear, 2002, *N. marmorata* Golovatch, Geoffroy & Mauriès, 2006, *N. pallida* Mauriès, 1988, *N. phulcokia* Mauriès, 1988, *N. pianma* Shear, 2002, *N. ringmoensis* Mauriès, 1988, *N. taiensis* Mauriès, 1988, *N. taplejunga* Shear, 1987, *N. thodunga* Shear, 1979, *N. tragsindola* Mauriès, 1988, *N. troglodytes* Liu, in Liu et al. 2017b, *N. vietnamica* Golovatch, 1983, *N. wangi* Liu, in Liu et al. 2017b, *N. siamensis* sp. nov.

**Distribution.** Nepal, southern China, Myanmar, northern and southeastern Thailand, and northern Vietnam (Fig. 1).

**A brief historical account.** The genus *Nepalella* was first established by Shear (1979), based on two new species from Nepal, including characters of the female vulvae (= cyphopods) added to both descriptions. Golovatch (1983) described a new species from northern Vietnam and, together with *Megalotyla*, assigned it to the family Megalotylidae. Shear (1987) added further two new species from Nepal, this time using only male specimens for descriptions.

Mauriès (1988) published ten new *Nepalella* species from Nepal, Myanmar or Thailand, including descriptions of female genitalia that followed Shear's (1979) pattern. Although the morphological differences in the vulvae were often found species-specific, Mauriès (1988) preferred not to describe new species based solely on female material.

Shear (1999, 2002) reviewed *Nepalella* and described five new species from China, including *N. magna*, the first to be named based on four female specimens alone. That species was particularly large in size, showed morphologically distinctive vulvae, and found coexisting in syntopy with both *N. griswoldi* and *Vieteuma longi* Shear, 2002, the latter taxon another chordeumatidan genus and family (Shear 2002).

Golovatch et al. (2006a, b) described a further three *Nepalella* from Chinese caves and provided a key to all species then known in the genus. More recently, Liu et al. (2017b) published four new species and two new records of *Nepalella*, including a key to, and a distribution map for, all 12 species of *Nepalella* from China. This latter study also pioneered barcoding in *Nepalella*, providing the first molecular-based phylogeny of a chordeumatidan genus outside Europe.

## Description of a new species

***Nepalella siamensis* sp. nov.**
http://zoobank.org/3768467C-2FB4-4E2F-88A8-3977AE5ADDFF
Figs 2–5

**Holotype.** ♂ (CUMZ), Thailand, Sa Kaeo Province, Ta Phraya District, Ta Phraya National Park, 183 m a.s.l., 14°08'22"N, 102°40'11"E, 27.10.2010, leg. N. Likhitrakarn and S.I. Golovatch. The holotype of *Nepalella siamensis* sp. nov. is housed in the Museum of Zoology, Chulalongkorn University (CUMZ), Bangkok, Thailand.

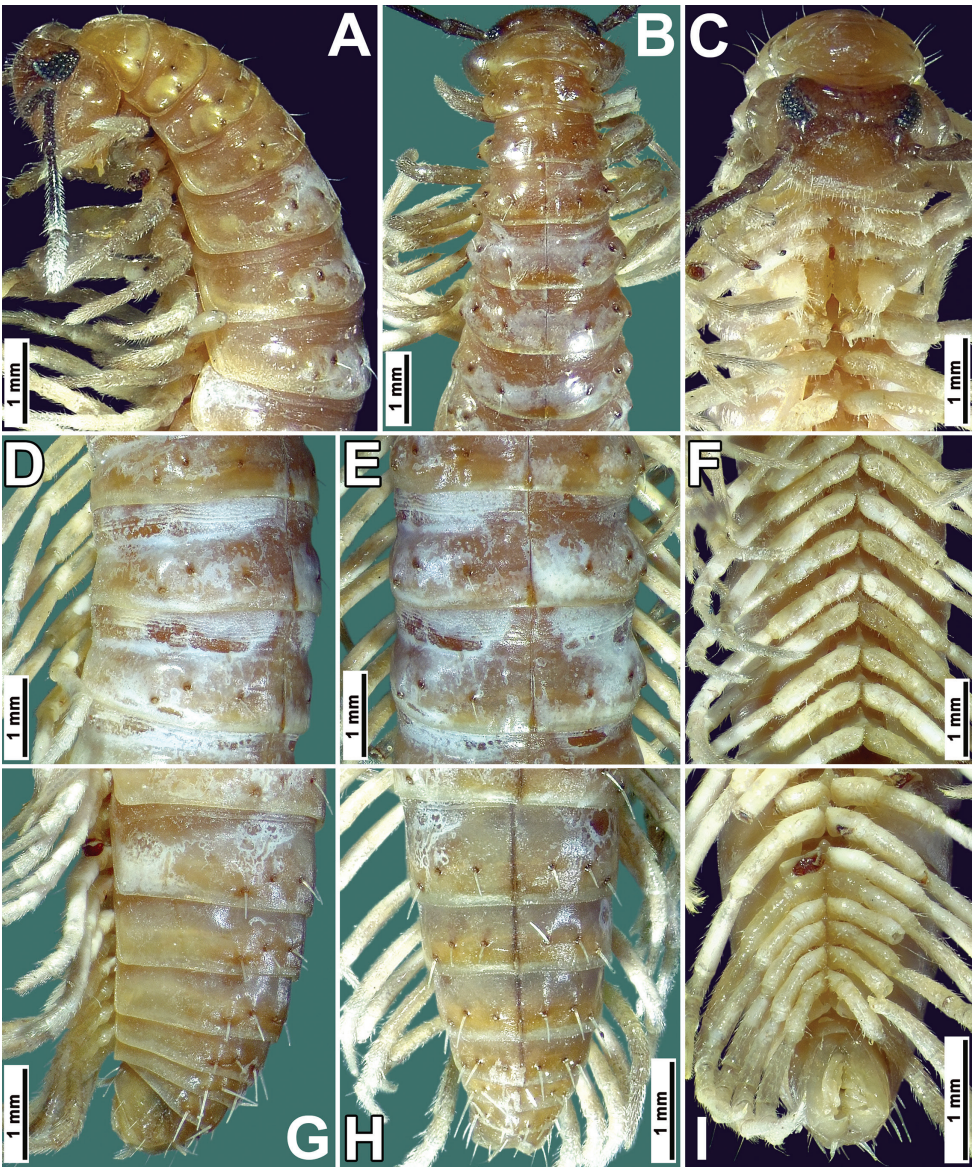


**Figure 2.** *Nepalella siamensis* sp. nov., ♂ holotype (CUMZ) **A–C** anterior part of body, lateral, dorsal and ventral views, respectively **D–F** body segments 8–10, sublateral, dorsal and ventral views, respectively **G–I** posterior part of body, lateral, dorsal and ventral views, respectively.

**Etymology.** To emphasize "Siam", referring to the former name of Thailand as the *terra typica*; adjective.

**Diagnosis.** Differs from the congeners by ♂ femora 3 and 4 each with a small mushroom-like protuberance (**mp**) ventrally (Fig. 3C); ♂ coxa 10 with a conspicuous horn-shaped process (**h**) dorsally (Fig. 3E, F); ♂ coxa 11 with a small, medial, digitiform process (**m**) and a high, basal, funnel-shaped process (**b**) (Fig. 3G, H); anterior

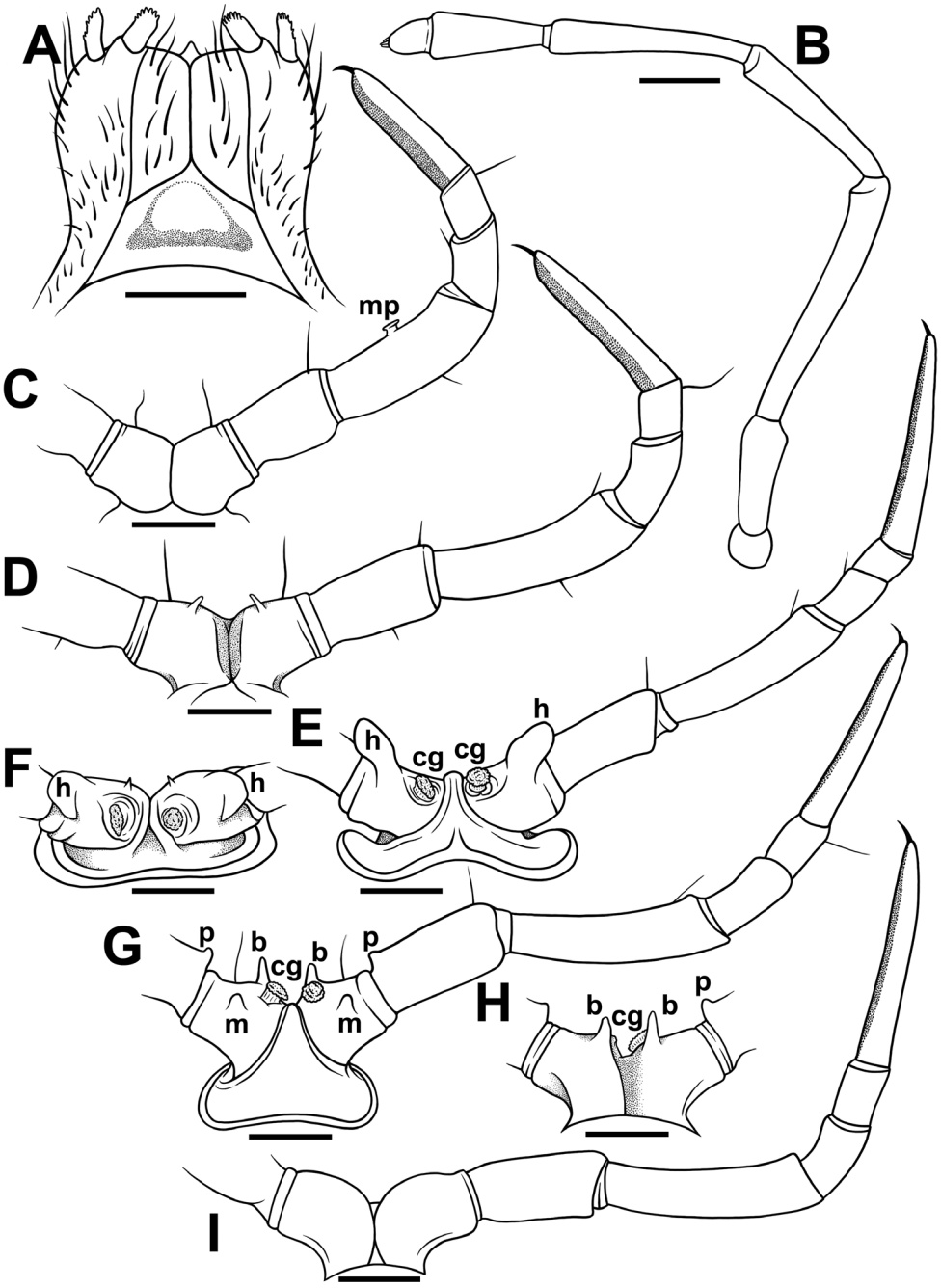


**Figure 3.** *Nepalella siamensis* sp. nov., ♂ holotype (CUMZ) **A** gnathochilarium, ventral view **B** antenna **C** leg 4, caudal view **D** leg 7, caudal view **E** leg 10, front view **F** coxa 10, subcaudal view **G** leg 11, front view **H** coxa 11, caudal view **I** leg 12, caudal view. Abbreviations: **b** basal process, **cg** coxal gland, **m** medial process, **mp** mushroom-shaped protuberance, **p** parabasal process, **h** horn-shaped process. Scale bars: 0.25 mm.

gonopod sternum carrying a median lobe and two small lateral lobules (Figs 4A, B, 5A), coupled with posterior gonopod equipped with a foot-shaped colpocoxite (**c**) and a rounded bulge (**r**) at base in frontal view (Figs 4C, D, 5C, D).

**Description.** Length of holotype ca 33 mm, maximum width 3.2 mm. Coloration light brown (Fig. 2A, B, D, E, G, H); head light brown, venter and legs light yellowish to pallid (Fig. 2C, F, I). Eye patches and antennae brownish black (Fig. 2A, C).

In width, collum < segment 2 < 3 < head with genae = segment 4 < 5 < 6 < 7 = 20; thereafter, body very gradually tapering towards telson.

Body with 30 segments (29 pleurotergites with free sternites, plus telson, or "rings", in terms of Enghoff et al. (1993, 2015)).

Head densely setose, clypeolabral region slightly convex. Eye patches triangular, each composed of 27 and 28 convex ommatidia (Fig. 2A, C).

Antennae very long and slender (Figs 2A, 3A), reaching past body segment 6 when stretched posteriorly; antennomere 7 with four apical cones.

Gnathochilarium without promentum (Fig. 3A).

Collum as usual (for heterochordeumatoideans), obcordate in shape, with rudimentary paraterga (Fig. 2A). Tegument smooth, shining, only prozonae distinctly and densely striolate transversely (Fig. 2D, E). Metatergal setation 3 + 3, typical of Chordeumatida; macrochaetae long, rather thick, pointed, placed on clear knobs (Fig. 2A, B, D, E, G, H); stricture between pro- and metazona shallow, inconspicuous (Fig. 2A, D, E, G, H). Paraterga poorly developed, with small dorsolateral bulges in anterior part of body (Fig. 2B), following segments rather regularly rounded in dorsal view (Fig. 2D, E, H).

CIX (ring 15) = 0.62; MIX (ring 15) = 0.87; MA (ring 15) ≈ 145°; PIX impossible to evaluate due to insufficiently developed paraterga. Axial suture distinct, pallid, as usual (Fig. 2B, D, E, H).

♂ legs long and slender, ca 1.5 times as long as midbody height. Legs 1 and 2 slightly reduced, tarsi with usual ventral brushes, but without papillae; ♂ coxa 2 with a distal mediocaudal cone perforated by gonopore orifice. All following legs conspicuously papillate on ventral face of tarsi (Fig. 3C, D, E, G, I). ♂ legs 3–7 distinctly and increasingly crassate, pairs 3 and 4 particularly so. Femora 3 and 4 each with a small, but evident mushroom-shaped protuberance (**mp**) at midway ventrally (Fig. 3C). Coxa 7 with a small, but evident distoventral digitiform outgrowth (Fig. 3D).

♂ legs 10 and 11 each with a small coxal gland (**cg**) (Fig. 3E–H); each coxa 10 dorsally with a large horn-shaped process (**h**) conspicuously enlarged at base (Fig. 3E, F); each coxa 11 with a small, medial, digitiform process (**m**) and a high, basal, funnel-shaped process (**b**) (Fig. 3G, H); prefemur 11 with a small parabasal process (**p**) ventrally (Fig. 3G, H). Claws simple, rather long.

Anterior gonopods (♂ leg-pair 8) very strongly reduced, sternum with a median lobe (**ml**) distally in oral view and with two small lateral lobules (**ll**); coxites (**cxi**) long, slender and horn-shaped (Figs 4A, B, 5A, B).

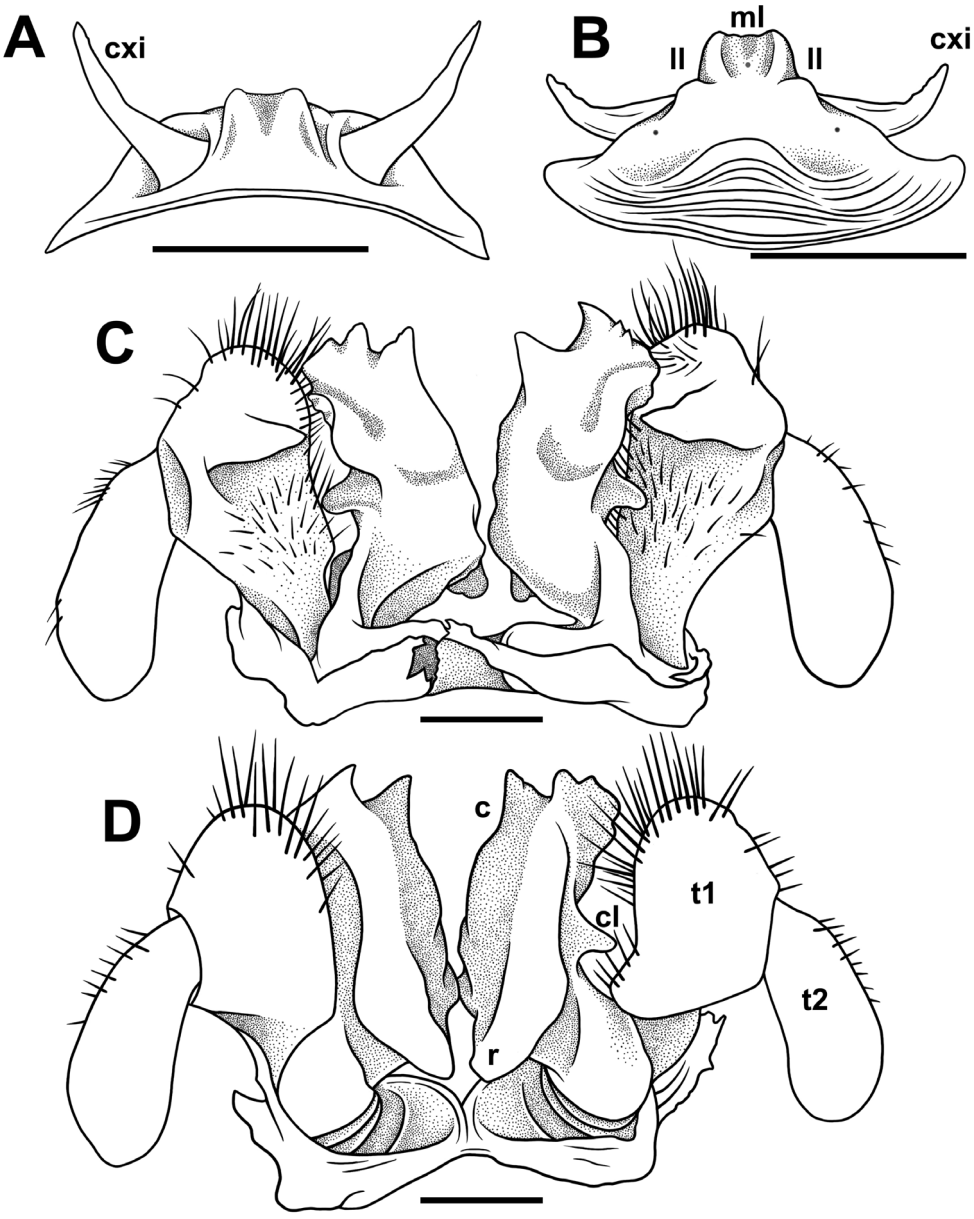


**Figure 4.** *Nepalella siamensis* sp. nov., ♂ holotype (CUMZ) **A, B** anterior gonopods, front and caudal views, respectively **C, D** posterior gonopods, caudal and front views, respectively. Abbreviations: **c** colpocoxite, **cl** lateral lobe, **cxi** coxites, **ll** lateral lobules, **ml** median lobe, **r** rounded bulge, **t1** telopoditomere 1, **t2** telopoditomere 2. Scale bars: 0.2 mm.

Posterior gonopods (♂ leg-pair 9) (Figs 4C, D, 5C, D, E, F) hypertrophied, each with a prominent, foot-shaped colpocoxite (**c**), this being higher than telopodite, and with three evident longitudinal lamellae in caudal view; a rather conspicuous lateral lobe

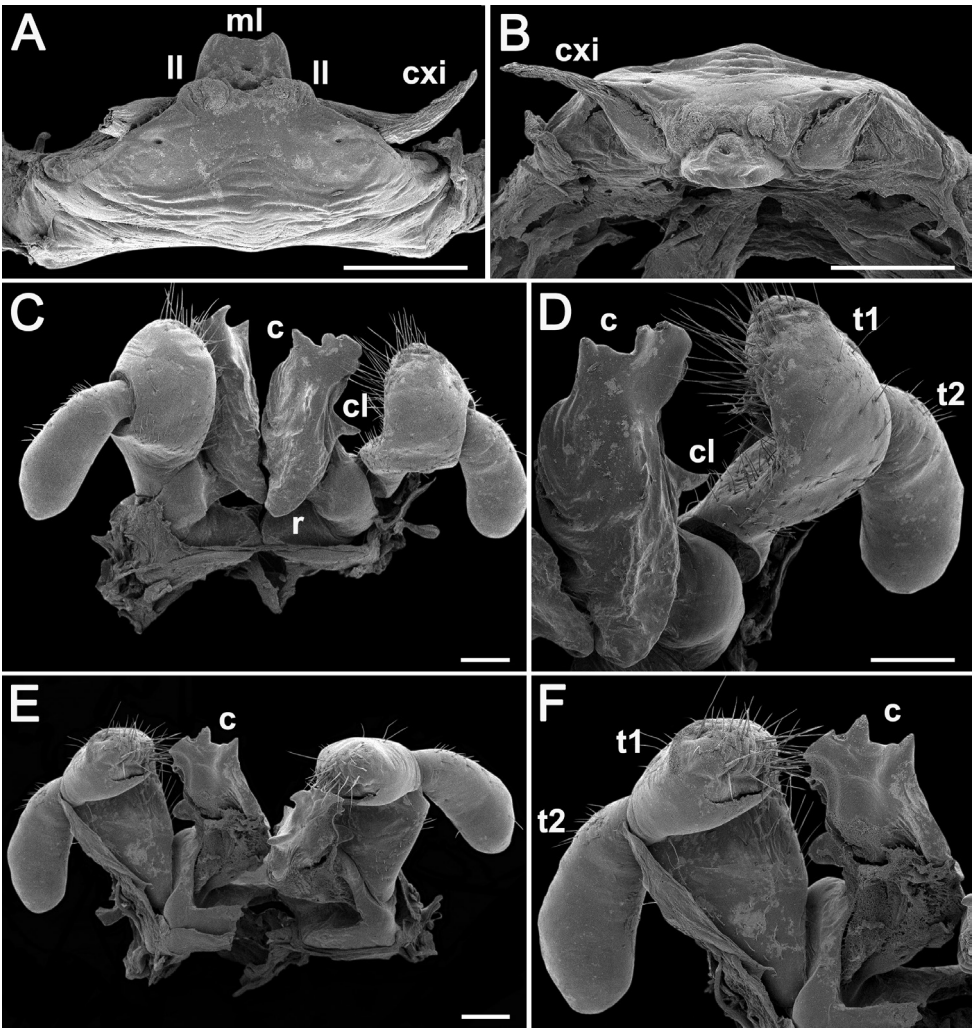


**Figure 5.** *Nepalella siamensis* sp. nov., SEM ♂ holotype (CUMZ) **A, B** anterior gonopods, caudal and superior views, respectively **C, E** posterior gonopods, front and caudal views, respectively **D, F** left gonopod, front and caudal views, respectively. Abbreviations: **c** colpocoxite, **cl** lateral lobe, **cxi** coxites, **ll** lateral lobules, **ml** median lobe, **r** rounded bulge, **t1** telopoditomere 1, **t2** telopoditomere 2. Scale bars: 0.2 mm.

(**cl**) at midway in caudal view; with a rounded bulge (**r**) at base in frontal view; telopoditomere 1 (**t1**) particularly strongly setose on posterior face, expanded apically, telopoditomere 2 (**t2**) subpyriform, likewise voluminous, only slightly setose laterally in basal half.

**Remark.** The specimen was collected by hand while it was moving very fast on the leaf litter surface. The type locality is situated in a dipterocarp forest on the side of a road near the Ta Phraya Waterfall. The species was found syntopically together with *Antheromorpha uncinata* (Attems, 1931) (Paradoxosomatidae, Polydesmida) (Likhitrakarn et al. 2016).

## Key (after adults) to the known species of *Nepalella*, modified after Golovatch et al. (2006b)

1 Adults with 28 body segments: 27 pleurotergites including telson ..... ***N. phulcokia***

– Adults with 30 body segments including telson ..... **2**

2 Body length ≥ 27 mm, width 2.5–3.5 mm ..... **3**

– Body length ≤ 26 mm ..... **10**

3 Midbody paraterga well developed, PIX(15) = 0.17–0.62 ..... **4**

– Midbody paraterga poorly developed, PIX(15) impossible to evaluate ..... **5**

4 Body length 27–35 mm, width 3.2–3.5 mm; coloration rather pale; each eye patch with 26 ommatidia; ♂ femora 3 and 4 each with a mushroom-like protuberance ventrally ..... ***N. lobata***

– Body length 36–38 mm, width 2.6–2.8 mm; coloration light brown; each eye patch with 8–11 ommatidia; ♂ legs 3 and 4 without such modifications ..... ***N. jinfoshan***

5 Each eye patch ≥ 25 ommatidia ..... **6**

– Each eye patch with 10–17 ommatidia ..... **7**

6 Each eye patch with 27–28 ommatidia; coloration light brown; Sa Kaeo Province, Thailand ..... ***N. siamensis* sp. nov.**

– Each eye patch with 25 ommatidia; coloration dark brown; Yunnan, China. ..... ***N. magna***

7 ♂ legs 2.0 times as long as midbody height; ♂ coxa 10 with a large process distoventrally; anterior gonopod sternum with a very large and broad median lobe ..... ***N. wangi***

– ♂ legs 1.4–1.8 times as long as midbody height; ♂ coxa 10 without such modifications; anterior gonopod sternum with either a small or an otherwise modified process ..... **8**

8 Body particularly large, ≥ 40 mm long; antennae very long, reaching past body segment 8 dorsally; anterior gonopod sternum with a high and evident median protuberance and two lateral lobes ..... ***N. grandis***

– Body smaller, ≤ 40 mm long; antennae shorter, reaching only past body ring 5 dorsally; anterior gonopod sternum with a small median protuberance .... **9**

9 ♂ legs 1.4 times as long as midbody height; coloration pale brown; ♂ femora 3 and 4 each with a small mushroom-shaped protuberance ventrally ..... ***N. marmorata***

– ♂ legs 1.8 times as long as midbody height; coloration entirely pallid to light yellowish; ♂ legs 3 and 4 without such modifications ..... ***N. grandoides***

10 Body pallid, but eye patches and antennae pigmented; body 2.6–2.7 mm wide due to paraterga well developed, in the form of distinct dorsolateral keels; tergal setae long; ♂ legs 3–7 not enlarged; Myanmar ..... ***N. pallida***

– Body either entirely pallid (cavernicole) or distinctly pigmented, eye parches and sometimes also antennae pigmented; body width ≤ 2.3 mm, paraterga

largely poorly developed, like indistinct dorsolateral swellings; tergal setae medium-sized at most; ♂ legs 3–7 very often crassate ..... **11**

11 Body length ≥ 18 mm, width ≥ 1.9 mm; coloration uniformly brown, ♂ coxa 10 without distinct processes ..... **12**

– Never all these three characters combined ..... **14**

12 Anterior gonopod sternum with a narrow and acute median process; only ♂ femur 4 roundly gibbose ventrally; Thailand ..... **13**

– Anterior gonopod sternum with a round and broad median process; ♂ femora 3 and 4 each with a fungiform protuberance ventrally; Nepal ..... ***N. gunsa***

13 Body length 24 mm, width 2.3 mm; posterior gonopods with colpocoxites divided distally into three branches; ♂ coxa 10 with two large processes distoventrally ..... ***N. taiensis***

– Body length 17 mm, width 2.0 mm; posterior gonopods with colpocoxites protruded distally and bend down; ♂ coxa 10 with a rather small process distoventrally ..... ***N. inthanonae***

14 Body entirely pallid; ommatidia < 9, reduced, only slightly pigmented and widely separated; cave in Guizhou Prov., China ..... **15**

– Body pigmented, > 20 dark and compact ommatidia ..... **16**

15 Body length 18 mm, width 1.6 mm; each eye patch with nine ommatidia; ♂ legs 3–7 not modified; anterior gonopod sternum with two short, acute, paramedian processes ..... ***N. caeca***

– Body length 20–26 mm, width 1.5–2.3 mm; each eye patch with 4–6 ommatidia; ♂ legs 3–5 distictly crassate; anterior gonopod sternum without median process ..... ***N. troglodytes***

16 Body 2.2 mm wide, paraterga well developed, shoulder-shaped; ♂ femur 4 with a distal knob subtending a distal depression on ventral side; Yunnan, China ..... ***N. griswoldi***

– Body width usually ≤ 1.9 mm; paraterga moderately to poorly developed; ♂ femur 4 either unmodified or modified otherwise ..... **17**

17 Tergal setae short and blunt; ♂ legs 3–7 crassate, but without further modifications; posterior gonopod telopodite relatively strongly reduced, much shorter than colpocoxites; Yunnan ..... ***N. pianma***

– Tergal setae short to medium-sized, acute; at least some of ♂ legs 3–7 usually with modifications; telopodite of posterior gonopods hypertrophied, (sub) equal in height to colpocoxite ..... **18**

18 Body width 1.8–2.0 mm; ♂ legs 3–7 with tarsal papillae and dorsally inflated prefemora; Yunnan ..... ***N. kavanaughi***

– Body width usually ≤ 1.9 mm; ♂ legs 3–7 with neither tarsal papillae nor dorsally enlarged prefemora ..... **19**

19 Tarsal papillae present on most ♂ legs; ♂ prefemur 11 with a long, digitiform, parabasal process; Vietnam ..... ***N. vietnamica***

– Tarsal papillae absent from ♂ legs; ♂ prefemur 11 devoid of processes ..... **20**

20 Claw simple; ♂ coxa 10 with a long process distoventrally; ♂ coxa 11 at most with one small process distoventrally, Nepal.....**21**
– Claw complex, with both a minute accessory claw dorsally and a long setoid filament ventrally at base; ♂ coxae 10 devoid of processes, ♂ coxa 11 with two small processes distoventrally; Myanmar .....***N. birmanica***
21 Coloration ochraceous, with four dark, brown, longitudinal stripes.....**22**
– Coloration ochraceous to brownish, with spots, or metazonae dark .....**25**
22 Colpocoxites of posterior gonopods divided into three branches or lobes.... **23**
– Colpocoxites of posterior gonopods poorly divided distally into only two short branches.....**24**
23 Larger: 16–17 mm long, 1.8–1.9 mm wide; colpocoxite of posterior gonopods divided into three lobes; ♂ coxa 10 with a C-shaped process ..... .....***N. tragsindola***
– Smaller: 10–12 mm long, 1.0–1.3 mm wide; colpocoxite of posterior gonopods divided into two lobes and a slender acuminate branch (solenomere?); ♂ coxa 10 with a coniform process topped by a rounded, microgranulate bulge .....***N. gairiensis***
24 Larger: 17 mm long, 1.6 mm wide (♂); both branches of colpocoxite very short and erect; ♂ coxa 10 with a bifid process .....***N. ringmoensis***
– Smaller: 11–14 mm long, 1.3–1.5 mm wide (♂, ♀); middle branch of three unequal branches of colpocoxite directed medially; ♂ coxa 10 with a subtruncate process.....***N. deharvengi***
25 ♂ coxa 10 with a straight, apically truncate process; ♂ prefemora 3–7 each with a distoventral knob; ♂ coxa 11 without gland, but with a small distomedial process .....***N. thodunga***
– ♂ coxa 10 with a curved, apically acuminate process; ♂ prefemora 3–7 either unmodified or only third and fourth with distoventral knobs; ♂ coxa 11 at most with a small gland, devoid of any processes .....**26**
26 ♂ coxa 10 with a strong unciform process directed caudally; ♂ femora 3–7 each with a ventral fungiform protuberance at midway.....***N. taplejunga***
– ♂ coxa 10 with a strong unciform process directed laterad; ♂ femora 3–7 unmodified.....**27**
27 Larger: ca 14 mm long, 1.4–1.5 mm wide; tergal setae medium-sized; ♂ prefemora 3 and 4 each with a distoventral knob .....***N. khumbua***
– Smaller: ca 10 mm long, 1.0 mm wide; tergal setae short; ♂ legs 3 and 4 without such modifications.....***N. jaljalae***

## Discussion

At the moment, 28 species of *Nepalella* have been described, mostly (22, ca 79%) from Nepal or China. In Nepal, many species have been encountered at very high elevations of 2200–3800 m a.s.l., although the occurrence in montane habitats

(>800 m a.s.l.) is typical of most congeners elsewhere. Allopatry prevails, but sympatry or even syntopy of two congeners has occasionally been recorded as well. As the distributions of all species, both epigean and cave-dwelling, tend to be highly localized, narrow endemism is most characteristic. Cavernicoly seems to be restricted to the karsts of the southern half of China alone, whereas more to the south, even in the abundant karsts of Thailand or Myanmar, all *Nepalella* encounters appear to be only epigean and increasingly sporadic (Table 1). Moreover, there seem to be no troglobionts among the Chordeumatida presently known to occur in Thailand or Myanmar, although at least the cave millipede faunas of Thailand and Indochina are quite well studied (e.g., Golovatch 2015; Likhitrakarn et al. 2015, 2016, 2017, 2018, 2020a, 2020b, 2021). The most common group, likewise both highly diverse and abundant, that clearly dominates the subterranean millipede faunas of Southeast Asia together with southern China is long known to be the family Cambalopsidae (Spirostreptida) (Golovatch 2015; Likhitrakarn et al. 2018, 2020a, b, 2021).

Basically, these characteristics and patterns strongly resemble those of many groups of Diplopoda such as the orders Polydesmida (4 families, 8 genera), Chordeumatida (3 families, 3 genera), Callipodida (3 families, 3 genera), Spirostreptida (2 families, 3 genera), Glomerida (1 family, 1 genus), and Julida (1 family, 1 genus) encountered in caves of southern China (Golovatch and Liu 2020). Thus, it is there that caves appear to be exceptionally rich in millipedes, often with 5–6 diplopod species, mostly very local endemics and presumed troglobionts (Golovatch 2015), occurring per cave. The animals are largely characterized by pronounced troglomorphic features such as reduced and mostly unpigmented eyes, unpigmented bodies, thinner and more delicate teguments, clearly elongated appendages (antennae, legs, claws, tergal outgrowths etc.), and often also the so-called "cave gigantism" (Liu et al. 2017a).

A few *Nepalella* species are among the largest Chordeumatida globally (e.g., *N. grandis*, which is up to 42 mm long) and nearly all appear to be restricted to subtropical rather than purely tropical environments lying between 23.5° and 34°N (Fig. 1). In contrast, lowland, typically tropical occurrences are only very few: *N. vietnamica* from Vietnam, and both *N. taiensis* and *N. inthanonae* from Thailand (Table 1). The new species, *N. siamensis* sp. nov., definitely joins the trio, at the same time representing the most lowland and the southernmost record of a *Nepalella*.

Liu et al. (2017b) recovered the phylogeny of five species of *Nepalella*, based both on morphological and molecular evidence. Barcoding results revealed that interspecific p-distances amounted to 8.5–15.9%, vs 0–6.8% for intraspecific p-distances. The genus was split into two groups associated with such morphological characters as the presence or absence of a median lobe on the sternum of the anterior gonopods. Because of a limited amount of *Nepalella* material used in that pioneering study, future investigations are required to confirm both hypotheses. There is little doubt that further novelties concerning the species diversity and distribution of *Nepalella* are ahead.

## Acknowledgements

This project was funded through grants received from TRF Strategic Basic Research BDG 6080011 (2017–2019) to CS and NL, and Center of Excellence on Biodiversity (BDC-PG4-163008) to SP. We thank the members of the Animal Systematics Research Unit for their invaluable assistance in the field. One of us (SIG) was partly supported by the Presidium of the Russian Academy of Sciences, Program No. 41 "Biodiversity of Natural Systems and Biological Resources of Russia". Special thanks go to William A. Shear (Virginia, U.S.A.) and an anonymous reviewer, as well as to Dragan Ž. Antić (Belgrade, Serbia), the editor, whose critiques and help have allowed us to considerably improve the paper.

## References

AVMA (2013) AVMA guidelines for the euthanasia of animals. https://www.avma.org/KB/Policies/Documents/euthanasia.pdf [Accessed on: 2021-11-11]

Enghoff H, Dohle W, Blower JG (1993) Anamorphosis in millipedes (Diplopoda) – the present state of knowledge with some developmental and phylogenetic considerations. Zoological Journal of the Linnean Society 109: 103–234. https://doi.org/10.1111/j.1096-3642.1993.tb00305.x

Enghoff H, Golovatch SI, Short M, Stoev P, Wesener T (2015) Diplopoda. In: Minelli A (Ed.) Treatise on Zoology—Anatomy, Taxonomy, Biology. The Myriapoda 2(16): 363–453. https://doi.org/10.1163/9789004188273_017

Golovatch SI (1983) Contributions to the millipede fauna of Vietnam (Diplopoda) I. Chordeumatida. Acta Zoologica Academiae Scientiarum Hungaricae 29(1–3): 123–127.

Golovatch SI (2015) Cave Diplopoda of southern China with reference to millipede diversity in Southeast Asia. ZooKeys 510: 79–94. https://doi.org/10.3897/zookeys.510.8640

Golovatch SI, Mikhaljova EV (1978) A new family of East-Palaearctic Chordeumida (Diplopoda), with a description of a new genus and a new species [in Russian]. Bulletin of the Moscow Society of Naturalists, Biological series 83(4): 66–71. [In Russian, a summary in English]

Golovatch SI, Liu W (2020) Diversity, distribution patterns, and fauno-genesis of the millipedes (Diplopoda) of mainland China. ZooKeys 930: 153–198. https://doi.org/10.3897/zookeys.930.47513

Golovatch SI, Geoffroy JJ, Mauriès JP (2006a) Four new Chordeumatida (Diplopoda) from caves in China. Zoosystema 28(1): 75–92.

Golovatch SI, Geoffroy JJ, Mauriès JP (2006b) Several new or poorly-known cavernicolous millipedes (Diplopoda) from southern China. Arthropoda Selecta 15(2): 81–89.

Likhitrakarn N, Golovatch SI, Panha S (2015) A checklist of the millipedes (Diplopoda) of Cambodia. Zootaxa 3973(1): 175–184. https://doi.org/10.11646/zootaxa.3973.1.7

Likhitrakarn N, Golovatch SI, Panha S (2016) Review of the Southeast Asian millipede genus *Antheromorpha* Jeekel, 1968 (Diplopoda, Polydesmida, Paradoxosomatidae). ZooKeys 571: 21–57. https://doi.org/10.3897/zookeys.571.7566

Likhitrakarn N, Golovatch SI, Jirapatrasilp P, Panha S (2017) A checklist of the millipedes (Diplopoda) of Myanmar, with an updated list of Leonardo Fea's collecting localities. Zootaxa 4350(1): 1–46. https://doi.org/10.11646/zootaxa.4350.1.1

Likhitrakarn N, Golovatch SI, Srisonchai R, Brehier F, Lin A, Sutcharit C, Panha S (2018) Two new species of the millipede family Cambalopsidae from Myanmar (Diplopoda: Spirostreptida). ZooKeys 760: 55–71. https://doi.org/10.3897/zookeys.760.24837

Likhitrakarn N, Golovatch SI, Jeratthitikul E, Srisonchai R, Sutcharit C, Panha S (2020a) A remarkable new species of the millipede genus *Trachyjulus* Peters, 1864 (Diplopoda, Spirostreptida, Cambalopsidae) from Thailand, based both on morphological and molecular evidence. ZooKeys 925: 55–72. https://doi.org/10.3897/zookeys.925.49953

Likhitrakarn N, Golovatch SI, Thach P, Chhuoy S, Ngor PB, Srisonchai R, Sutcharit C, Panha S (2020b) Two new species of the millipede genus *Plusioglyphiulus* Silvestri, 1923 from Cambodia (Diplopoda, Spirostreptida). ZooKeys 938: 137–151. https://doi.org/10.3897/zookeys.938.51234

Likhitrakarn N, Golovatch SI, Jantarit S (2021) Two new species of the millipede genus *Glyphiulus* Gervais, 1847 (Diplopoda, Spirostreptida, Cambalopsidae) from caves in northern Thailand. ZooKeys 1056: 173–189. https://doi.org/10.3897/zookeys.1056.71395

Liu W, Golovatch SI, Wesener T, Tian M (2017a) Convergent evolution of unique morphological adaptations to a subterranean environment in cave millipedes (Diplopoda). PLoS ONE 12(2): e0170717. https://doi.org/10.1371/journal.pone.0170717

Liu W, Wesener T, Golovatch SI, Tian M (2017b) Contributions to the millipede genus *Nepalella* Shear, 1979 from China, with four new species and first results on phylogeny based on DNA-barcoding (Diplopoda, Chordeumatida, Megalotylidae). Zootaxa 4243(3): 455–482. https://doi.org/10.11646/zootaxa.4243.3.3

Mauriès JP (1988) Myriapodes du Népal. II. Diplopodes craspédosomides nouveaux de l'Himalaya et de la région indo-malaise (Craspedosomidea et Chordeumidea). Revue suisse de Zoologie 96 (1): 3–49. https://doi.org/10.5962/bhl.part.79638

Shear WA (1979) Diplopoda from the Nepal Himalayas. Chordeumida with comments on the Asian chordeumid fauna. Senckenbergiana biologica 60(1–2): 115–130.

Shear WA (1987) Chordeumatid Diplopoda from the Nepal Himalayas, II. Courier Forschungsinstitut Senckenberg 93: 229–240.

Shear WA (1999) A new troglobitic milliped of the genus *Nepalella* from China (Diplopoda, Chordeumatida, Megalotylidae). Myriapodologica 6(1): 1–10.

Shear WA (2002) Five new chordeumatidan millipeds from China: new species of *Vieteuma* (Kashmireumatidae) and *Nepalella* (Megalotylidae). Proceedings of the California Academy of Sciences 53(6): 63–72.

Spelda J (2001) Review of the millipede genus *Pterygophorosoma* Verhoeff, 1897 (Diplopoda, Chordeumatida, Craspedosomatidae). Andrias 15: 29–48.